FOCAL MECHANISMS AND VARIATIONS IN TECTONIC STRESS FIELDS IN EASTERN CANADA (WESTERN QUEBEC AND SOUTHERN ONTARIO)

By

PARISA ASGHARZADEH SADEGH

A thesis submitted to the Department of Geological Sciences

and Geological Engineering in conformity with

the requirements for the degree of

Master of Science

Queen's University,

Kingston, Ontario, Canada

June 2012

Abstract:

Earthquakes in western Quebec and southern Ontario present a major contribution to the natural hazards in south eastern Canada due to their proximity to major population centres. However, the seismic characteristics of the events in these regions have not been well documented. Improved knowledge of earthquake distribution and seismic controlling mechanisms provides a great benefit for earthquake hazard analysis in eastern Canada.

The available information about the tectonic stress indicators, including focal mechanisms, was compiled for Canada prior to 1994. The present research is concentrated mainly on determination of the focal mechanisms and hypocentre locations of the earthquakes after 1993 with M > 3.5 to characterize the present-day regional and local stress fields in southern Ontario and western Quebec. An attempt was also made to differentiate local zones with comparatively homogeneous tectonic stresses orientation and seismic regimes, thus providing information for future re-assessment of the seismic hazard in each region.

Considering seismic parameters such as the trend of the epicentres, focal depths and the state of stress of the events along with their tectonic settings, ten distinct clusters have been proposed for western Quebec and two clusters of events were determined for southern Ontario with comparatively consistent focal mechanisms. The locations and characteristics of seismicity clusters appear to be consistent with the hypothesis that they are near the locations of large historic and prehistoric events, and represent exceptionally persistent aftershocks of past large earthquakes.

Acknowledgements:

I would like to express my sincere gratitude to my supervisors, Dr. Savka Dineva and Dr. Laurent Godin, whose valuable support, advice and comments made this work possible. I would like to acknowledge Dr. Bob Mereu for providing the opportunity to work with (PLTSEK) software. A special thanks to General Mapping Tools (GMT) and Ruhr University for donating the software used to complete my studies. I also thank Dr. Stephen McKinnon for insightful questions and discussions during my thesis examination. I would like to thank Dr. St-Onge in Natural resources Canada for helping me to understand the nature of deformation in the earth's crust.

I am thankful to all friends, staff and colleagues in the Department of Geological Sciences and Geological Engineering.

I would like to extend a special thanks to my brothers and parents, especially my mother, for their love and support through these years. My special thanks goes to my spouse, Mohammad Rayhani, and my lovely daughter for their endless support and patience.

Table of Contents

Chapter 6: Conclusions and Recommendations

List of Figures

List of Tables

Abbreviations

CNSN: Canadian National Seismic Network.

ERH: The standard error in the epicentre in km given by √(SDX2 + SDY2), where SDX and SDY are the standard errors in latitude and longitude.

ERZ: The standard error in the focal depth in km.

GSC: Geological Survey of Canada.

IRIS: Incorporated Research Institution for Seismology.

PmP: P wave reflected at Moho Discontinuity.

PmS: P wave reflected and converted into S-wave at Moho Discontinuity.

Pn and **Sn**: P and S waves refracted from Moho Discontinuity.

Pg and **Sg**: Direct P- and S-waves in the crust.

POLARIS: Stands for "Portable Observatories for Lithospheric Analysis and Research Investigating Seismicity.

RMS: Root-Mean Square.

SAC: Seismic Analysis Code.

SEED: Standard format for Exchange of Earthquake Data.

UWO file: File in The University of Western Ontario format - developed and accepted for use with PLTSEK software.

CHAPTER 1

INTRODUCTION

1.1 Introduction

Eastern Canada is part of the stable interior of the North American plate. Our knowledge of the cause of seismic activity in Eastern Canada is far from complete. Regional seismicity plays an important role in the study of tectonic processes and can contribute to the understanding of the nature of these processes and to the evaluation of the seismic hazard. Accurate locations for earthquake hypocentres are important in identifying potential seismogenic features and developing a relationship between seismicity and the tectonic structures and features. Other source parameters such as focal mechanisms can also provide information on the tectonic structures on which the earthquakes occur. The earthquake source parameters also provide information about the regional and local stress distributions within the plates, as well as the geometry and kinematics of fault slips. Accurate estimation of the magnitude of the seismic events can also provide insight into the size of the active faults. Earthquakes with magnitude of $m_N \leq 3$ have rupture sizes in the order of 1-100 metres with slips of less than a few centimetres, while earthquakes with larger magnitudes ($m_N > 5$) may have rupture dimensions at the scale of kilometres (e.g. Johnston, 1993).

Earthquakes in western Quebec and southern Ontario present a major contribution to the natural hazards in south-eastern Canada due to their proximity to major population centres, e.g., Montreal, Ottawa and Toronto (Adams and Halchuk, 2003) (Figure 1.1). Unfortunately, the seismic characteristics of the events in these regions have not been sufficiently documented. Without full understanding of the earthquake source parameters and mechanisms involved in the occurrence of these earthquakes, there are uncertainties in earthquake hazard analysis in eastern Canada.

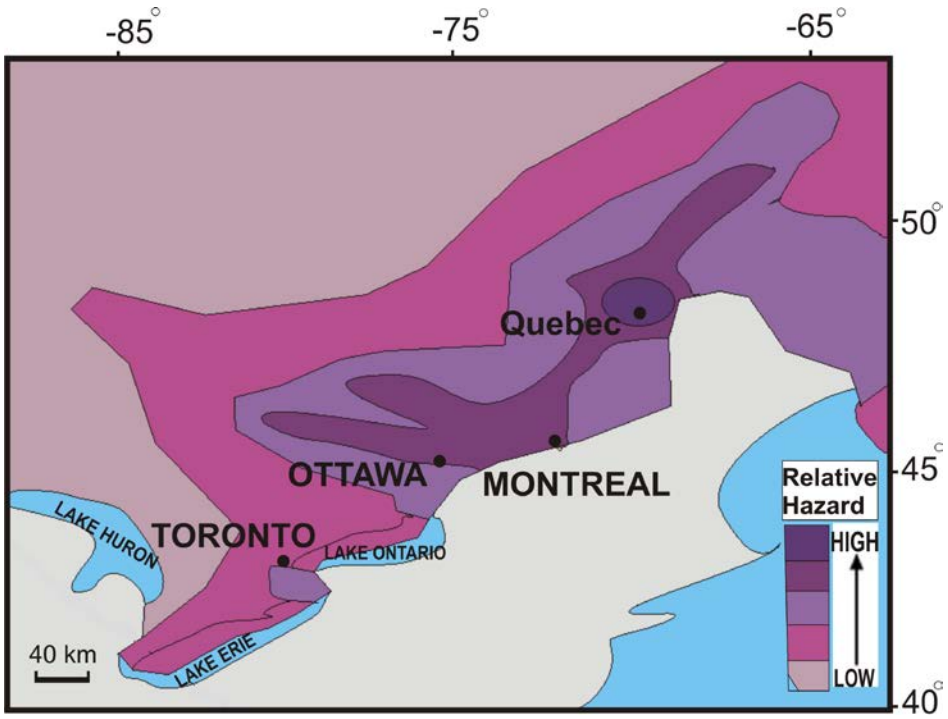

Figure 1.1: Simplified seismic hazard map of Canada. The estimated hazard in south eastern Ontario is greatest along the St. Lawrence and Ottawa Rivers, but moderate hazard is also present in other areas including densely populated southern Ontario (http://earthquakescanada.nrcan.gc.ca/hazard-alea/simphaz-eng.php).

Upgrades to the seismic networks in the last 20 years provide an opportunity for further study of the earthquake parameters and investigation of the relationships between geological setting and seismic source properties. The Southern Ontario Seismic Network (SOSN) (Mereu et al., 2002), the POLARIS network (Portable Observatories for Lithospheric Analysis and Research Investigating Seismicity) (Eaton et al. 2005) and the recent expansion of the Lamont-Doherty Cooperative Seismographic Network (LCSN) have improved the seismic network coverage in this area, providing better observational constraints on the recent seismicity. Most of the POLARIS stations use satellite communication technology, which allows for the installation of seismometers in remote areas. This has enabled the development of extensive seismic network coverage in parts of eastern Canada where significant but poorly understood seismicity may exist.

The objectives of this Thesis are to obtain several key source parameters (hypocentre locations, refined focal depths, and focal mechanisms) for earthquakes with magnitude (m_N) over 3.5 from 1992 to 2011 in western Quebec and southern Ontario. The new data, combined with the existing data in the Canadian Stress Database and various other publications, are used to examine the hypotheses for underlying tectonic controls on earthquake locations through comparison of hypocentre locations with seismogenic structures and other geological data. The threshold magnitude 3.5 was chosen because earthquakes stronger than 3.5 are well recorded by many stations and the locations and focal mechanisms can be reliably estimated. Smaller events usually do not generate enough data for estimation of the focal mechanism.

1.2 Organization of Thesis

Chapter 1 provides a description of the problem, scope, and layout of this thesis. Chapter 2 consists of a comprehensive survey of geological features as well as historical seismicity of the study area. Chapter 3 discusses the data set and methods used to determine the seismic parameters of earthquake data in southern Ontario and western Quebec. A brief review of the software packages used in this study is presented. Chapter 4 reports the results of the study including epicentre locations, focal depths and focal mechanisms for each studied earthquake. Chapter 5 is a discussion of the seismic source parameters in the study area along with a comparison to tectonic features of western Quebec and southern Ontario. All together, ten distinct clusters of events were identified and discussed. Finally, Chapter 6 summarizes the findings of the research and makes recommendations for future research.

CHAPTER 2

GEOLOGICAL SETTINGS AND SEISMICITY OF THE STUDY AREA

2.1 Introduction

Plate tectonics can explain most of the distribution of earthquakes around the world. Although earthquakes occur primarily along plate boundaries or in broad regions along the plate boundaries, numerous earthquakes also occur within the plates, causing loss of life and damage to properties (Adams and Basham, 1989). Unlike seismicity along the plate boundaries, the seismicity inside the plates has received very little attention. The earthquakes are not evenly distributed inside the plates. For example Sykes (1978) recognised that most events in northeastern America occur within the crust in areas that were affected by the last major orogenesis prior to the opening of Atlantic Ocean. The present seismicity could be the result of reactivation of existing fault zones, failed rifts, and other tectonic boundaries such as the late Proterozoic to Paleozoic rift systems along the St. Lawrence and Ottawa Rivers (Thomas, 2006).

Eastern Canada is located within the North American Plate and, therefore, has a relatively low rate of earthquake activity. However, large earthquakes do occur in the region, and may pose significant societal risk. Approximately 450 earthquakes occur in

eastern Canada each year, of which perhaps four exceed magnitude 4, thirty exceed magnitude 3, and about twenty-five events are reported felt (Geological Society of Canada, GSC). On average, a decade will include three events greater than magnitude 5. A magnitude 3 event is sufficiently strong to be felt in the immediate area, and a magnitude 5 event is generally the threshold of damage.

2.2 Background Geology

Figure 2.1 shows the major geologic units in the study area. The Superior Province, which is north of the study area, is the largest Archean craton on Earth and forms the ancient core of the North American continent (Ludden and Hynes, 2000). It is subdivided into a number of generally east–west trending juvenile trains, ranging in age from 2.72 Ga to 2.6 Ga (Hoffman, 1988). The Huronian Supergroup, also north of the study area, is a 15-km thick wedge of supracrustal rocks that records pre 2.1 Ga rifting and the subsequent establishment of a passive margin along the southern edge of the Superior craton (Hoffman, 1988). This region later experienced metamorphism during the 1.9 Ga Penokean Orogeny, a relatively early component of an extensive period of collisional orogenesis that produced the proto-North American landmass known as Laurentia (Hoffman, 1988).

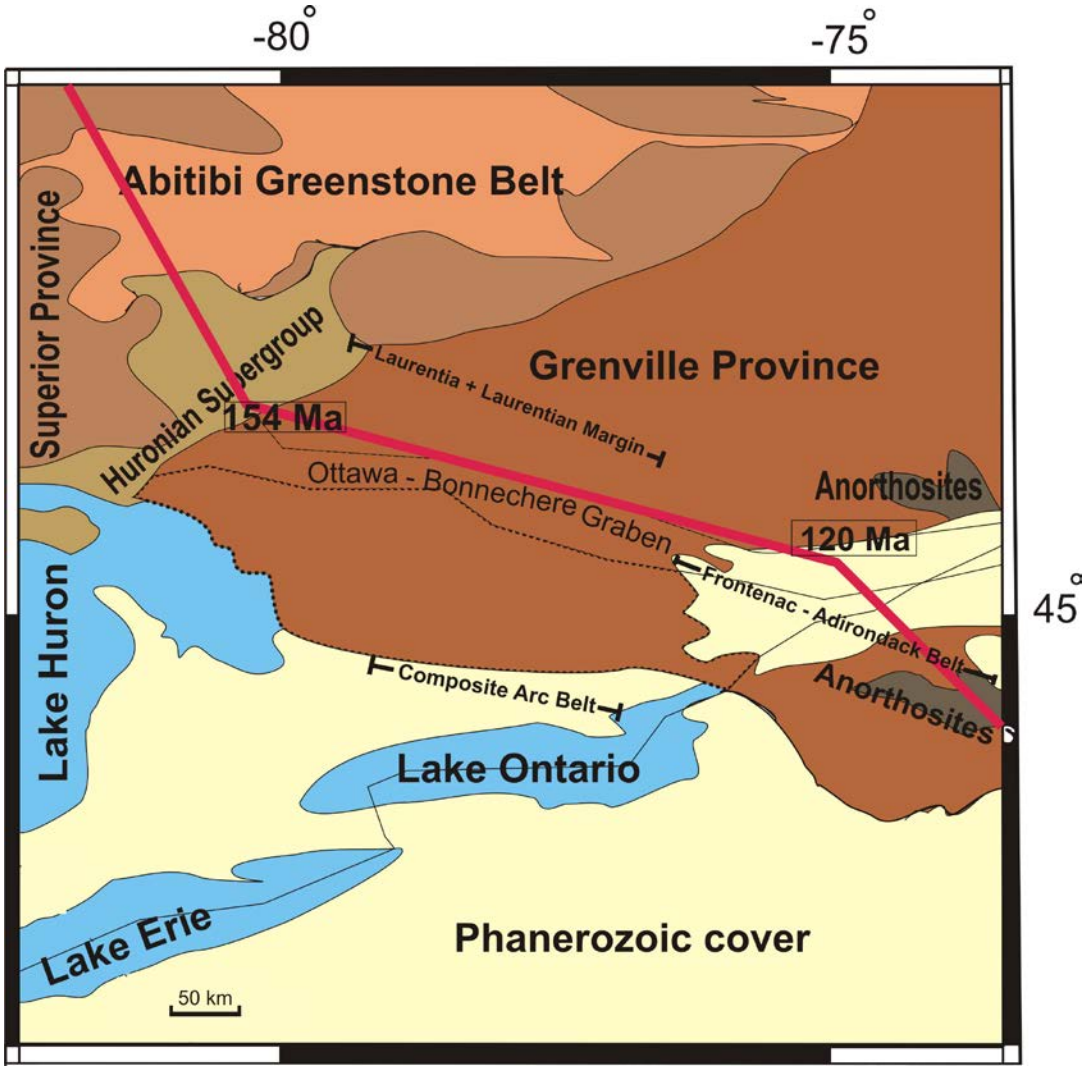

Figure 2.1: Geologic sketch map of southern Ontario and southwestern Quebec. (modified from Ludden and Hynes (2000); Red line is the approximate location of the hot spot track according to Heaman and Kjarsgaard, 2000. The numbers in Ma show igneous activities along this track. (Carr et al,. 2000).

Three main tectonic elements of the Frontenac–Adirondack, Laurentia and its pre-Grenvillian margin and the Composite Arc Belt have formed the Grenville Province (Carr et al., 2000). The pre-Grenvillian Laurentian margin extends from the Central

Metasedimentary Belt boundary tectonic zone (CMBbtz) in the southeast to the Grenville Front tectonic zone (GFtz) in the northwest (Figure 2.2). This margin contains Paleoproterozoic and Mesoproterozoic rocks (1800-1350 Ma), which were formed by Andean-style arcs (Carr et al., 2000). The pre-Grenvillian Laurentian margin has a long tectonic history including ca. 1700 and 1450 Ma deformation, magmatism and metamorphism, and was progressively reworked during the ca. 1120-980 Ma Grenville orogen (Rivers 1997). The main tectonic elements of the Grenville province (the Grenville Front tectonic zone, CMBbtz, and the Elzevir Frontenac boundary zone (EFbz) are divided by major shear zones several kilometres wide (Easton, 1992). These zones are characterized by deformed rocks with northeast striking, shallow southwest-dipping tectonic fabric, and southeast-plunging mineral lineation (Carr et al., 2000).

The Composite Arc Belt (1300-1250 Ma) is predominantly composed of Mesoproterozoic volcanic arcs and sedimentary rocks from various arcs and marginal basins (Carr et al., 2000). This belt extends from the Central Metasedimentary Belt boundary thrust zone (CMBbtz) in the northwest to the Elzevir Frontenac boundary zone (EFbz) in the southeast (Easton, 1992; Carr et al., 2000) (Figure 2.2). Carr et al. (2000) interpreted this belt as a series of island arcs that were accreted and thrust onto Laurentia. The arcs are also interpreted to have formed an offshore oceanic crust and were probably amalgamated by ca. 1240 Ma (White et al. 2000).

The Frontenac–Adirondack Belt southeast of the EFbz is characterized by supracrustal marbles, granitic rocks, and quartzo-feldspathic gneisses. These rocks formed within continental crust or arc segments of uncertain age and were deformed by

ca. 1170 Ma, likely in a tectonic setting offshore from the pre-Grenvillian Laurentian margin (White et al. 2000). The Frontenac-Adirondack region was amalgamated with the Composite Arc Belt at ca. 1165 Ma and translated toward the craton at ca. 1120-980 Ma (Carr et al., 2000).

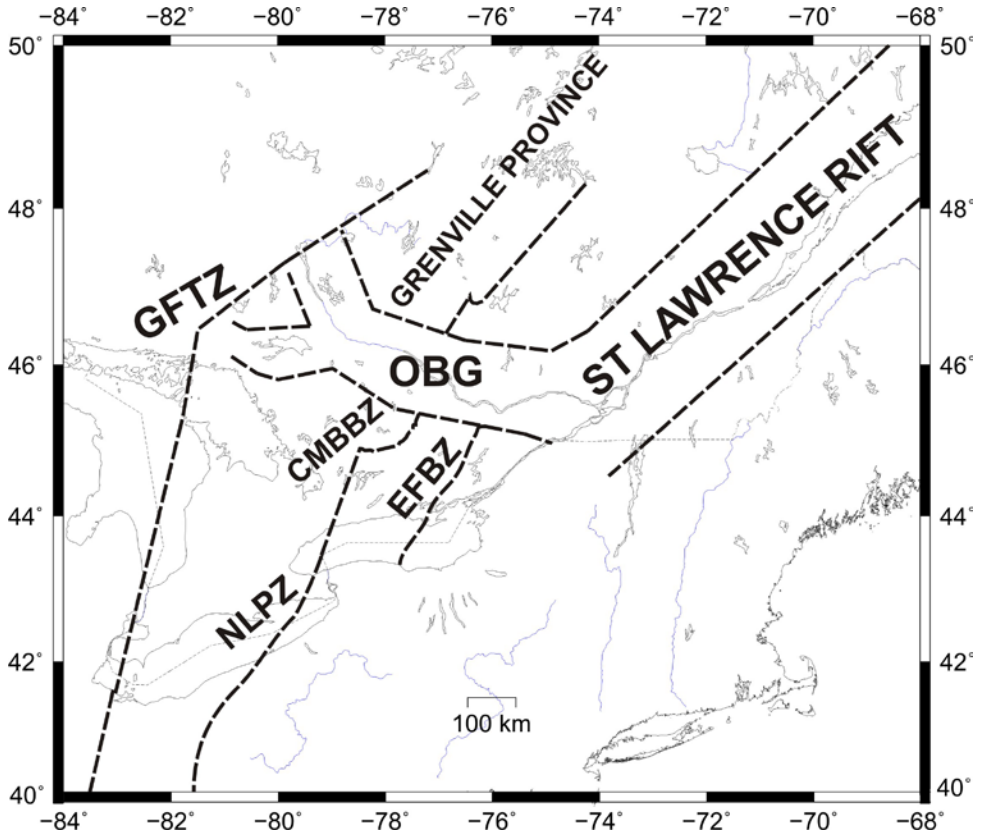

Figure 2.2: Simplified tectonic setting in Western Quebec and southern Ontario.

GFTZ–Grenville Front tectonic zone; CMBBZ–Central Metasedimentary Belt boundary tectonic zone; EFBZ–Elzevir Frontenac boundary zone; NPLZ–Niagara Pickering Linear Zone; OBG–Ottawa Bonnechere graben. (Compiled from Kumarapeli and Saul, 1966; Adams and Basham, 1989; Rivers et al., 1989; Easton 1992).

The Grenville Front tectonic zone (GFtz) is a southeast dipping zone which underwent ductile thrusting at ca. 1000 Ma (Easton, 1986). The Central Metasedimentary Belt boundary thrust zone is a northwest-directed ductile thrust (Hanmer and McEachern, 1992) that carried rocks of the Composite Arc and Frontenac-Adirondack belts over the pre-Grenvillian Laurentian margin. The Elzevir Frontenac boundary zone is a 10-35 km wide zone extended from the Elzevir and Frontenac terranes (Forsyth et al., 1994a), and consists of plutonic rocks with various metamorphic grades ranging in age from 1280-1170 Ma.

Late Precambrian rifting of Rodinia is manifested in this region by 590 Ma extensional faulting and dike intrusion (Kamo et al., 1995) along a series of NW-trending grabens that extend across the Grenville province and into the Superior province (Fig. 2.1). The Ottawa–Bonnechere graben, approximately corresponding to the current Ottawa River valley, is generally associated with the Mesozoic opening of the Atlantic Ocean (Easton, 1992). Normal faults trending west-northwest deformed the Precambrian surface forming the Ottawa–Bonnechere graben and the Block Mountains of the Madawaska Highlands (Kay, 1942). The most recent tectonic activity is associated with the emplacement of kimberlites at ~180 Ma (Kirkland Lake) and alkaline intrusions at ~130–120 Ma (Monteregian igneous province) (Crough, 1981).

2.3 Regional Seismicity

The intraplate seismicity of eastern Canada is concentrated in the following four areas of higher seismic activity that have potential for strong earthquakes: the Western

Quebec Seismic Zone (WQSZ), the Charlevoix Seismic Zone (CSZ), the Lower St. Lawrence Seismic Zone (LSZ) and the Southern Ontario Seismic Zone (SOSZ) (Figure 2.3) (Adams and Basham, 1989), likely associated with the reactivation of late Proterozoic to Paleozoic and Mesozoic rift systems along the St. Lawrence and Ottawa Rivers (Thomas, 2006). Figure 2.3 shows the distribution of recent seismic events in eastern Canada. As can be seen from this figure, earthquakes are generally concentrated in a few seismically active zones including the NE-striking bands of earthquakes along the St. Lawrence valley and the Appalachian Mountains, and the NW-striking band of seismicity consistent with the locations of kimberlite intrusions and other igneous activity along the inferred continental track of the Great Meteor hotspot (Heaman and Kjaarsgaard, 2000). There is also a seismically active area around the west end of Lake Ontario and south of Lake Erie. Adams and Basham (1989) argued that most of the events in southeastern Canada were associated with the reactivation of a Late Proterozoic to Paleozoic and Mesozoic rift system along the St. Lawrence and Ottawa Rivers (Thomas, 2006). Adams and Basham (1989) grouped the seismicity into four seismic zones (Figure 2.3):

- The Western Quebec Seismic Zone (WQSZ) (northeast of Ottawa River)
- The Lower St.Lawrence Seismic zone (LSZ)
- The Charlevoix Seismic zone (CSZ)
- Southern Ontario Seismic Zone (SOSZ)

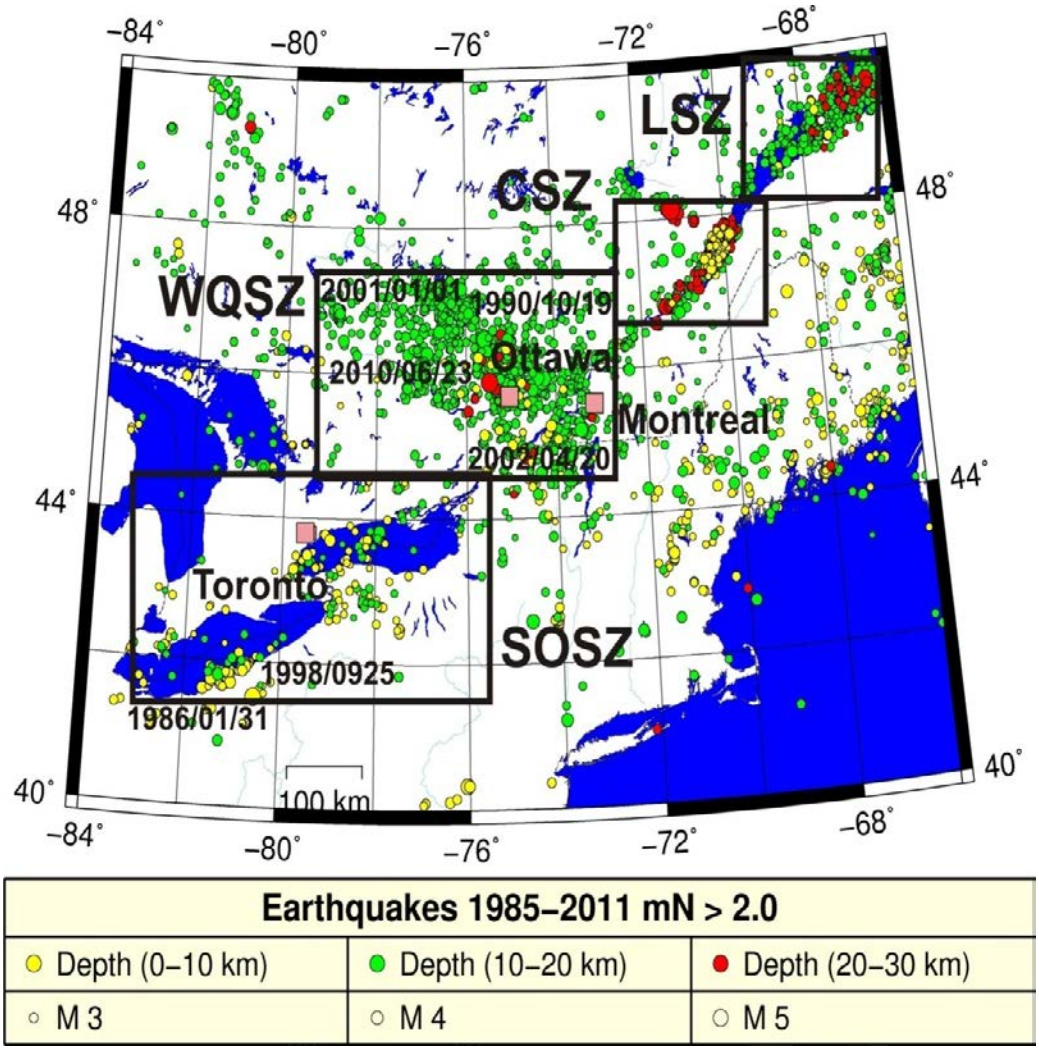

Figure 2.3: Seismicity in the study area; LSZ (Lower St. Lawrence Zone); CSZ (Charlevoix Seismic Zone); WQSZ (Western Quebec Seismic Zone); SOSZ (Southern Ontario Seismic Zone).

(Data is extracted from the Canadian National Earthquake Database (NEDB)-Earthquakes Canada, GSC, *Earthquake Search (On-line Bulletin)*, http://seismo.nrcan.gc.ca/stnsdata/nedb/bull_e.php, Nat. Res. Can., accessed June 2011).

This study focuses on the seismicity of the WQSZ and the SOSZ, but short descriptions of the tectonics and seismicity of the other two seismic zones (CSZ and LSZ) are also included.

2.3.1 The Western Quebec Seismic zone (WQSZ)

The Western Quebec Seismic Zone, which was first defined by Basham et al. (1979), is a 160 km wide zone extending 500 km from the Timiskaming region of Quebec (~47.5°N, 79°W) to the Adirondack Highlands of upstate New York (~43.5°N, 73.5°W) (Figure 2.3). This zone is situated over the Mesozoic track of the Great Meteor hotspot (Crough, 1981). Adams and Basham (1989) divided the WQSZ into two regions. The first region is along the Ottawa River from Timiskaming to Ottawa and the second region is parallel to the first from Montreal to Baskatong Reservoir, about 200 km north of Ottawa. Adams and Basham (1989) suggested that the seismicity of the first region could be associated with a zone of normal faulting along the Ottawa River, while the second region could be due to crustal fractures formed during the passage of North America over the hot spot between 140 and 120 million years ago (Crough, 1981).

Tectonic features in the WQSZ were formed over a long time interval, from 2.8 Ga within the Superior Province (Laurentian craton) to 115 Ma intrusions along the track of the Great Meteor hotspot. The major orogenic belt of the Mesoproterozoic Grenville orogeny (1.2-1.0 Ga) transects this region (Faill, 1997). The Grenville orogen comprises the youngest rocks of the Canadian Shield and extends beneath Phanerozoic sedimentary rocks (Figure 2.1). The similarity between the tectonic setting of the Grenville orogen and the modern Alpine-Himalayan orogen suggests that they both formed as a consequence of

broadly similar continent-continent collisional processes (Carr et al. 2000). The thickness of the crust within the Grenville province varies between 30 and 48 km, with generally thinner crust in the vicinity of the WQSZ (Eaton et al. 2006).

The Great Meteor Hotspot track, with its SE-NW direction, crosses the whole WQSZ (Crough, 1981; Morgan, 1983; Sleep, 1990; McHone, 1996). Igneous crystallization ages increase monotonically from southeast to northwest (Heaman and Kjaarsgaard, 2000). Surface features such as small-volume kimberlite eruptions can also be attributed to the hotspot (Heaman and Kjaarsgaard, 2000). Other surface features like intermediate-volume alkaline magmas that occur near the edge of the craton and within the Appalachian orogen, could be related to the hotspot (Zartman, 1977; Eby, 1984). This change in the inferred near-surface expression of the hotspot proposes an evolution from kimberlitic melts to more voluminous crustal magmatism, as the inferred hotspot interacted with a progressively thinner lithosphere due to the motion of the overriding plate (Ma, 2009).

Sykes (1980) and Ma and Atkinson (2006) suggested that the regional seismicity in the WQSZ might be localized along the hotspot track. Many large historical events occurred along this trend in the Boston region, including the 1755 Cape Ann M 6.2 earthquake (Ebel, 2002), the 1727 M 7 (Ebel et al., 2000), and 1638 M 6.5 (Ebel, 1998). Ma and Atkinson (2006) proposed that the hot spot track exerts control on the location of seismicity, either by thermal rejuvenation of antecedent faults, or by stress concentration due to a predicted large strength contrast between mafic and felsic rock in the middle crust, similar to the events in Georgian Bay (Dineva et al., 2007).

The WQSZ is known as the second most active seismic zone in eastern Canada (Figure 2.4). Recent studies have suggested that larger historic earthquakes with magnitudes around 7 may have happened between 4550 and 7060 years B.P. (Aylsworth et al. 2000). In 1732 an earthquake with an estimated magnitude of 5.8 occurred near Montreal, causing significant damage to houses and properties. Many people were also injured with one possible death (Smith., 1962). In 1935 the area of Timiskaming, in the most northern part of the seismic zone, was shaken by an earthquake with a magnitude of 6.2 (Basham et al., 1989). In 1944, an earthquake with a magnitude of 5.6 caused significant damage to the area of Cornwall-Massena (Hodgson, 1945). Inversion of regional waveform recordings performed by Bent (1996a) showed that this earthquake occurred in the mid-crust at a depth of about 20 km with an oblique thrust mechanism, similar to the mechanism for other events in the WQSZ and consistent with the regional stress field. The area is also occasionally shaken by moderate earthquakes. Between 1980 and 2000, 16 earthquakes were recorded with a magnitude of around 4.0 m_N. Recently, in January 2000, an earthquake with a magnitude of 5.2 m_N occurred in Kipawa, close to the epicentre of the 1935 event, which was felt up to 500 km away (Bent et al. 2002). In April 2002, an event with a moment magnitude of 5.5 M_W occurred in the Adirondack Mountains in New York State (Seeber et al. 2002). On June 23, 2010 an earthquake with moment magnitude M_W 5.0 hit Val-des-Bois, Quebec, with ground shaking felt over a large area of eastern Canada and northeast United States.

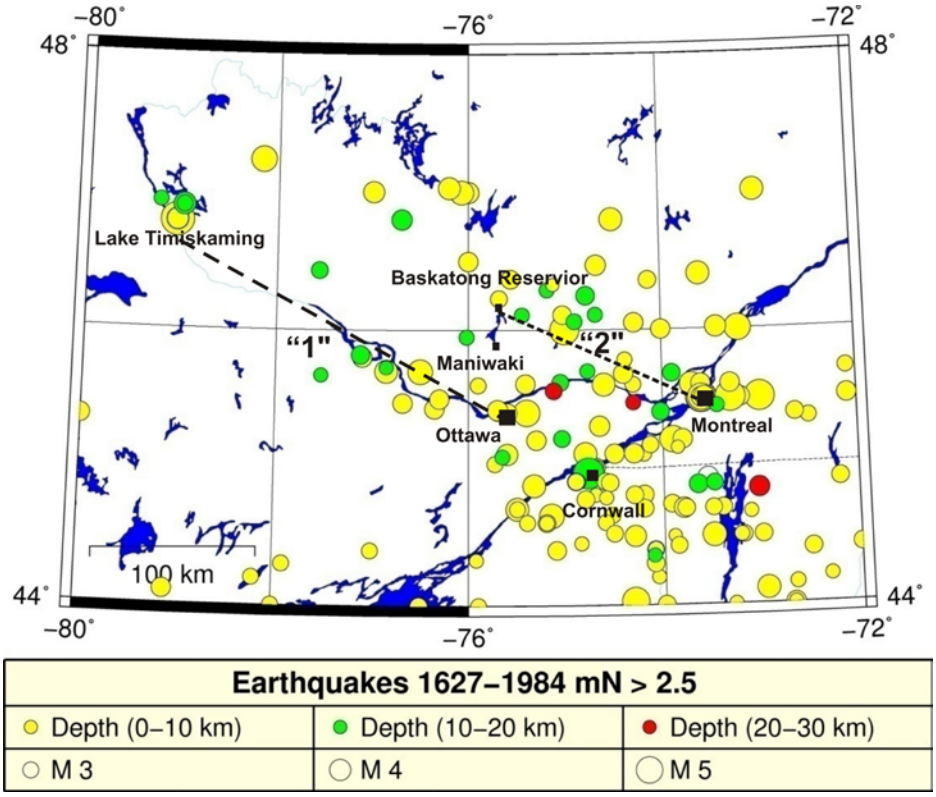

Figure 2.4: Historical earthquakes in Western Quebec Seismic Zone (1627-1984)

(Data is extracted from the Canadian National Earthquake Database (NEDB)- Earthquakes Canada, GSC, *Earthquake Search (On-line Bulletin)*, http://seismo.nrcan.gc.ca/stnsdata/nedb/bull_e.php, Nat. Res. Can., accessed June 2011).

Seismic activity within the WQSZ contributes significantly to the seismic hazard in the south eastern Canadian cities of Ottawa and Montreal (Adams and Halchuk, 2003). The pattern of historical seismic activity shows that the earthquake concentration is mainly focused along the Ottawa River and in the Montreal-Maniwaki region (Figure 2.4).

Previous studies have suggested that earthquakes along the southwestern margin of the WQSZ zone demonstrate a reverse-sense reactivation of Paleozoic normal faults within the Ottawa-Bonnechere Graben (e.g., Kay, 1942; Adams and Basham, 1991; Bent et al. 2002). However, most earthquakes in the north-eastern part of the WQSZ have not shown any spatial relationships with the surface features of Grenvillian shear zones or any other rift-related faults (Forsyth, 1981; Adams and Basham, 1991). Previous authors have proposed hypotheses relating pre-existing tectonic structures, including Mesoproterozoic shear zones associated with the Grenville orogeny (Forsyth, 1981) and late Precambrian and early Palaeozoic normal faults associated with the Ottawa-Bonnechere Graben (Adams and Basham, 1991; Bent et al., 2002), to earthquake locations. However, the nature of seismicity in the WQSZ is not well understood mainly due to the lack of realistic models relating the earthquakes within the region to the main seismogenic structures of the WQSZ. One of the reasons for this is probably the large error in the routinely calculated epicentres (~ 0.03° average error for the latitude and longitude and a default depth of 18 km for most of the earthquakes in the GSC catalog). Some events in this zone have more accurate hypocentre locations but they do not cover the whole area nor long period of time.

2.3.2 The Charlevoix Seismic zone (CSZ)

The Charlevoix region, located in southern Quebec along the St. Lawrence River 150 km NE of Quebec City, is historically the most active earthquake zone in eastern Canada *(e.g.* Buchbinder et al. 1988) (Figure 2.3). This region has been monitored by a microseismic array since 1977, yielding accurate locations of earthquake hypocentres. Large historical

earthquakes have occurred within the St. Lawrence valley in the Charlevoix seismic zone northeast of Quebec City in 1663 (M~ 7; Basham et al. 1979), 1791 (M~ 6), 1860 (M~ 6), 1870 (M~ 6.5) and 1925 (M~ 6.2).

The Charlevoix seismic zone is structurally controlled by the Iapetan rift and a meteorite impact structure (Adams and Basham, 1991). Lamontagne et al. (2004) stated that this region was cut by faults created during four tectonic events: the Grenvillian collision (1100 to 900 Ma), the rifting episode related to the opening of the Iapetus ocean (700 Ma), the Taconian reactivation of these faults at the closing of the ocean, Mesozoic extension/rift related to Atlantic opening (450 Ma), and the meteorite impact (350 Ma). The CSZ contains part of a meteorite crater with a diameter of 54 km, consisting of a basin with a central uplift. This structure was identified as a meteorite crater in 1965 with the discovery of shatter cones. Lamontagne (1987) proposed that the meteor impact weakened the rift faults, although meteor impacts are not generally associated with high levels of seismicity (Solomon and Duxbury, 1987). Earthquakes in this zone are mainly thrust, or combination of thrust and strike-slip, events (Lamontagne, 1999) and the seismicity seems to be clustered along a segment of the St. Lawrence rift, which is overlapped by the meteorite impact crater (Baird et al., 2009). This localization can be explained by low-strength bounding faults and stress channelling between them (Baird et al., 2009).

2.3.3 The Lower St. Lawrence Seismic Zone (LSZ)

The LSZ is located at the estuary of the St. Lawrence River, between Baie-Comeau and Sept-Iles (Figure 2.3). This zone is known as the third most active seismic zone in

eastern Canada with earthquake frequency of about 50-100 events per year with magnitude predominantly less than 5 m_N. Lamontagne et al. (2003) proposed that most earthquakes in this zone occur beneath the St. Lawrence River at focal depths between about 7 and 25 km, well within the Precambrian shield. The trend of the normal faults in the LSZ zone seems to be east-west. Lamontagne et al. (2003) have also suggested that local faults in this zone could be weak due to crustal fluids at depth, probably under hydrostatic pressure, which leads to a lower internal friction.

2.3.4 Southern Ontario Seismic Zone

The Southern Ontario Seismic Zone includes Southern Ontario and the areas just south of Lake Erie and Lake Ontario. This is a zone with low to moderate earthquake activity. Moderate seismic events such as the 1986 Cleveland, Ohio earthquake with a magnitude of 5 m_N, the 1929 Attica earthquake with a magnitude of m_N 5.2, and the 1998 Pymatuning earthquake with a magnitude of m_N 5.4 (Armbruster et al., 1998) occurred in this zone (Figure 2.5). Strong seismic events with magnitudes above 6 have not been recorded or felt since 1800 (Stevens, 1994). On average, 2 to 3 per year earthquakes with magnitude 2.5 or larger have been recorded in this region from 1984 to 2011 (Natural Resources Canada).

The seismicity in this area is mainly associated with normal faults (Adams & Basham, 1991; Adams 1995). Excluding the Ottawa River area, seismicity focuses primarily in clusters south of Lake Erie and around western Lake Ontario. Some of the localized clusters include the western Lake Ontario Zone (Seeber and Armbruster, 1993), also named the Burlington-Niagara Falls cluster (Adams & Basham, 1991); the Attica

cluster, which is considered part of the western New York State Zone (Ebel and Kafka, 1991; Seeber and Armbruster, 1993); the Northeast Ohio Seismic Zone located south of Lake Erie on the Ohio-Pennsylvania border (Seeber and Armbuster, 1993); and the Niagara Seismic Zone (Seeber and Armbruster, 1993; Dineva et al, 2004).

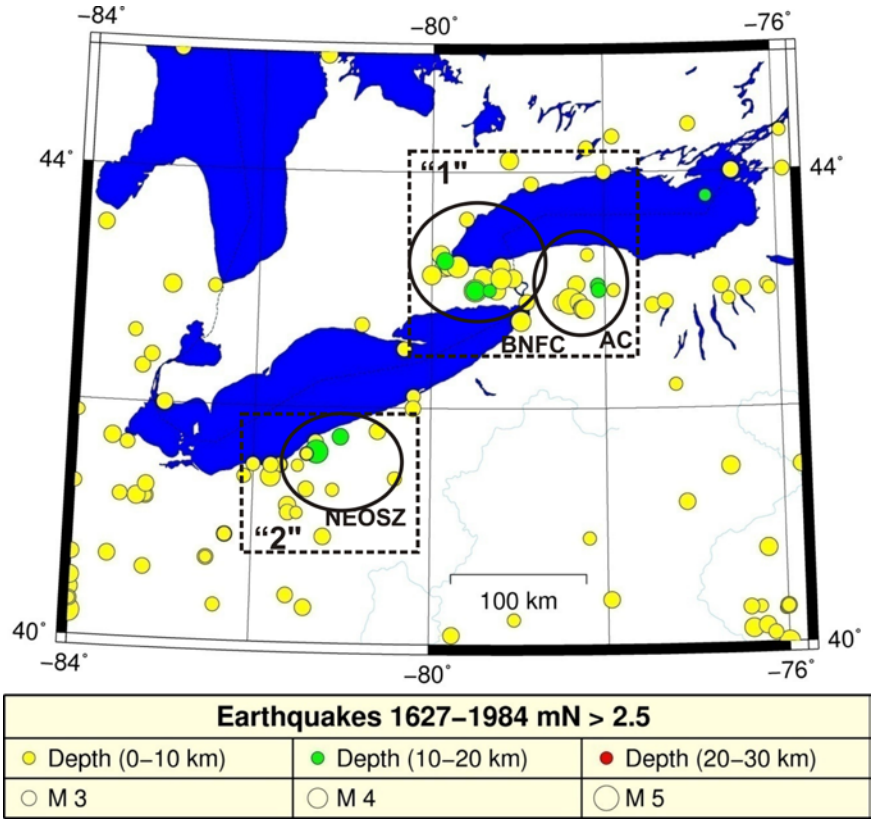

Figure 2.5: Historical seismicity in southern Ontario (1627-1984)

(Data is extracted from the Canadian National Earthquake Database (NEDB)- Earthquakes Canada, GSC, *Earthquake Search (On-line Bulletin)*, http://seismo.nrcan.gc.ca/stnsdata/nedb/bull_e.php, Nat. Res. Can., accessed June 2011).

Southern Ontario is structurally underlain by the northeast-striking, relatively shallow southeast-dipping thrust faults of the Grenville orogen (Easton, 1992). Many

researchers investigated the tectonic features of the Grenville orogen by deep seismic reflection imagery from seismic surveys (e.g., White et al., 2000; Forsyth et al., 1994a,b). White et al. (2000) proposed a seismic-based cross-section for the southwest Grenville Province. This section shows that domains within the lithotectonic settings are separated by a series of northwest-directed thrust sheets. Seismic sections proposed for the orogen beneath the Great Lakes by Forsyth et al., (1994a,b) and that proposed for areas farther east in Quebec by Martignole & Calvert (1996) demonstrate similar crustal features. Seismic reflection images of the GFtz, CMBbtz, and EFbz display shallow to moderate east-dipping reflections that continue to mid-crustal depths (12-20 km) (Green et al., 1988; Milkereit et al., 1992; White et al., 1994). Culotta et al. (1990) proposed that the boundary between the Elzevir and Frontenac terranes could be the eastern edge of the crustal block of west-dipping features that extends south-west to Alabama.

Southern Ontario has continuously experienced relatively small seismic events. Stevens (1994) described the seismicity of this region as “intermittent scattered activity” with no preferred trends. Other authors, however, suggested a link between seismic activity of this region and magnetic lineaments associated with basement shear zones (e.g., Thomas et al., 1993; Mohajer, 1993; Wallach et al., 1998). Some authors have also made a connection between basement features and current seismicity (Mohajer, 1993; Seeber & Armbruster, 1993; Wallach et al., 1998; Boyce & Morris, 2002). However these studies have been primarily qualitative in nature. Godin et al., (2002) proposed a glaciotectonic origin for most of the deformation features observed in the Rouge River valley in the region of Toronto. Mereu et al. (2002) summarized the existing publications on seismicity and revised the hypocentre locations in the region for the period 1990 –

2001. All events seemed to occur in the upper part of the crust at depths less than 18 km, and most events occurred at depths less than 10 km. The epicentres of studied events are concentrated beneath Lake Ontario and south of Lake Erie and exhibit statistically significant clustering and a northeast alignment. Dineva et al. (2004) recognized five distinct clusters, four around the western Lake Ontario-Niagara Falls area and one on the Ohio-Pennsylvania border near Lake Erie. The inferred spatial correlations between modern seismicity and magnetic anomalies and the proximity of seismicity to the Great Lakes suggested that seismicity in the region tends to be localized mostly in areas where pre-existing tectonic structures are favourably oriented with respect to the present-day stress field.

2.4. Focal Mechanism and Tectonic Stress

Evaluation of focal mechanisms for several seismic events in eastern Canada demonstrates a change from a strike-slip regime in the central eastern United States to a thrust regime in the southeastern Canada-U.S. border region (e.g. Zoback, 1992b; Du et al., 2003; Baird et al. 2009). The earthquake hypocentres were also shown to be deeper on the Canadian side (5–28 km) versus much shallower depths (2–8 km) on the U.S. side (Du et al., 2003). This transition seems to occur near the former margin of the Laurentide ice sheet (Stewart et al., 2000). Adams and Basham, (1989) thus suggested that the seismicity in this region may be partially a result of stress perturbations induced by postglacial rebound.

Stress data for intraplate North America up to 2008 are well summarized by Heidbach, et al., (2008). They proposed a *S*Hmax (maximum horizontal stress component) orientation throughout the region, varying between northeast and east and averaging east-northeast. Analysis of the stress field in southern Ontario shows a misalignment between the direction of tectonic loading and the orientation of the major horizontal principal stress. This could be due to the fault slip which rotates the stress field toward the strike of the faults (Baird and McKinnon, 2007).

This study aims to further investigate the seismicity of southern Ontario and western Quebec through detailed studies of earthquakes with magnitudes over 3.5 that occurred from 1993-2010 within the region, and to do a thorough comparison of hypocentre locations and focal mechanisms with seismogenic structures and geological data.

CHAPTER 3

DATA SET AND METHODS

3.1 Introduction

This chapter describes the methodology of earthquake parameter estimation in western Quebec and southern Ontario. The hypocentre location, origin time, focal depth and focal mechanism solutions were obtained for more than 50 earthquakes with magnitude m_N > 3.5 from 1992 to 2010 in the Western Quebec (WQSZ) and Southern Ontario (SOSZ) seismic zones, covering an area within latitudes from 40.5°N to 48°N and longitudes from 81.5°W to 71.5°W.

3.2 Data

Since the installation of the Southern Ontario Seismic Network (SOSN, Mereu et al., 2002) in 1991, the density of the existing permanent stations of the Canadian National Seismic Network (CNSN) has been increased. Since 2001, both southern Ontario and part of western Quebec are covered by more than 30 Portable Observatories for Lithospheric Analysis and Research Investigating Seismicity (POLARIS; Eaton et al., 2005) stations

(partially updated SOSN stations). POLARIS is a Canadian geophysical research consortium focused on investigation of structure and dynamics of the Earth's lithosphere and the prediction of earthquake ground motion. The seismic instrumentation of the dense POLARIS Ontario array in Southern Ontario is complimented by a broadly spaced array covering the rest of the province, funded by the Federal Economic Development Initiative for Northern Ontario (FedNor) (Eaton et al., 2005).

In this thesis the data from the Canadian National Seismic Network (CNSN) and from a few seismic networks in the Unites States are added to the data from SOSN/POLARIS stations. Figure 3.1 shows the distribution of the POLARIS stations, the FedNor stations, the CNSN stations, and the US seismic stations in the study area. Seismometers broad-band and short-period have been used at all stations. The CNSN stations are equipped with both types with corresponding sample rates of 40 samples per second (sps) and 100 sps. POLARIS and FedNor have broad-band stations with sample rate of 100 sps. The older SOSN stations have short-period instruments with sample rate of 100 sps. The US stations contain mixed broad-band and short-period stations with sample rates of 50 sps and 100 sps.

For the period between 1992 and 2010, 145 different stations recorded 53 earthquakes with magnitude (m_N) larger than 3.5 (Appendix C).

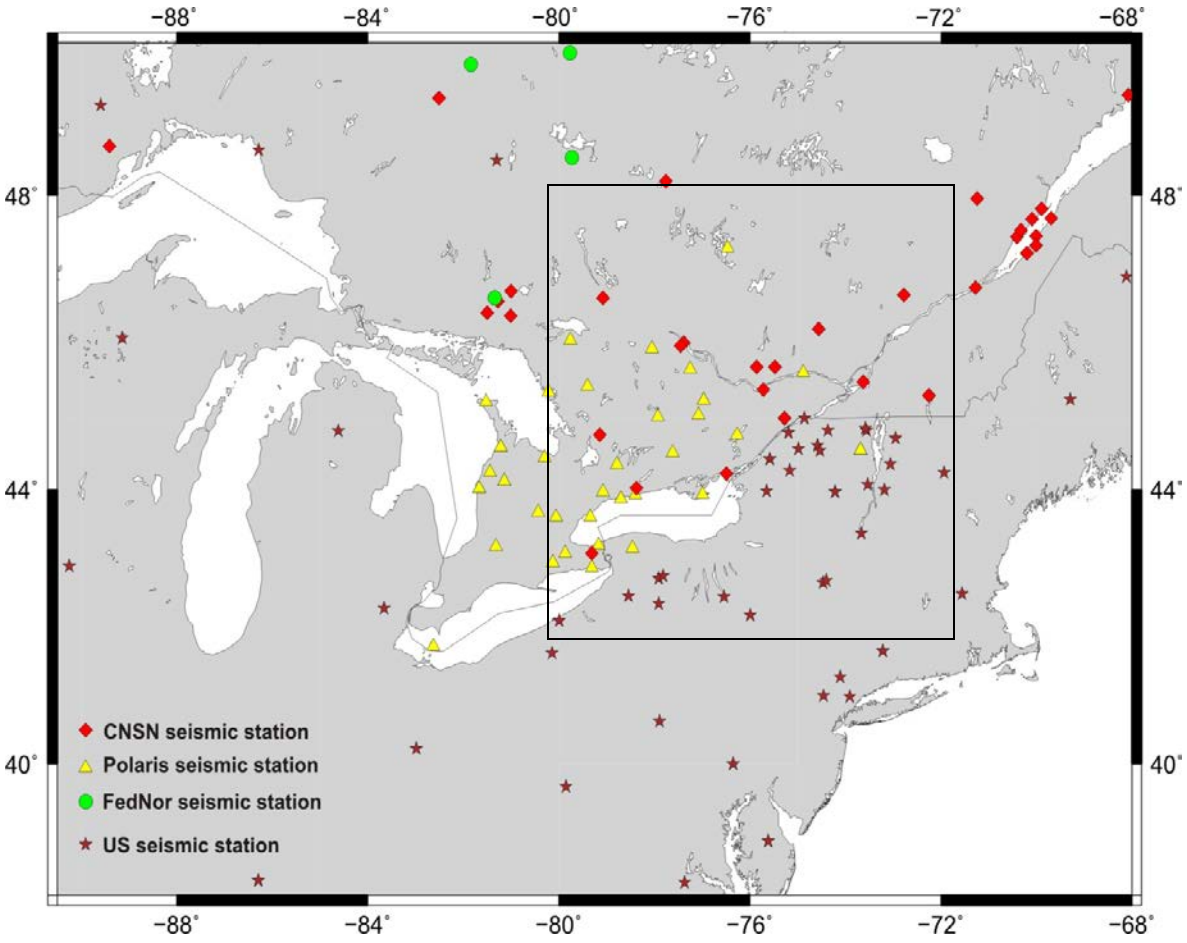

Fig. 3.1: Locations of seismic stations used in this study. Seismic networks: Canadian National Seismic Network (CNSN), SOSN/POLARIS, FedNor, and US stations (different networks). The rectangular area shows the boundary of the study area.

Only the events that were recorded by a minimum of ten stations were studied, reducing the number of the studied events to 50. Five events were recorded by more than 90 stations. The majority of the events were recorded by 30 to 40 stations, especially the events that occurred after 2002 (after the installation of the POLARIS seismic stations) (Figure 3.2). The list of the studied events was compiled from the Canadian National Earthquake Database (http://earthquakescanada.nrcan.gc.ca/stndon/NEDB-BNDS/index-

eng.php). All of the studied events have magnitudes between m_N 3.5 and 5.5. The strongest event was the m_N 5.7 10 km SE from Val-des-Bois (23th of Jun 2010). Most of the events (about 30 of them) have magnitudes of m_N ~4.

Digital waveforms were extracted from all possible Canadian seismic stations at distances up to 1000 km using the AutoDRM service of Geological Survey of Canada (GSC) (http://earthquakescanada.nrcan.gc.ca/stndon/AutoDRM/index-eng.php). This includes the CNSN, POLARIS, and FedNor stations. Data from the US stations were extracted using the BREQ_FAST service of the Incorporated Research Institution for Seismology database (IRIS) (http://www.iris.edu/manuals/breq_fast.htm#4). All extracted waveforms started around 2 minutes before the origin time and were 600 sec long. Data was extracted from both short-period and broad-band instruments. Arrival time data for all studied events were provided by Geological Survey of Canada.

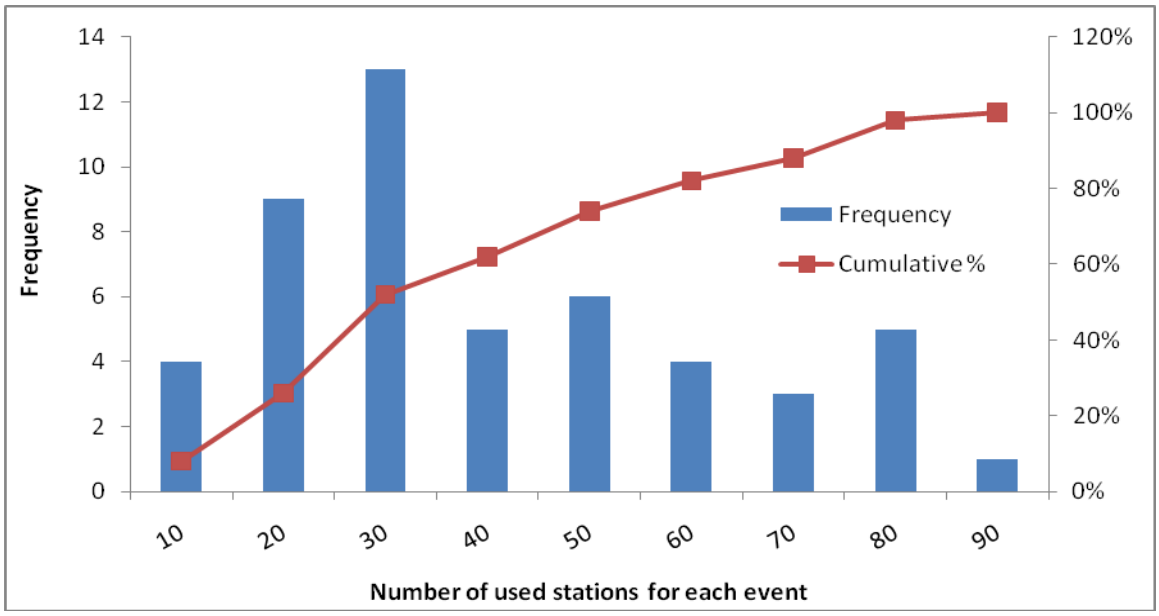

Figure 3.2: Number of stations used versus frequency of the events and their cumulative number.

Figure 3.3 shows the map distribution of the studied events (*N*=50) from 1992 to 2010. The events are not uniformly distributed, but instead appear to be concentrated in several discrete areas. Among the 50 events studied here only 12 events (m>3.5) occurred in southern Ontario, and 38 of them occurred in western Quebec. Most of the earthquakes in western Quebec are concentrated along the Ottawa River and Montreal-Maniwaki region with a strong NNW-NW trend, transverse to the Appalachians and the St. Lawrence River valley. There is no obvious concentration of earthquake epicentres in the northwestern part of the western Quebec (Figure 3.3). A similar relative absence of earthquakes is also present in the historical data (Chapter 2, Figure 2.3). In southern Ontario the earthquakes are concentrated either south of Lake Erie or in western Lake Ontario and there is only one event in Georgian Bay (Figure 3.3).

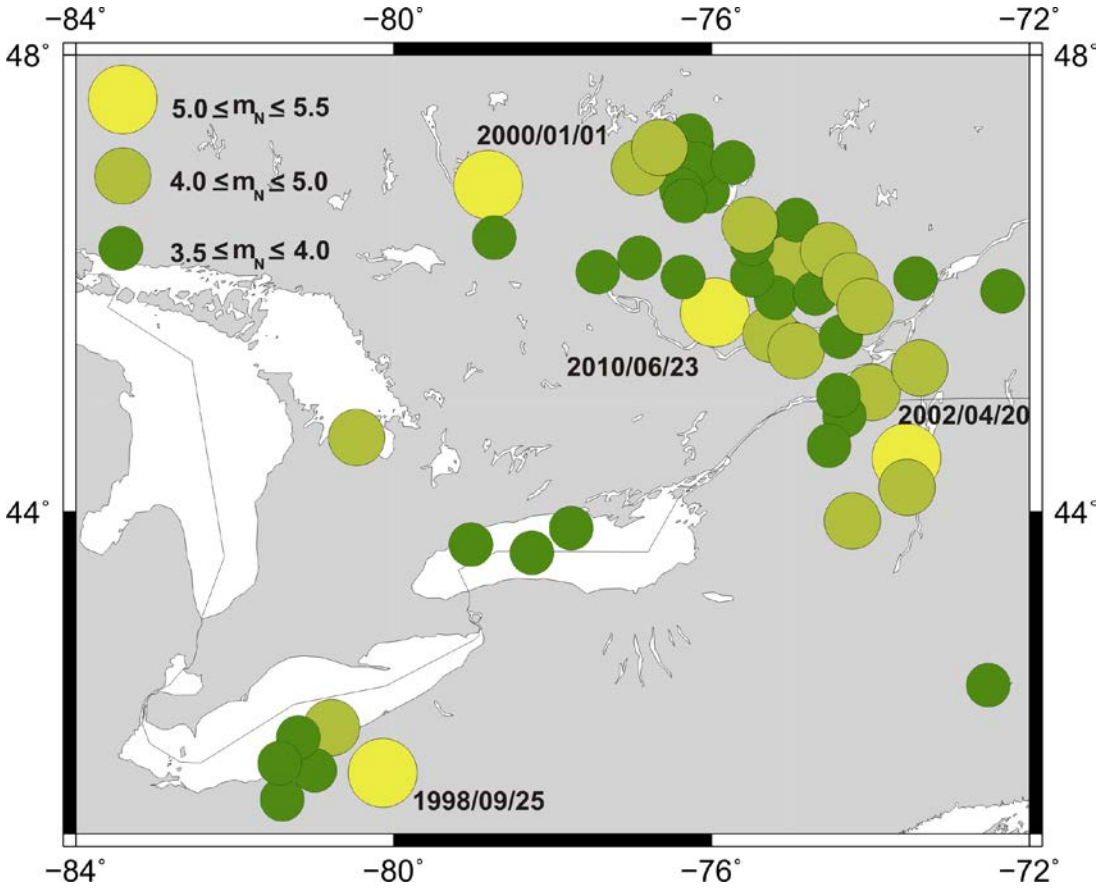

Fig. 3.3: Epicentres of earthquakes studied (m_N >3.5) in Western Quebec Seismic Zone (WQSZ) and Southern Ontario Seismic Zone (SOSZ) for the period 1992-2010. The largest studied earthquakes ($m_N \geq 5$) are labelled with the date when they occurred.

The magnitude distribution of the events is shown in Figure 3.4. Out of 50 events in the study area, 4 events had magnitude m_N over 5, 15 had magnitude m_N between 4-5, and 31 events had magnitude m_N between 3.5 – 4.0. The largest magnitude for events in the SOSZ is the m_N 5.4 1998 earthquake near Ohio-Pennsylvania border (4.5 M_W, Maceira et al., 2000). The 5.7m_N (5.0 M_W) June 23, 2010 Val-des-Bois earthquake was

the strongest recorded event in the WQSZ (m_N is the Nuttli Sg/Lg-wave magnitude - Nuttli, 1973 modified by Wetmiller and Drysdale, 1982 and M_W is the moment magnitude – Hanks and Kanamori, 1979).

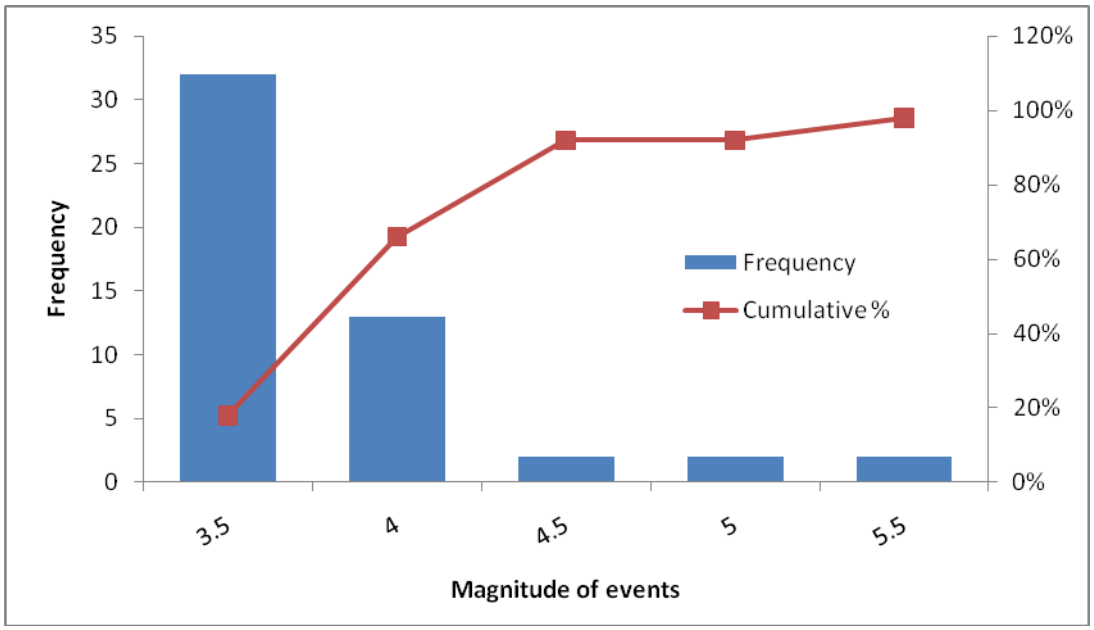

Figure 3.4: Magnitude m_N distribution of the studied events and their cumulative number.

3.3 Data Processing

3.3.1 Earthquake Source Parameters

Figure 3.5 shows the definitions of the source parameters analysed. The Hypocentre is the point of the actual focus where the fault movement starts. The epicentre is the point on the earth surface directly above the focus/hypocentre and is the location normally shown on the maps. The earthquake focal mechanism, also known as fault plane solution,

provides constraints on the possible fault geometry, which can be compared with known geological structures. One plane of focal plane solution represents the fault plane and contains the slip vector $\hat{d}$, while the other plane, known as the auxiliary plane, is oriented normal to the slip vector $\hat{d}$. Figure 3.5 also shows the dip (δ) and strike (ϕ_1) of the fault plane and the rake angle of the slip vector (λ), which are part of the parameters defined by the focal mechanism. The focal mechanism provides important information about the orientations of the tectonic strains in the source (Pressure P and Tension T axes). The T axis is at 45° to the compression quadrants (with positive polarity of the first P-wave arrival) and P axis is in the middle of the dilatation quadrants.

3.3.2 Methods and Data Analysis

Three different software packages were used to pick the arrival times of seismic waves and to calculate the earthquake source parameters (hypocentre locations and focal mechanisms). The PLTSEC program was used to analyse the waveforms and determine the arrival times and polarities for each seismic wave for each event (Mereu, 2003a, b). The HYPOCENTER program was used to calculate hypocentre locations using the arrival times (Lienert and Havskov, 1995; Havskov and Ottemöller, 2003). The FOCMEC program was used to calculate the focal mechanism using the locations from HYPOCENTER and the defined polarities of the first (Pg or Pn) arrivals (Snoke et al., 1984).

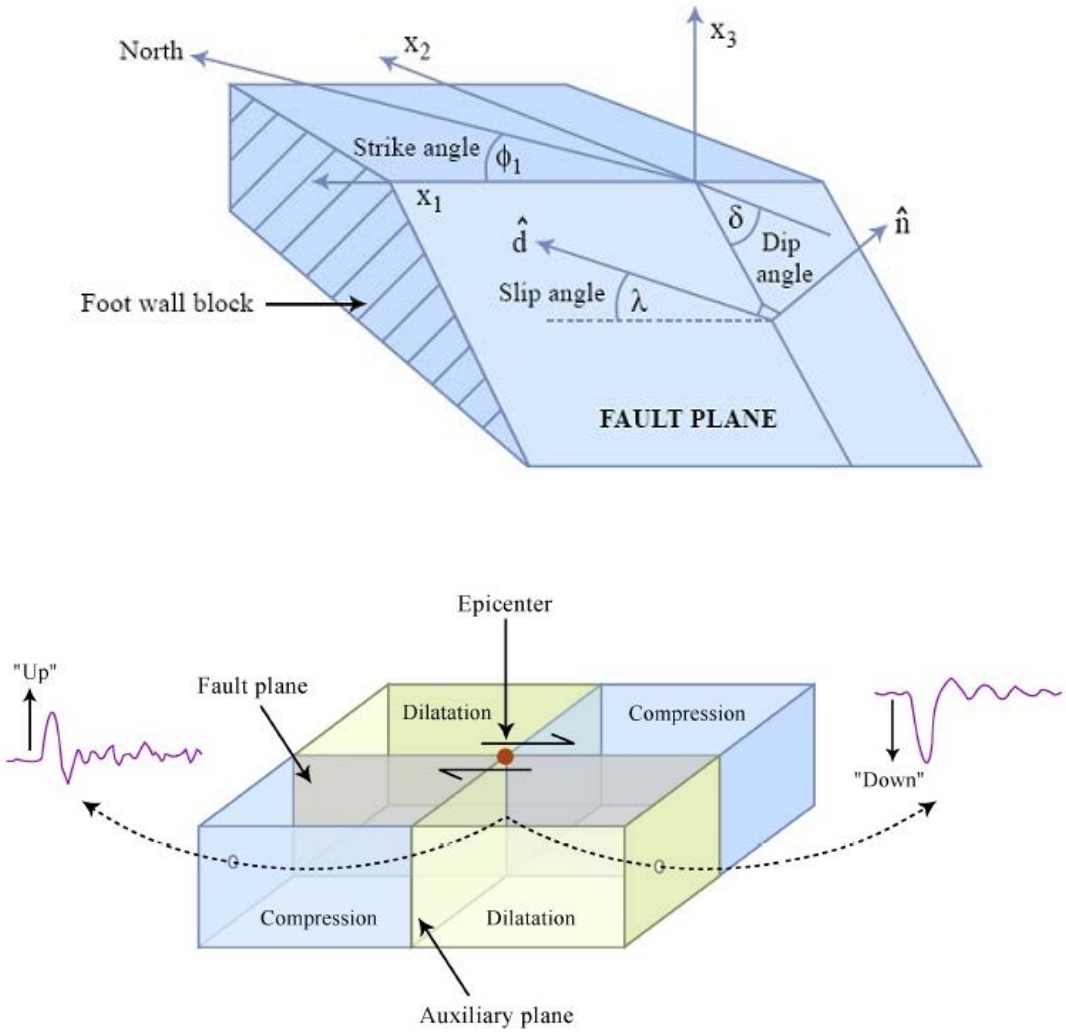

Figure 3.5: Earthquake source parameters determined in this study: ($\hat{d}$, slip vector; δ, dip; ϕ_1, strike; and λ, rake angle) adapted from Stein and Wysession, 2003.

3.3.3. Earthquake Waveform Analysis

PLTSEK program facilitates the display and analysis of earthquake data recorded by seismic stations (Mereu, 2003a,b). The program has an option to display the waveforms for analysis and manually pick the arrival times for different phases of the seismic

waveform (Pn, Pg, Sn, Sg, PmP, SmS, pPg, pPmP. sPg, sPmP, etc.) and polarity of first arrival times of P-waves and to manually assign weights for the picks. The waveform data in SEED format for each event were initially obtained with duration of 600 seconds and various sample rates (40, 50 or 100 samples-per-second (sps)). These files were converted into SAC files using rdseed program (IRIS) and subsequently to a special UWO format used in the PLTSEK program. Data were analysed using a sample rate of 50 sps. The two data sets for each event (one from the Canadian and one from the US stations) were combined to form one UWO file for each event. These files were then used in PLTSEK for visualization and analysis of the waveforms and for picking the arrival times (Pn, Pg, Sn, and Sg, etc.) and the polarities of P-waves (Pg, Pn).

The weights of the arrival times were assigned manually based on the quality of first arrival: sharp and clear or unclear. Numbers 0, 1, 2, 3, 4 (0 for best and 4 for poor arrivals) were assigned corresponding to the weighting scheme in the HYPOCENTER program. The accurate arrival time is important for finding the exact location of the event. The smallest uncertainties for P- and S arrival picks for all stations are 0.02 sec, but in many cases they are up to 0.06 sec because of the presence of noise. Usually the P-arrivals (Pg or Pn) can be picked with better accuracy than the subsequent arrival (Sn, Sg, etc.) because they have to be distinguished only from the background ambient noise. The secondary arrivals come at the coda of the P-waves and it is much more difficult to distinguish because of the presence of P-coda and lower signal to noise ratio. Figure 3.6 shows examples of the arrival time picks for P- and S-waves. On Figure 3.6a the signal to noise ratio is large and P_g and S_g are clear. In cases where the signal to noise ratio is small, picking the first arrival times is comparatively difficult (Fig. 3.6b, top left).

The amplitudes of the seismic waves decrease with distance. For the comparatively strong seismic events studied here (m_N > 3.5) it was possible to pick arrival times for stations at epicentral distances up to 900 km. An example of seismic records for one of the studied events aligned by the distance is shown in Figure 3.7.

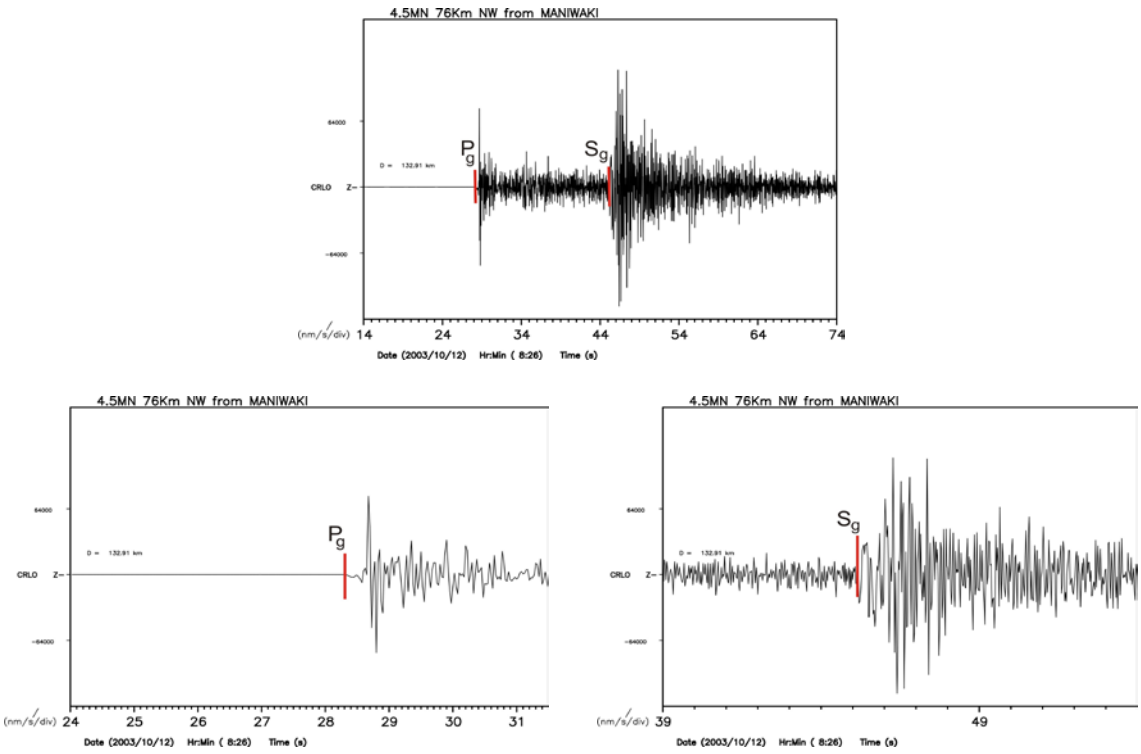

Figure 3.6a: Example of arrival times picking for Pg and Sg –waves for station CRLO at epicentral distance 133 km from m_N 4.5 earthquake NW from Maniwaki.

When possible, the polarity (compression or dilatation) of the first arrivals on the vertical component was defined. In some cases it was possible to define the polarities of both Pn and Pg waves on the same waveform (Figure 3.6). No filter was used when the polarities were picked to avoid distortion of the signal and change of the original polarity

(Figure 3.8). The polarities were assigned only if they were clear and there was no doubt about them.

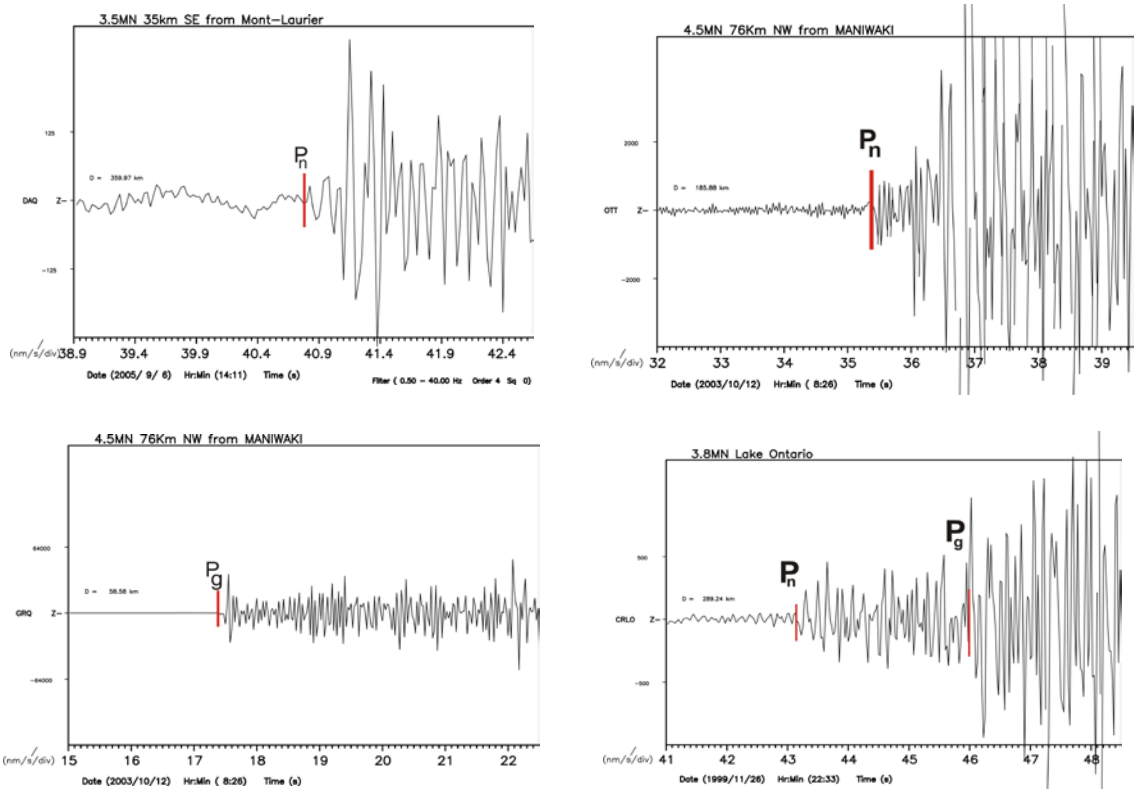

Figure 3.6b: Examples of arrival times picking for P (Pn, Pg) –waves for stations: DAQ (distance 359 km), OTT (186 km), and GRQ (58 km) with waveforms from m_N 4.5 earthquake NW from Maniwaki; station CRLO (289 km) with waveform from m_N 3.8 earthquake in Lake Ontario.

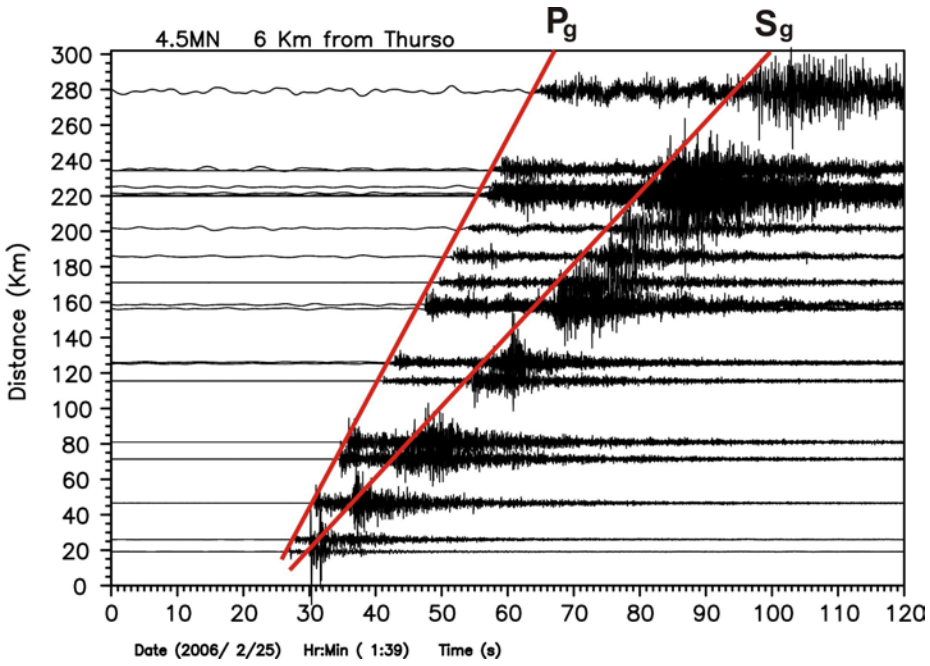

Figure 3.7: Vertical component waveforms of the earthquake on February 25, 2006 (m_N 4.5) recorded at epicentral distance up to 300 km. The approximate Pg- and Sg- arrivals are shown by red lines.

The arrival times of all possible phases (Pg, Pn, Sg, Sn) were picked on all stations up to 1000 km for all 50 studied earthquakes. The arrival times obtained from the Geological Survey of Canada were used as preliminary estimation of the arrival times. The output file from the PLTSEK program with the arrival times with their weights and the polarities of P-waves was a TPK file for each event. These files were converted to HYPOCENTER input file (NORDIC format) for hypocentre location.

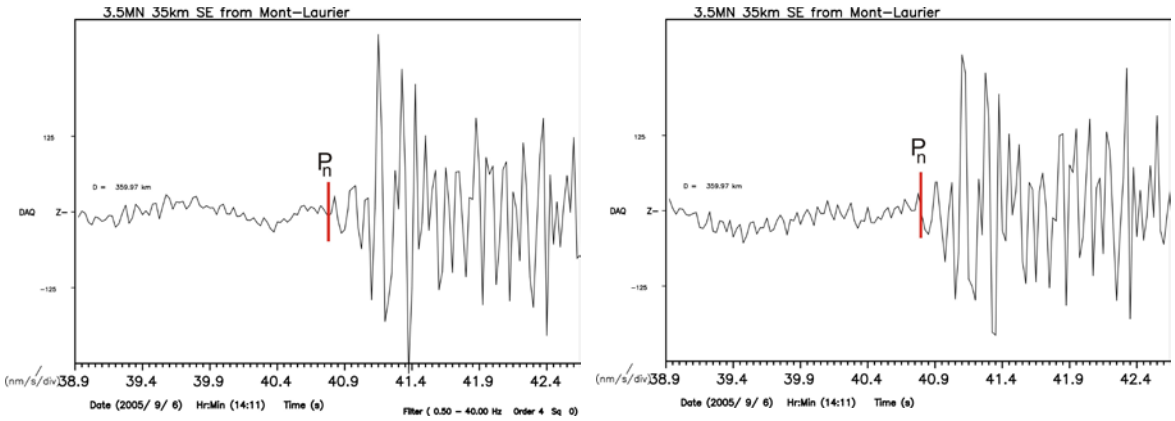

Figure 3.8: Effect of filter (band pass 0.5-40 Hz) on event waveform; with filter (left) and without filter (right).

3.3.4. Hypocentre Locations

The epicentre location and the focal depth are critical parameters for seismic hazard assessment, seismological research, and seismotectonic study. The accuracy of hypocentre location determination depends on several factors. These factors include the network geometry, available phases, accuracy of arrival-time, and knowledge of the crustal structure (Pavlis, 1986; Gomberg et al., 1990). The accurate reading of the arrival time, by itself, plays a critical role in estimating the hypocentre location. The methodology for the hypocentre location is also important. Different hypocentre location software can give slightly different results with different accuracy. The HYPOCENTER program used in this thesis proved to give stable results and to work well for local and regional earthquakes in Ontario and Quebec (Dineva et al., 2004; 2007).

HYPOCENTER program

The HYPOCENTER program (Lienert et al., 1986; Lienert and Havskov, 1995) was employed to determine hypocentre location and origin time of the earthquakes. The program calculates the location and origin time for a single event by tracing the rays through a given 1-D velocity (both direct and refracted waves) model and adjusting earthquake parameters using a conventional least-squares approach. There are two weighting options. The first weighting option is related to the accuracy of the arrival times. User specified weights (ω_i) are assigned by a single integer value in the range 0 to 4 for a given phase (the weights assigned manually in PLTSEK program). These numbers correspond to weighting factors of 1, 0.75, 0.5, 0.25 or 0.0 for that phase. The second option is a distance weighting given by the following relationship (Havskov and Ottemöller, 2003):

$$\omega_i = (xfar - D_i)(xfar - xnear) \quad (3.1)$$

The parameters *xnear* and *xfar* are read from the STATION0.HYP file, where xnear is the distance at which distance weighting starts and xfar is a distance at which distance weighting is zero, beyond xfar, the phase is not used, and D is the epicentral distance. (All distances are in km). The xnear and xfar in this study were 300km and 600 km, respectively.

The residual time is defined as the difference between the observed times t_i and predicted arrival times ($T_i(x,y,z) + t_0$) (Havskov and Ottemöller, 2003):

$$\Delta t = t_i - T_i(x,y,z) - t_0 \quad (3.2)$$

where $T_i(x,y,z)$ is the travel time from the source to the receiver (function of the coordinates) and t_0 is the origin time. The weighted residual is (Havskov and Ottemöller, 2003):

$$\tau_i = \omega_i \, (t_i - T_i(x,y,z) - t_0). \quad (3.3)$$

Here ω_i is the product of all weighting factors (the first and second weighting options combined). This program uses the least squares solution which minimizes the sum of the weighted squared residuals from n observation (Havskov and Ottemöller, 2003):

$$e = \sum_i \tau_i^2 \quad (3.4)$$

The root mean squared residual RMS for the hypocentre solution is defined as (Havskov and Ottemöller, 2003):

$$RMS = \sqrt{e/n} \, . \quad (3.5)$$

The standard error in the hypocentre location in a horizontal plane ERH (in km) $\sqrt{SDX^2 + SDY^2}$, where SDX and SDY are the standard errors in latitude and longitude. ERZ defines the standard error in the focal depth (in km).

The method uses both direct and refracted waves. The arrival times are weighted according to their accuracy and additionally by the epicentral distance and the time residuals. For the cases in which only P or S was given (no indication of the type of the

wave – e.g. Pg or Pn, Sg or Sn), the fastest (first possible) phase is assigned by the program.

Phase arrival times, station co-ordinates and a crustal velocity model are required as input data. HYPOCENTER reads the arrival time information from a Nordic format input phase file, and the station and velocity information from the station input file STATION0.HYP .

The program has a set of TEST parameters that define different options for the hypocentre location (included in STATION0.HYP). For this study only a few of these parameters were used:

TEST (31) = Max degrees of freedom for determining origin time and hypocentre: 3

TEST (57) = Distance to calculate travel times: 1000 km (max)

TEST (66) = Print out of travel time calculation errors: 1.0

TEST (70) = Maximum depth that the hypocentre is allowed to move to: 30 km

TEST (72) = Auto phase identification for distant events: 1.0 (yes)

TEST (74) = Print input phase data in print.out: 1.0 (yes)

TEST (88) = RMS residual (sec) at which residual weighting is applied for distant events

The output from the program is in three different files: *hyp.out, print.out*, and hypsum.out. The '*hyp.out'* file contains the arrival times used for the hypocentre location, the hypocentre locations with the location errors, and the time residuals for each arrival. The main output file '*print.out'* shows the TEST parameters and contains more detailed information showing not only the arrival times and the final locations with their errors but

also how the hypocentre location is obtained (the RMS for each of the iteration steps), the reliability of the depth estimation, number of phases, the number of degrees of freedom in the spatial solution (maximum 3), rms damping, the resolution matrix and summary of the average station residuals for all hypocentre locations. The file *hypsum.out* is a summary file only with the locations and their errors. An example of the input and output files is given in Appendix A.

3.3.5. Crustal Model

A crustal velocity model is required for obtaining the hypocentre location and ultimately the focal mechanism. Winardhi and Mereu (1997) proposed a 1D gradient velocity model for almost the same area as the present study area based on data from crustal refraction experiments across pre-Grenvillian Laurentia and its margin (Lithoprobe project) (Figure 3.9a). The data contained over 10,000 *Pg* observations. Winardhi and Mereu (1997) used seismic refraction tomography to image the overall seismic velocity combined with delay-time analysis of the Pg waves. A study of wide-angle reflected waves from the Moho (PmP) provided constraints on the crustal thickness and the nature of the crust. The Moho was shown as a well-defined sharp discontinuity beneath the Central Gneiss belt of the Grenville orogen. The velocity model includes a 40-km-thick crust with a linear velocity gradient where the velocity of P-waves *Vp* varies from 6.21 km/sec at the surface to 7.0 km/sec at Moho. The layer density varies from 2.65 to 2.70 Mg/m3 and the velocity of P- and S-waves have a ratio *Vp/Vs* of 1.73. *Vp* and *Vs* for the upper mantle are 8.1 km/sec and 4.52 km/sec, respectively. The density of the upper mantle layers is considered to be 3.4 Mg/m3 in this model. Figure 3.9b shows the approximation of this

model for P-wave velocity with multiple layers and some possible variations, since the HYPOCENTER program works only with layered models and not gradient models (Dineva et al., 2004). The crustal thickness of 40 km represents a good average for the whole region (Eaton et al., 2006). It was shown that this model gives very good results for the hypocentre locations in Ontario and Western Quebec (Dineva et al., 2004).

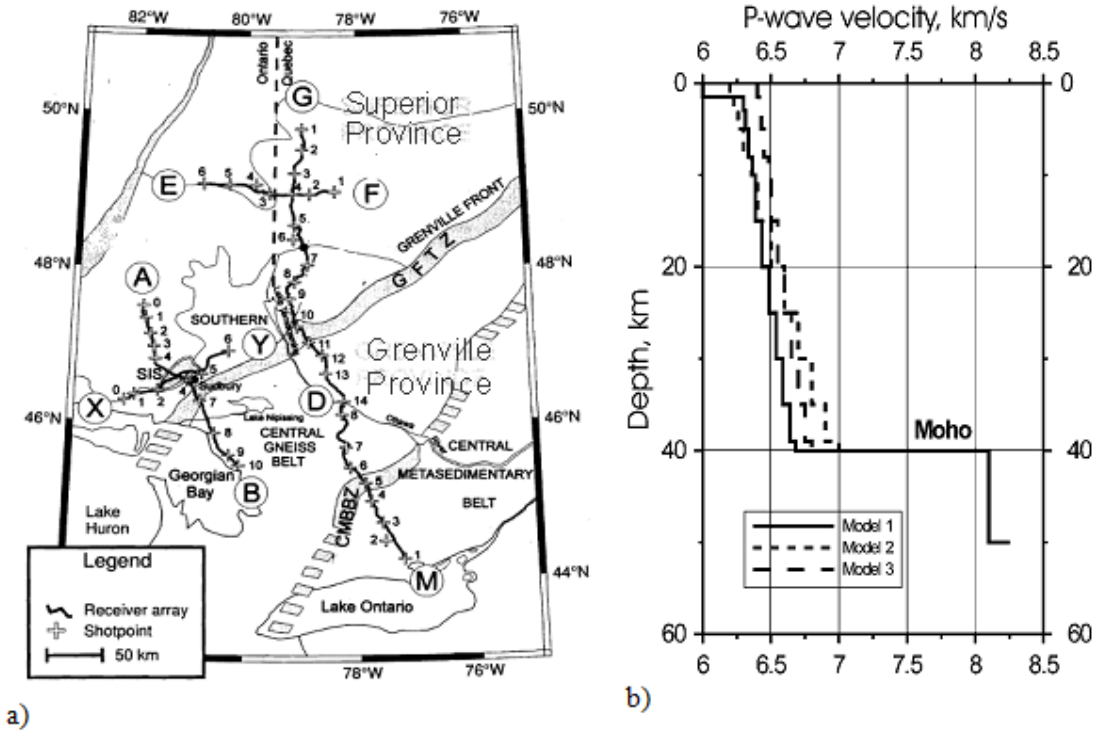

Figure 3.9: a) Shot points and seismic lines in the study area (Location of the 1992 Lithoprobe Abitibi-Grenville seismic refraction survey, with simplified regional geology. CMBBZ, Central Metasedimentary Belt Boundary Zone; GFTZ, Grenville Front Tectonic Zone (Winardhi and Mereu 1997), and b) P-wave gradient model adapted from Dineva et al., (2004).

3.3.6. Focal Mechanisms

The focal mechanism can be obtained manually or by using software. Data used for the focal mechanism can be the polarities of the P-waves or the amplitude information for P- and S-waves. An important feature of this kind of software is an output not only as a single solution but as a set of all possible solutions for a specific confidence level. The FOCMEC program uses both the polarities and the amplitude ratios, and gives a set of possible solutions.

FOCMEC program

FOCMEC (Snoke et al., 1984) was used to evaluate the focal mechanism for each earthquake. The program uses the distances, azimuths, and the take-off angles from the HYPOCENTRE output. FOCMEC produces four output files: 1) 'focmec.dat' contains the input parameters for FOCMEC, 2) 'focmec.lst' shows the input data and all details of all possible solutions (dip, strike, and rake of the nodal planes, trend and plunge of P, T, and B axes, total number of polarities and the stations with wrong polarities); 3) 'focmec.out' contains only the strike, dip and rake for one of the nodal planes for all solutions with the number of wrong polarities and grid step in degrees; 4) 'focmec.eps' is a Postscript plot file of the latest plot. An example of the output files for one seismic event is given in Appendix B. The program uses grid-search algorithm over the entire focal sphere to define all possible solutions with option of misfit polarity. The minimum number of polarity errors and degree increment in the grid search can be entered manually. After several trials, the best solution of each event has been selected based on the minimum number of polarity misfit.

CHAPTER 4

RESULTS

In this chapter the earthquake source parameters obtained for Western Quebec and Southern Ontario seismic zones based on seismic data from 1992-2011 (Figure 4.1) are presented and discussed.

4.1. Hypocentre Location

The hypocentre locations, including the depth and origin time with their errors were calculated with the HYPOCENTER program for all studied events. The weighting for the hypocentre location distance was applied for distances > 300 km (*xnear* in eq. 4.1). The weight decreases linearly to zero between 300 km and 600 km (*xfar* in eq. 3.1). This distance range of the weighting was chosen after a test with different *xnear* and *xfar* distances (Table 4.1.). The final distance weighting (300 km – 600 km) was chosen because at this range there was an optimum trade-off between the total residual of all solutions, the average number of stations for good azimuthal coverage, the number of the events with solutions, and also the solution for the depth was stable. The hypocentres and

origin times of the remaining 52 events were calculated using the HYPOCENTER program (26 stations on average).

Table 4.1: Results from distance weighting tests.

Distance weighting range (km)	Total RMS for all events	Number of events with solutions	Average number of stations
150-350	33.97	48	18
200-350	35.40	48	17
250-350	35.42	48	19
300-500	42.56	50	25
300-600	44.50	52	26
350-550	44.30	51	26
350-650	49.84	50	25
400-550	45.76	50	26
400-600	46.10	50	26

The distribution of the RMS for all individual solutions is shown in Figure 4.1. The majority of the RMS is smaller than 0.60 s (60%) with an average value of 0.45 s for all events. The maximum RMS is 0.8 sec. The distribution of the azimuthal gaps is also shown on Figure 3.10. The minimum azimutal gap of the events is 56˚and the largest azimutal gap is 300˚ (only for two events). Around 60% of all events have azimuthal gaps of less than 180°. A smaller azimuthal gap would give better solution for the hypocentre location.

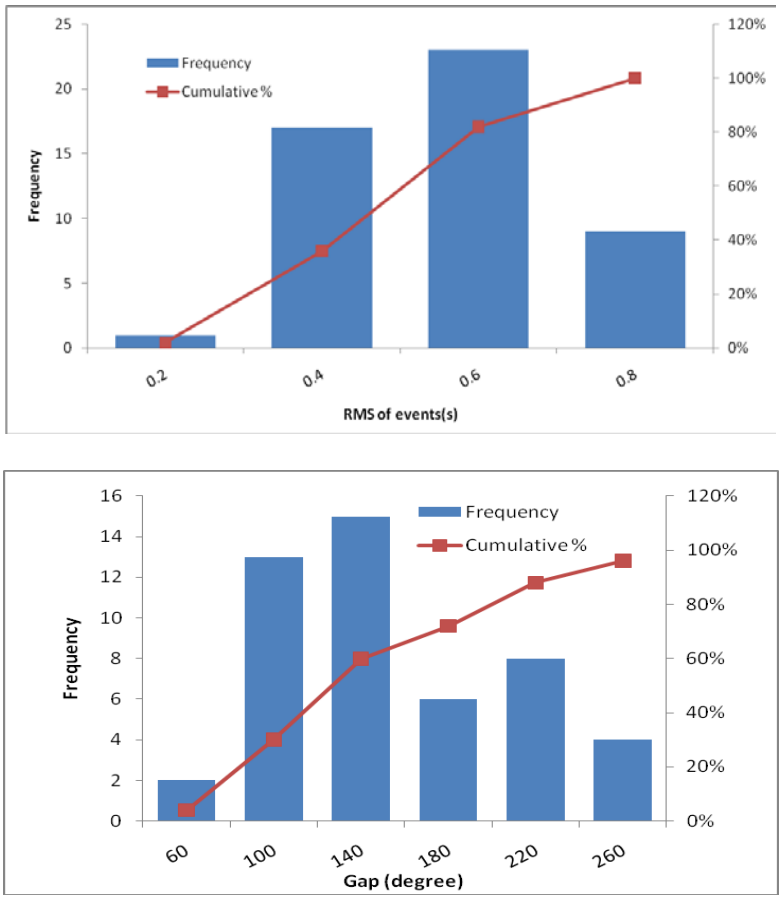

Figure 4.1: Distribution of RMS of the hypocentre solutions (top) and azimuthal gap distribution (down) for all 52 events in the study area.

The results from the hypocentre location with the estimated errors are presented in Table 4.2. Figure 4.2 shows histograms of the focal depth distribution of the events separately for southern Ontario and Western Quebec. As it can be seen, the main peaks of the two respective depth distributions differ. The maximum depth for southern Ontario is between 8 and 12 km, and for Western Quebec between 20 and 24 km. In average the focal depth of the Western Quebec events appears greater than that of the Southern Ontario seismic zone, which is consistent with previous studies (e.g., Ma and Atkinson, 2006). The median depth calculated by the HYPOCENTER program is 19.5 km for

western Quebec seismic zone and 8.2 km for the southern Ontario seismic zone. Focal depths higher than 18 km are observed for 24 events in the region, which reflects the depths for clusters of seismicity in the western Quebec (near the St. Lawrence River). Events with shallower depths are mainly located in Southern Ontario Seismic Zone.

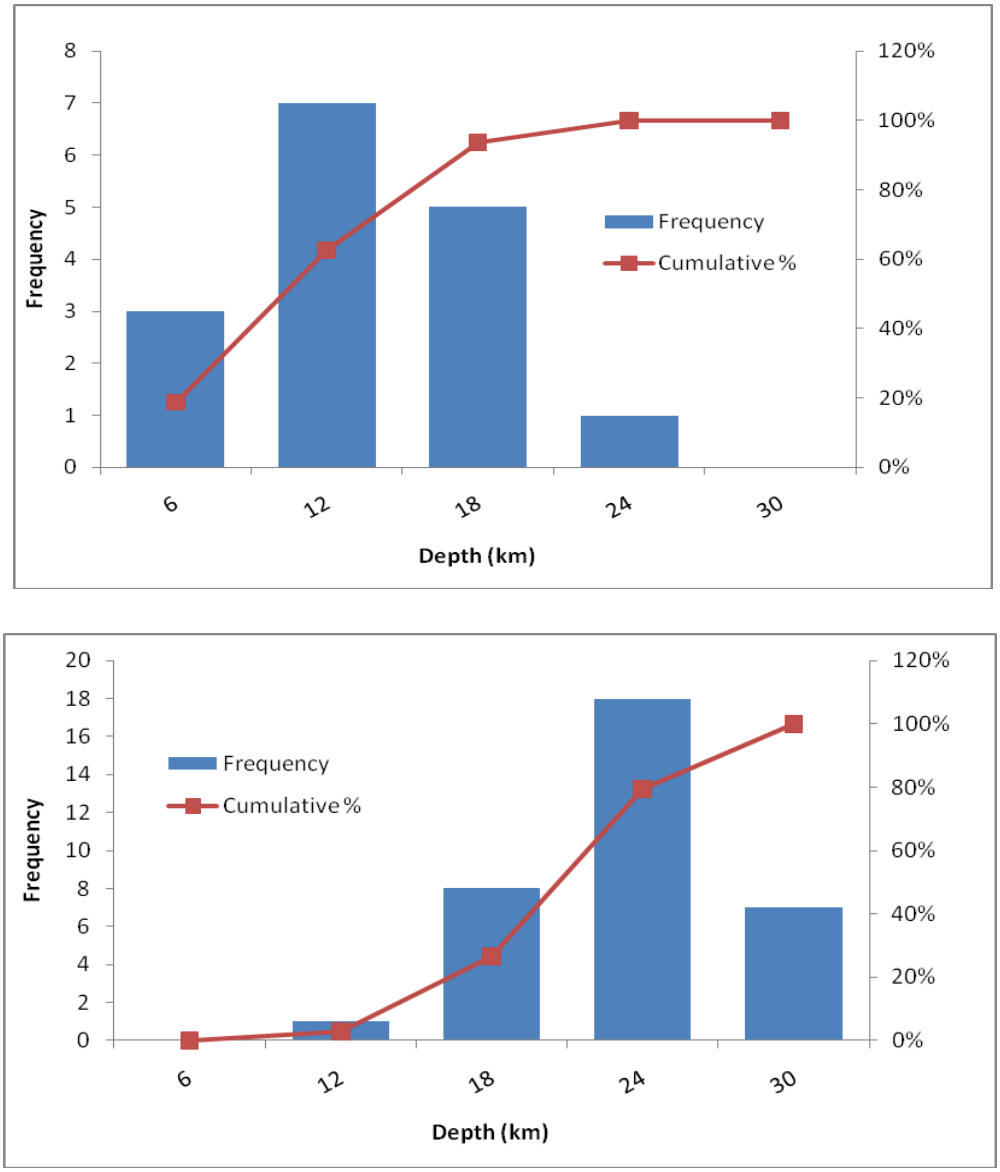

Figure 4.2: Distribution of focal depths for the events in a) Southern Ontario, and b) Western Quebec.

Table 4.2: Earthquake parameters (hypocentres and origin times) obtained in this study.

No.	Date	Error (s)	Lat (deg)	Error (km)	Long (deg)	Error (km)	Depth (km)	Error (km)	RMS	# Station	Az gap
1	16/11/1993	0.45	45.225	5.7	-73.474	3.9	19.4	6.9	0.35	11	177
2	25/12/1993	0.28	46.519	2.4	-75.515	2.8	19.2	5.6	0.18	13	158
3	02/10/1994	0.34	42.230	7.8	-72.300	6.3	10.0	0.0	0.66	10	243
4	15/02/1995	0.64	45.931	6.6	-75.095	4.2	18.3	8.2	0.74	16	143
5	03/06/1995	0.66	47.100	5.3	-76.220	5.3	18.0	0.0	0.40	10	181
6	16/06/1995	0.42	44.180	4.4	-71.570	3.9	15.0	3.0	0.53	19	217
7	12/09/1995	0.36	45.583	2.7	-74.427	1.7	23.4	5.3	0.35	18	128
8	10/10/1995	0.63	46.280	4.3	-78.480	6.2	30.0	7.0	0.60	11	151
9	14/03/1996	0.85	46.172	8.0	-74.508	6.6	30.0	8.4	0.36	24	112
10	03/04/1997	0.56	45.590	3.5	-72.220	5.5	17.0	9.0	0.44	12	123
11	24/05/1997	0.84	45.925	2.5	-74.232	2.7	22.2	4.5	0.56	39	78
12	26/02/1998	0.36	46.096	1.5	-76.367	1.6	15.2	6.6	0.45	24	90
13	18/04/1998	0.79	45.559	2.3	-74.997	2.9	21.5	4.8	0.30	30	101
14	30/07/1998	0.35	46.227	5.1	-74.690	4.1	10.0	5.0	0.30	10	214
15	25/09/1998	0.76	41.340	6.7	-80.143	13.4	5.0	0.0	0.76	20	246
16	25/12/1998	0.41	43.853	7.4	-77.820	4.5	15.0	8.0	0.59	17	247
17	18/06/1999	0.80	46.481	3.8	-75.149	3.9	27.5	6.0	0.74	24	119
18	26/11/1999	0.32	43.664	8.7	-78.980	6.4	10.0	5.0	0.42	16	292
19	01/01/2000	0.40	46.870	2.8	-78.887	2.7	14.6	2.9	0.43	21	132
20	20/04/2000	0.74	43.927	2.4	-74.264	3.1	12.2	4.1	0.51	32	79
21	06/08/2000	0.55	46.227	2.9	-75.008	3.0	25.1	4.7	0.48	24	120
22	06/10/2000	0.80	45.077	6.6	-73.986	4.4	20.1	6.0	0.27	26	184
23	26/01/2001	0.66	41.912	4.5	-80.867	8.2	5.0	3.0	0.74	25	194
24	19/03/2001	0.45	47.084	3.5	-76.249	2.2	20.5	5.3	0.51	34	132
25	11/04/2001	0.79	47.108	6.1	-76.103	5.1	19.4	7.1	0.25	26	121
26	24/12/2001	0.56	46.905	5.2	-76.488	3.3	19.4	6.3	0.45	14	181
27	11/02/2002	0.64	46.083	2.9	-73.438	3.6	15.9	4.3	0.26	44	93
29	20/04/2002	0.75	44.523	2.2	-73.728	2.7	17.4	4.5	0.37	45	81
28	20/04/2002	0.67	44.483	1.8	-73.683	2.3	7.3	3.5	0.41	54	91

30	07/09/2002	0.70	47.047	1.9	-76.237	2.8	24.5	2.8	0.42	51	100
31	08/04/2003	0.73	44.630	3.3	-74.362	2.5	19.0	4.9	0.44	50	178
32	30/06/2003	0.36	41.648	7.5	-81.150	9.9	7.0	3.0	0.63	27	322
33	20/08/2003	0.39	46.012	1.4	-74.951	1.8	19.0	2.6	0.40	43	101
34	12/10/2003	0.60	47.059	2.3	-76.322	2.0	21.0	2.4	0.36	73	139
35	04/08/2004	0.80	43.672	1.6	-78.241	1.6	6.4	2.1	0.54	73	123
36	03/03/2005	0.50	45.038	2.7	-74.189	2.3	18.4	3.7	0.24	72	158
37	25/05/2005	0.54	46.290	1.3	-75.620	1.6	23.8	1.7	0.34	84	77
38	04/07/2005	0.50	46.264	1.2	-76.912	1.7	16.7	2.2	0.28	79	82
39	23/07/2005	0.54	47.037	2.6	-75.799	2.3	19.5	2.7	0.28	70	112
40	06/09/2005	0.46	46.282	1.6	-75.287	2.1	23.1	2.4	0.78	52	94
41	20/10/2005	0.49	44.671	1.5	-80.470	2.1	16.4	2.3	0.40	37	68
42	09/01/2006	0.49	45.031	1.2	-73.897	1.6	15.0	2.7	0.54	60	56
43	25/02/2006	0.59	45.664	1.4	-75.246	1.7	18.7	1.8	0.59	50	70
44	20/06/2006	0.38	41.799	2.4	-81.202	2.3	9.1	5.3	0.46	46	213
45	12/03/2007	0.47	41.377	6.1	-81.394	5.1	7.0	2.5	0.58	29	243
46	30/09/2007	0.41	46.924	2.5	-76.510	2.0	15.4	3.9	0.47	44	105
47	01/10/2007	0.52	47.069	1.6	-76.862	2.4	19.8	3.6	0.63	62	103
48	23/12/2007	0.60	46.163	2.3	-77.350	2.6	25.9	2.3	0.64	40	74
49	09/01/2008	0.33	41.758	3.6	-81.395	2.7	6.0	4.0	0.44	30	214
50	23/06/2010	0.63	45.882	2.0	-75.495	1.8	25.9	2.5	0.56	76	49

The focal depth calculated here is compared with the depth calculated in previous studies using depth phases (*sPg, sPmP,* and *sPn)* (so called RDPM – regional depth phase modelling). Table 4.3 shows the comparison of focal depth calculated in this study with those calculated by Ma and Atkinson (2006) and Ma and Eaton (2007) for the same events. In overall the focal depth calculated in Ma and Atkinson (2006) is smaller or at the lower end of the confidence intervals of the depth calculated here using the HYPOCENTER program. On the other hand the focal depth in Ma and Eaton (2007) is very close to the depth calculated here and only in two out of six cases is lower.

There are a few possible reasons for the discrepancies between the depth determined in this study using the HYPOCENTER program and RDPM results. The accuracy of absolute hypocentre locations (e.g. HYPOCENTER) is controlled by various factors, including seismograph network geometry, the accuracy of the arrival times of the used phases, the crustal-velocity structure, etc. (Pavlis, 1986; Gomberg et al., 1990). In comparison, the accuracy of the RDPM is affected by the accurate identification of the depth phases, the velocity model, and the focal mechanism that can affect the waveform shapes and amplitudes, and thus may cause error in reading the phase-arrival times (Ma and Atkinson, 2006).

The focal depths for the 9 events compared here with the results from Ma and Atkinson (2006) are estimated using similar velocity model by the two methods. To explain the difference between the depths there is a possibility that either the depth estimated by the HYPOCENTER program is affected by a trade-off between the epicentre location and/or the depth estimated by the RDPM is affected by error in the identification of the depth

phase. As the RDPM depths in Ma and Atkinson (2006) and in Ma and Eaton (2007) are estimated from only one station it is difficult to define their actual error.

Table 4.3: Comparison of focal depths for the region obtained in the present study and in Ma and Atkinson (2006) and Ma and Eaton (007)

Event No.	Date year/month/day	Focal depths calculated in the present study (km)	Focal depths reported by Ma and Atkinson (2006) (km)
2	1993/12/25	19.2 ± 5.6	12.0
9	1996/03/14	30.0 ± 8.4	22.0
12	1998/02/26	15.2 ± 6.6	10.0
18	1999/11/26	9.9 ± 12	5.0
21	2000/08/06	25.1 ± 4.7	9.0
22	2000/10/06	20.1 ± 6	12.0
26	2001/12/24	19.4 ± 6.3	13.0
28	2002/04/20	17.4 ± 4.5	12.0
31	2003/04/08	19.0 ± 4.9	8.0
No.	Date year/month/day	Focal depths calculated in the present study (km)	Foca depth (Ma and Eaton, 2007)
37	2005/05/25/	23.8 ± 1.7	24
38	2005/07/04/	16.7 ± 2.2	15
40	2005/07/06	23.1 ± 2.4	17
41	2005/10/20	16.4 ± 2.3	11
42	2006/01/09	15.0 ± 2.7	15
43	2006/02/25	18.7 ± 1.8	19

4.2 Focal Mechanism

Fault plane solutions were determined for 50 earthquakes using the FOCMEC program (Snoke et al. 1984). Only P-wave polarities were used for the calculation. An average between 13 and 14 polarities (*Pg or/*and *Pn*) were picked from the seismograms for each event. The grid search to obtain all possible solutions was made at 2° grid. Individual

focal mechanism beach-ball diagrams were plotted using the lower-hemisphere equal area projection.

The quality of the focal mechanism solutions is divided in four groups depending on the range of the possible solutions and the number of polarity errors. Figure 4.4 shows a sample solution for each quality. Half of the solutions (23 events) were determined without any polarity error and assigned group A; 18 solutions were computed mostly with one polarity error (group B); seven events were categorized in group C; and just two of the events were in group D.

The determined focal mechanisms with all possible solutions and the polarities used for the determination are presented in Appendix C. Each solution is characterised with the number of polarities, the number of the error polarities, and the quality A, B, C (Figure 4.3). For the cases with only one type of solution (quality A or B), the possible values for each focal mechanism parameter (e.g. strike, dip, trend, plunge) were obtained from the output file. The average value and the variations for each one of the parameters are calculated and the final solution is presented with both of them. The average values for the parameters must satisfy the requirement that the fault plane and the auxiliary plane are perpendicular to each other and the P- and T-axes are at 45° from these planes. For cases with more than one solution, the values and variations for each parameter as well as the type of solution were obtained. At the end only one solution was chosen for further analysis. This was made based on the number of possible solutions for each type and the number of their error polarities. The final single solution for the fault plane solutions for the 50 earthquakes analysed in this study are given in Table 4.4.

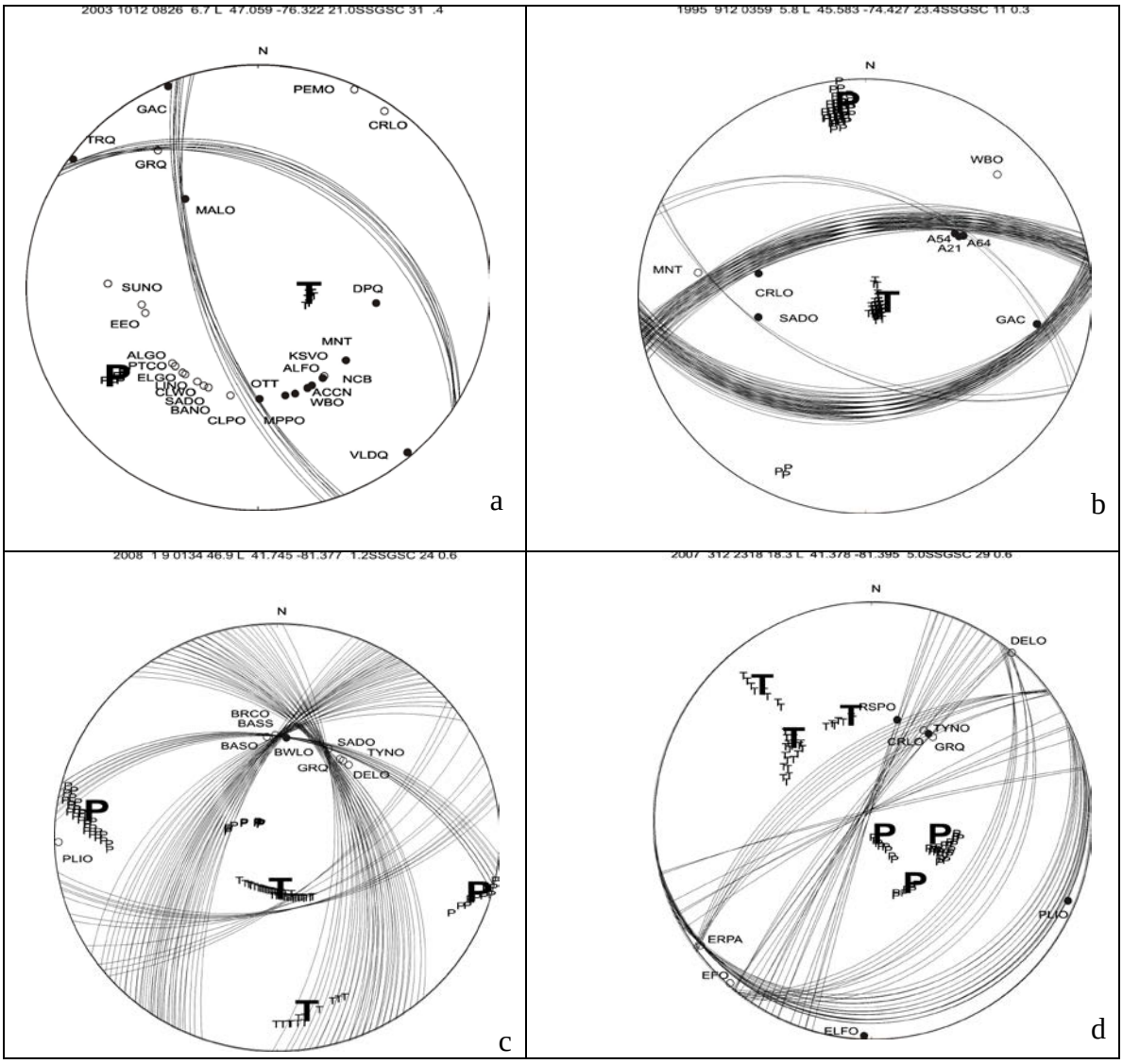

Figure 4.3: Samples of focal mechanis solutions with different quality : a: Excellent solution; b: Very good solution; c: Usable solution (with a few options); d: Poor solution. (T: Tension axis; P: Compression axis)

Figure 4.4 shows a map with the geographic locations of the 50 earthquakes and the lower hemisphere beach-ball diagrams. Among the 50 events studied here, 29 are thrust fault events and the other 21 events have focal mechanisms that are dominantly reverse with a small component of strike-slip movement. In terms of the regional distribution, all events in the WQSZ have a reverse-sense focal mechanism, although

some spatial variability of the orientation of the fault planes is apparent. In general, the focal mechanism solutions are similar and show thrusting on NNW or NW strikes. This NNW-NW strike of the planes is almost parallel to the general trend in seismicity.

The events in southern Ontario have different nodal plane strike orientations to the WQSZ (Figure 4.5 – right). They have mostly NNE-SSW direction with an average strike of 34°. The pressure axes there are mostly subhorizontal but they are rotated compared to Western Quebec and have an average EW trend (~N280°). Events in southern Ontario and more specifically in Lake Ontario and south of Lake Erie are mainly of strike-slip character. The results are consistent with the focal mechanisms reported by Adams et al. (1989) and Bent et al. (1999) for the western Quebec and southern Ontario using P polarities and Sv/P amplitude ratio information. A recent event in Georgian Bay (around 100 km from Lake Ontario) had a focal mechanism very similar to those in the WQSZ (Dineva et al., 2007).

Figure 4.5b the dip angle of the nodal planes indicate that: in Western Quebec there are two clusters for both nodal planes. One of the planes is dipping in the NE direction (~ 40°) and the other one in SW direction (~ 220°). In Southern Ontario the majority of the nodal planes yield dip angles around 54°-55° towards the SE (~107°) and NW (~143°) directions.

Table 4.4: Focal mechanisms obtained in this study.

	Date	Dip (1)	Strike (1)	Rake (1)	Dip (2)	Strike(2)	Rake (2)	Trend(P)	Plunge (P)	Trend(T)	Plunge (T)	solution	polarity	polarity error	Quality
1	19931116	45 ±4	169 ±6	90 ±2	45 ±4	349 ±7	90 ±2	169 ±7	3 ±2	135 ±20	86 ±2	50.0	11.0	0.0	A
2	19931225	40 ±4	136 ±14	90 ±0	50 ±3	316 ±14	90 ±0	46 ±14	5 ±3	226 ±14	85 ±3	40.0	8.0	0.0	B
3	19941002	48 ±2	14 ±10	90 ±0	42 ±2	194 ±12	90 ±0	104 ±11	3 ±2	284 ±11	87 ±2	23.0	7.0	0.0	C
		78 ±9	296 ±3	-90 ±0	12 ±8	116 ±1	-90 ±0	206 ±2	57 ±9	26 ±1	33 ±8	20.0	7.0	0.0	C
4	19950215	61 ±7	125 ±9	64 ±5	38 ±1	349 ±4	127 ±10	233 ±6	12 ±3	350 ±6	65 ±8	5.0	10.0	0.0	A
5	19950603	50 ±15	100 ±15	69 ±12	44 ±5	311 ±15	113 ±20	205 ±20	3 ±10	305 ±30	73 ±15	22.0	7.0	0.0	B
		65 ±11	77 ±11	54 ±6	43 ±4	317 ±14	141 ±15	192 ±9	13 ±7	301 ±17	55 ±7	21.0	7.0	0.0	B
6	19950616	70 ±7	352 ±6	44 ±8	49 ±1	243 ±15	152 ±12	114 ±7	12 ±3	217 ±4	45 ±13	12.0	10.0	0.0	C
		62 ±15	135 ±10	-56 ±10	43 ±4	259 ±0	-137 ±20	93 ±5	58 ±18	201 ±5	11 ±10	7.0	10.0	0.0	C
7	19950912	54 ±5	259 ±5	85 ±1	36 ±7	87 ±6	97 ±2	353 ±4	9 ±6	148 ±20	80 ±5	39.0	8.0	0.0	B
		50 ±6	116 ±2	90 ±0	40 ±1	296 ±1	90 ±0	206 ±1	5 ±1	26 ±1	85 ±1	3.0	8.0	0.0	B
8	19951010	45 ±5	134 ±20	76 ±4	47 ±5	333 ±12	104 ±3	54 ±10	1 ±4	318 ±35	80 ±3	48.0	7.0	0.0	A
9	19960314	69 ±7	96 ±14	60 ±7	36 ±0	334 ±7	143 ±15	208 ±10	18 ±5	327 ±10	55 ±10	25.0	9.0	0.0	B
		71 ±3	249 ±5	-58 ±2	36 ±2	7 ±3	-147 ±6	198 ±7	53 ±3	316 ±5	20 ±3	25.0	9.0	0.0	B
10	19970403	9±4	78 ±20	-63 ±20	82 ±5	231 ±10	-94 ±3	137 ±10	53 ±4	325 ±10	37 ±4	30.0	11.0	0.0	C
		82 ±3	232 ±4	-90 ±0	8 ±3	52 ±5	-90 ±0	142 ±4	53 ±3	322 ±4	37 ±3	11.0	11.0	0.0	C
11	19970524	36 ±0	116 ±13	83 ±14	54 ±14	305 ±8	95 ±4	31 ±6	9 ±20	236 ±25	80 ±18	49.0	17.0	0.0	C
		6 ±0	89 ±0	89 ±0	84 ±0	270 ±0	90 ±0	360 ±0	39 ±0	180 ±0	51 ±0	1.0	17.0	0.0	C
12	19980226	42 ±4	309 ±13	53 ±10	57 ±5	174 ±15	119 ±7	244 ±15	8 ±4	137 ±7	64 ±5	46.0	13.0	1.0	B
13	19980418	80 ±5	275 ±3	74 ±6	19 ±6	155 ±15	149 ±15	19 ±7	33 ±4	166 ±8	52 ±5	50.0	10.0	0.0	A
14	19980730	34 ±2	174 ±6	90 ±0	56 ±3	354 ±10	90 ±0	84 ±9	11 ±3	264 ±8	79 ±3	25.0	13.0	0.0	C
		10 ±2	114 ±4	90 ±0	80 ±5	294 ±4	90 ±0	24 ±4	35 ±5	204 ±4	55 ±5	18.0	13.0	0.0	C
15	19980925	46 ±1	356 ±3	53 ±1	55 ±1	224 ±3	122 ±1	292 ±3	4 ±2	193 ±6	64 ±0	8.0	8.0	0.0	C
		40 ±1	305 ±11	-109 ±7	53 ±1	149 ±5	-75 ±9	107 ±7	70 ±5	221 ±4	9 ±1	8.0	7.0	0.0	C
16	19981225	42 ±0	328 ±0	24 ±0	74 ±0	221 ±0	130 ±0	282 ±0	19 ±0	171 ±0	46 ±0	1.0	11.0	0.0	A
17	19990618	34 ±10	178 ±6	90 ±0	56 ±6	358 ±10	90 ±0	88 ±10	11 ±3	268 ±10	79 ±3	31.0	10.0	0.0	B
		10 ±4	114 ±4	90 ±0	80 ±5	294 ±4	90 ±0	24 ±4	35 ±5	204 ±4	55 ±5	19.0	10.0	0.0	B
18	19991126	72 ±11	2 ±2	90 ±0	18 ±11	182 ±2	90 ±0	92 ±2	27 ±11	272 ±2	63 ±11	33.0	11.0	0.0	B
19	20000101	56 ±9	126 ±3	90 ±0	34 ±9	306 ±3	90 ±0	216 ±3	11 ±9	36 ±3	79 ±9	31.0	15.0	0.0	B
20	20000420	49 ±1	270 ±3	51 ±2	54 ±3	141 ±3	126 ±2	207 ±2	3 ±2	112 ±5	62 ±2	10.0	17.0	0.0	A
21	20000806	55 ±2	308 ±5	73 ±5	38 ±1	156 ±5	113 ±7	50 ±3	9 ±2	171 ±6	73 ±4	6.0	17.0	0.0	A

22	20001006	50 ±3	134 ±10	90 ±0	40 ±3	314 ±10	90 ±0	224 ±10	5 ±2	44 ±10	85 ±3	39.0	10.0	0.0	B
23	20010126	43 ±5	259 ±20	-46 ±10	60 ±8	26 ±9	-123 ±2	246 ±20	60 ±7	139 ±12	10 ±7	25.0	9.0	0.0	D
24	20010319	34 ±10	4 ±3	90 ±0	56 ±10	184 ±3	90 ±0	274 ±3	11 ±10	94 ±3	79 ±10	34.0	8.0	1.0	B
25	20010411	59 ±10	4 ±12	90 ±0	31 ±10	184 ±8	90 ±0	95 ±3	14 ±10	273 ±10	76 ±10	50.0	12.0	1.0	B
26	20011224	65 ±11	279 ±11	54 ±7	43 ±5	159 ±5	141 ±17	34 ±8	13 ±9	143 ±2	55 ±10	21.0	10.0	0.0	B
		55 ±2	122 ±8	73 ±6	38 ±1	330 ±3	113 ±9	224 ±5	9 ±1	345 ±11	73 ±5	20.0	10.0	0.0	B
27	20020211	46 ±7	273 ±18	59 ±14	52 ±2	137 ±4	118 ±10	207 ±10	3 ±3	110 ±11	68 ±8	46.0	16.0	0.0	B
28	20020420)	28 ±7	10 ±5	86 ±3	62 ±7	195 ±5	92 ±10	283 ±6	17 ±5	110 ±6	73 ±6	27.0	22.0	0.0	B
		6 ±1	36 ±8	90 ±0	84 ±4	216 ±8	90 ±0	306 ±8	39 ±4	126 ±8	51 ±4	24.0	22.0	0.0	B
29	20020420	38 ±1	188 ±7	80 ±10	52 ±2	21 ±13	98 ±7	105 ±9	7 ±1	326 ±27	81 ±3	21.0	19.0	1.0	A
30	20020907	43 ±3	173 ±5	75 ±12	49 ±5	13 ±10	103 ±4	93 ±6	3 ±3	347 ±15	80 ±8	20.0	9.0	0.0	B
31	20030408	86 ±5	127 ±3	82 ±3	9 ±4	11 ±25	154 ±30	225 ±7	40 ±5	29 ±6	48 ±5	50.0	12.0	0.0	B
		27 ±4	312 ±1	76 ±5	64 ±5	147 ±6	97 ±2	232 ±5	19 ±5	71 ±7	70 ±4	50.0	12.0	0.0	B
32	20030630	39 ±0	302 ±0	12 ±0	82 ±0	202 ±0	128 ±0	263 ±0	27 ±0	147 ±0	40 ±0	1.0	16.0	0.0	A
33	20030820	79 ±5	257 ±3	51 ±2	40 ±1	154 ±7	163 ±7	16 ±2	24 ±4	130 ±3	42 ±1	9.0	13.0	0.0	A
34	20031012	35 ±3	302 ±2	57 ±2	62 ±3	160 ±3	111 ±3	235 ±1	14 ±3	109 ±8	67 ±1	8.0	26.0	1.0	A
35	20040804	65 ±3	298 ±2	-18 ±4	74 ±6	36 ±3	-154 ±3	259 ±2	29 ±3	166 ±3	5 ±6	26.0	24.0	0.0	B
		77 ±3	137 ±2	-25 ±2	65 ±3	233 ±2	-166 ±3	93 ±3	27 ±2	187 ±2	8 ±2	25.0	24.0	0.0	B
36	20050303	68 ±11	140 ±4	90 ±0	22 ±11	320 ±4	90 ±0	230 ±4	23 ±11	50 ±4	67 ±11	35.0	11.0	0.0	B
37	20050525	24 ±15	138 ±3	90 ±0	66 ±14	318 ±4	90 ±0	48 ±4	21 ±18	228 ±4	69 ±12	46.0	13.0	0.0	B
38	20050704	50 ±0	289 ±3	80 ±1	40 ±1	125 ±1	102 ±2	27 ±1	5 ±0	148 ±4	81 ±1	3.0	18.0	0.0	A
39	20050723	40 ±2	103 ±7	58 ±10	56 ±4	322 ±10	114 ±8	35 ±10	8 ±2	283 ±10	68 ±7	50.0	9.0	0.0	A
40	20050906	38 ±0	134 ±0	80 ±0	52 ±0	327 ±0	98 ±0	52 ±0	7 ±0	272 ±0	81 ±0	1.0	12.0	0.0	A
41	20051020	40 ±3	291 ±16	39 ±9	66 ±6	169 ±12	123 ±2	235 ±11	14 ±5	123 ±16	56 ±5	50.0	19.0	1.0	A
42	20060109	40 ±0	290 ±0	87 ±3	50 ±0	114 ±3	93 ±2	202 ±2	5 ±0	44 ±10	85 ±1	3.0	15.0	2.0	A
43	20060225	54 ±1	126 ±0	70 ±0	41 ±0	337 ±0	115 ±0	230 ±2	7 ±0	342 ±3	72 ±4	2.0	28.0	2.0	A
44	20060620	49 ±6	243 ±10	-51 ±5	54 ±7	13 ±12	-126 ±6	222 ±20	62 ±2	127 ±7	3 ±5	50.0	20.0	2.0	A
45	20070312	56 ±8	233 ±5	-80 ±1	35 ±8	36 ±1	-104 ±1	174 ±14	76 ±6	316 ±1	11 ±8	30.0	8.0	0.0	D
46	20070930	30 ±8	126 ±7	90 ±0	60 ±8	306 ±8	90 ±0	36 ± 7	15 ±9	216 ±8	75 ±7	50.0	11.0	0.0	A
47	20071001	47 ±1	131 ±3	47 ±5	58 ±2	5 ±3	126 ±2	70 ±3	6 ±3	330 ±3	59 ±4	16.0	13.0	0.0	A
48	20071223	38 ±3	248 ±9	70 ±9	55 ±3	93 ±6	105 ±7	172 ±5	9 ±3	47 ±15	75 ±5	50.0	16.0	1.0	A
49	20080109	48 ±10	336 ±15	44 ±10	58 ±10	212 ±15	128 ±5	276 ±8	6 ±8	177 ±18	57 ±2	47.0	9.0	0.0	C
		39 ±0	281 ±4	-71 ±13	53 ±5	77 ±15	-105 ±8	296 ±13	76 ±7	177 ±5	7 ±4	15.0	9.0	0.0	C
50	20100623	65 ±4	132 ±5	59 ±6	39 ±2	7 ±8	139 ±12	244 ±3	15 ±3	359 ±4	58 ±7	24.0	47.0	2.0	A

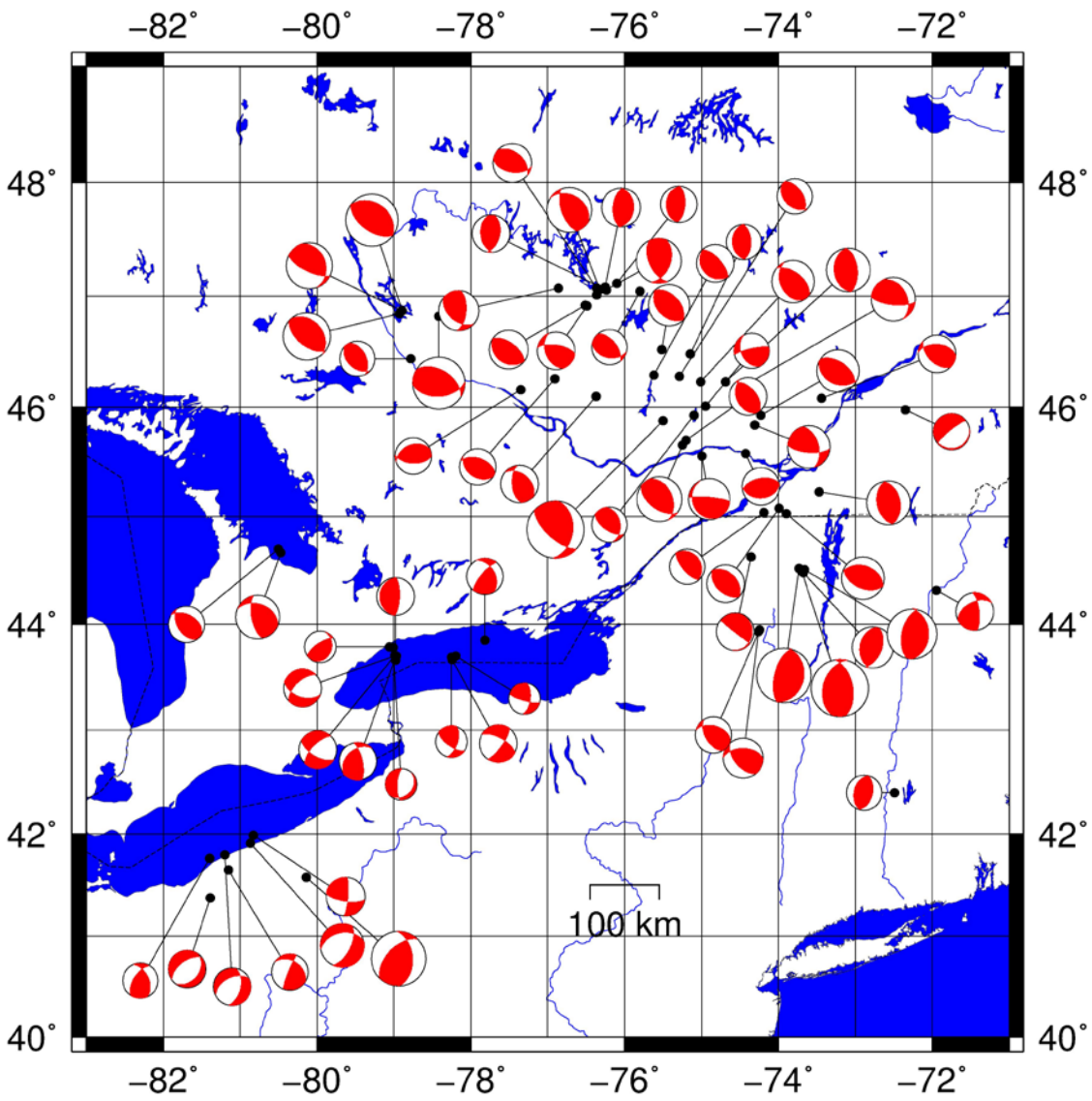

Fig. 4.4: Spatial distribution of fault plane solutions for 50 events in the study area.

(Red: compression quadrant; White: tension quadrant).

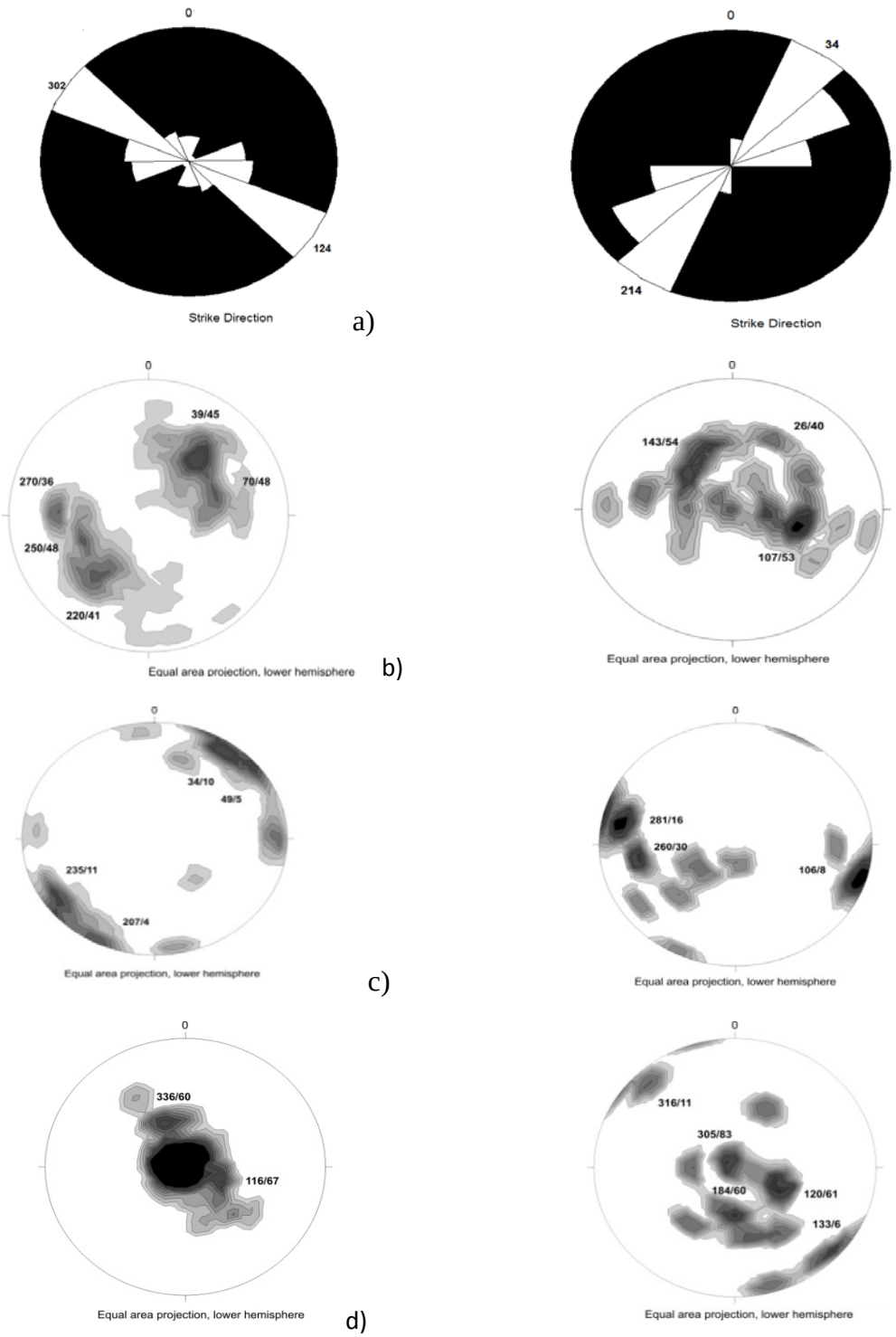

Western Quebec Southern Ontario

Fig. 4.5: Average focal mechanism parameters for the 50 studied events; a) rose diagram of the strike orientation, b) lower hemisphere equal area projection of the dipping angle, c) P-axes and d) T-axes for the events in Western Quebec (left) and Southern Ontario (right). The numbers show the trend/plunge of data

CHAPTER 5

ANALYSIS AND DISCUSSION

5.1 Introduction

Previous studies have attempted to discern trends in seismicity and relate them to regional geology or tectonics, which led to increased efforts to map basement fault zones and to re-evaluate seismic hazard in many areas of Eastern North America which were formerly regarded as low risk areas (Barosh, 1986; Jacobi and Fountain, 1993; Seeber and Armbruster, 1993; Talwani, 1999). Sbar and Sykes (1973) proposed that earthquakes in Eastern North America occur in areas of high stress along existing fault zones of late Paleozoic or younger age. Yang and Aggarwal (1981) distinguished two seismogenic provinces, that is, the Adirondack–western Quebec province and the Appalachian province, using the locations of 364 earthquakes of magnitude 2 to 5, and 22 focal mechanism solutions. Adams and Basham (1989) defined four seismic zones in southeastern Canada and argued that most of the events were associated with the reactivation of late Proterozoic to Paleozoic rift system along the St. Lawrence and Ottawa Rivers. In this chapter seismic source parameters (focal depth strike orientation, plunging angle P-axes and T-axes) determined in the present study are combined with the

results from other similar studies, and analysed and compared with tectonic features of the study area.

5.2 Focal Depths

Depth is one of the main parameters considered in the seismic hazard. It plays an important role in determination of the seismogenic layer in earthquake zones. Figure 5.1 shows the distribution of studied earthquakes with their focal depth. There is obviously a distinct geographic difference in the depths of the seismic events in western Quebec and southern Ontario.

The southern Ontario events and the events and south of Lake Erie occur at shallow depths between 4 and 20 km (Figure 5.1) but most of them are with hypocentres around 10 km. The depth range of these events is similar to the range of depths suggested by White et al. (2000) for the Grenville province in southern Ontario (possibly Grenville rocks under Palaeozoic cover).

The western Quebec events are generally deeper – between 12 to 30 km but most of them are around 18 - 20 km. The hypocentres around 18 km and deeper are restricted mostly in the eastern part of Western Quebec Seismic Zone. Considering a felsic composition of rock types at depths lower than 18 km and the temperature in such depths (≥350ºC) (Mareschal et al., 2000) the state of the crust in this zone seems to be close to the ductile/brittle transition. The depth interval for the hypocentres in western Quebec seems to be consistent with the depth of the Mesoproterozoic shear zone on the LlTHOPROBE seismic profile (Figure 5.2a). Based on this correlation, it may be concluded that the distribution of earthquakes in the WQSZ may be locally influenced by

Precambrian structures associated with the Grenville orogeny and rifting associated with opening of the Iapetus Ocean (Ma and Eaton, 2007). To be able to make more precise correlation between the earthquake locations (hypocentres) and the faults in depth it would be necessary to have larger number of accurately estimated hypocentres and especially depths.

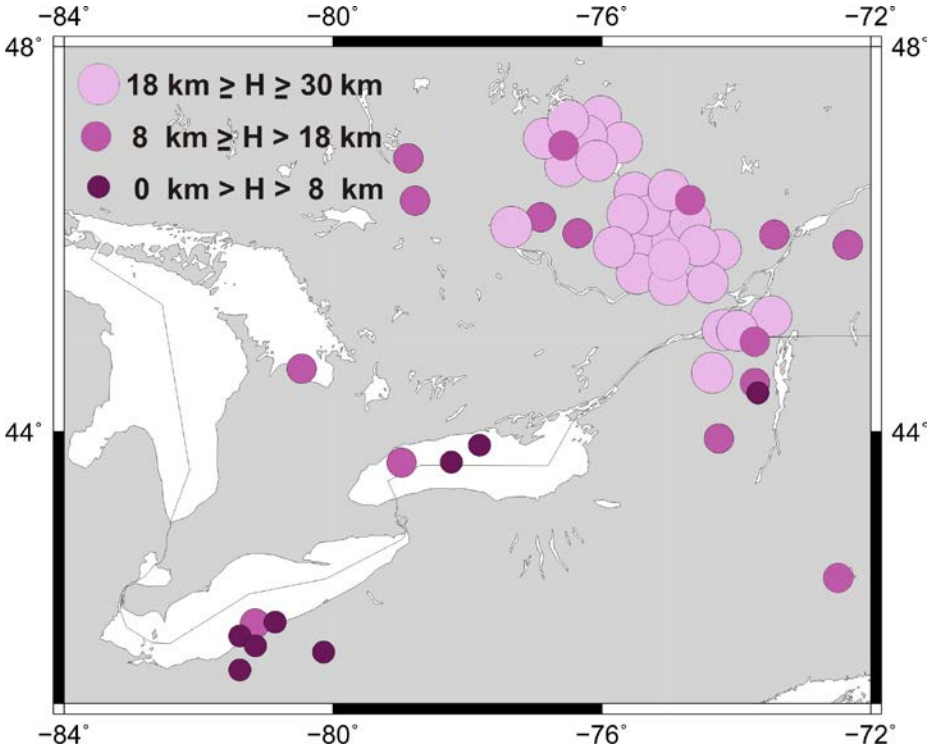

Figure 5.1: Epicentral map of studied events from 1992 to 2010 with magnitude m_N 3.5-5.7 with their focal depth in three different ranges: 0-8 km, 8-18 km, and 18-30 km.

Maximum focal depth is assumed to be controlled by either a rheological change from a brittle rupture to ductile flow or a transition in fault frictional behaviour from velocity weakening to velocity strengthening (Sibson, 1982; Scholz, 1990). Both transitions are closely related to the temperature–depth profile. The maximum depth of seismic events is found to correlate with heat flow values (or the tectonic ages) in the

source region (e.g. Chen and Molnar, 1983; Chen, 1988). Those areas with increasing tectonic ages are known generally to have decreasing surface heat flow values (Parsons and Scalter, 1977; Sclater et al., 1980; Willett et al., 1985). The mean heat flow in the older Grenville province is estimated at 43 ± 8 mW/m^2, while the average heat flow for the Grenville province in southern Ontario is significantly higher (58 ± 15 mW/m^2) (Guillou-Frottier et al., 1995; Mareschal et al., 2000), which correlates with the crust thickness and hence the depths of events in western Quebec and southern Ontario. In western Quebec there is comparatively lower heat flow with older and thicker crust and in southern Ontario there is younger and thinner crust with higher heat flow.

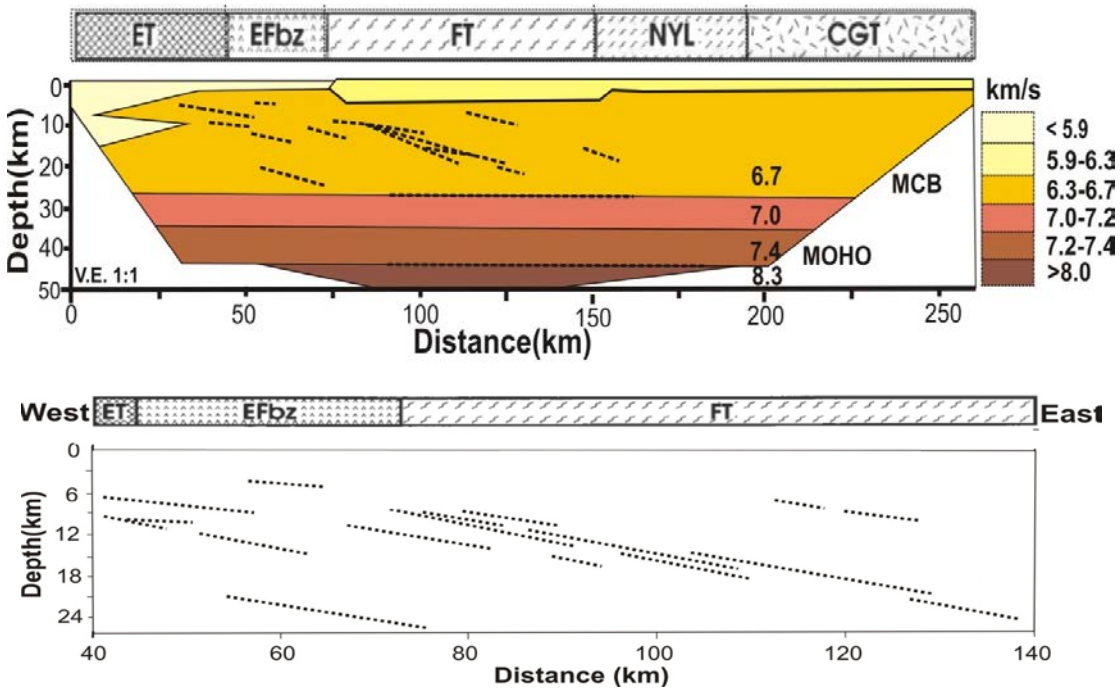

Figure 5.2: Seismic reflection cross section in the study area: a) P-wave velocity model for Western Quebec Seismic Zone; b) The east-dipping reflectors for the same profile with equal horizontal and vertical scale. MCB denotes mid-crustal boundary; ET, Elzevir terrain; EFbz, Elzevir-Frontenac boundary zone; FT, Frontenac terrain; CGT, Central Granulite Terrain (after Zelt et al., 1994).

5.3 State of Stress

Stress data for intraplate North America up to 2008 are summarized by Heidbach et al., (2008). Through examining the focal mechanisms of 32 earthquakes in eastern North America, she estimated a horizontal stress orientation throughout the region, varying between northeast and east and averaging east-northeast. This orientation is consistent with the North American plate motion and mainly attributed to plate boundary forces such as Mid-Atlantic Ridge push (Zoback, 1992a; Richardson, 1992).

P and T axes from earthquake focal mechanisms are one of the most commonly used tectonic stress indicators, although borehole breakouts yield more consistent results (Mazzotti and Townend, 2010). Principal stress axis orientations obtained from individual fault-plane solutions, however, are not reliable measures because P and T axes cannot be converted with certainty to the greatest and least principal stress directions (Zoback and Zoback, 1980; Scholz, 1990). These uncertainties result from the fact that most earthquakes occur on pre-existing faults that can be mis-oriented with respect to the current stress tensor. Therefore, individual focal mechanisms can only constrain the stress direction within 35°–45° (Zoback and Zoback, 1980). McKenzie (1969) proposed a restriction on the greatest principal stress imposed by the fault plane solution in which this stress direction should lie in the same quadrant as the P axis but could, in fact, be nearly normal to the P direction. It appears that the best method of analysing focal mechanism data is to consider a number of events that occur on different faults in a particular area and then to rely on their average P and T directions as measures of the orientations of the maximum and minimum principal stresses (Zoback and Zoback, 1980). A large number of mechanisms from a small volume can be used for a stress

estimate using a stress inversion technique (e.g. Gephart &Forsyth, 1984; Mitchael, 1984; Arnold & Townend, 2007). In the current study the available focal mechanisms are combined within spatial clusters and analyzed to verify their consistency so that later this kind of stress inversion can be made for each cluster.

Mazzotti and Townend (2010) determined the state of stress in nine seismic zones in central and eastern North America from focal mechanisms using a Bayesian analysis. The axis of maximum horizontal compressive stress determined from earthquake focal mechanisms in seismic zones (S_{HS}) and from borehole data near but outside the seismic zones (S_{HB}) showed a similar pattern in Gatineau (N038° vs N043°) and Montreal (N058° vs N044°) area. In Lower St. Lawrence and Charlevoix areas S_{HS} revealed a rotation of 20° to 40° clockwise compared to S_{HB}. The North Appalachian region shows indications of similar clockwise rotations but at a low confidence level.

The summary of the results for the P-axes for western Quebec obtained in the current study (Figure 4.6c, left) shows that the P-axes are mostly sub-horizontal, with plunge values less than 30°. Most of the events yield northeast-southwest-trending P axes, between approximately 30° and 50°, although some events yield P-axes trending from north-south to east-west. These results are generally consistent with the trends of the horizontal stresses (30° to 45°) defined by Zoback (1992b). In southern Ontario, the P axes predominantly have east-west orientation and are mostly horizontal but vary to almost vertical. The average orientations of the P-axes for southern Ontario and Western Quebec are calculated and shown on Figure 5.3.

The variations in P- and T-axes in western Quebec and southern Ontario suggest local perturbations in the stress field, similar to the results obtained in Wahlstrom (1987)

and Adams (1989), in contrast to studies that favor a regionally homogeneous eastern North American stress field (Sbar and Sykes, 1977; Zoback and Zoback, 1991). For example, Sbar and Sykes (1997) suggest that the Adirondack and western Quebec form a continuous seismic zone with a uniform stress pattern of ENE compression. In contrast Adams (1989) proposes that, within the mid-plate stress province, there are stress anomalies. Mazzotti and Townend (2010) argue that the intraplate state of stress may be affected by stress perturbation sources: postglacial rebound and local stress (induced by spatial and temporal interplay of regional stress sources) concentrators, such as low-friction faults. This implies that local conditions can significantly modify the regional stress field. Locally, some earthquake focal mechanisms (including those in a 50 km radius around Ottawa) indicate P-axes normal to the regional trend. These variations may be caused by local stress in a nearly isotropic field. The present study confirms the lack of uniformity of the stress field inferred from focal mechanism studies (Figure 5.3).

Comparisons of the axis of maximum horizontal compressive stress determined from earthquake focal mechanisms in this study and those proposed by Mazzotti and Townend (2010) show a similar stress orientation for western Quebec (Figure 5.3). The average orientation of the P-axes in southern Ontario is slightly rotated compared to the average orientation of the compression obtained by Zoback (1992a). Details for the stress patterns proposed by Mazzotti and Townend (2010) for eastern Canada and those determined in this study for the defined clusters of events in western Quebec and southern Ontario are shown in Figure 5.3.

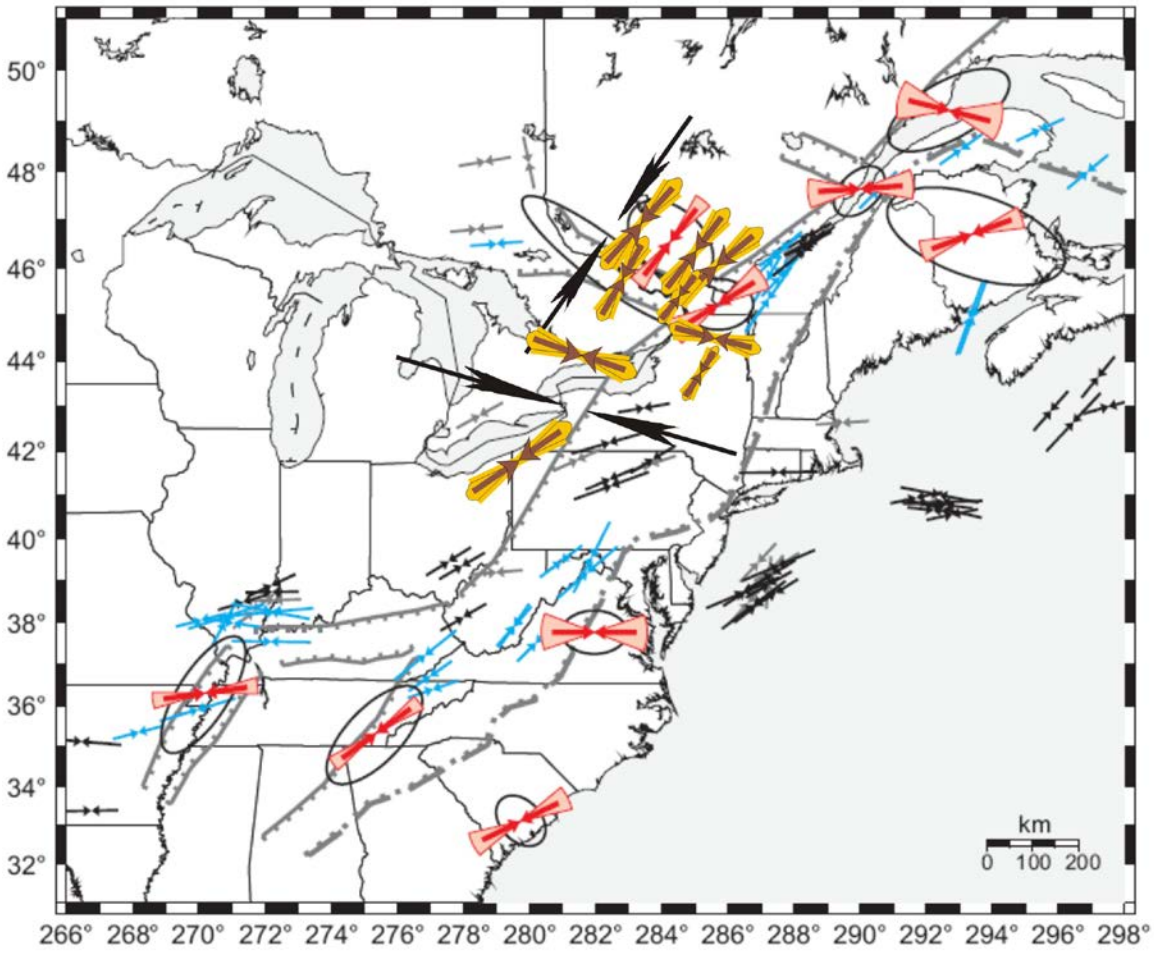

Figure 5.3: Stress pattern for all events in the study area (modified from Mazzotti and Townend, 2010). Orange symbols with brown arrows indicate the orientation of the P-axes in each cluster and large black arrows indicate the average orientation of P-axes for southern Ontario and Western Quebec from this study. The red arrows and angular sectors indicate stress orientation obtained by Mazzotti and Townend, 2010; Solid and gray arrows show S_{HB} orientation from borehole observation. Blue arrows show borehole observations used by Mazzotti and Townend, (2010).

5.4 Spatial variation of focal mechanism parameters

The spatial variations of the focal mechanism parameters were studied using the focal mechanism data obtained in the current study combined with all available focal mechanism solution data in the literature (Appendix D). The solutions were selected and manually analysed based on the accuracy and quality of the results provided for each event. In some cases the strike and dip of the nodal planes were calculated manually from the trend and plunge of the T and P axes. Only one focal mechanism solution for each earthquake was considered, based on the quality, for the subsequent analysis. All earthquake epicentres of the events with focal mechanisms and with magnitude $m_N > 3.5$ are shown in Figures 5.4a. The events were combined into clusters using the density distribution of the earthquakes in the study area (Figure 5.4b) and manually checked for consistency of the focal mechanisms of closely spaced events. The clusters outlined by previous researchers within the study area were also taken into account. This clustering can be improved in future by including more earthquakes with well-defined hypocentres for longer period of time and wider magnitude range. The data for the focal mechanisms (nodal planes, P- and T-axes) were analysed separately for each cluster.

The earthquake activity in western Quebec is suggestive of a strong NNW-NW trend, where most of events are focused along the Ottawa River, from Montreal to Baskatong (Figure 2.4). Earthquake epicentres along the Ottawa River appear to correlate with a zone of Paleozoic or younger normal faults along the Ottawa River (Forsyth, 1981). Another series of epicentres are located from Montreal to west of the Baskatong Reservoir trend northwest. Forsyth (1981) suggested that earthquakes of the second band (from Montreal to the west of the Baskatong) are occurring on or between structural

boundaries of the Central Metasedimentary Belt. There is no obvious concentration of earthquake epicentres northwest and southeast of the western Quebec seismic zone (Figure 5.4). A similar relative absence of earthquakes is also present in the historical data (1627-1984) (Figure 3.1). Similarly, in the southern Ontario region most of the earthquakes appear to be clustered either around the region of eastern Lake Erie, western Lake Ontario or along the Ottawa River (Figure 5.4).

Detailed investigation in the trend of epicentres in both the western Quebec and the southern Ontario suggests some distinct seismic clusters (e.g. Ma and Eaton, 2007; Dineva et al. 2004). However, trends in earthquake epicentres alone are not enough either to establish seismic zones or to rule out the existence of seismic zones. Similarly, seismic zones cannot be defined solely on the basis of past geologic history of the region (Yang and Aggarwal, 1981). In fact, a combination of seismic parameters and geological patterns should be used to identify and isolate those parameters that may influence present-day earthquake processes in the region. Dineva et al. (2004) and Ma and Eaton (2007) have developed a simple statistical approach to characterize the spatial clustering of seismicity. The method is implemented by subdividing the area of interest into square bins and counting the number of events that fall within each bin. An attempt is made in this thesis to recognise potential seismic clusters in both the western Quebec and the southern Ontario by means of the earthquake parameters and geological features in the region. This classification is based on earthquake parameters such as epicentre locations, focal depth, focal mechanism solutions, the pressure and tension stress directions (P- and T-axes) inferred from focal mechanism solutions, and specific lineaments inferred from geologic data such as faults.

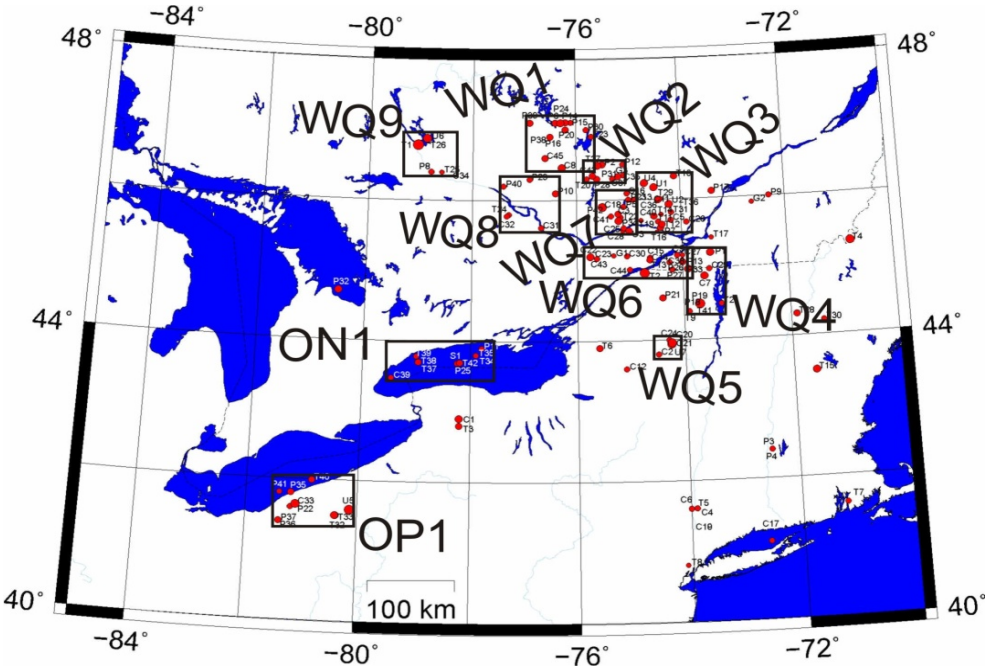

a)

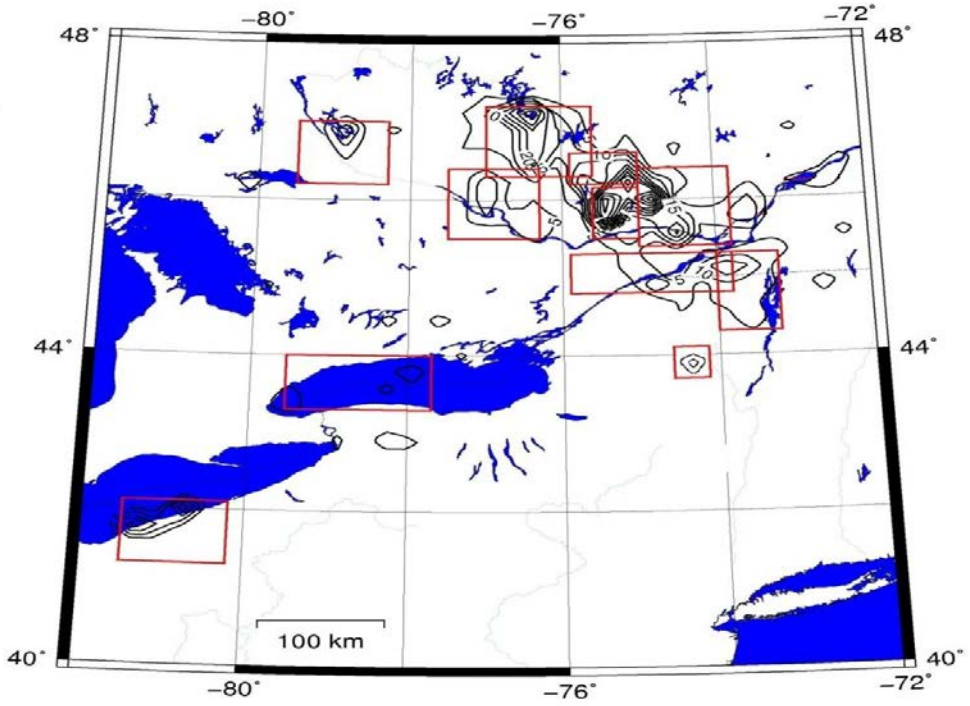

b)

Figure 5.4: Defined clusters of earthquake epicentres in western Quebec and southern Ontario (m_N>3.5, 1993-2011); a) Epicentres of the events in the study area: Maniwaki Cluster (WQ1), Mont Laurier Clusters (WQ2 and WQ3), Adirondack Clusters (WQ4 and WQ5), Ottawa River Clusters (WQ6, WQ7, WQ8), Timiskaming Cluster (WQ9), southern Ontario (ON1) cluster (The Burlington-Niagara Falls Cluster (BNFC)), Ohio-Pennsylvania Cluster (OP1); b) Contour density map for the events with $m_N > 2$, for the Western Quebec (WQSZ) and Southern Ontario (SOSZ) seismic zones.

In Western Quebec Seizmic Zone (WQSZ) nine smaller clusters have been identified (Figure 5.4) within a few distinct clusters: Timiskaming, Maniwaki, Mont Laurier, and Adirondack. Similar larger clusters have been proposed by Ma and Atkinson (2006). Only one cluster - the Timiskaming cluster (WQ1), located close to the epicentre of the 1935 Timiskaming earthquake, has events with focal depths around 10 km. All other clusters in WQSZ have events with depth between 14 km and 30 km. A few clusters with shallow depth are identified within the southern Ontario seismic zone: OP1 and ON1. These clusters are similar to previously identified Burlington-Niagara Falls cluster (Adams and Basham, 1991; Dineva et al. 2004), also known as Western Lake Ontario cluster (Seeber and Armbruster, 1993) and the Ohio-Pennsylvania border cluster (Northeast Ohio seismic zone) (Seeber and Armbuster, 1993; Dineva et al. 2004).

The parameters of the focal mechanisms in each cluster including the orientation of the nodal planes, the maximum compressive stress directions inferred from the focal mechanism, and the relationship between seismicity and pre-existing tectonic structures are discussed in the following sections. The predominant orientation of the compression axis in each cluster is compared with those proposed by Zoback (1992a) and Mazotti and Townend, (2010).

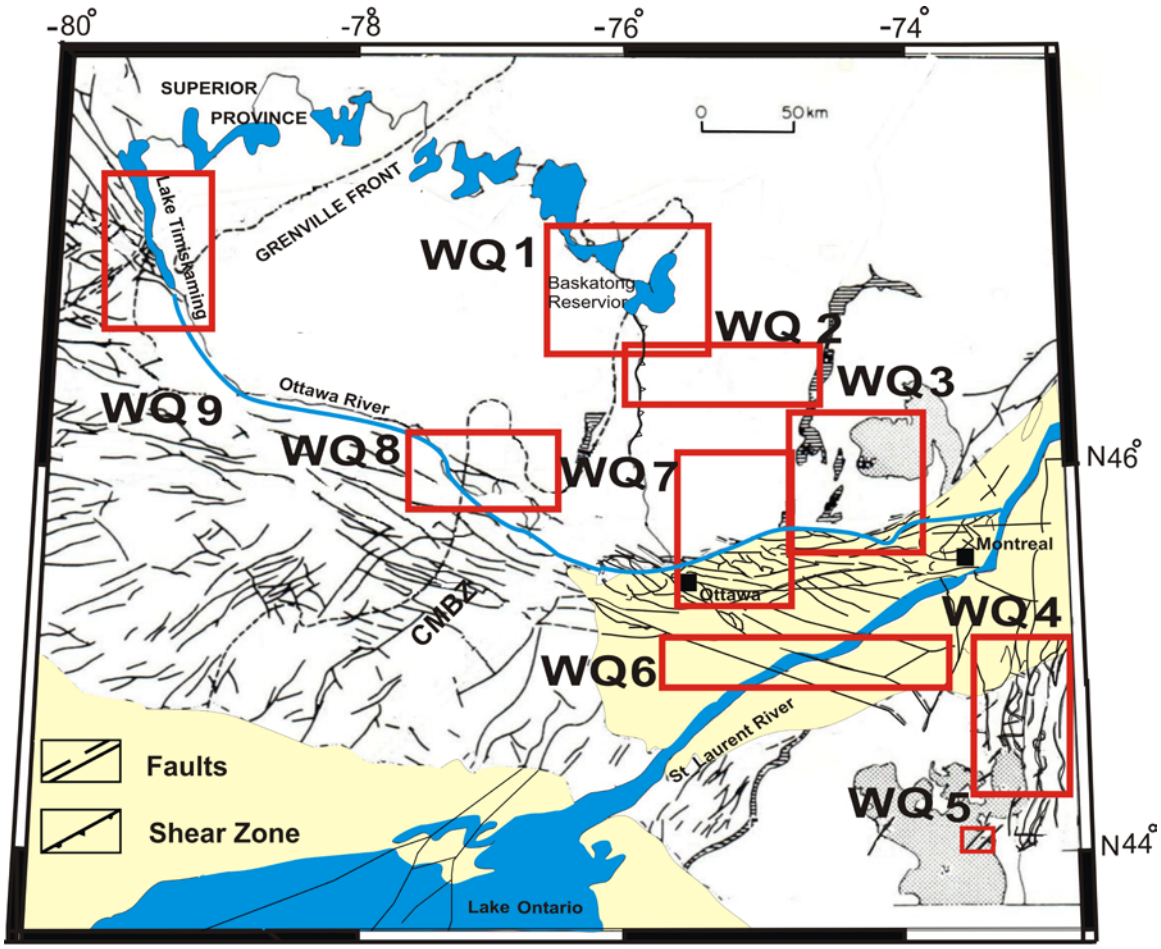

Figure 5.5: Regional fault map with approximate position of the WQ clusters

The grey areas show anothosite bodies and lined areas indicate cataclastic/mylonite zones. Yellow coloured areas in south and southeast indicate Paleozoic cover. The dotted lines indicate interpreted faults in southern Ontario. Geological province subdivisions are indicated with dashed lines (modified from Forsyth 1981).

5.4.1 Maniwaki Cluster (WQ1)

The Maniwaki (WQ1) cluster is located in the northwest corner of the WQSZ within the Grenville Province (from latitude 46° to 47.5°and longitude -75.5° to -77.5°). There are 12 events with focal mechanisms in this cluster. Most earthquakes in this cluster are

deeper than 20 km (20 km to 26 km). The distribution of hypocentres (Figure 5.1) with respect to the major tectonic elements imaged by the crustal seismic profile (Figure 5.2) suggests some evidence for local controls on the distribution of seismicity by the pre-existing Precambrian structures. Figure 5.6a shows the fault plane solutions for events in the Maniwaki cluster (WQ1). All of the events are of reverse fault type. The nodal planes strike is NNE-SSW (~ 10° - 190°) and ESE-WNW (~125° – 305°). The first strike orientation correlates well with the fault orientation which is mainly in N-S direction (Figure 5.7). Most planes have dip angle from 45° to 48° in SW direction and 54° to 57° in NE direction (Figure 5.6c). The P-axes are sub-horizontal and with average NE orientation (Fig. 5.6d).

From 1992 to 2011 there were 12 events with $m_N > 3$ recorded in this cluster. These events have similar recorded waveforms, although different magnitude. This similarity suggests that these events have essentially the same source mechanism (Ma and Atkinson, 2006). Figure 5.8 shows an example of recorded earthquake waveforms for two events within this cluster recorded by station GAC (Figure 5.6a). As it can be seen, this similarity might be a result of repeating seismicity in this cluster. The recurrence intervals of these events vary from about 6 months to 6 years. Schaff and Richards (2004) propose that repeating events with interval of 6 months or more could be due to creep loading of stuck fault patches (slow movement of fault planes) (Figure 5.6). Possibly the most recent tectonic activity around this cluster is associated with emplacement of kimberlites at ~180 Ma and alkaline intrusions at ~130 Ma –120 Ma (Crough, 1981).

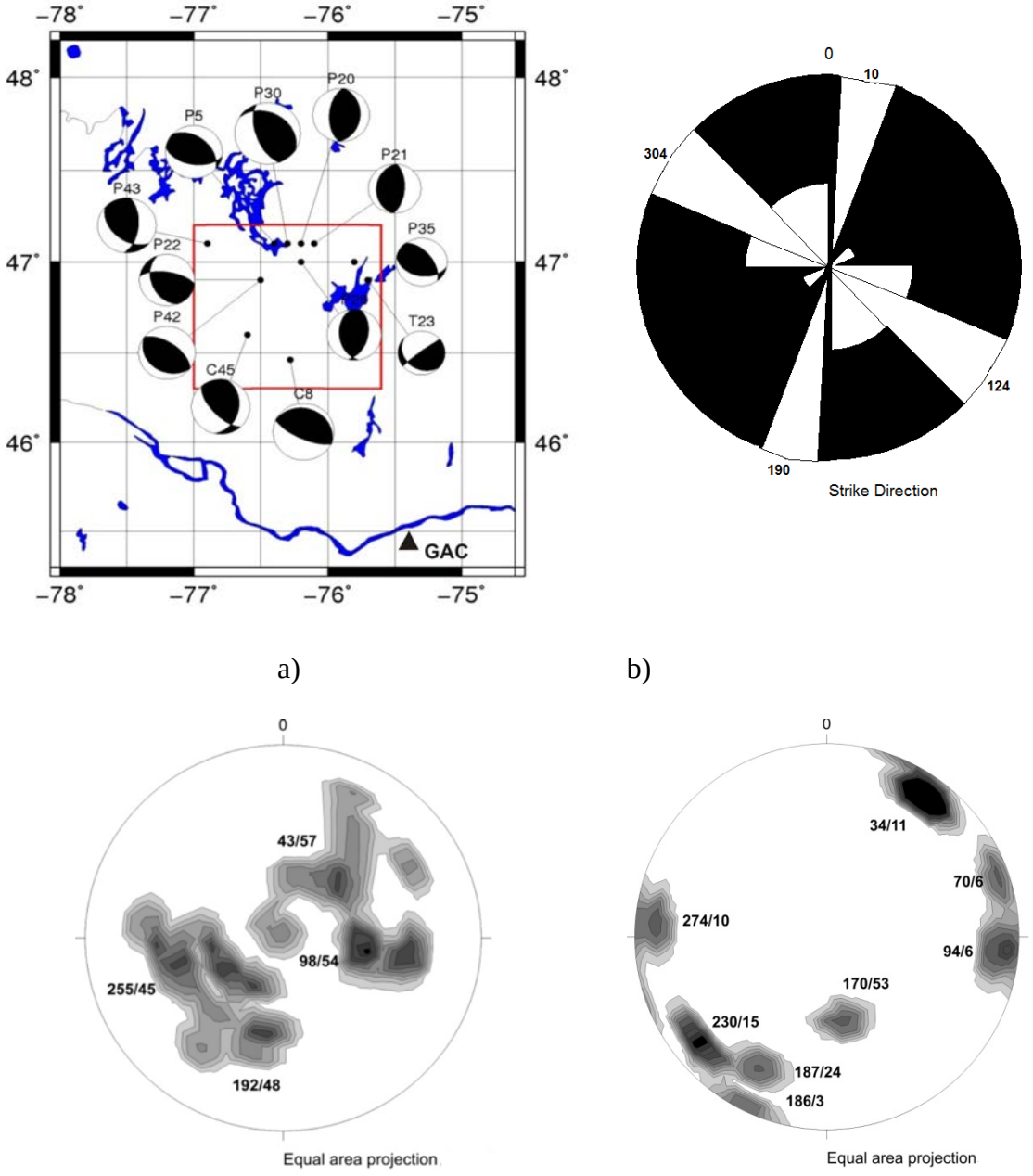

Figure 5.6: Summary of the focal mechanism parameters for the WQ1 (Maniwaki) cluster. a) Fault plane solutions, b) Rose-diagram for the strike of both nodal planes, c) Distribution of the dip angle of both nodal planes, and d) Distribution of pressure (P) axes. The labels of the events on the map are the same as in Appendix C.

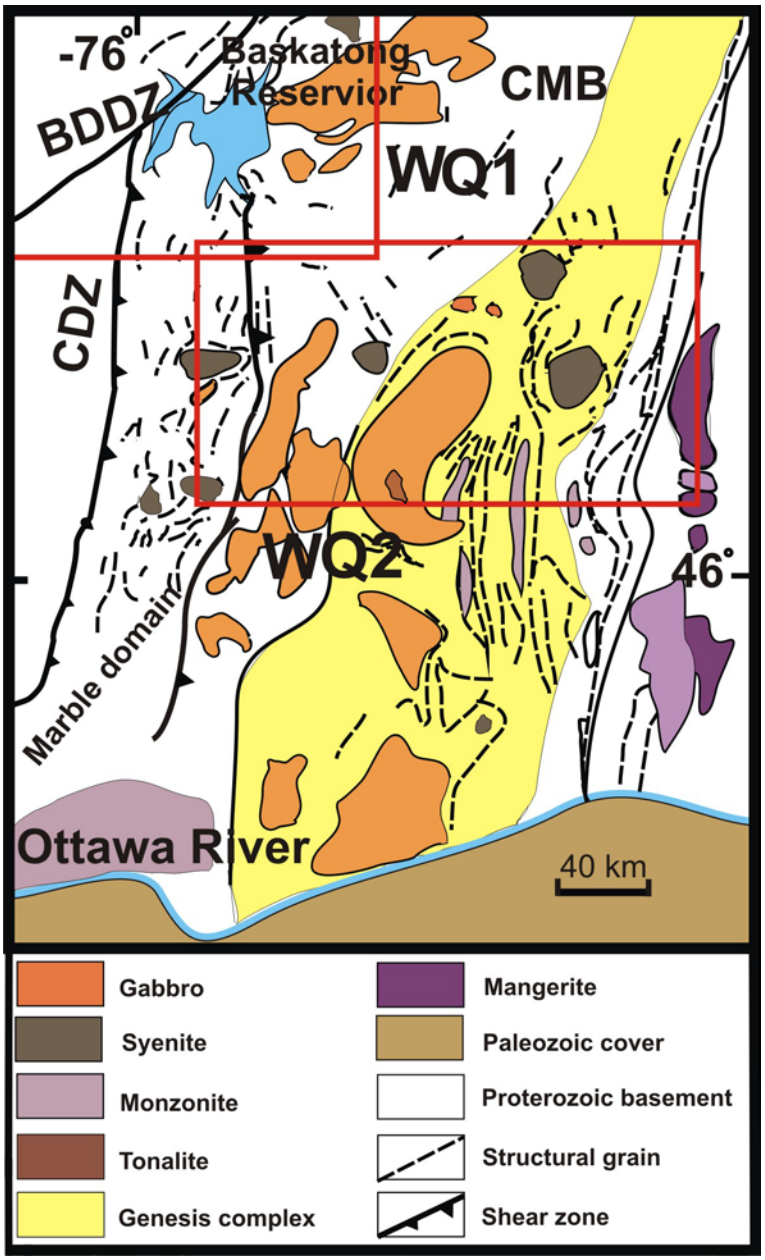

Figure 5.7: Geologic features of WQ1 and WQ2 in the Central Metasedimentary Belt (modified from Harris et al., 2001).

BDDZ, Baskatong-Desert deformation zone (Sharma et al., 1995), and CDZ, Caymant deformation zone (Sharma et al., 1995).

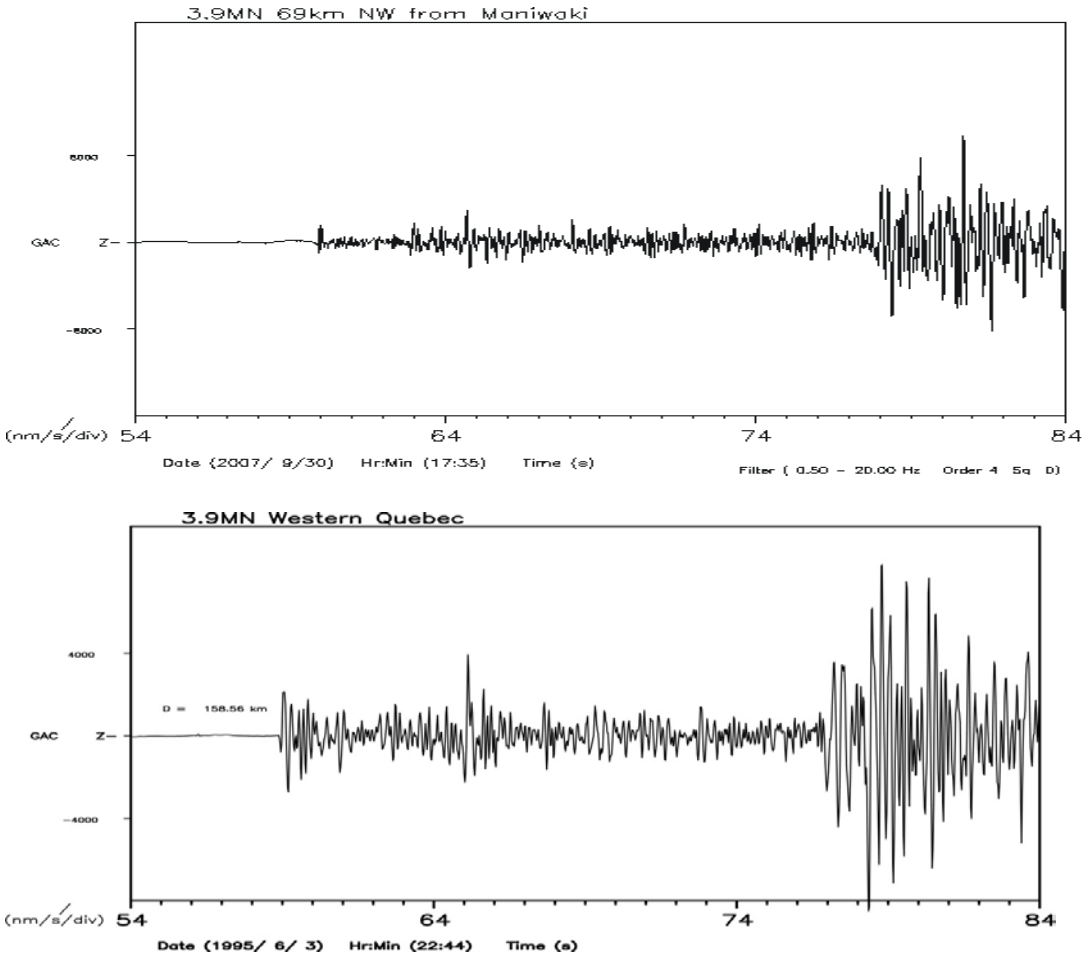

Figure 5.8: Waveform comparison for two events within the Maniwaki cluster (WQ1).

5.4.2 Mont Laurier Clusters (WQ2 and WQ3)

The Mont Laurier region is located in the northern area of the WQSZ within the Grenville province between latitude 45.4° to 46.6° and longitude -73.8° to -75°. There are 27 studied events with focal depth between 18 km to 28 km in this cluster. Seismicity in the Mont Laurier cluster is characterized by a slightly lower Gutenberg-Richter *b* value (0.76) than the Maniwaki cluster and higher *b* value than other clusters in the region (Ma,

2009). The Mont-Laurier earthquake occurred in 1990 with a magnitude m_N 5.0 approximately 9 km southwest of Mont-Laurier, Quebec.

From a geological point of view, the Mont-Laurier epicentres are located in the northern Central Metasedimentary Belt (CMB) division of the western Grenville Province (Wynne-Edwards, 1972) (Fig. 2.2). The CMB is characterized by supracrustal and plutonic rocks (ca. 1.3 to 1.0 Ga) that appear as a stack of crustal slices emplaced along a series of east dipping, top to the northwest ductile thrust zones (Forsyth et al., 1994a). Earthquakes in this region seem to be occurring on or between structural boundaries of the CMB (Forsyth, 1981) (Figure 5.7). Adams and Basham (1989) proposed a correlation between the earthquake locations and the assumed passage of this region over a hot spot. Goodacre et al. (1993) suggested that crustal zones of weakness delineated by the drainage pattern and, to a lesser extent, positive aeromagnetic anomalies and the Helikian (Mid-Proterozoic) paragneiss may be controlling the location of microearthquakes in the central part of the seismic zone. Lamontagne et al. (1994) argued that the current earthquake activity in this area may be explained by relatively small zones of weakness distributed over the whole CMB.

Based on the concentration of epicentres in this region, two clusters of events can be recognised: WQ2 (10 events) and WQ3 (17 events) (Figures 5.3). WQ2 formed in the north-western part of the Mont Laurier region, while the other cluster is formed in south-eastern part, named WQ3 cluster. In WQ2 cluster the focal mechanisms are mostly of reverse type, although two events yield significant strike-slip component (Figure 5.9a). The strike orientation of the nodal planes for most events in this cluster is NW-SE (~ N124° - N304°) (Figure 5.9b), while most structural features of the area are NE. This

could be attributed to possible buried deep cross structures as suggested by Dufréchou et al., (2011). The dip angles of the nodal planes vary in average from 32° to 60° to the SW direction and between 52° and 58° to the NE (Figure 5.9c). The P-axes are mainly subhorizontal and their average orientation is NE-SW. The regional compression stress orientation proposed by Zoback and Zoback (1991) is similar to this orientation.

WQ3 is located in south-eastern part of the Mont Laurier region, Figure 5.10a shows the focal plane solutions for the events in WQ3 cluster. Most of the events in this cluster show reverse type focal mechanism. There are only a few events with a strike-slip component and one event (C13) which is almost pure strike-slip. The strike orientation of the nodal planes in this cluster varies in wide angle around almost E-W direction (~ 100 - 280°) and some in NE-SW. This direction is consistent with the trend of pre-existing faults or shear zones in general E-W direction within this cluster (Figure 5.5). There are also some planes with NNE-SSW strike (~22 - 202°). The dip angles of the nodal planes vary between 36° and 84°. The pressure axes for this cluster are sub-horizontal, mostly with NE-SW trend (~50 -240°), varying from N-S to E-W.

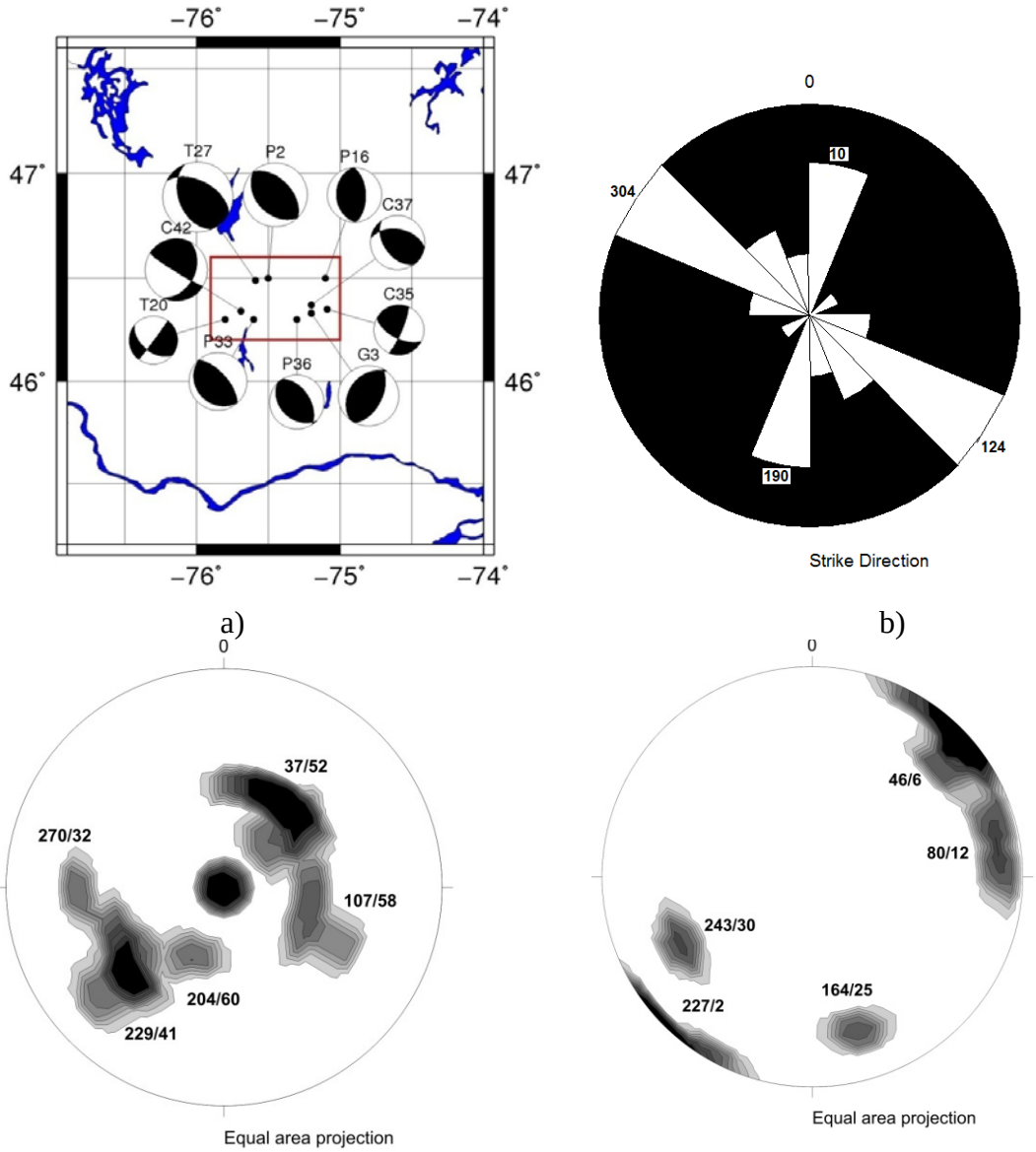

Figure 5.9: Summary of the focal mechanism parameters for the WQ2 (Mont Laurier) cluster. a) Fault plane solutions, b) Rose-diagram for the strike of nodal planes, c) Distribution of the dip angle, and d) Distribution of pressure (P) axes. The labels of the events on the map are the same as in Appendix C.

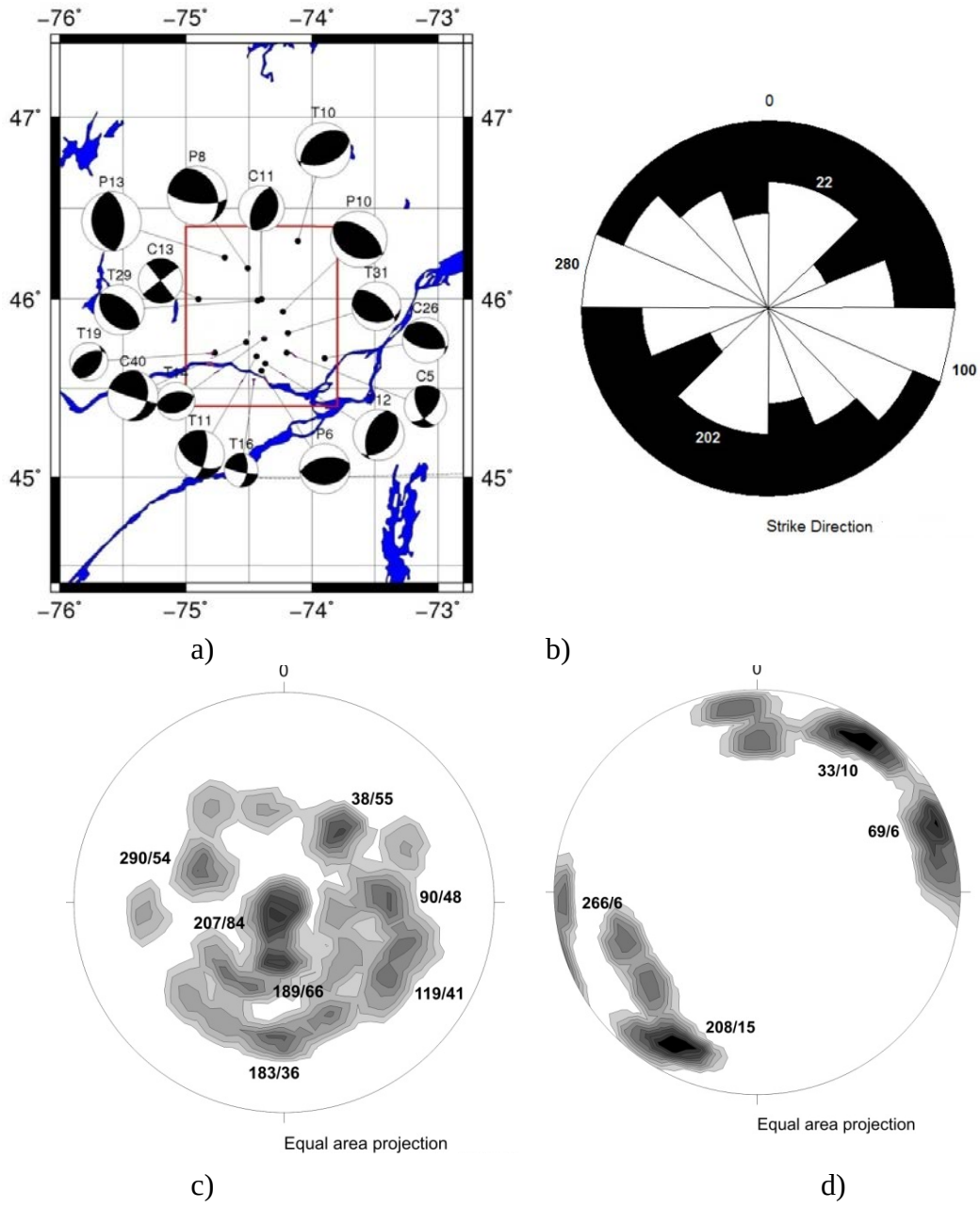

Figure 5.10: Summary of the focal mechanism parameters for the WQ3 (Mont Laurier) cluster. a) Fault plane solutions, b) Rose-diagram for the strike of both nodal planes, c) Distribution of the dip angle of both nodal planes, and d) Distribution of pressure (P) axes. The labels of the events on the map are the same as in Appendix C.

5.4.3 Adirondack Clusters (WQ4 and WQ5)

The Adirondack region is located in the south-eastern part of the WQSZ in the south-eastern part of Grenville Province. The Adirondack region has a dome-like structure with the Lower Paleozoic beds outcropping around the margins and with the basement complex of Precambrian igneous and metamorphic rocks exposed in the interior (Quinn, 1993). The earthquakes in this region are at the edge of the Grenville Adirondack massif and near the front of the Appalachian system.

Two clusters of events can be recognised in the Adirondack region. WQ4 covers an area from latitude 44.3 to 45.35° and longitude -73.1° to -74°. There are 8 events with focal depths from 7 to 18 km in this cluster. WQ5 is located in an area from latitude 43.7 to 44.1°and longitude -74.1 to -74.6° containing 5 events with focal depths from 5 km to 12 km (Figure 5.1). The Gutenberg-Richter *b* value is estimated to be about 0.65 for this cluster (Ma and Atkinson, 2006), slightly higher than the Timiskaming cluster, but much less than for the other clusters in the WQSZ.

Figure 5.11a shows the focal plane solutions for the WQ4 cluster. Most of the events in this cluster have reverse type focal mechanisms; one of the events is almost pure dip-slip (T9) and one has strike-slip component (T21). The nodal planes in this cluster have predominantly N-S strike, consistent with the known fault orientations (Figure 5.5 and Figure 5.11). The plane dip angles vary widely from 2 to 75° but the majority have dip angles 42 to 51° (Figure 5.11c). The compression axes in this cluster have mainly E-W direction, which is different from the average regional tectonic stress (Figure 5.11d).

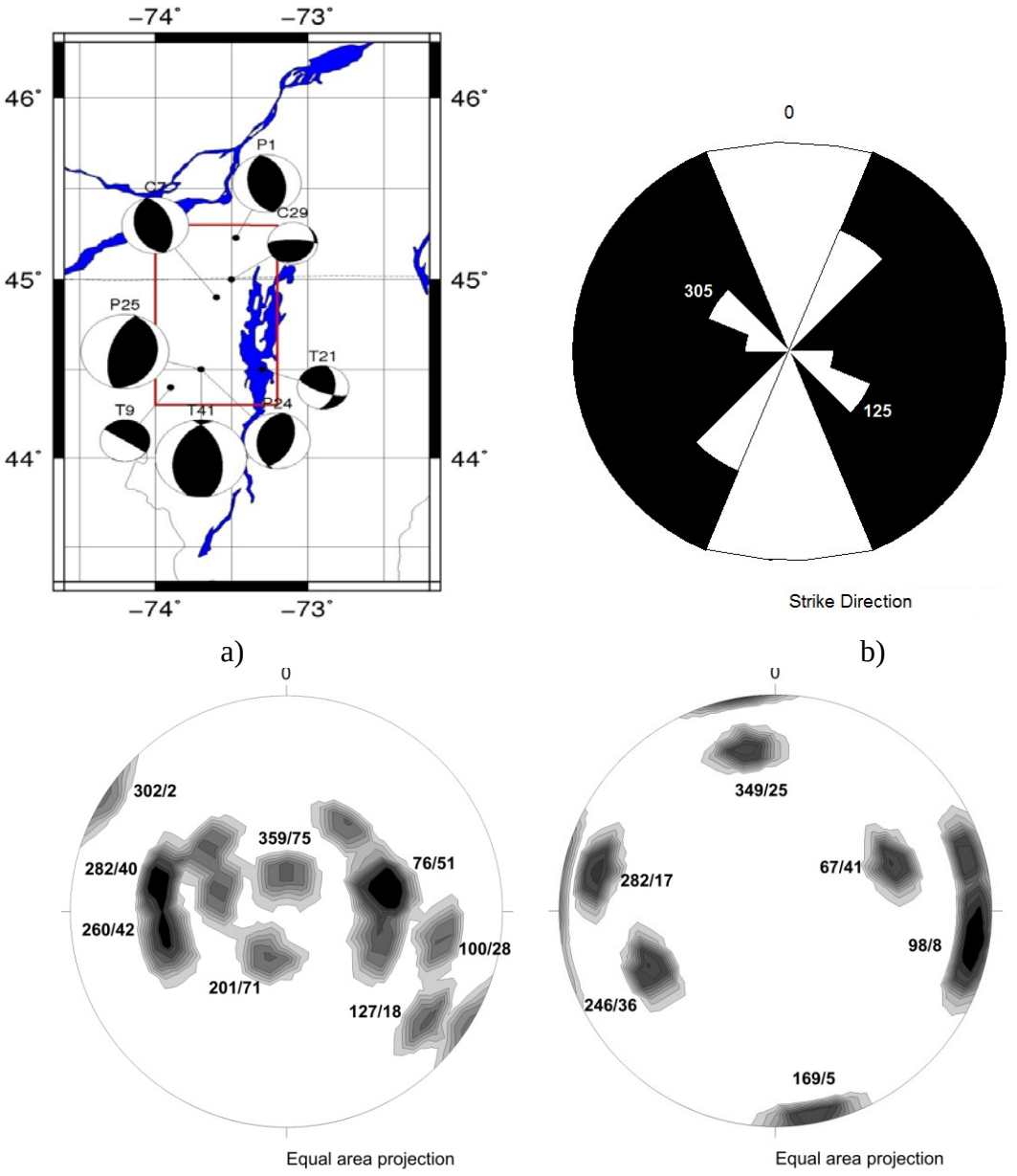

Figure 5.11: Summary of the focal mechanism parameters for the WQ4 (Adirondack) cluster. a) Fault plane solutions, b) Rose-diagram for the strike of both nodal planes, c) Distribution of the dip angle of both nodal planes, and d) Distribution of pressure (P*)* axes. The labels of the events on the map are the same as in Appendix C.

WQ5 is located in the southern part of the Adirondack. Two different nodal plane strikes are noticeable in the cluster; one with almost N-S orientation and the other with NW-SE. The dip angles in NE-SW direction vary from 22° to 70° and in the NW-SE direction vary from 44° to 50° (Fig. 5.12c). The *P*-axes indicate NE-WS orientation in average but there are variations in wide angle around it (Fig. 5.12d).

Figure 5.13 shows the tectonic setting and geologic features for the Adirondack region. As discussed above, tectonic activity in this region may be affected by a simple buttressing effect of weak Palaeozoic rocks against Precambrian shield rocks. This buttressing orientation is consistent with the strike of events in both clusters (WQ4, WQ5) and the pressure direction is similar to the arch axis shown in E-W direction. Therefore the seismicity could be due to reactivation of pre-existing faults (such as ancient rifts) (Figures 5.13). The strike of the focal mechanisms of the events in this region is mainly in N-S direction, while local faults are mostly in NE-SW direction.

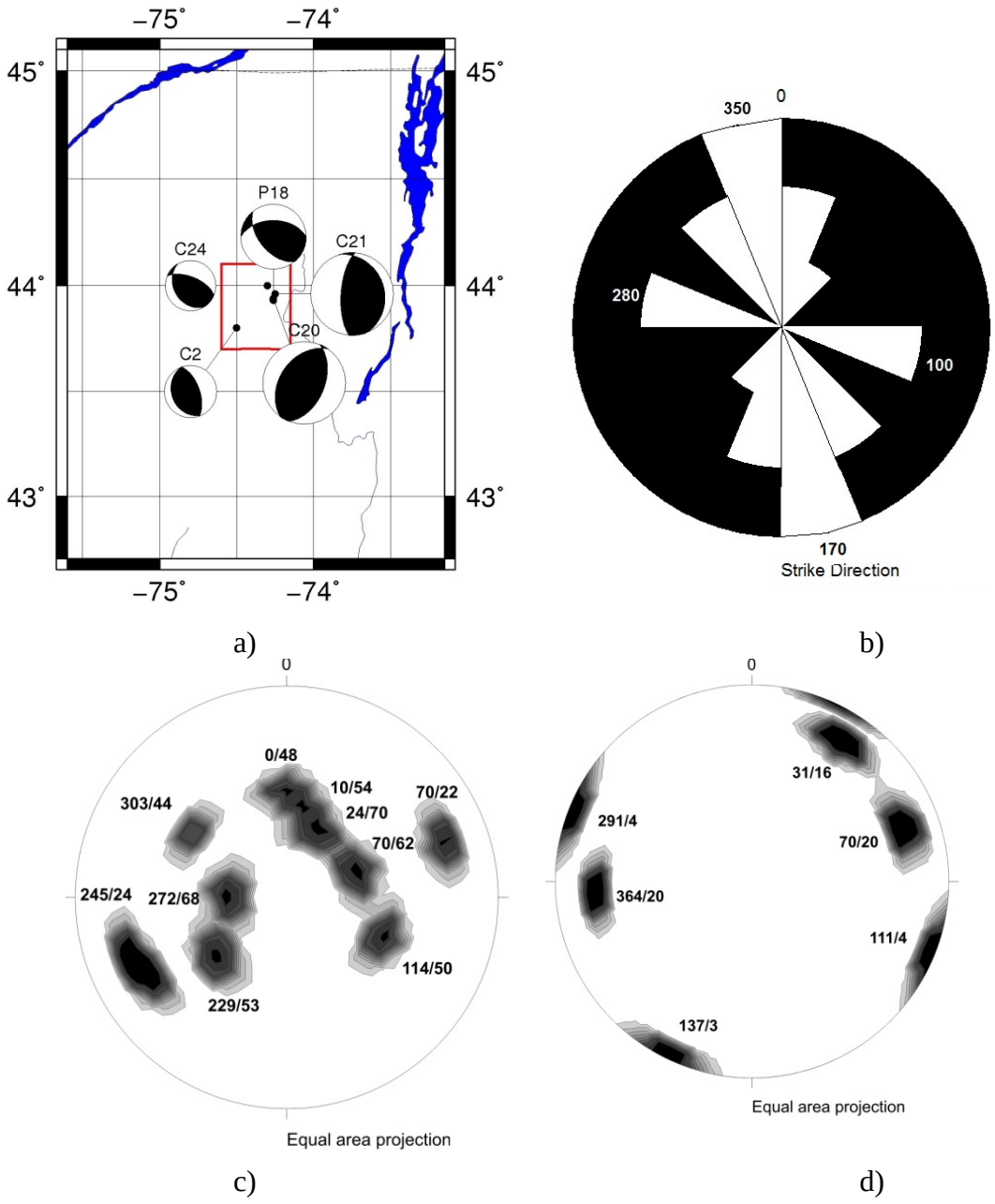

Figure 5.12: Summary of the focal mechanism parameters for the WQ5 (Adirondack) cluster. a) Fault plane solutions, b) Rose-diagram for the strike of both nodal planes, c) Distribution of the dip angle of both nodal planes, and d) Distribution of pressure (P) axes. The labels of the events on the map are the same as in Appendix C.

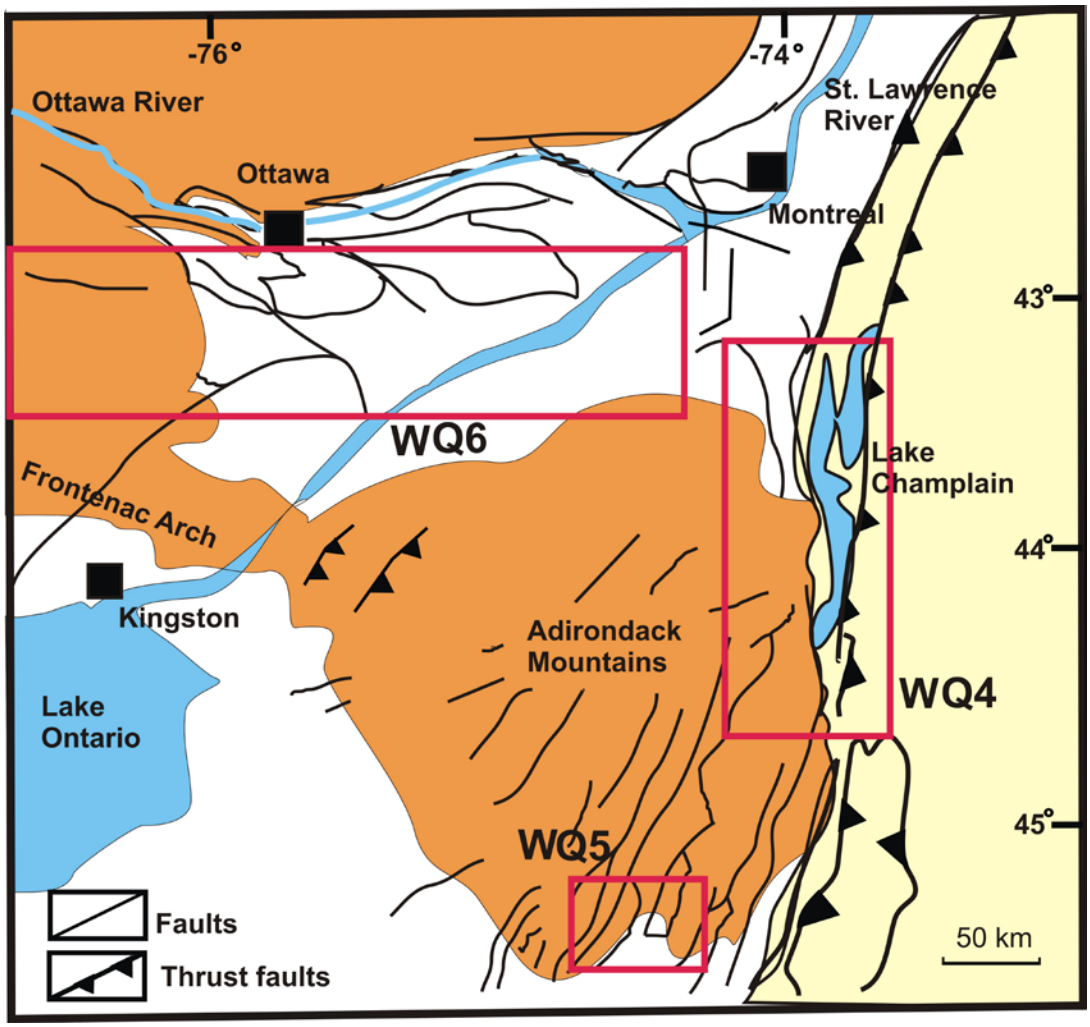

Figure 5.13: Geological features of the Adirondack region (Dix and Molgat, 1998).

5.4.4 Ottawa River Clusters (WQ6, WQ7, WQ8)

The Ottawa River clusters are located in the mid-western part of the WQSZ. The geology of the Ottawa Valley consists of Paleozoic sedimentary rocks of the Ottawa Valley-St. Lawrence Lowland regions, and Grenvillian basement consisting of metasedimentary and metavolcanic rocks intruded by plutons (1160-970 Ma) (Hewitt, 1964; Williams et al., 1992). The Ottawa graben is bounded by steeply dipping, EW- to WNW-striking faults (Rimando and Benn, 2005) (Fig. 5.5). A dense network of approximately east-west

striking faults is located in the south-eastern part of the Ottawa River (Figure 5.5). There was little information known on the seismicity of this area prior to the augmentation of the regional seismic network beginning in 2002 (POLARIS). The earthquakes in Ottawa River area is divided into three clusters: WQ6, WQ7 and WQ8 (Figure 5.3).

Cluster WQ6 is in the south-eastern part of the Ottawa River region from latitude 44.8° to 45.3°and longitude -73.8 to -75.9°. There are 15 events in this cluster with focal depths ranging from 12 km to 18 km. The 1944 Cornwall-Massena earthquake with magnitude of 5.6 m_N is the strongest event in this cluster (event T2). The fault plane of this event is oriented NNW-SSE, which is similar to the strike of most of the events in this cluster (Figure 5.14). Most of the events have reverse type focal mechanism; some of them yield a small strike-slip component. There is one event of a normal type. The rose diagram for the strike of the nodal planes in this cluster shows predominantly NW-SE orientation (~ 124°-304°) but there are nodal planes striking almost N-S (~10-190°) and ENE-WSW. Only the NW-SE oriented nodal planes are consistent with the fault orientation on Figure 5.5 and Figure 5.13. The dip angles of the nodal planes are smaller (~27°) in NNW direction, and vary between 41° and 48° for all other deractions. There are some nodal planes with dip angle around 71° (in N direction).

WQ7 is located in the northern part of the Ottawa River region from latitude 45.5 to 46.15°and longitude -74.9 to -77.7° with 12 events. The Focal depths of the events are mainly between 16 km to 26 km. The 2010 Val-de-Bois earthquake (m_N 5.7) is the strongest event in this cluster. Most of the events have reverse type focal mechanisms. There are a few events of predominant strike-slip type. The strongest event here and most other events have NW-SE strike (~124°-304°) (Figure 5.15b). This orientation is

consistent with regional fault map (Figure 5.5). The dip angles vary widely between 20 and 90° (Figure 5.15c). P-axes for the events are mostly in NE direction.

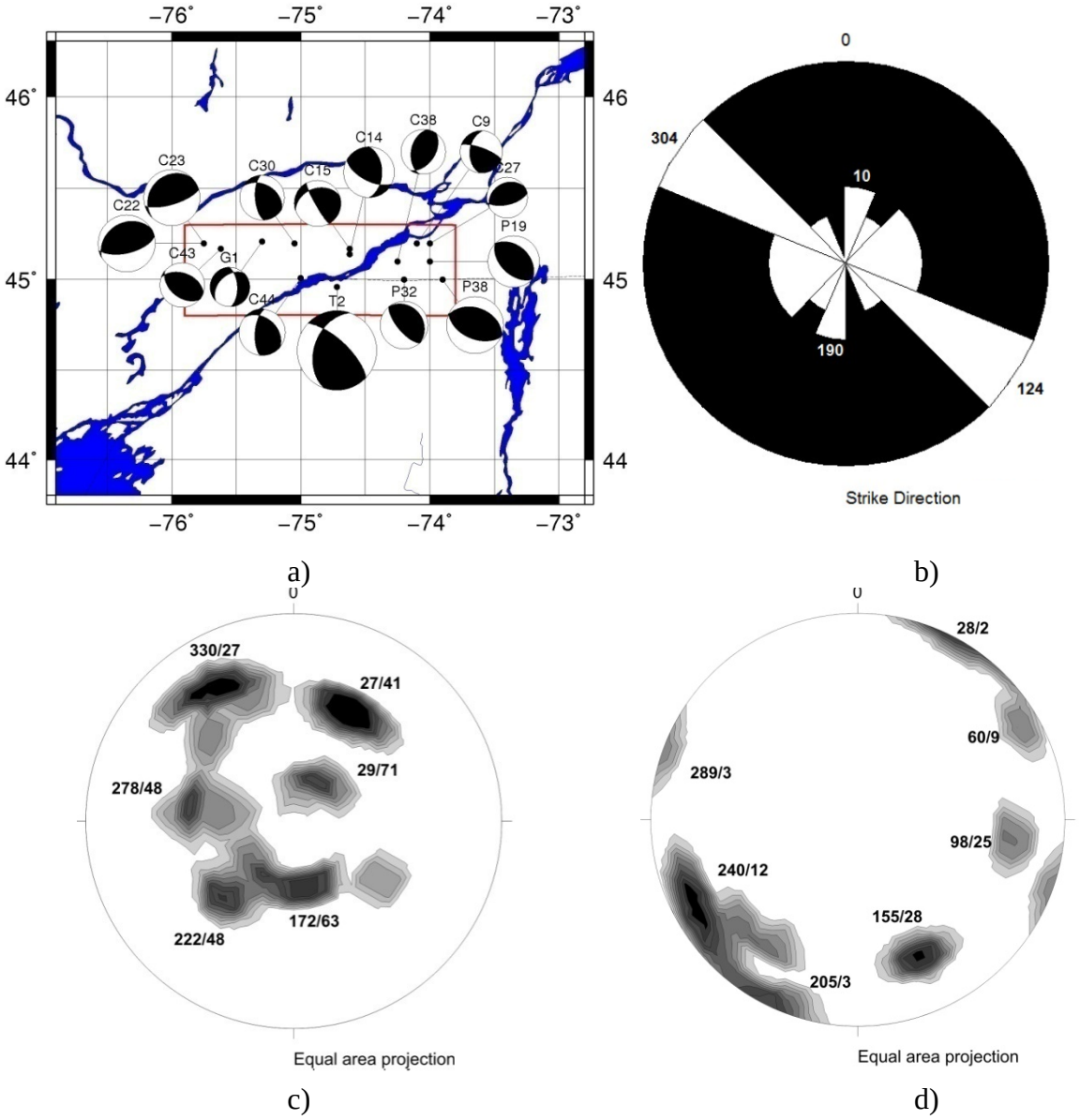

Figure 5.14: Summary of the focal mechanism parameters for the WQ6 (Ottawa River) cluster. a) Fault plane solutions, b) Rose-diagram for the strike of both nodal planes, c) Distribution of the dip angle of both nodal planes, and d) Distribution of pressure (P) axes. The labels of the events on the map are the same as in Appendix C.

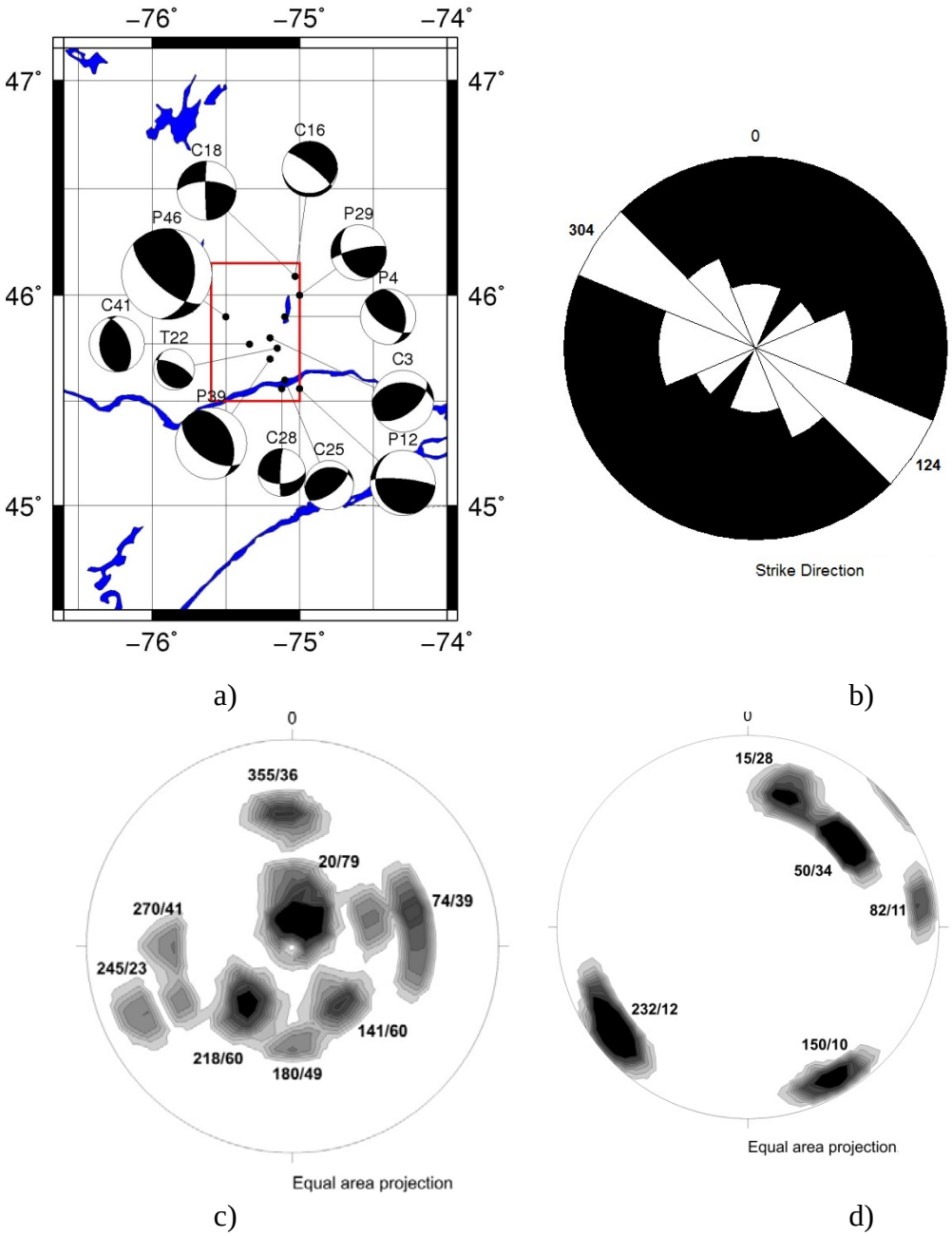

Figure 5.15: Summary of the focal mechanism parameters for the WQ7 (Ottawa River) cluster. a) Fault plane solutions, b) Rose-diagram for the strike of both nodal planes, c) Distribution of the dip angle of both nodal planes, and d) Distribution of pressure (P) axes. The labels of the events on the map are the same as in Appendix C.

WQ8 is locatedin the north-western part of the Ottawa River from latitude 45.5 to 46.4° and longitude -77.5 to -76.3° with five events at focal depths ranging from 13 to 26 km. The events in this cluster to the north of the Ottawa River have different focal mechanism (reverse type) from those to the south of it (normal type). (Figure 5.16a). The events to the north of the river show mainly NW-SE strike for the nodal planes, while two events to the south of the river have almost N-S strike and one event E-W strike. Comparison of the strike of the nodal planes with the geological features in this area shows that most of the events have the same strike as the faults within the region (Figure 5.5). Exceptionally, a few events have a N-S strike. The dip angles vary widely between 24° and almost 80°. The P-axes show diverse orientation but most of them are sub-horizontal with trends varying from N-S to E-W. The regional stress field is oriented in NE-SW in this region which is comparatively similar to the average trend of P-axes of the WQ6, WQ7, and WQ8 in the study area.

Comparison of the focal plane solutions (Figures 15.16) and the faults within this region (Figure 5.5) indicates that seismicity in this area could be related to reactivation of faults, although many researchers link the seismicity to the Great Meteor Hotspot Track (e.g., Crough, 1981).

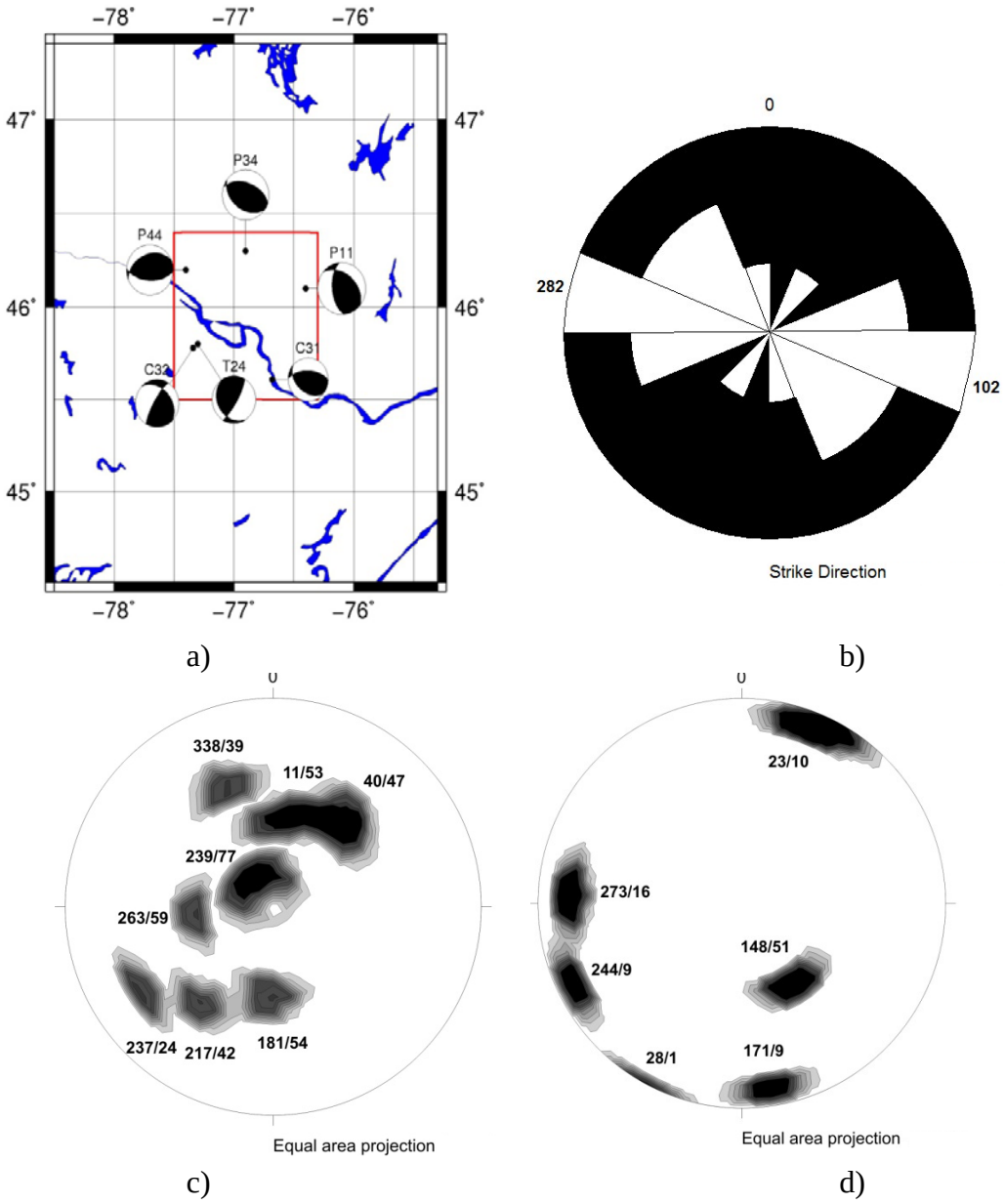

Figure 5.16: Summary of the focal mechanism parameters for the WQ8 (Ottawa River) cluster. a) Fault plane solutions, b) Rose-diagram for the strike of both nodal planes, c) Distribution of the dip angle of both nodal planes, and d) Distribution of pressure (P) axes. The labels of the events on the map are the same as in Appendix C.

5.4.5 Timiskaming Cluster (WQ9)

The Timiskaming cluster, which partly lies in eastern part of the western Quebec seismic zone, covers an area from latitude 46° to 47.5° and latitude -78 to -79.5° and contains five events with focal depth of 10 km to 18 km. The epicentre of the 1935 M6.2 earthquake is located in this cluster. The north-western part of this cluster coincides with a 15-km thick wedge of supracrustal rocks (The Huronian Supergroup) that records pre 2.1 Ga rifting and subsequent establishment of a passive margin along the southern edge of the Superior craton (Frederiksen et al., 2006).

Figure 5.17 shows the fault plane solutions for the earthquake events in this cluster. Most of the events have reverse-sense focal mechanisms with NW striking nodal planes (~125- 325°). The nodal planes in this cluster dip at angles from 26 to 43° in N-E direction and from 10 to 58° in S-W direction (Figure 5.18c). Focal mechanisms within this cluster (Figure 5.17d) reveal a fairly coherent pattern of northeast-southwest trending P-axes consistent with the overall regional stress field (Figure 5.22). The nodal planes generally indicate thrust or oblique thrust strike-slip faulting, and most solutions have at least one northwest-striking nodal plane. The characteristics of the WQ9 cluster differs from the characteristics of the other clusters (Mont Laurier, Adirondack). For example, this cluster is characterized by a lower Gutenberg-Richter *b* value (0.56) than the other clusters (0.83) (Ma and Atkinson, 2006).

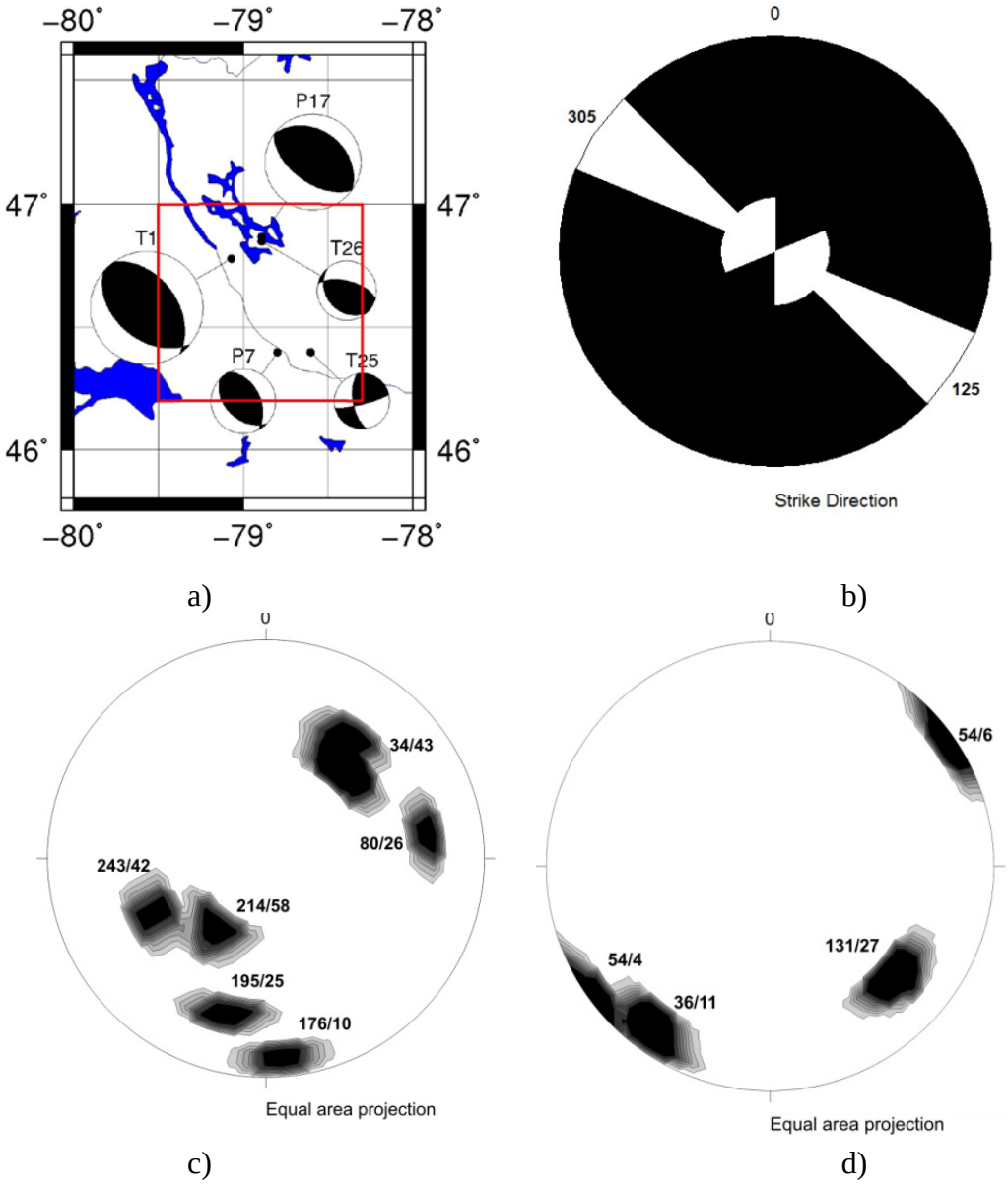

Figure 5.17: Summary of the focal mechanism parameters for the WQ9 (Timiskaming) cluster. a) Fault plane solutions, b) Rose-diagram for the strike of both nodal planes, c) Distribution of the dip angle of both nodal planes, and d) Distribution of pressure (P) axes. The labels of the events on the map are the same as in Appendix C.

The known faults in WQ9 cluster are shown in more details in Figure 5.18. The strike of the nodal planes in this cluster is consistent with the mapped faults that make up the Timiskaming graben (Bent, 1996b). The most obvious northwest trending features in the region are the Ottawa River and Lake Timiskaming, from which the rivers flows. These features were considered to be part of the St. Lawrence Rift System (Kumarapeli and Saull, 1966). Seismicity in this region is compatible with faulting on these reactivated rift structures.

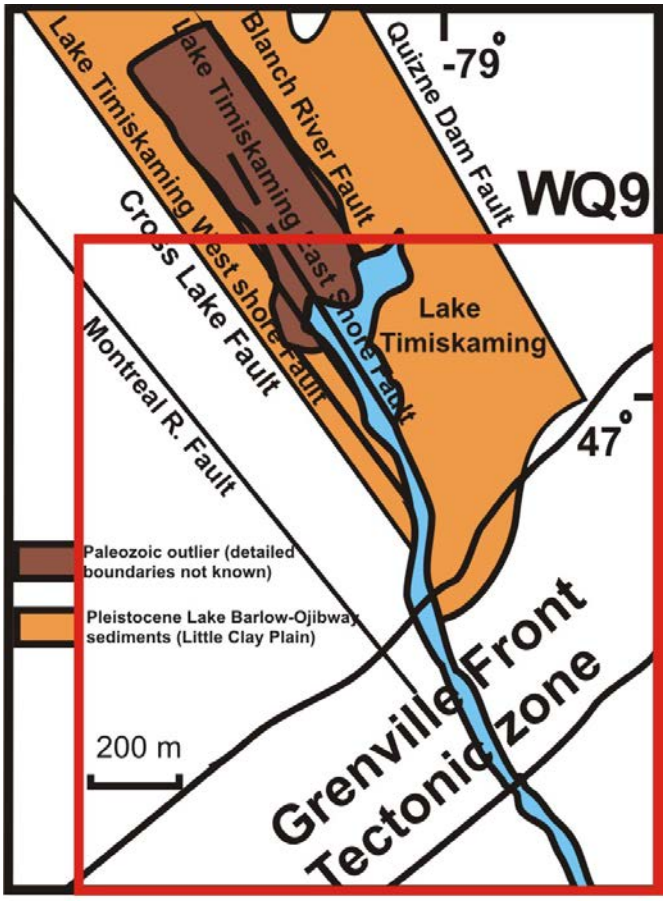

Figure 5.18: Fault map around Timiskaming cluster (modified from Lovell and Caine, 1970; Dix et al 2007).

5.4.6 Southern Ontario cluster (ON1) (The Burlington-Niagara Falls Cluster (BNFC))

The Burlington-Niagara Falls (ON1) cluster also known as the Western Lake Ontario cluster is located in the west end of Lake Ontario from latitude 43.3 to 44° and longitude -77° to -79.5°. This area is structurally underlained by the northeast striking relatively shallow southeast-dipping thrust faults of the Grenville orogen (Easton, 1992). The seismicity in Lake Ontario has been characterized by Stevens (1994) as "intermittent scattered" based on the available data at that time but other researchers have attributed apparent linear trends of seismicity (e.g., Mohajer et al., 1992; Mohajer, 1993, 1995a,b; Wallach et al., 1998; Dineva et al, 2004).

Eight earthquakes, with magnitude of $m \geq 3.5$ were recorded in this region after 1992. Focal mechanisms for the Western Lake Ontario cluster are typically oblique with pressure orientation almost NNE and NE. The focal depth of the events in this cluster varies from 5 km to about 10 km depth. Figure 5.20 shows the distribution of the major faults and geological structures in southern Ontario. The nodal planes in this cluster dip at angles from 66 to 77° in E-S direction and 45° in N direction (Figure 5.19c). The orientation of the major horizontal principal stress, estimated from the focal mechanisms in this region differs from the direction of regional tectonic field. The orientation of the P-axes varies from EES to WWN direction. The compressive stress field instead appears to be oriented sub-parallel to the major terrain boundaries such as the Grenville Front, the Central Metasedimentary Belt boundary zone and the Elzevir Frontenac boundary zone. This suggests that the stress field has been modified by these deep crustal scale deformation zones (Baird & McKinnon, 2007).

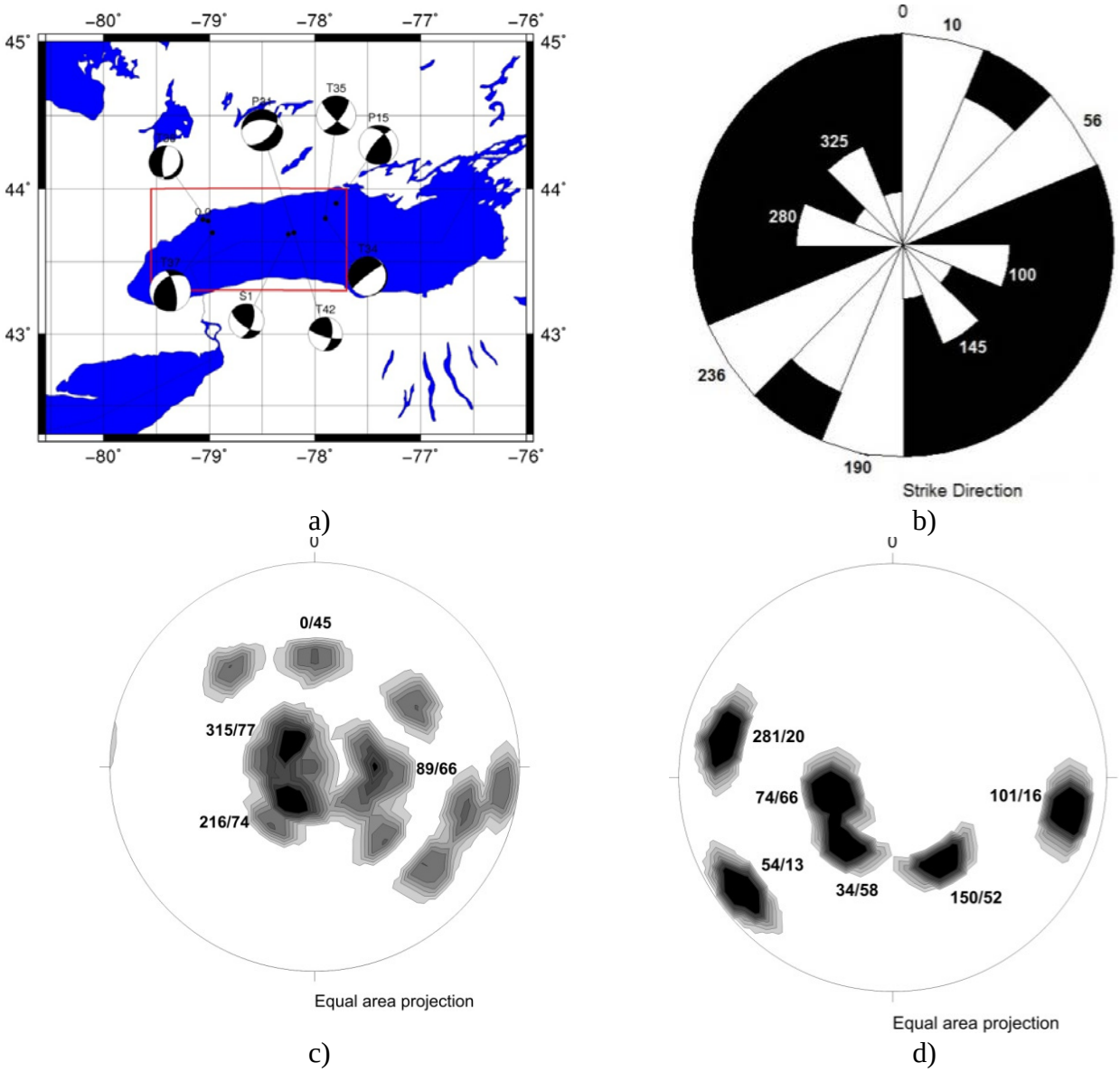

Figure 5.19: Summary of the focal mechanism parameters for the ON1 (Burlington-Niagara Falls Cluster) cluster. a) Fault plane solutions, b) Rose-diagram for the strike of both nodal planes, c) Distribution of the dip angle of both nodal planes, and d) Distribution of pressure (P*)* axes. The labels of the events on the map are the same as in Appendix C.

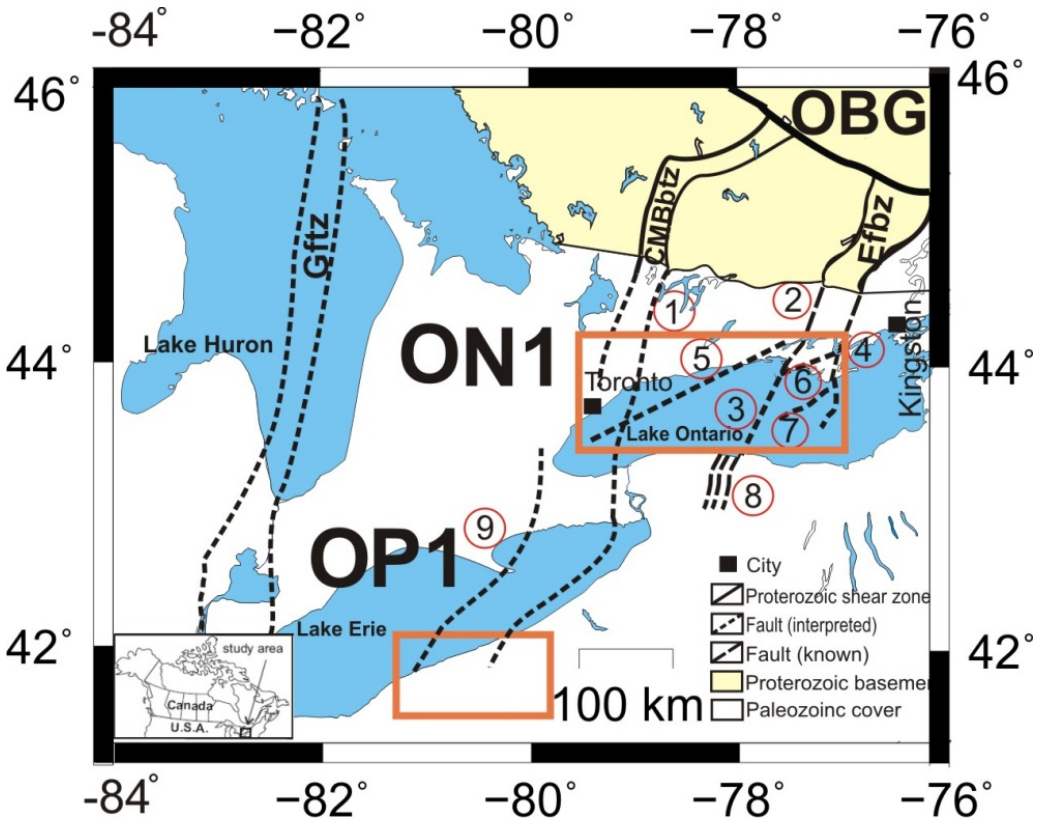

Figure 5.20: Simplified tectonic map of the southern Ontario. No. 1, Niagara Pickering linear zone; 2, Salmon river Fault; 3, Scotch Bonnet Rise; 4, Picton Fall; 5, Hamilton Presqu-ile Lineament; 6, Wellington Fault; 7, Salmon Point Fault; 8, CLF- Clarendon-Linden Fault; 9, Hamilton-Lake Erie magnetic lineament; OBG, Ottawa Bonnechere garben; GFTZ-Grenville front tectonic zone; CMBbtz, Central Metasedimentry Belt boundry tectonic zone; EFbz, Elzevir Frontenac boundary zone; (compiled from Baird 2010; Ontario Geological survey 1991; McFall 1993).

5.4.7 Ohio-Pennsylvania Cluster (OP1)

The Ohio-Pennsylvania border or Northeast Ohio (OP1) cluster is located south of Lake Erie from latitude 41.3 to 42.1° and longitude -79.9 to -81.5°. From 1992-2011 there were six earthquakes with magnitude higher than 3.5 and focal depth of 5 to 10 km

recorded within this cluster. As it can be seen from Figure 5.21, most of the events have oblique-slip focal mechanisms. The dip angles of the nodal planes in this cluster are 38° to 58° in NW-SE direction and 34° to 71° in NE-SW direction (Figure 5.21c). The pressure axes varies from E-W to EES orientations. (Figure 5.21d), similar to the northeast strike of the boundary zones dividing the main tectonic segments of the Grenville province (the GFtz, CMBbtz, and EFbz) (Easton, 1992). Seismicity in this region is compatible with reactivation of pre-existing fault zones in this zone (Figure 5. 20).

A comparison of the strike of the nodal planes for all clusters in the study area and the known tectonic features is shown in Figure 5.22. As discussed in details the general average strike of focal mechanisms of the events in southeastern part of the Western Quebec seismic zone is N-S, which is compatible with the faults and other pre-existing shear zones in this area. For the rest of western Quebec, the strike of the focal mechanisms is generally in NW-SE direction, which is also compatible with local faults and structures in most cases, as discussed above. For southern Ontario, the strike of the focal mechanisms of the events is mostly in N-S to NE-SW. This is consistent with the direction of major shear zones in this area. As the structural dip can affect both the depth and epicentres of the earthquakes they may line up on the surface but not at depth. For comparison of the hypocentre locations with the faults in depth there will be necessary to have more high-quality hypocentres. This discussion is based on a limited number of earthquakes studied here, and more detailed analyses with larger earthquake database is required to define if there is a correlation between the hypocentre locations and the faults.

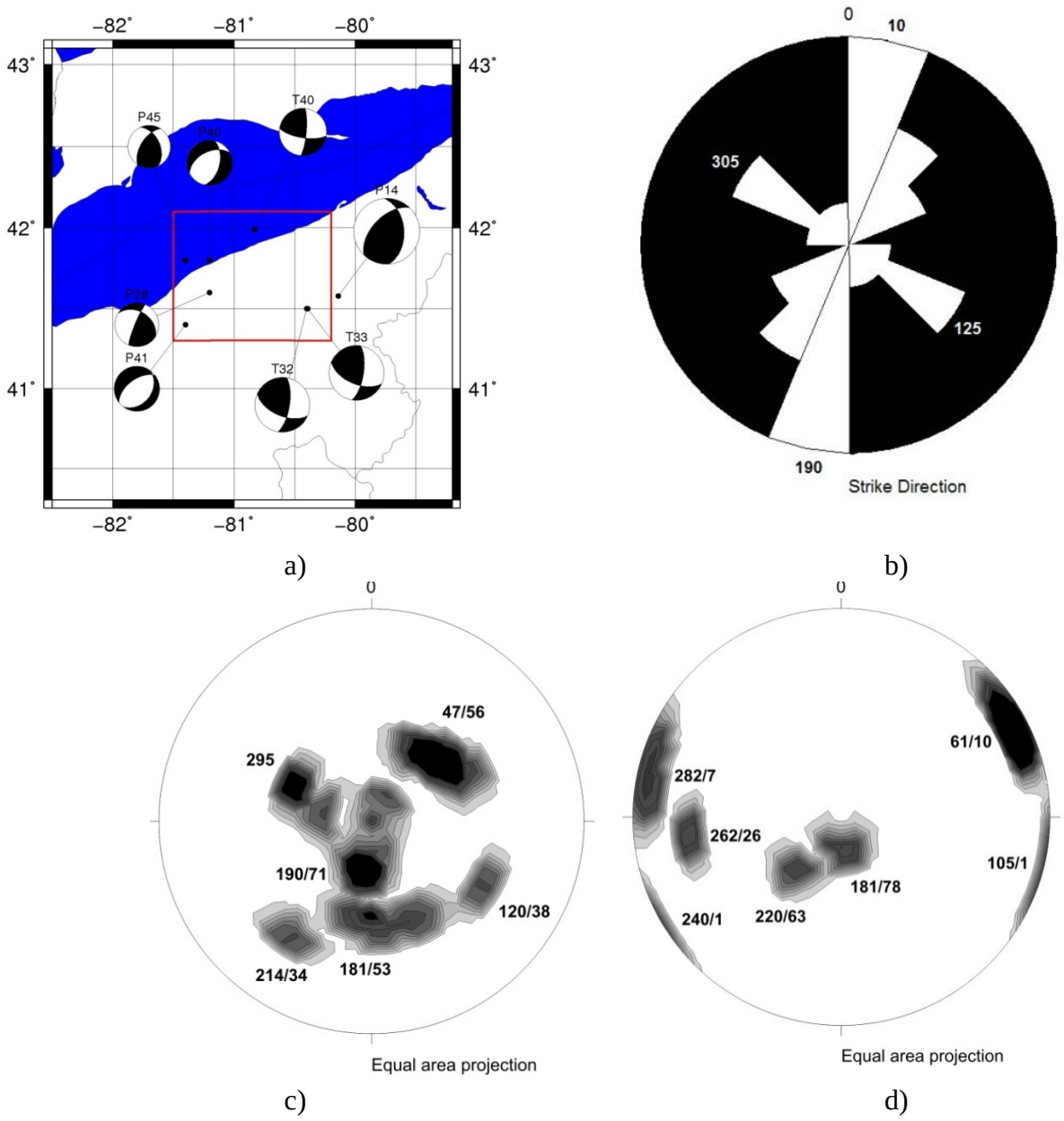

Figure 5.21: Summary of the focal mechanism parameters for the OP1 (Ohio-Pennsylvania) cluster. a) Fault plane solutions, b) Rose-diagram for the strike of both nodal planes, c) Distribution of the dip angle, and d) Distribution of pressure (P) axes. The labels of the events on the map are the same as in Appendix C.

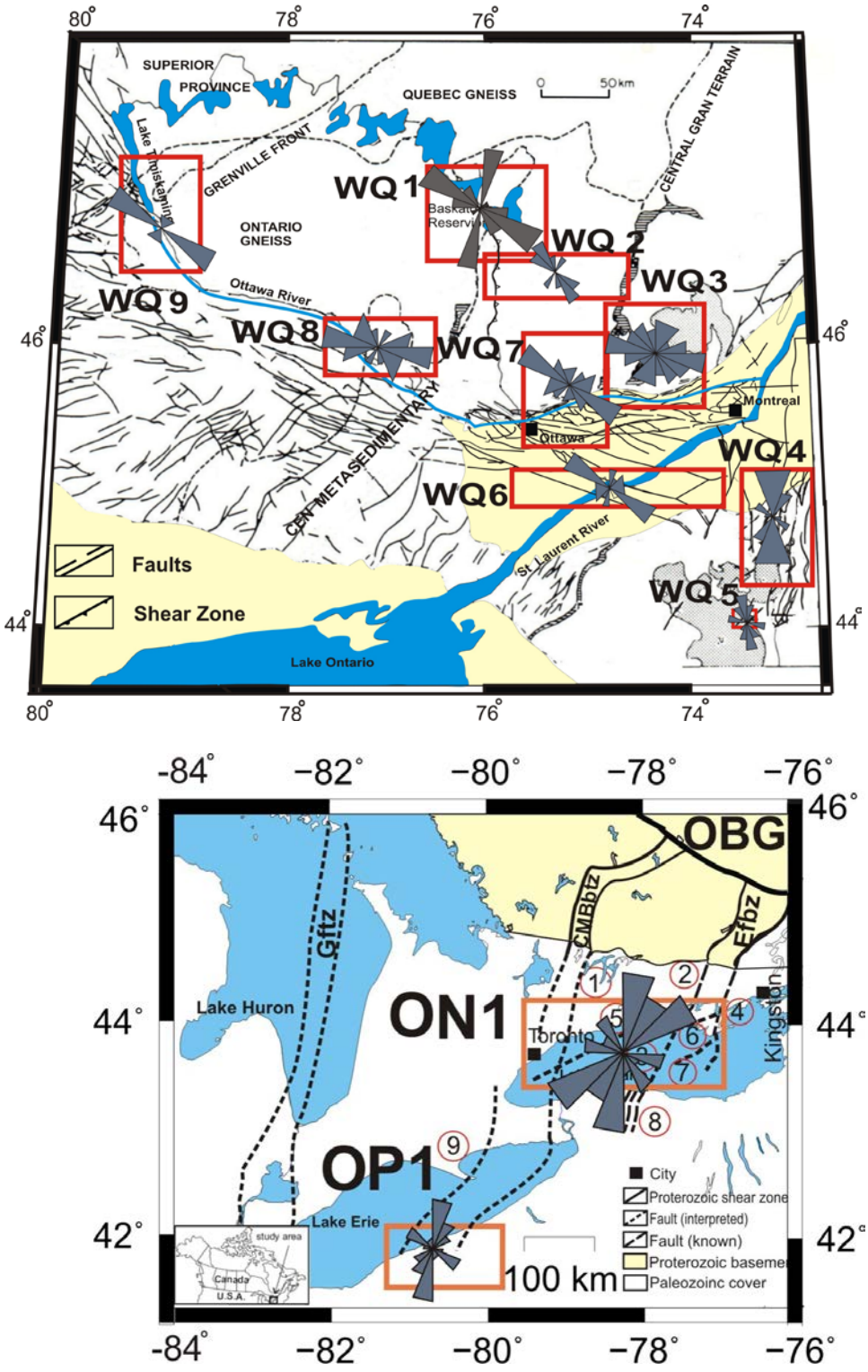

Figure 5.22: Nodal plane strike for all clusters in the study area compared to the known tectonic features; a) Plane strike in western Quebec; b) Plane strike in southern Ontario (tectonic maps compiled from Forsyth, 1981; Baird, 2010; Ontario Geological survey 1991; McFall, 1993).

CHAPTER 6

CONCLUSIONS AND RECOMMENDATIONS

6.1 Conclusions

This study focused on the seismicity of southern Ontario and western Quebec through detailed studies of earthquakes with magnitude over 3.5 between 1992 and 2011 and combining these new data with data previously published. The parameters (hypocentre locations and focal mechanisms) of 50 earthquakes with magnitude m_N 3.5 - 5.7 were determined. Earthquake source parameters were determined using data from all possible seismic stations in Canada and the US. The earthquake source parameters like nodal plane orientation, focal depth, and compression orientation were compared with the available tectonic and geological data. The conclusions from this study can be summarized as follows:

- Most of the events in western Quebec seismic zone are concentrated along the Ottawa River and Montreal-Maniwaki region. There is no obvious concentration of earthquake epicentres in the northwest and southeast regions of the western Quebec Seismic Zone. In southern Ontario most of the earthquakes appear to be

restricted to western Lake Ontario or along the Ottawa river and along the Ohio-Pensylvania border within a cluster south of Lake Erie.

- The focal depth for all earthquakes in the study area is less than 30 km. The focal depth of the Western Quebec events appears greater than that of the Southern Ontario seismic zone. All 16 events in southern Ontario occurred at shallow depths less than 19 km. The western Quebec events, however, are generally deeper, with depths from 18 to 30 km. The median depth of events is 8.2 km for the southern Ontario seismic zone and 20 km for western Quebec seismic zone.
- Among the 50 events studied, 29 are thrust fault events and 21 have focal mechanisms that are predominantly strike-slip with a small component of dip-slip movement. In terms of regional distribution, almost all events in the WQSZ have a reverse-sense focal mechanism with some spatial variability in the nodal plane orientation. Events in southern Ontario and more specifically in Lake Ontario and south of Lake Erie are mainly of strike-slip character. The dipping angle of the nodal plane in Western Quebec varies around 45° towards NE-SW, but in Southern Ontario it is around 50° towards NW-SE.
- The average orientation of the compression (P) axes for western Quebec was found to be almost NE-SW and for southern Ontario NW-SE, which are consistent with previous studies.
- Investigation of such parameters as density of the epicentres, focal depths, and type of the focal mechanism as well as tectonic setting in both the western Quebec and the southern Ontario suggest some distinct seismic clusters. Using a simple statistical approach (Dineva et al. 2004; Ma and Eaton, 2007), nine distinct

clusters have been outlined for western Quebec, one in southern Ontario, and one in Pennsylvania. The seismic characteristics of each cluster including focal mechanism solutions, the maximum compressive stress directions inferred from FMS, and relationship between seismicity and pre-existing tectonic settings were studied. The locations and characteristics of seismicity clusters appear to be consistent with the hypothesis that they are mainly near the locations of pre-existing faults or shear zones.

- The orientation of the nodal planes and P-axes varies from cluster to cluster within the same seismic zone. The orientation of P-axes varies from N019 to N274° for WQSZ and from ~N110° to N280° for southern Ontario.

- The results in this study show more detailed variations in the compression orientation compared to the results obtained by Mazzotti and Townend (2010) for Western Quebec.

6.2 Recommendations

This thesis provides an insight to our understanding of relationship between seismicity and tectonic features in western Quebec and southern Ontario. Source parameters of recent earthquakes have been analyzed and a possible link between the earthquakes and tectonics in the region was proposed. However, there is still room for more detailed investigations. Due to the large study area, it was not possible to discuss these relations in details.

More detailed look at the relationship between earthquake focal mechanisms and geologic features in each of the clusters discussed in this study will complement this research and provide a comprehensive understanding of the earthquake occurrence mechanisms.

Some statistics of the pressure and tension axes was obtained in the study and the orientation of the pressure axes was compared with the regional stress field. The results from this study can be used for a stress inversion to obtain the local variations in the stress field (principal stresses). Future detailed analysis could clarify the influence of different factors, e.g. the structural weaknesses (e.g., pre-existing faults or shear zones) on the variations of the stress field.

This study focused on earthquakes with magnitude 3.5 and above (up to $5.7m_N$). Future analysis of earthquakes with magnitude below 3.5 would complement this research and can give even more detailed picture of the local variations of the stress field.

7. REFERENCES

Adams, J. and Basham, P. (1989). The seismicity and seismotectonics of Canada east of the Cordillera. Geos. Ca., 16**,** 3-16.

Adams, J. and Basham, P. (1991). The seismicity and seismotectonics of eastern Canada. In Slemmons, D. B., Engdahl, E. R., Zoback, M. D and Blackwell, D. D, eds., Neotectonics of north America, p.261-275. Geol. Soc. Am., Boulder, Colorado, United States.

Adams, J., and Halchuk, S. (2003). Fourth generation seismic hazard maps of Canada: values for over 650 Canadian localities for the 2005 National Building Code of Canada. Geol. Surv. Can., Open File, 4459, 155.

Adams, J., Sharp, J., and Stagg, M. C. (1989). New focal mechanisms for southeastern Canadian earthquakes. Geol. Surv. Canada Open File.

Adams, J. (1989). Crustal stresses in eastern Canada. In: Gregerson, S., Basham, P. W. (Eds), Earthquakes at North Atlantic passive margins: neotectonics and postglacial rebound. Kluwer academic publishers, Boston, 355-370.

Adams, J. (1995). The Canadian crustal stress database a compilation to 1994. Geol. Surv. Can., Open File. 3122, 226.

Adams, J. and Basham, P. (1991). The seismicity and seismotectonics of eastern Canada. Neotectonics of North America (Edited by Slemmons, D.B., Engdahl, E.R., Zoback, M.D., & Blackwell, D.D.), 261-276.

Armbruster, J. G., Barton, H., Bodin, P., Buckwalter, T. F., Cox, J., Cranswick, E., Dewey, J., Fleeder, G. M., Hopper, M., Horton, S., Hoskins, D., Kieb, D., Meremonte, M., Metzger, A., Risser, D. W., Seeber, L., Shedlock, K., Stanley, K., Withers, M., and Zirbes, M. (1998). Preliminary results from the investigation of the Pymatuning earthquake of September 25. Geology, 29, 2–14.

Arnold, R., and Townend, J. (2007). A Bayesian approach to estimateing tectonic stress from seismological data. Geoph. J. Inter., 170, 1336_1356.

Aylsworth, J. M., Lawrence, D. E., and Guertin J. (2000). Did two massive earthquakes in the Holocene induce widespread landsliding and near-surface deformation in part of the Ottawa Valley Canada. Geology, 28, 903-906.

Baird, W.A. F. (2010). Crustal stress and seismicity in intraplate setting: relationship to geology and driving forces. Thesis. Ph.D. Queen's university 2010.

Baird, W.A. F., and McKinnon, S. D. (2007). Linking stress field deflection to basement structures in southern Ontario: results from numerical modeling. Tectonophysics, 432, 89-100.

Baird, A. F., McKinnon, S. D., and Godin, L. (2009). Stress channelling and partitioning of seismicity in the Charlevoix seismic zone, Quebec, Canada. Geoph. J. Intern., 179(1), 559-568.

Barosh, P.J. (1986). Neotectonic movement, earthquakes and stress state in the eastern United States. Tectonophysics, 132, 117–152.

Basham, P.W., Weicheret, D. H., Anglin, F. M., and Berry, M.J. (1982) New probabilistic strong seismic ground motion maps of Canada: a compilation of earthquake source zones, methods and results. Earth Phys., 82-33.

Basham, P. W., Weichert. D. H, and Berry. M. J. (1979). Regional asseeement of seismc risk in Eastern Canada. Bulle. Seism. Soc. Ame., 69, 1567-1602.

Bent A. L. (1996a). Source parameters of the damaging Cornwall-Massena earthquake of 1944 from regional waveforms. Bull. Seism. Soc. Am., 86, 489-497.

Bent A. L. (1996b). An improved source mechanism for the 1935 Timiskaming, Quebec earthquake from regional waveforms. Pu. App. Geoph., 146**,** 5-20.

Bent, A. L., Lamontagne, M., Adams, J., Woodgold, C. R. D., Halchuk, S., Drysdale, J., Wetmiller, R. J., Ma, S., and Dastous, J-B. (2002).The Kipawa, Quebec "Millennium" earthquake. Seism. Res. Lett., 73, 285-297.

Bent, A. L., Lamontagne, M., and Wetmiller, R .J. (1999). Two moderate earthquakes near Ste-Agathe-des-Monts, Quebec. Seism. Rese. Lett., 70.

Bent, A. L., and Perry, C. (1999). Focal mechanisms for eastern Canada earthquakes: 1 January 1996–30 June 1998. Geol. Surv. Can., Open File, 3698.

Bent, A. L., Drysdale, J., and Perry, C. (2003). Focal mechanisms for eastern Canadian earthquakes, 1994-2000. Seism. Re., Lett., 74. 452-468.

Boyce, J. I., and Morris, W. A. (2002). Basement-controlled faulting of Paleozoic strata in southern Ontario, Canada: new evidence from geophysical lineament mapping. Tectonophysics, 353, 151–171.

Buchbinder, G. G. R., Lambert, A., Kurtz, R.D., Bower, D. R., Anglin, F. M.,and Peters, J. (1988). Twelve years of geophysical research in the Charlevoix seismic zone. Tectonophysics, 156, 193– 224.

Carr, S. D., Easton, R. M., Jamieson, R. A., and Culshaw, N. G. (2000). Geologic transect across the Grenville orogen of Ontario and New York. Can. J. Earth Sci., 37, 193–216.

Chen, W.-P. (1988). A brief update on the focal depths of intracontinental earthquakes and their correlations with heat flow and tectonic age. Seism. Res. Lett., 59**,** 263–272.

Chen, W.-P., and Molnar, P. (1983). Focal depths of intracontinental and intraplate earthquakes and their implications for the thermal and mechanical properties of the lithosphere. J. Geoph. Res., 88, 4183– 4214.

Crough, S. T. (1981). Mesozoic hotspot epeirogeny in eastern North America. Geology, 9. 2-6.

Culotta, R. C., Pratt, T., and Oliver, J. (1990). A tale of two sutures: COCORP's deep seismic survey of the Grenville province in the eastern U.S. midcontinent. Geology, 18, 646-649.

Dineva, S., Eaton, D., Ma, S., and Mereu, R. (2007). The October 2005 Georgian Bay (Canada) earthquake sequence: Mafic dykes and their role in the mechanical heterogeneity of Precambrian crust. Bulle. Seism. Soc. Ame., 97, 457–473.

Dineva, S., Eaton, D., and Mereu, R. (2004). Seismicity of the Southern Great Lakes: Revised Earthquake Hypocentres and Possible Tectonic Controls. Bulle. Seism. Soc. Ame., 94, 1902–1918.

Dix, G. R., Coniglio, M., Riva, J. F. V., and Achab, A. (2007). The Late Ordovician Dawson point formation (Timiskaming outlier, Ontario): Key to a new regional synthesis of Richmondian carton. Ca. J. Earth Sci., 44, 1313-1331.

Dix, G., and Molgat, M. P. (1998). Character of the Middle Ordovician Sauk-Tippecanoe sequence boundary in the Ottawa Embayment (eastern Ontario): Possible evidence for platform-interior, Taconic tectonism. Can. J. Earth Sci., 603 – 619.

Du, w. x., Kim, w. Y. and Sykes, L. R. (2003) Earthquake source parameters and state of stress for northeastern United States and southeastern Canada from analysis of regional seismograms. Bull. Seism. Soc., 93, 1633–1648.

Dufréchou. G., Odonne, F. and Viola, G., (2011) Analogue models of second order faults genetically linked to a circular strike-slip fault system. J. Struc. Geol., 33, 1193-1205.

Easton, R. M. (1986). Geochronology of the Grenville Province, The Grenville Province. (Edited by Moore, J. M., Davison, A., and Baer, A. J). Spec. Pap. Geol. Assoc. Can., 32, 125-173.

Easton, R.M. (1992). The Grenville Province and the Proterozoic history of central and southern Ontario. Geology of Ontario. Capt. 19. Edited by Thurston, P. C., Williams, H. H., and Stott, G. M. On. Geo. Sur., especial volume 4, part 2, 714 -904.

Eaton, D. W., Adams, J., Asudeh, I., Atkinson, G.M., Bostock, M.G., Cassidy, J.F., Ferguson, I.J., Samson, C, Snyder, D.B., Tiampo, K.F. and Unsworth, M.J. (2005). Investigating Canada's lithosphere and earthquake hazards with portable arrays, EOS. Tran. Am. Geo. Un., 86, 169-176.

Eaton, D., Dineva, S., and Mereu, R. (2006). Crustal thickness and Vp/Vs variations in the central Grenville orogen (Ontario, Canada) from analysis of teleseismic receiver functions. Tectonophysics, 420**,** 223-238.

Eaton, D. W., and Fredericksen, A. (2007). Seismic evidence for convection-driven motion of the North American plate. Nature, 446, 428-431.

Ebel, J. E., Bonjer, K. P. and Oncescu, M. C. (2000), Paleoseismicity: Seismicity evidence for past large earthquakes. Seism. Res. Lett., 71, 283-294.

Ebel, J. E., and Kafka, A. L. (1991). Earthquake activity in the northeastern United States in Neotectonics of North America, D. B. Slemmons. (Edited by Engdahl, E. R., Zoback, M. D., and Blackwell, D. D.), Geol. Soc. Am., Boulder, Colorado, 277–290.

Ebel, J. E., Tuttle, M. (2002). Earthquakes in the Eastern great lakes basin from a regional perspective. Tectonophysics, 353 17-30.

Ebel, J. E. (1998). Speculations on the source parameters of the 1638 earthquake in the northeastern United States using inferences from modern seismicity, paper presented at the 70th Annual Meeting. East. Sect. Seismol. Soc. of Am., Millersville, Pa., 18–20 .

Eby, G. N. (1984). Geochronology of the Monteregian Hills alkaline igneous province, Quebec. Geology, 12, 468-470.

Faill, R. T. (1997). A geologic history of the north-central Appalachians; Part 1, Orogenesis from the Mesoproterozoic through the Taconic Orogeny. Am., Jour. Sci., 297, 551-619.

Forsyth, D.A., Milkereit, B., Davidson, A., Hanmer, S. (1994a). Seismic images of a tectonic subdivision of the Grenville Orogen beneath lakes Ontario and Erie. Can. J. Earth Sci., 31, 229–242.

Forsyth, D.A., Milkereit, B., Zelt, C.A., White, D.J., Easton, R.M., Hutchinson, D.R. (1994b). Deep structure beneath Lake Ontario: crustal scale Grenville subdivisions. Can. J. Earth Sci.,31, 255–270.

Forsyth, D. A. (1981). Characteristics of the western Quebec seismic zone. Can. J. Earth Sci.,18, 103-119.

Frederiksen, A. W., I.J. Ferguson, D. Eaton, Miong, S. K., Gowan, E. (2006). Mantle fabric at multiple scales across an Archean–Proterozoic boundary, Grenville Front, Canada. Phys. Earth Planet. Inter., 158, 240–263.

Gephart, J. W. And Forsyth, D. W. (1984). An improved method for determining the regional sress tensor using earthquake focal mechanism data; application to the San Fernando earthquake sequence. J. Geoph. Res., 89, 9305_9320

Godin, L., Brown, R. L., Dreimanis, A., Atkinson, G. M., and Armstrong, D. K. (2002). Analysis and reinterpretation of deformation on features in the Rouge River Valley, Scarborough, On. Can. J. Earth Sci. 39, 1373-1391.

Gomberg, J. S., Shedlock, K. M. and Roecker, S. W. (1990). The effect of S-wave arrival times on the accuracy of hypocentre estimation. Bull. Seism. Soc. Am, 80, 1605- 1628.

Goodacre, A. K., Bonham-Carter, G. F., Agterberg, F. P., and Wright, D. F. (1993). A statistical analysis of the spatial association of seismicity with drainage pattern and magnetic anomalies in Wetern Quebec. Tecnophysics, 217, 285-305.

Green, A. G., Milkereit, B., Davidson, A., Spencer, C., Hutchinson, D. R., Cannon, W. F., Lee, M. W., Agena, W. F., Behrendt, J. C. (1988). Crustal structure of the Grenville front and adjacent terranes. Geology, 16, 788-792.

Guillou-Frottier, L., Mareschal, J. C., Jaupart, C., Gariépy, C., Lapointe, R., and Bienfait, G. (1995). Heat flow variations in the Grenville Province, Canad., Earth Planet. Sci. Lett., 136, 447–460.

Hanks, T.C. and Kanamori, H. (1979). Moment magnitude scale. J. Geol. Res., **84** (B5), 2348–50.

Hanmer, S., Mceachern, S. (1992). Kinematical and rheological evolution of a crustal-scale ductile thrust zone, Central Metasedimentary Belt, Grenville orogen, Ontario. Can. J. Earth Sci., 29.

Harris, L.B., Rivard, B., Corriveau, L. (2001). Structure of the Lac Nominingue-Mont- Laurier region, Central Metasedimentry Belt, Quebec Grenville Province. Can. J. Earth Sci., 38.

Havskov, J., and Ottemöller, L. (2003). SEISAN package, Institute of Solid Earth. Physics, University of Bergen, Norway.

Heaman, L. M. And Kjarsgaard, B. A. (2000). Timing of eastern North American kimberlite magmatism: continental extension of the Great Meteor hotspot track? Earth Planet. Sci. Lett., 178, 253-268.

Heidbach, O., Tingay, M., Brath, A., Reinecher, J., KurfeB, D., and Muller, B. (2008).The 2008 release of the World Stress Map. URL http://www.world-stress-map.

Herrmann, R. B., (1979). Surface wave focal mechanisms for eastern North American earthquakes with tectonic implications. J. Geoph. Res., 84, 3543-3552.

Hewitt, D. F. (1964). Geological notes for maps nos. 2053 and 2054 Madoc-Gananoque area. Geological circular no. 12, Ontario department of Mines.

Hodgson, E. A. (1945). Indastrial earthquake hazard in eastern Canada. Bull. Seism. Soc. Am. 35.

Hoffman, P. F. (1988). United Plates of America, the birth of a craton: early Proterozoic assembly and growth of Laurentia . Ann. Rev. Earth Planet. Sci., 16, 543-603.

Kamo, S. L, Krogh, T. E. and Kumarapeli, P. S. (1995). Age of the Grenville dyke swarm, Ontario-Quebec: implications for the timing of Iapetan rifting. Can. J. Earth Sci, 32, 273-280.

Kay, G. M. (1942). Ottawa-Bonnechere graben and lake Ontario homocline. Bull. Geol. Soc. Am., 53, 585-646.

Kim, W.-Y., Dineva, S., Ma, S., and Eaton, D., (2006). The 4 August 2004 Lake Ontario, earthquake. Seism. Res. Lett., 77, 65–73.

Kumarapeli, P.S., Saull, V.A. (1966). The St. Lawrence Valley system: a North American equivalent of the east African rift valley system. Can. J. Earth Sci., 3.

Jacobi, R., Fountain, J. (1993). The southern extension and reactivations of the Clarendon–Linden fault system. Géographie Physique et Quaternaire, 47, 285–302.

Johnston, A. C. (1993). Average stable continental earthquake source parameters based on constant stress drop scaling. Seism. Res. Lett., 64, 261.

Lamontagne, M. (1987). Seismic activity and structural features in the Charlevoix region, Quebec. Can. J. Earth Sci., 24, 2118-2129.

Lamontagne, M. (1999). Rhelogical and geological constraints on the earthquake distribution in the Charlevoix seismic zone, Quebec, Canada. Geol. Surv. Ca. Open File, D3778, 1 CD-ROM.

Lamontagne, M., Haseggawa, H. S., Forsyth, D. A., Buchbinder, G. R., and Cajka, M. (1994). The Mont-Laurier, Quebec, earthquake of October 1990 and its seismotectonic environment. Bull. Seism. Soc. Am., 84, 1506-1522.

Lamontagne, M., Keating, P., and Perreault, S., (2003). Seismotectonic characteristics of the Lower St. Lawrence Seismic Zone, Quebec: insights from geology, magnetics, gravity, and seismic. Can. J. Earth Sci., 40, 317-336.

Lamontagne, M., Beauchemin, M., and Toutin, T., (2004). Earthquakes of the Charlevoix seismic zone. Quebec, CSEG record, 41-44.

Lienert, B. R. E (1991). Report on modifications made to Hypocentre. Institute of solid earth physics, uni. Bergen.

Lienert, B. R. E., Berg, E., and Frazer, L. N. (1986). Hypocenter: An earthquake location method using centered, scaled, and adaptively least square. BSSA, Vol 76, 771-783.

Lienert, B. R. and Havskov, J. (1995). A computer program for locating earthquakes both locally and globally. Seism. Res. Lett., 66, 26–36.

Lovell, H. L., and Caine, T.W. (1970). Lake Timiskaming rift valley. Minens Misc, 39, 1-16

Ludden, J., and Hynes, A. (2000). The Lithoprobe Abitibi-Grenville transect: two billion years of crust formation and recycling in the Precambrian Shield of Canada. Can. J. Earth Sci., 37, 459–476.

Ma, S. (2009). Seismicity and seismotectonics in eastern Canada and vicinity. Ph. D. Thesis**,** Uni. Western Ontario.

Ma, S., and Eaton, D. (2007). Western Quebec seismic zone (Canada): clustered, mid-crustal seismicity along a Mesozoic hotspot track. J. Geoph. Res., 112.

Ma, S., and Eaton, D. (2009). Anatomy of a small earthquake swarm in southern Ontario. Can. J. Earth Sci., 80, 222 -231.

Ma, S., and Atkinson, G. M. (2006). Focal Depths for Small to Moderate Earthquakes (mN _2.8) in Western Quebec, Southern Ontario, and Northern New York. Bulle. Seism. So. Ame., 96, 609–623.

Ma, S., and Adams, J. (2002). Estimation of moment tensor for moderate earthquakes in eastern Canada and its vicinity by modeling surface waveforms,.internal report, Nat. Resour. Can., 110.

Maceira, M., Ammon, C. J., and Herrmann, R. B. (2000). Faulting parameters of the September 25, 1998 Pymatuning, Pensylvania earthquake. Seism. Res. Lett., 71. 742-752.

Mareshal, J., and Zhu, P. D. (1989). Focal mechanisms of small earthquakes and the stress field in the western Quebec Adriondack region. Tectonophysics, 166, 163-174.

Mareschal, J.C., Jaupart, C., Gariepy, C., Cheng, L.Z., Guillou-Frotier, L., Bienfait, G., and Lapointe, R. (2000). Heat flow and deep thermal structure near the southeastern edge of the Canadian Shield. Can. J. Earth Sci., 37, 399–414.

Martignole, J., and Calvert, A. J. (1996). Crustal-scale shortening and extension across the Grenville province of western Quebec. Tectonics, 15, 376-386.

Mazzotti, S. and Townend, J. (2010). State of stress in central and eastern North American seismic zones. Lithosphere, 2, 76-83.

McFall, G.H. (1993). Structural elements and neotectoic of Prince Edward Country, southern Ontario. Geograph. Phys. Quater., 47(3), 303-312.

McHone, J. G. (1996). Constraints on the mantle plume model for Mesozoic alkaline intrusions in northeastern North America. Can. Mineral., 43, 325-334.

McKenzie, D.P., (1969). Speculations on the consequences and causes of plate motions. Geoph., 18, 491-514.

Mereu, R. F., Asmis, H. W., Dunn, B, Brunet, J, Eaton, D, Dineva, S, and Yapp, A. (2002). The seismicity of Western Lake Ontario Area: results from the Southern Ontario Seismic Network (SOSN). Seism. Res. Lett., 73, 534-551.

Mereu,R.F. (2003a). A user friendly computer program to display and analyze POLARIS earthquake data. Eastern Section of the Seism. So. Ame.

Mereu, R.F. (2003b). Simulating a mechanical pen recorder with a computer Program. Seism. Res. Lett., 74, 44-45.

Milkereit, B., Forsyth, D.A., Green, A.G., Davidson, A., Hanmer, S., Hutchinson, D.R., Hinze, W.J., Mereu, R.F. (1992). Seismic images of a Grenvillian terrane boundary. Geology, 20, 1027– 1030.

Michael, A. J. (1984). Determination of stress from slip data: faults and folds. J. Geoph. Res., 89, 11517_11526.

Mohajer, A. A. (1993). Seismicity and seismotectonics of western Lake Ontario region. Geogr. Phys. Quat., 47, 353–362.

Mohajer, A., Eyles, N., and Rogojina, C. (1992). Neotectonic faulting in metropolitan Toronto: implications for earthquake hazard assessment in the Lake Ontario region. Geology, 20**,** 1002–1006.

Mohajer, A. A. (1995a). Faults in the metropolitan Toronto area; active vs dormant faults, in Program, List of participants and abstracts from the Atomic Energy Control Board Workshop of Seismic Hazard Assessment in Southern Ontario. Ottawa, Ontario, 19–21 June 1995, INFO-0604-1, C61–C74.

Mohajer, A. A. (1995b). Local seismic monitoring east of Toronto, in Program, List of participants and abstracts from the Atomic Energy Control Board Workshop of Seismic Hazard Assessment in Southern Ontario. Ottawa, Ontario, June 1995, INFO-0604-1.

Morgan, W. J. (1983). Hotspot tracks and the early rifting of the Atlantic. Tectonophysics, 94, 123-139.

Natural Recourses Canada: http://www.earthquakescanada.nrcan.gc.ca/zones/eastcan-eng.php#SGLSZ

Nguyen, B. V., and Herrmann, R. B. (1992). Determination of source parameters for centeral and eastern North America earthquakes (1982-1986). Seism. Res. Lett., 63.

Nuttli, O.W. (1973) Seismic wave attenuation and magnitude relations for eastern North America, J. Geophy. Res. 78, 876-885.

Ontario Geological Survey. 1991. Bedrock geology of Ontario, southern sheet. On. Geo. Sur., Map 2544, scale 1: 1 000 000.

Parsons, B., and Scalter, J. G. (1977). An analysis of the variation of ocean floor bathymetry and heat flow with age. J. Geoph. Res., 82**,** 803– 827.

Pavlis, G. L. (1986). Appraising earthquake hypocenter location errors: a complete, practical approach for single-event locations. Bull. Seism. Soc. Am., 76, 1699- 1717.

Quinn, A. W. (1993). Normal faults of the Lake Champlain region. J. Geol., 41, 11-143.

Richardson, R. M. (1992). Ridge forces, absolute plate motions, and the intraplate stress field. J. Geoph. Re., 97.

Rimando, R. E., and Benn, K. (2005). Evolution of faulting and paleo-stress field within the Ottawa graben, Canada. J. Geody., 39, 337-360.

Rivers, T. (1997). Lithotectonic elements of the Grenville Province: review and tectonic implications. Precambrian Res., 86, 117-154.

Rivers, T., Martingnole, J., Gower, C.F., Davidson, T. (1989). New tectonic divisions of the Grenville Province. Tectonics, 8, 63– 84

Sbar, M.L., Sykes, L.R. (1973). Contemporary compressive stress and seismicity in eastern North America: an example of intraplate tectonics. Geol. Soc. Ame. Bull., 84, 1861– 1882.

Sbar, M.L., Sykes, L.R. (1977). Seismicity and lithosphere stress in New Yourk and adjacent areas. J. Geophys. Res., 82, 5771-5786.

Scholz, C. H. (2002). The mechanics of earthquakes and faulting. Cambridge U Press, New York.

Seeber, L., and Armbruster, J. G., (1993). Natural and induced seismicity in the Lake Erie-Lake Ontario region: reactivation of ancient faults with little neotectonic displacement. Geogr. Phys. Quat., 47**,** 363–378.

Seeber, L., Kim, W-Y., Armbruster, J. Du, W-X., and Lerner-Lam, A. (2002). The 20 April 2002 Mw5.0 earthquake near Au Sable Forks, Adirondacks, New York: A first glance at a new sequence. Seism. Res. Lett., 73, 480-489.

Schaff, D. P, and Richards. P. (2004). Repeating Seismic Events in China. Science, 303**,** 1176 -1178.

Sclater, J. G., Jaupart, C, and Galson, D. (1980). The heat flow through oceanic and continental crust and the heat loss of the Earth. Rev. Geoph. Space Phys, 18**,** 269–311.

Sharma, K. N. M., Singhroy, V. H. And Levesque, J. (1995). Discussion: a two-stage emplacement for the Cabonga allochthon (central part of the Grenville province): evidence for orthogonal and oblique collision during the Grenville orogeny. Can. J. Earth Sci., 32, 1474-1778.

Sibson, R. H. (1982). Fault zone models, heat flow, and the depth distribution of earthquakes in the continental crust of the United States. Bull. Seism. Soc. Am., 72**,** 151–163.

Sleep, N. H. (1990). Monteregian hotspot track: a long-lived mantle plume. J. Geoph. ites., 95,21,983-21,990.

Smith, W. E. T. (1962). Earthquakes of eastern Canada and adjacent areas 1534–1927. Publ. Dominion Obs. Ottawa, 26, 269– 301.

Snoke, J. A., Munsey, J. W., Teague, A. G., and Bollinger, G. A. (1984). A program for Focal mechanism determination by combined use of polarity and SV-P amplitude data (abstract). Earthquake Not., 55(3), 15.

Solomon, S. C. And Duxbury, E. D. (1987). A test of the longevity of impact-induced faults preferred sites for later tectonic activity. J. Geoph. Res., 92(B4), 759-769.

Stein, S., and Wysession, M. (2003), An Introduction to Seismology, Earthquakes, and Earth Structure. Blackwell, Malden, Mass.

Stevens, A. E. (1994). Earthquakes in the Lake Ontario region: intermittent scattered activity, not persistent trends. Geo. Ca., 21**,** 105–111.

Stewart, I. S., J. Sauber, and Rose, J. (2000). Glacio-tectonics: Ice sheets, crustal Deformation, and seismicity. Quat. Sci. Rev., 19, 1367– 1389.

Sykes, L.R. (1978). Intraplate seismicity, reactivation of preexisting zones of weakness, alkaline magmatism and other tectonism post-dating continental fragmentation. Rev. Geoph., 16, 621–688.

Sykes, L. R. (1980). Earthquakes and other processes within lithospheric plates and the reactivation of pre-existing zones of weakness, in The Continental Crust and Its Mineral Deposits, edited by D. W. Strangway. Geol. Assoc. Can. Spec. Pap., 20, 215–237.

Talwani, P. (1999). Fault geometry and earthquakes in continental interiors. Tectonophysics, 305, 371– 379.

Thomas, R.L., Wallach, J.L, McMillan, R.K., Bowlby, J.R., Frape, S., Keyes, D. and Mohajer, A. A. (1993). Recent deformation in the bottom sediments of western and southeastern Lake Ontario and its association with major structures and seismicity. In J.L. Wallach and J.A. Heginbottom, eds., Neotectonics of the Great Lakes Area. Géogr. Phys. Quater., 47.

Thomas, W. A. (2006). Tectonic inheritance at a continental margin. GSA Today, 16(2).

Wallach, J. L., Mohajer,A. A., and Thomas, R. L. (1998). Linear zones, seismicity, and the possibility of a major earthquake in intraplate western Lake Ontario area of eastern North America. Can. J. Earth Sci, 35, 7.

Wahlstrom, R. (1987) Focal mechanisms of earthquakes in southern Quebec, southeastern Ontario, and northeastern New York with implications for regional seismotectonics and stress field characteristics. Bull. Seism. Soc. Amer., 77, 891-924.

Wetmiller, R., and J. Drysdale (1982). Local magnitudes of eastern Canadian earthquakes by an extended Mb(Lg) scale (abstract). Earthquake Notes 53, 40.

White, D. J., Easton, R. M., Culshaw, N. G., Milkereit, B., Forshyth, D. A., Carr, S., Green, A. G., and Davidson, A. (1994). Seismic images of the Grenville Orogen in Ontario. Can. J. Earth Sci., 31, 293-307.

White, D. J., Forsyth, D.A., Asudeh, I., Carr, S.D., Wu, H., Easton, R.M., and Mereu, R.F. (2000). A seismic-based cross-section of the Grenville Orogen in southern Ontario and western Quebec. Can. J. Earth Sci., 37, 183.

Willett, S. D., Chapman, D. S., and Neugebauer, H. J. (1985). A thermo mechanical model of continental lithosphere. Nature, 314**,** 520–523.

Williams, D. A., Telford, P. G., McCracken, A. D., Brunton, F. R. (1992). Cambrian-Ordovician geology of the Pttawa region fieldtrip guidebook No. 2. In: Canadian Paleontology conference- II, Ottawa, P. 51.

Winardhi, S., and Mereu, R. F. (1997). Crustal velocity structure of the Superior and Grenville of the southeastern Canadian Shield. Can. J. Earth Sci., 34**,** 1167–1184.

Wynne-Edwards, H. R. (1972). The Grenville Province. In variations in tectonic style in Canada Edited by Price, R. A. And Douglas, R. J. W. Geological association of Canada, 263-334.

Yang, J., and Aggarwal, Y. P. (1981). Seismotectonicosf northeastern United Statesa and adjacent Canada. J. Geologi. Res., 86, NO, 4981-4998.

Zartman, R. E. (1977). Geochronology of some alkaline rock provinces in eastern and central United States. Ann. Rev. Earth Planet. Sci., 5, 257– 286.

Zelt, C. A., Frsyth, D. A., Milkereit, B, White, D. J., Asudeh, I. (1994). Seismic structure of the Central Metasedimentary Belt, southern Grenville Province. Can. J. Earth Sci., 31, 243-254.

Zoback,M.D., and Zoback,M.L. (1991). Tectonic stress field of North America and relative plate motions. In: Slemmons. (Edited by Engdahl, D. B., Zoback, E. R., Blackwell, M.). Neotect. North Am., 339–366.

Zoback,M.L. and Zoback,M.D. (1980). State of stress in the conterminous United States. Geoph. Res., 85, 6112-6156.

Zoback, M.L. (1992a). First- and second-order patterns of stress in the lithosphere: The World stress map project. Geoph. Re., 97(B8).

Zoback, M.L. (1992b). Stress field constraints on intraplate seismicity in eastern North America. J. Geoph. Res., 97.

APPENDIX A: Examples of Input and Output Files for

HYPOCENTRE Program

Example of input file for one event

Heather information

Date of the event: 2006/02/25; Origin time: 1^{h}:39^{m}:22.2^{s}

Latitide: 45.65°N

Longtitude: 75.23°W

Depth: 20 km

All starting data is from the GSC data file.

Arrival time data

Column 1: station code

Column 2: component

Column 3: type of the phase

Column 4: assigned weight

Column 5: polarity of P-wave arrival

Column 6: arrival time (hour/minute/seconds)

```
2006  225  139 22.2   45.652 -75.230 20.0SS
 FRNY BZ  PG  3 C  139 46.65
 FRNY BZ  SG  4    140  5.70
 ACCN BZ  SG  4    140 37.73
 ACCN BZ  PN  4    140  2.85
 WLVO BZ  SG  2    140 48.25
 WLVO BZ  PN  3 C  140  6.48
 MPPO BZ  PG  1 D  139 42.45
 MPPO BZ  SG  2    139 58.30
 BANO BZ  PG  3 C  139 56.73
 BANO BZ  PN  3    139 55.20
 BANO BZ  SN  4    140 20.95
 DELO BZ  PG  3 D  139 57.35
 DELO BZ  SG  4    140 23.93
 DELO BZ  PN  2 D  139 55.55
 PECO BZ  PG  3 D  139 58.95
 PECO BZ  PN  1 D  139 57.32
 LINO BZ  SG  4    140 46.55
 LINO BZ  PN  4    140  5.57
 LINO BZ  SN  2    140 39.70
 ALGO BZ  PG  3 D  139 56.82
 ALGO BZ  SG  4    140 22.70
 ALGO BZ  PN  3    139 54.88
 BUKO BZ  SG  4    140 49.50
 BUKO BZ  PN  3    140  7.20
 ALFO BZ  PG  0 D  139 27.88
 ALFO BZ  SG  2    139 31.45
 PLVO BZ  PG  0 D  139 47.40
 PLVO BZ  SG  4    140  6.45
 GAC  BZ  PG  1 C  139 27.00
 GAC  BZ  SG  2    139 30.07
 CRLO BZ  PN  1 C  139 48.80
```

CRLO	BZ	SN	3		140	9.82
EEO	BZ	SG	4		140	48.02
EEO	BZ	PN	1	C	140	6.63
EFO	BZ	SG	3		141	19.02
EFO	BZ	PN	3		140	20.18
GRQ	BZ	PG	0	D	139	41.15
GRQ	BZ	SG	2		139	54.40
KGNO	BZ	PN	1	D	139	51.25
KGNO	BZ	SN	3		140	13.27
OTT	BZ	PG	0	D	139	30.73
OTT	BZ	SG	2		139	36.63
A11	BZ	SG	4		141	15.68
A11	BZ	PN	3		140	20.95
A21	BZ	SG	3		141	31.70
A21	BZ	PN	3		140	27.23
A54	BZ	SG	3		141	15.80
A54	BZ	PN	3		140	19.20
A61	BZ	PN	3		140	23.46
CNQ	BZ	SG	3		142	26.40
CNQ	BZ	PN	4		140	49.65
CNQ	BZ	SN	2		141	56.51
DAQ	BZ	PN	3		140	16.38
DPQ	BZ	SG	4		140	22.13
DPQ	BZ	PN	1	D	139	55.73
DPQ	BZ	SN	4		140	21.23
KAPO	BZ	PN	4		140	52.27
KAPO	BZ	SN	4		141	59.32
LMQ	BZ	SG	4		141	18.38
LMQ	BZ	PN	3		140	20.63
MNT	BZ	PG	1	D	139	42.22
MNT	BZ	SG	2		139	57.27
QCQ	BZ	SG	3		140	50.63
QCQ	BZ	PN	3		140	9.43
VLDQ	BZ	Sg	3		140	55.93
VLDQ	BZ	PN	2	C	140	9.90
VLDQ	BZ	SN	3		140	44.75
GSQ	BZ	PN	3		140	55.55
LMN	BZ	PN	2	D	141	7.70
LMN	BZ	SN	2		142	27.00
MNQ	BZ	PN	4	D	140	56.35
MNQ	BZ	SN	3		142	7.92
ICQ	BZ	SG	4		142	41.10
ICQ	BZ	PN	3		140	57.30
SMQ	BZ	PN	3		141	6.70
TRQ	BZ	PG	0	D	139	35.75
TRQ	BZ	SG	2		139	45.73
WBO	BZ	PG	0	D	139	34.50
WBO	BZ	SG	2		139	43.05
MOQ	BZ	PN	1	C	139	57.57
MOQ	BZ	SN	2		140	24.68
MALO	BZ	PN	3		140	40.30
MALO	BZ	SN	4		141	37.88
KILO	BZ	SG	4		141	28.95
KILO	BZ	PN	3		140	24.90
KILO	BZ	SN	2		141	10.63
SUNO	BZ	SG	4		141	32.90
SUNO	BZ	PN	3		140	27.00

```
SUNO BZ  SN  3    141 15.29
SADO BZ  SG  4    140 49.32
SADO BZ  PN  3 D  140  6.80
PNPO BZ  SG  3    143 25.82
PNPO BZ  PN  3    141 17.80
PNPO BZ  SN  2    142 44.88
TIMO BZ  SG  4    141 53.90
TIMO BZ  PN  3    140 36.50
TIMO BZ  SN  2    141 31.45
DRLN BZ  PN  4    142 17.37
DRLN BZ  SN  4    144 28.77
ACSO BZ  SG  4    143 17.73
ACSO BZ  PN  3    141 15.45
ALLY BZ  SG  4    142  4.35
ALLY BZ  SN  2    141 40.02
ARNY BZ  SG  3    141 35.38
BGR  BZ  PG  4    139 40.10
BGR  BZ  SG  4    139 54.35
CBN  BZ  PN  3    141 11.65
CBN  BZ  SN  3    142 32.67
ERPA BZ  PN  4    140 36.02
ERPA BZ  SN  4    141 29.17
HRV  BZ  PN  2    140 23.98
MVL  BZ  PN  3    140 46.82
NCB  BZ  PN  3 C  139 53.30
NCB  BZ  SN  2    140 17.25
PAL  BZ  SG  4    141 43.75
PAL  BZ  PN  2 D  140 33.20
```

Example of output file (hyp.out file) Heather information (calculate parameters)
Date of the event: 2006/02/25
Origin time: 01:39:22.2
Latitude: 45.664°N
Longitude: 75.246°W
Focal depth: 18.7 km
Azimutal gap: 70°
Origin time error: 0.59 s
Latitude error: 1.4 km
Longitude error: 1.7 km
Focal depth error: 1.8 km

Data
Column 1: station code
Column 2: component
Column 3: type of the phase
Column 4: assigned weight;
Column 5: polarity of P-wave;
Column 6: arrival time of the phase (hour/minute/seconds);
Column 7: take off angle (°);
Column 8: rms (room mean square) error (s)

Column 9: hypocentral distance to the station (km);
Column 10: azimuth to the station (°)

```
2006  225 0139 22.2   45.664 -75.246 18.7SSGSC
 GAP= 70        0.59       1.4     1.7  1.8
 GAC  BZ  PG  1 C  139 27.00                      134    0.36 7 18.9 284
 GAC  BZ  SG  2    139 30.07                      134    0.37 5 18.9 284
 ALFO BZ  PG  0 D  139 27.88                      122    0.1010 28.2  98
 ALFO BZ  SG  2    139 31.45                      122   -0.22 5 28.2  98
 OTT  BZ  PG  0 D  139 30.73                      110    0.2110 47.7 231
 OTT  BZ  SG  2    139 36.63                      110    0.22 5 47.7 231
 WBO  BZ  PG  0 D  139 34.50                      102    0.0710 73.8 182
 WBO  BZ  SG  2    139 43.05                      102   -0.13 5 73.8 182
 TRQ  BZ  PG  0 D  139 35.75                      100    0.1010 81.8  40
 TRQ  BZ  SG  2    139 45.73                      100    0.43 5 81.8  40
 BGR  BZ  SG  4    139 54.35                      96     0.15 0  115 143
 GRQ  BZ  PG  0 D  139 41.15                      96     0.3510  115 336
 GRQ  BZ  SG  2    139 54.40                      96     0.19 5  115 336
 BGR  BZ  PG  4    139 40.10                      96    -0.70 0  115 143
 MPPO BZ  PG  1 D  139 42.45                      95    -0.29 7  128 219
 MPPO BZ  SG  2    139 58.30                      95     0.75 5  128 219
 MNT  BZ  PG  1 D  139 42.22                      95    -0.51 7  128  98
 MNT  BZ  SG  2    139 57.27                      95    -0.26 5  128  98
 PLVO BZ  SG  4    140  6.45                      93     0.36 0  159 245
 FRNY BZ  PG  3 C  139 46.00                      93    -0.97 2  159 125
 PLVO BZ  PG  0 D  139 40.00                      93    -0.2710  159 245
 FRNY BZ  SG  4    139 5.70                       93    -0.30 0  159 125
 CRLO BZ  PN  1 C  139 48.80                      53    -0.44 7  171 285
 CRLO BZ  SN  3    140  9.82                      53     1.02 2  171 285
 KGNO BZ  PN  1 D  139 51.25                      53    -0.02 7  188 212
 KGNO BZ  SN  3    140 13.27                      53     0.96 2  188 212
 NCB  BZ  PN  3 C  139 53.30                      53    -0.11 2  205 156
 NCB  BZ  SN  2    140 17.25                      53     1.23 5  205 156
 DPQ  BZ  SG  4    140 22.13                      92    -0.57 0  221  58
 ALGO BZ  PG  3 D  139 56.82                      92    -0.35 2  221 279
 DPQ  BZ  PN  1 D  139 55.73                      53     0.29 7  221  58
 DPQ  BZ  SN  4    140 21.23                      53     1.70 0  221  58
 ALGO BZ  PN  3    139 54.88                      53    -0.48 2  221 279
 ALGO BZ  SG  4    140 22.70                      92     0.19 0  221 279
 BANO BZ  PN  3    139 55.20                      53    -0.38 2  222 252
 BANO BZ  PG  3 C  139 56.73                      92    -0.70 2  222 252
 BANO BZ  SN  4    140 20.95                      53     1.19 0  222 252
 DELO BZ  PN  2 D  139 55.55                      53    -0.50 5  226 237
 DELO BZ  PG  3 D  139 57.35                      92    -0.68 2  226 237
 DELO BZ  SG  4    140 23.93                      92    -0.08 0  226 237
 MOQ  BZ  SN  2    140 24.68                      53     1.72 5  237  98
 PECO BZ  PG  3 D  139 58.95                      91    -0.73 2  237 216
 PECO BZ  SN  2    140 22.82                      53    -0.01 5  237 216
 MOQ  BZ  PN  1 C  139 57.57                      53     0.14 7  237  98
 PECO BZ  PN  1 D  139 57.32                      53    -0.03 7  237 216
 ACCN BZ  PN  4    140  2.85                      53    -0.16 0  283 153
 ACCN BZ  SG  4    140 37.73                      91    -1.41 0  283 153
 LINO BZ  PN  4    140  5.57                      53    -1.38 0  315 244
 LINO BZ  SN  2    140 39.70                      53     0.26 5  315 244
 LINO BZ  SG  4    140 46.55                      91    -1.19 0  315 244
 EEO  BZ  PN  1 C  140  6.63                      53    -0.42 7  315 292
```

EEO	BZ	SG	4		140	48.02	91	0.09	0	315	292
WLVO	BZ	PN	3	C	140	6.48	53	-0.59	2	316	233
WLVO	BZ	SG	2		140	48.25	91	0.22	5	316	233
SADO	BZ	PN	3	D	140	6.80	53	-1.07	2	322	253
SADO	BZ	SG	4		140	49.32	91	-0.42	0	322	253
BUKO	BZ	PN	3		140	7.20	53	-1.11	2	325	267
BUKO	BZ	SG	4		140	49.50	91	-1.18	0	325	267
QCQ	BZ	PN	3		140	9.43	53	0.48	2	330	67
QCQ	BZ	SG	3		140	50.63	91	-1.37	2	330	67
VLDQ	BZ	PN	2	C	140	9.90	53	-0.26	5	340	327
VLDQ	BZ	SN	3		140	44.75	53	-0.24	2	340	327
VLDQ	BZ	Sg	3		140	55.93	91	1.30	2	340	327
DAQ	BZ	PN	3		140	16.38	53	-0.97	2	398	49
A54	BZ	PN	3		140	19.20	53	-0.85	2	421	60
A54	BZ	SG	3		141	15.80	91	-0.43	2	421	60
A11	BZ	PN	3		140	20.95	53	0.34	2	425	64
A11	BZ	SG	4		141	15.68	91	-1.82	0	425	64
LMQ	BZ	PN	3		140	20.63	53	-0.70	2	431	59
LMQ	BZ	SG	4		141	18.38	91	-0.64	0	431	59
EFO	BZ	PN	3		140	20.18	53	-1.26	2	432	230
EFO	BZ	SG	3		141	19.02	91	-0.29	2	432	230
A61	BZ	PN	3		140	23.46	53	-0.73	2	454	58
HRV	BZ	PN	2		140	23.98	53	-0.71	5	458	139
KILO	BZ	PN	3		140	24.90	53	-0.46	2	464	314
KILO	BZ	SN	2		141	10.63	53	-0.66	5	464	314
KILO	BZ	SG	4		141	28.95	91	1.15	0	464	314
A21	BZ	PN	3		140	27.23	53	-0.30	2	481	60
A21	BZ	SG	3		141	31.70	91	-0.87	2	481	60
SUNO	BZ	PN	3		140	27.00	53	-0.84	2	484	285
SUNO	BZ	SN	3		141	15.29	53	-0.29	2	484	285
SUNO	BZ	SG	4		141	32.90	91	-0.30	0	484	285
ARNY	BZ	SG	3		141	35.38	91	-0.31	2	493	169
PAL	BZ	PN	2	D	140	33.20	53	-0.16	5	529	168
PAL	BZ	SG	4		141	43.75	90	-1.49	0	529	168
ERPA	BZ	PN	4		140	36.02	53	0.22	0	548	226
ERPA	BZ	SN	4		141	29.17	53	-0.17	0	548	226
TIMO	BZ	PN	3		140	36.50	53	-0.24	2	556	306
TIMO	BZ	SN	2		141	31.45	53	0.48	5	556	306
TIMO	BZ	SG	4		141	53.90	90	1.35	0	556	306
MALO	BZ	PN	3		140	40.30	53	-0.80	2	591	327
ALLY	BZ	SN	2		141	40.02	53	0.48	5	596	223
ALLY	BZ	SG	4		142	4.35	90	1.02	0	596	223
MVL	BZ	PN	3		140	46.82	53	0.25	2	636	189
CNQ	BZ	PN	4		140	49.65	53	-1.74	0	675	51
CNQ	BZ	SN	2		141	56.51	53	0.20	5	675	51
CNQ	BZ	SG	3		142	26.40	90	1.93	2	675	51
KAPO	BZ	PN	4		140	52.27	53	-0.99	0	690	310
KAPO	BZ	SN	4		141	59.32	53	-0.23	0	690	310
GSQ	BZ	PN	3		140	55.55	53	-0.58	2	713	57
MNQ	BZ	PN	4	D	140	56.35	53	-1.23	0	724	39
MNQ	BZ	SN	3		142	7.92	53	0.90	2	724	39
ICQ	BZ	PN	3		140	57.30	53	-1.74	2	737	52
ICQ	BZ	SG	4		142	41.10	90	-0.04	0	737	52
LMN	BZ	PN	2	D	141	7.70	53	-0.64	5	812	85
LMN	BZ	SN	2		142	27.00	53	1.36	5	812	85
SMQ	BZ	PN	3		141	6.70	53	-1.02	2	814	48
CBN	BZ	PN	3		141	11.65	53	-1.00	2	847	193

APPENDIX B: Examples of Input and Output Files for FOCMEC Program

Focmec input file

Date of the event: 2006/02/25
Calculated origin time: 01:39:22.2
Calculated latitude: 45.664°
Calculated longitude: -75.246°
Calculated focal depth: 18.7 km
Azimutal gap: 70
Calculated origin time error: 0.59
Calculated latitude error: 1.4
Calculated longitude error: 1.7
Calculated focal depth error: 1.8
First column: station code; Second column: network channel; Third column: phase of the wave; Forth column: assigned weight; Fifth column: picked polarity; Sixth column: arrival time of each phase in each station (h/min/sec); Seventh column: take off angle(°); Eight column: rms of each station; Ninth column: hypocentral distance to each station(km); Tenth column azimuth of each station(°)

```
2006  225 0139 22.5   45.664 -75.246 18.7SSGSC
 GAP= 70        0.59        1.4     1.7  1.8
 GAC  BZ  PG  1 C  139 27.00                    134    0.36 7 18.6 284
 ALFO BZ  PG  0 D  139 27.88                    122    0.0310 28.5  98
 OTT  BZ  PG  0 D  139 30.73                    110    0.2110 47.4 231
 WBO  BZ  PG  0 D  139 34.50                    102    0.0310 73.8 182
 TRQ  BZ  PG  0 D  139 35.75                    100    0.0310 82.0  41
 GRQ  BZ  PG  0 D  139 41.15                     96    0.3310  115 336
 MPPO BZ  PG  1 D  139 42.45                     95   -0.30 7  128 219
 MNT  BZ  PG  1 D  139 42.22                     95   -0.59 7  128  97
 PLVO BZ  PG  0 D  139 47.40                     93   -0.2710  159 245
 FRNY BZ  PG  3 C  139 46.65                     93   -1.05 2  159 125
 CRLO BZ  PN  1 C  139 48.80                     53   -0.44 7  171 285
 KGNO BZ  PN  1 D  139 51.25                     53   -0.04 7  188 212
 NCB  BZ  PN  3 C  139 53.30                     53   -0.17 2  205 156
 ALGO BZ  PG  3 D  139 56.82                     92   -0.34 2  220 279
 DPQ  BZ  PN  1 D  139 55.73                     53    0.22 7  222  58
 BANO BZ  PG  3 C  139 56.73                     92   -0.69 2  222 252
 DELO BZ  PN  2 D  139 55.55                     53   -0.51 5  226 237
 DELO BZ  PG  3 D  139 57.35                     92   -0.68 2  226 237
 PECO BZ  PN  1 D  139 57.32                     53   -0.05 7  237 216
 PECO BZ  PG  3 D  139 58.95                     91   -0.74 2  237 216
 MOQ  BZ  PN  1 C  139 57.57                     53    0.06 7  237  98
 WLVO BZ  PN  3 C  140  6.48                     53   -0.61 2  315 233
 EEO  BZ  PN  1 C  140  6.63                     53   -0.43 7  315 292
 SADO BZ  PN  3 D  140  6.80                     53   -1.08 2  322 253
 VLDQ BZ  PN  2 C  140  9.90                     53   -0.28 4  340 327
```

```
 PAL  BZ  PN  2 D  140 33.20                        53   -0.21 1  529 168
 MNQ  BZ  PN  4 D  140 56.35                        53   -1.29 0  725  39
 LMN  BZ  PN  2 D  141  7.70                        53   -0.72 0  812  85
```

Focmec.out LST

First column: the station coda; second column: azimuth of the station(°); Third column: take off angle(°); Forth column: polarity.

```
  GAC      284.0      134.0    C
  ALFO      98.0      122.0    D
  OTT      231.0      110.0    D
  WBO      182.0      102.0    D
  TRQ       41.0      100.0    D
  GRQ      336.0       96.0    D
  MPPO     219.0       95.0    D
  MNT       97.0       95.0    D
  PLVO     245.0       93.0    D
  FRNY     125.0       93.0    C
  CRLO     285.0       53.0    C
  KGNO     212.0       53.0    D
  NCB      156.0       53.0    C
  ALGO     279.0       92.0    D
  DPQ       58.0       53.0    D
  BANO     252.0       92.0    C
  DELO     237.0       53.0    D
  DELO     237.0       92.0    D
  PECO     216.0       53.0    D
  PECO     216.0       91.0    D
  MOQ       98.0       53.0    C
  WLVO     233.0       53.0    C
  EEO      292.0       53.0    C
  SADO     253.0       53.0    D
  VLDQ     327.0       53.0    C
  PAL      168.0       53.0    D
  MNQ       39.0       53.0    D
  LMN       85.0       53.0    D
 There are   28 polarities and    2 allowed errors


     Dip,Strike,Rake     52.97   126.77    74.90
     Dip,Strike,Rake     39.58   330.90   109.05
+                                                  :Auxiliary Plane

     Trend & Plunge of B    136.00    12.00
     Trend, Plunge of P,T    227.46     6.85   346.56    76.13

Polarity error at    BANO BANO WLVO WLVO

++++++++++++++++++++++++++++++++++++++++++++++++++++++++++++++++++++++++

     Dip,Strike,Rake     53.71   125.85    70.00
     Dip,Strike,Rake     40.76   337.43   114.97
```

```
+                                                                    :Auxiliary Plane

     Trend & Plunge of B    138.00    16.00
     Trend, Plunge of P,T    229.94     6.73   342.01    72.57

Polarity error at    BANO BANO WLVO WLVO
 ++++++++++++++++++++++++++++++++++++++++++++++++++++++++++++++++++++++++++++++

 There are    2 acceptable solutions
```

Fomec.out plt file

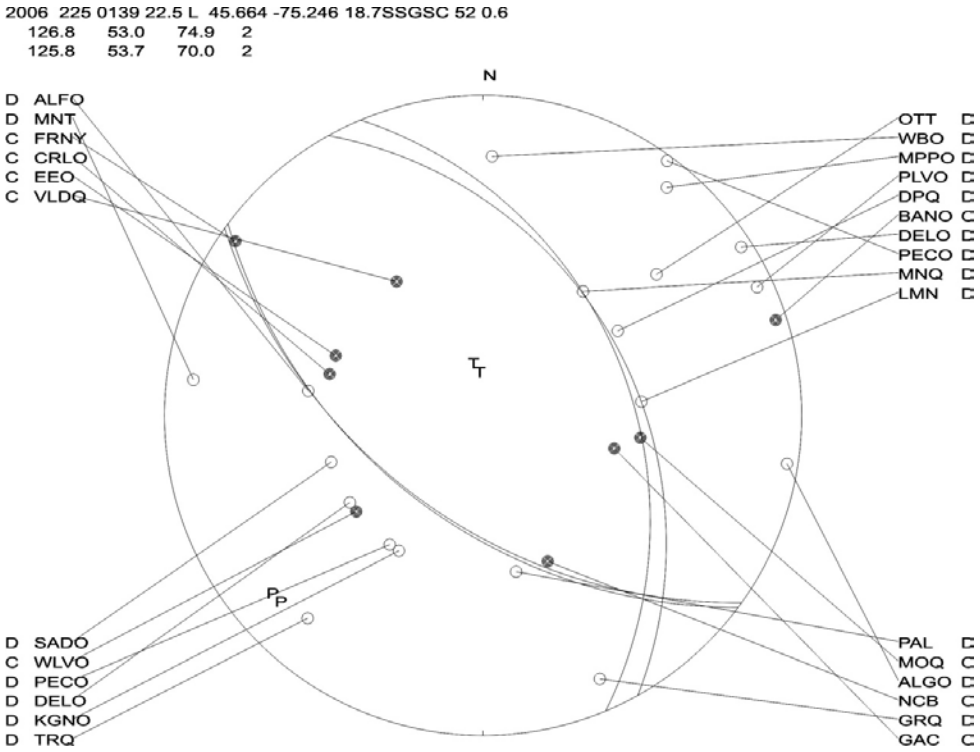

APPENDIX C: Faults Plane Solutions for Each Event in the Study Area (New Solutions and Available Solutions in the Literature)

The positive polarities (dark circles) and negative polarities (open circles) are shown with the code of the station next to them. ‘P’ are pressure axes and ‘T’ are the tension axes for individual solutions.

Focal mechanisms solutions in black are calculated in the current study and compared with previous available focal mechanism solutions (in blue)

Date: Date of the event:yyyymmdd.
Lon: Longitude of the event (°).

Lat: Latitude of the event (°).Depth: Focal depth of the event (km)

M: Magnitude of the event

Strike(1), Dip(1) and Rake(1): strike, dip and rake of the plain(1)

Strike(2), Dip(2) and Rake(2): strike, dip and rake of the plain(2)

Trend(p): Trend of p axes

Plunge(p): Plunge of P axes

Trend(T): Trend of T axes

Plunge(T): Plunge of T axes

Trend(B): Trend of B axes

Plunge(B): Plunge of B axes

Number	Date	OriginTime	Lat ,N	Long ,W	Depth, km	Magnitude, m_N
1	1993/11/16	$09^h31^m45^s$	$45^\circ.225$	$73^\circ.474$	19.4	4.3

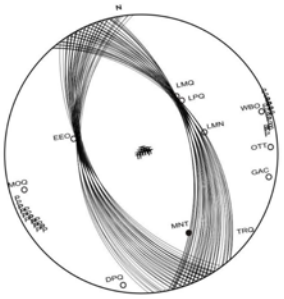

11 Polarities, 0 allowed errors
50/813 acceptable solutions
Quality:A

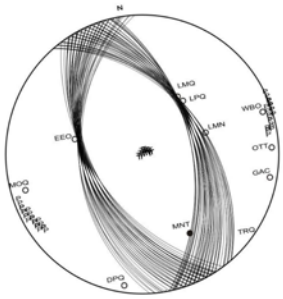

Average solution1

Dip(1)	Strike(1)	Rake(1)
45.0	169.2	90.2
± 4.0	±6.5	±2.0

Dip(2)	Strike(2)	Rake(2)
45.0	349.2	90.2
± 4.0	±7.5	±2.5

Trend(P)	Plunge(P)	Trend(T)	Plunge(P)	Trend(B)	Plunge(B)
169.1	3.0	135.3	86.4	169.0	0.0
± 7.0	± 2.0	20.0	±2.0	± 7.5	±1.0

Du et al., 2003

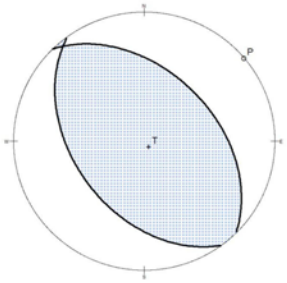

Lon	Lat	Depth
-77.9	43.8	13.0

Dip(1)	Strike(1)	Rake(1)
45.0	144.0	96.0

Dip(2)	Strike(2)	Rake(2)
45.0	316.0	84.0

Trend(P)	Plunge(P)	Trend(T)	Plunge(P)
50.0	0.0	142.0	86.0

Number	Date	OriginTime	Lat ,N	Long ,W	Depth, km	Magnitude, m_N
2	1993/12/25	$16^h44^m23^s$	$46^\circ.519$	$75^\circ.515$	19.2	4.1

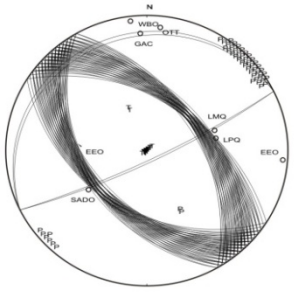

8 Polarities, 0 allowed errors
50/3114 acceptable solutions
Quality:B

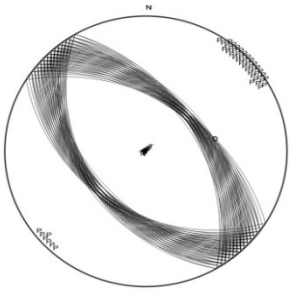

Average solution1

Dip(1)	Strike(1)	Rake(1)
40	136	90
± 4	±14	± 0

Dip(2)	Strike(2)	Rake(2)
50	316	90
± 3	±14	± 0

Trend(P)	Plungr(P)	Trend(T)	Plunge(T)	Trend(B)	Plunge(B)
46	5	226	85	136	0
±14	± 3	±14	± 3	±14	±0

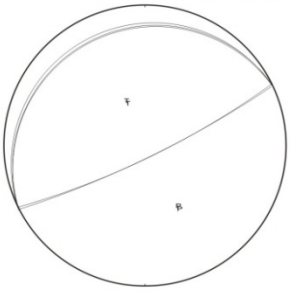

Average solution2

Dip(1)	Strike(1)	Rake(1)
80	64	90
± 1	± 0	± 0

Dip(2)	Strike(2)	Rake(2)
10	244	90
± 1	± 0	±0

Trend(P)	Plungr(P)	Trend(T)	Plunge(T)	Trend(B)	Plunge(B)
154	35	334	55	64	0
± 0	± 1	±0	± 1	± 0	±0

Number	Date	OriginTime	Lat ,N	Long ,W	Depth, km	Magnitude, m_N
3	1994/10/02	$11^h:27^m:23^s$	$42^\circ.230$	$72^\circ.300$	10	3.5

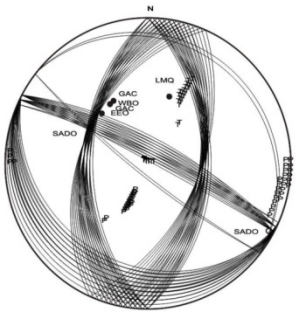

7 Polarities, 0 allowed errors
50/33644 acceptable solutions
Quality:C

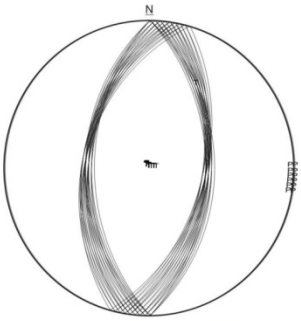

Average solution1

Dip(1)	Strike(1)	Rake(1)
48	14	90
± 2	±10	± 0

Dip(2)	Strike(2)	Rake(2)
42	194	90
± 2	±12	± 0

Trend(P)	Plungr(P)	Trend(T)	Plunge(T)	Trend(B)	Plunge (B)
104	3	284	87	14	0
±11	± 2	±11	± 2	±11	± 0

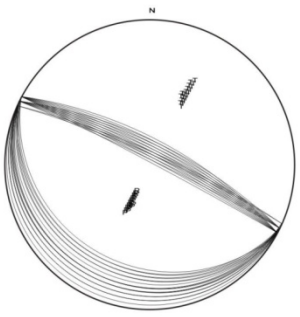

Average solution2

Dip(1)	Strike(1)	Rake(1)
78	296	-90
± 9	± 3	± 0

Dip(2)	Strike(2)	Rake(2)
12	116	-90
± 8	± 1	±0

Trend(P)	Plungr(P)	Trend(T)	Plunge(T)	Trend(B)	Plunge(B)
206	57	26	33	116	0
± 2	± 9	± 1	± 8	± 2	± 0

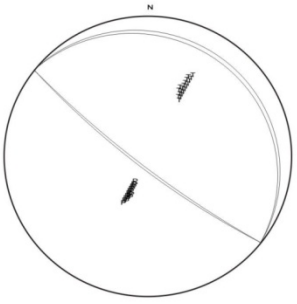

Average solution3

Dip(1)	Strike(1)	Rake(1)
46	0	90
± 1	± 0	± 0

Dip(2)	Strike(2)	Rake(2)
44	180	90.57
± 1	± 0	± 0

Trend(P)	Plungr(P)	Trend(T)	Plunge(T)	Trend(B)	Plunge(B)
89.59	1	247.94	88.92	359.59	0.4
± 0	± 1	±10	± 1	± 0	± 0

Number	Date	OriginTime	Lat ,N	Long ,W	Depth, km	Magnitude, m_N
4	1995/02/15	$05^h53^m59^s$	$45^\circ.931$	$75^\circ.095$	18	3.5

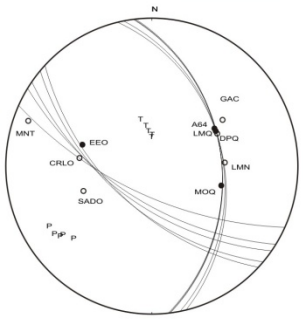

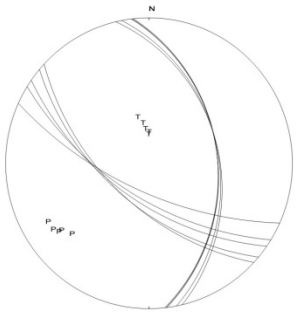

Average solution1

Dip(1)	Strike(1)	Rake(1)
60.57	124.83	64.53
± 7	± 9	± 5

Dip(2)	Strike(2)	Rake(2)
38.16	348.94	127.32
± 1	± 4	±10

10 Polarities, 0 allowed errors
5 acceptable solutions
Quality:A

Trend(P)	Plungr(P)	Trend(T)	Plunge(T)	Trend(B)	Plunge(B)
232.94	12.04	349.65	64.61	138	22
± 6	± 3	±6	± 8	± 9	±6

Number	Date	OriginTime	Lat ,N	Long ,W	Depth, km	Magnitude, m_N
5	1995/06/03	$10^h44^m32^s$	$47^\circ.1$	$76^\circ.22$	18	3.9

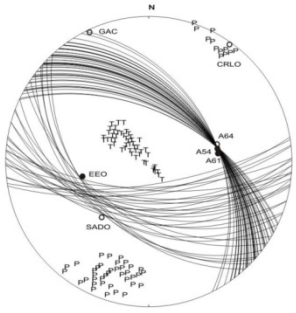

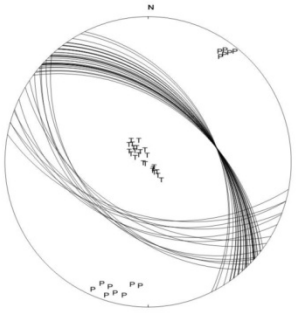

Average solution1

Dip(1)	Strike(1)	Rake(1)
49.97	100.06	68.9
± 15	± 15	±12

Dip(1)	Strike(1)	Rake(2)
44.41	311.02	113.2
± 5	± 15	±20

7 Polarities, 0 allowed errors
50/212 acceptable solutions
Quality:B

Trend(P)	Plunge(P)	Trend(T)	Plunge(T)	Trend(B)	Plunge(B)
204.83	2.88	304.77	73.73	114	16
± 20	± 10	±30	± 15	± 10	±14

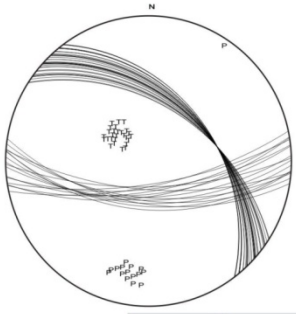

Average solution2

Dip(1)	Strike(1)	Rake(1)
64.91	76.99	54.19
± 11	±11	± 6

Dip(1)	Strike(1)	Rake(2)
42.74	316.55	141.33
± 4	±14	±15

Trend(P)	Plunge(P)	Trend(T)	Plunge(T)	Trend(B)	Plunge(B)
192.1	12.7	300.8	55	94	32
± 9	± 7	±17	± 7	± 10	±6

Number	Date	OriginTime	Lat ,N	Long ,W	Depth, km	Magnitude, m_N
6	1995/06/16	$12^h13^m13^s$	$44.^\circ180$	$71.^\circ570$	15	3.8

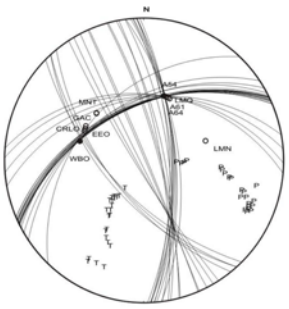

7 Polarities, 0 allowed errors
50/212 acceptable solutions
Quality:B

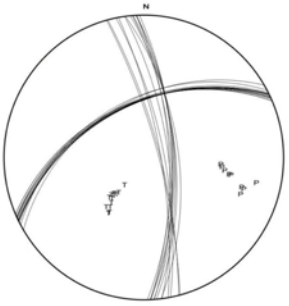

Average solution1

Dip(1)	Strike(1)	Rake(1)
69.58	352.42	44.44
± 7	± 6	± 8

Dip(2)	Strike(2)	Rake(2)
48.99	243.53	152.46
± 1	± 15	±12

Trend(P)	Plunge(P)	Trend(T)	Plunge(T)	Trend(B)	Plunge(B)
113.6	12.5	216.6	45.3	12	42
± 7	± 3	± 4	± 13	± 8	±10

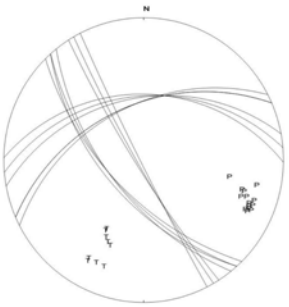

Average solution2

Dip(1)	Strike(1)	Rake(1)
62.68	135.35	-55.75
± 15	±10	±10

Dip(2)	Strike(2)	Rake(2)
42.74	259.33	-137.45
± 4	± 0	±20

Trend(P)	Plunge(P)	Trend(T)	Plunge(T)	Trend(B)	Plunge(B)
93.22	57.55	201.42	11.23	298	30
± 5	±18	±5	±10	± 15	±15

Du et al., 2003

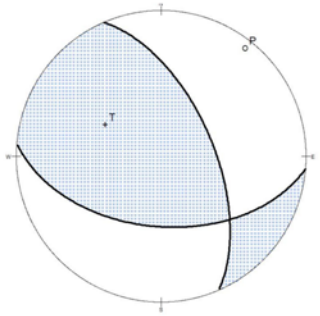

Lon	Lat	Depth
-71.9	44.3	6.0

Dip(1)	Strike(1)	Rake(1)
50.0	95.0	40.0

Dip(2)	Strike(2)	Rake(2)
61.0	337.0	132.0

Trend(P)	Plunge(P)	Trend(T)	Plunge(P)
38.0	6.0	300.0	53.0

Number	Date	OriginTime	Lat ,N	Long ,W	Depth, km	Magnitude, m_N
7	1995/09/12	$03^h:59^m:06^S$	$45^\circ.583$	$74^\circ.427$	23.4	3.7

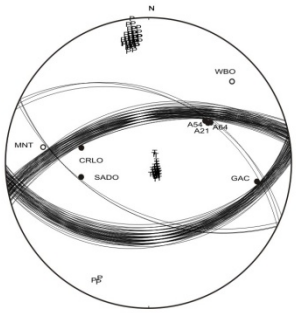

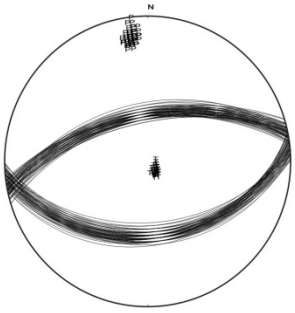

Average solution1

Dip(1)	Strike(1)	Rake(1)
54.1	259.1	85.06
± 5	± 5	± 1

Dip(2)	Strike(2)	Rake(2)
36.19	87.48	96.78
± 7	± 6	± 2

8 Polarities, 0 allowed errors
50/773 acceptable solutions
Quality:B

Trend(P)	Plunge(P)	Trend(T)	Plunge(P)	Trend(B)	Plunge(B)
352.63	8.98	148.23	80.16	262	4
± 4	± 6	±20	± 5	± 4	±1

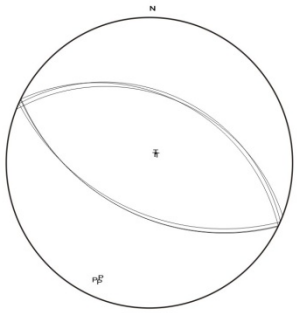

Average solution2

Dip(1)	Strike(1)	Rake(1)
50	116	90
± 6	± 2	± 0

Dip(2)	Strike(2)	Rake(2)
40	296	90
± 1	± 1	±0

Trend(P)	Plunge(P)	Trend(T)	Plunge(P)	Trend(B)	Plunge(B)
206	5	26	85	116	0
± 1	± 1	±1	± 1	± 1	±0

Number	Date	OriginTime	Lat ,N	Long ,W	Depth, km	Magnitude, m_N
8	1995/10/10	$07^h:19^m:20^S$	$46^\circ.280$	$78^\circ.480$	30	3.5

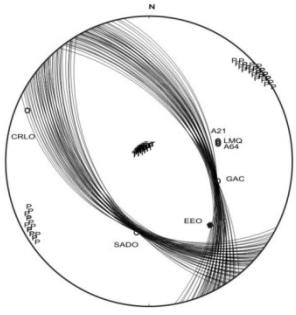

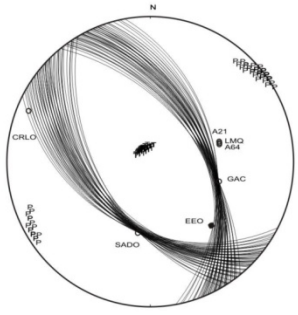

Average solution1

Dip(1)	Strike(1)	Rake(1)
44.89	133.81	75.76
± 5	± 20	± 4

Dip(1)	strike(2)	Rake(2)
46.83	333.52	103.77
± 5	± 12	± 3

7 Polarities, 0 allowed errors
50/3223 acceptable solutions
Quality:A

Trend(P)	Plunge(P)	Trend(T)	Plunge(T)	Trend(B)	Plunge(B)
53.83	0.98	318.26	79.95	144	10
± 10	± 4	±35	± 3	± 12	± 2

Number	Date	OriginTime	Lat ,N	Long ,W	Depth, km	Magnitude, m_N
9	1996/03/14	$10^h 42^m 28^s$	$46.^\circ 172$	$74.^\circ 508$	30	4.4

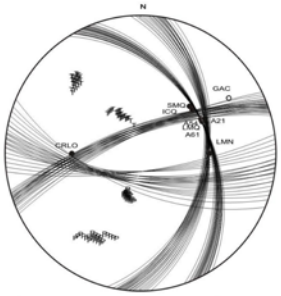

9 Polarities, 0 allowed errors
50/161 acceptable solutions
Quality:B

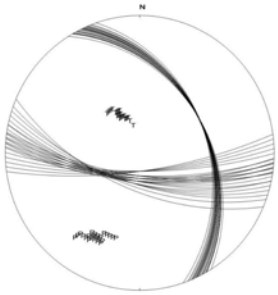

Average solution1

Dip(1)	Strike(1)	Rake(1)
68.95	96.19	59.8
± 7	±14	± 7

Dip(2)	Strike(2)	Rake(2)
36.23	334.52	142.59
± 0	± 7	±15

Trend(P)	Plungr(P)	Trend(T)	Plunge(T)	Trend(B)	Plunge(B)
208.22	18.45	327.27	55.52	108	28
±10	± 5	±10	±10	±15	± 7

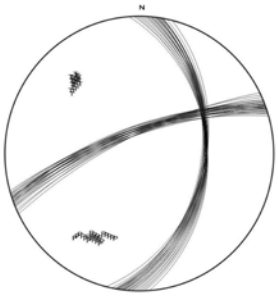

Average solution2

Dip(1)	Strike(1)	Rake(1)
71.07	249.42	-58.09
± 3	± 5	± 2

Dip(2)	Strike(2)	Rake(2)
36.59	6.94	-147.02
± 2	± 3	±6

Trend(P)	Plungr(P)	Trend(T)	Plunge(T)	Trend(B)	Plunge(B)
197.67	52.86	316.02	19.78	58	30
± 7	±3	±5	±3	±4	±2

Bent et al., 2003

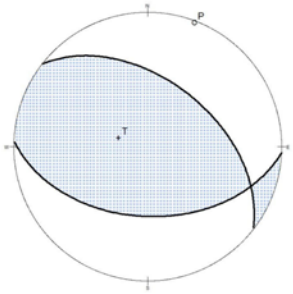

Lon	Lat
-74.93	45.93

Dip(1)	Strike(1)	Rake(1)
49.0	308.0	115.0

Dip(2)	Strike(2)	Rake(2)
47.0	94.0	65.0

Du et al., 2003

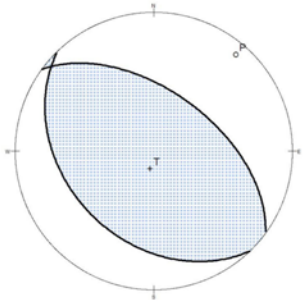

Lon	Lat	Depth
-74.43	45.99	18.0

Dip(1)	Strike(1)	Rake(1)
36.0	136.0	98.0

Dip(2)	Strike(2)	Rake(2)
54.0	306.0	84.0

Trend(P)	Plunge(P)	Trend(T)	Plunge(P)
40.0	9.0	191.0	80.0

Number	Date	OriginTime	Lat ,N	Long ,W	Depth, km	Magnitude, m_N
10	1997/04/03	$04^h 44^m 13^s$	$45^\circ.590$	$72^\circ.220$	17	3.2

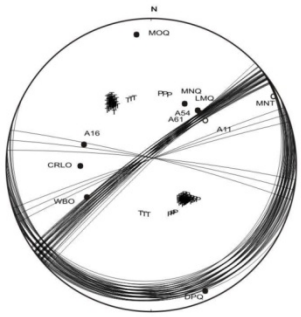

11 Polarities, 0 allowed errors
50/732 acceptable solutions
Quality:C

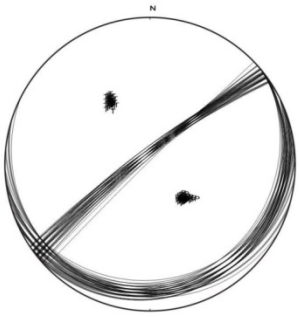

Average solution1

Dip(1)	Strike(1)	Rake(1)
8.94	78.4	-63.32
± 4	±20	±20

Dip(2)	Strike(2)	Rake(2)
82.02	231.44	-94.04
± 5	±10	± 3

Trend(P)	Plungr(P)	Trend(T)	Plunge(T)	Trend(B)	Plunge(B)
136.71	52.82	325.01	36.89	232	4
±10	± 4	±10	± 4	± 12	± 3

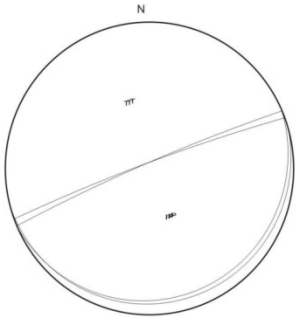

Average solution2

Dip(1)	Strike(1)	Rake(1)
82	232	-90
± 3	± 4	± 0

Dip(2)	Strike(2)	Rake(2)
8	52	-90
± 3	± 5	±0

Trend(P)	Plungr(P)	Trend(T)	Plunge(T)	Trend(B)	Plunge(B)
142	53	322	37	52	0
± 4	±3	±4	±3	± 4	± 0

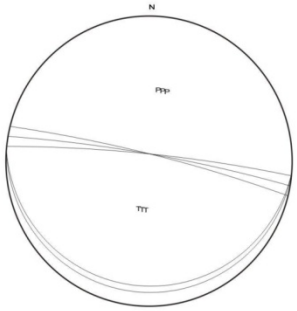

Average solution3

Dip(1)	Strike(1)	Rake(1)
5.65	94.93	85.05
± 0	± 2	± 2

Dip(2)	Strike(2)	Rake(2)
84.37	279.9	90.49
± 0	± 4	±0

Trend(P)	Plungr(P)	Trend(T)	Plunge(T)	Trend(B)	Plunge(B)
9.45	39.36	190.45	50.63	99.85	0.49
± 4	± 0	±4	±0	± 4	± 0

Number	Date	OriginTime	Lat ,N	Long ,W	Depth, km	Magnitude, m_N
11	1997/05/24	$18^h 52^m 10^s$	$45.^\circ 925$	$74.^\circ 232$	22	4.2

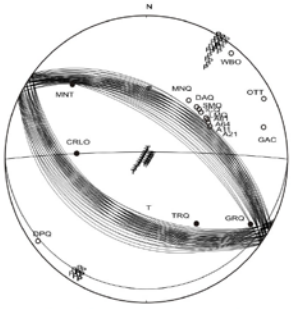

17 Polarities, 0 allowed errors
50/49200 acceptable solutions
Quality:B

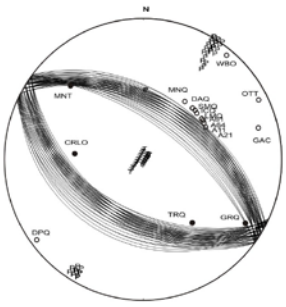

Average solution1

Dip(1)	Strike(1)	Rake(1)
36.19	116.52	83.22
± 0	± 13	±14

Dip(2)	Strike(2)	Rake(2)
54.1	304.9	94.94
± 14	± 8	± 4

Trend(P)	Plungr(P)	Trend(T)	Plunge(T)	Trend(B)	Plunge(B)
31.37	8.98	235.77	80.16	122	4
± 6	± 20	±25	± 18	± 4	± 2

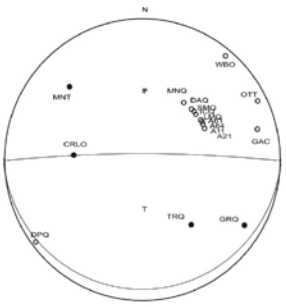

Average solution2

Dip(1)	Strike(1)	Rake(1)
5.65	89.07	89.06
± 0	± 0	± 0

Dip(2)	Strike(2)	Rake(2)
84.35	270.01	90.09
± 0	± 0	±0

Trend(P)	Plungr(P)	Trend(T)	Plunge(T)	Trend(B)	Plunge(B)
359.93	39.35	180.11	50.65	90	0.09
± 0	± 0	± 0	± 0	± 0	± 0

Bent et al., 2003

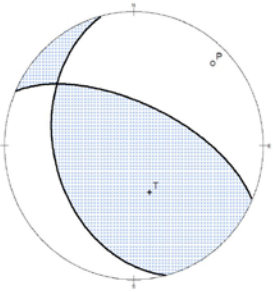

Lon	Lat
-74.19	45.81

Dip(1)	Strike(1)	Rake(1)
64.0	294.0	61.0

Dip(2)	Strike(2)	Rake(2)
38.0	165.0	135.0

Du et al., 2003

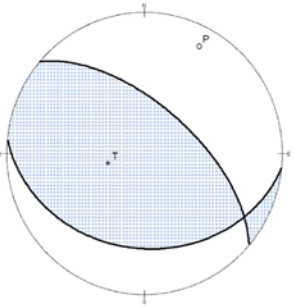

Lon	Lat	Depth
-74.19	45.81	22.0

Dip(1)	Strike(1)	Rake(1)
33.0	96.0	60.0

Dip(2)	Strike(2)	Rake(2)
62.0	311.0	108.0

Trend(P)	Plunge(P)	Tren(T)	Plunge(T)
27.0	15.0	256.0	68.0

Number	Date	OriginTime	Lat ,N	Long ,W	Depth, km	Magnitude, m_N
12	1998/02/26	$14^h 20^m 32^s$	$46^\circ.096$	$76^\circ.367$	15.2	3.7

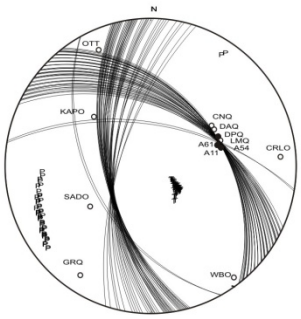

13 Polarities, 1 allowed errors
50/737 acceptable solutions
Quality:B

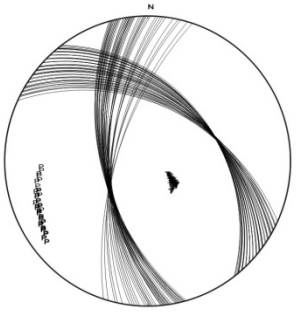

Average solution1

Dip(1)	Strike(1)	Rake(1)
42.4	308.8	52.9
± 4.0	± 13.0	± 10.0

Dip(2)	Strike(2)	Rake(2)
57.5	174.5	118.8
± 5.0	± 15.0	±7.0

Trend(P)	Plunge(P)	Trend(T)	Plunge(T)	Trend(B)	Plunge(B)
244.3	8.2	136.7	64.5	338.0	24.0
±15.0	± 4.0	±7.0	± 5.0	±17.0	±7.0

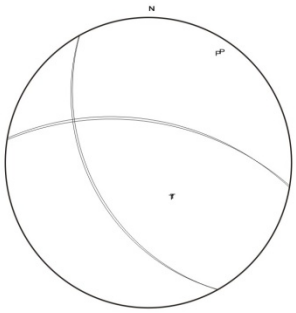

Average solution2

Dip(1)	Strike(1)	Rake(1)
57	279.86	56
± 1	± 0	± 1

Dip(2)	Strike(2)	Rake(2)
45.9	151	130.8
± 0	± 0	±1

Trend(P)	Plunge(P)	Trend(T)	Plunge(T)	Trend(B)	Plunge(B)
33.3	6.2	134.66	61.2	300	28
± 1	± 1	± 1	± 1	± 1	± 0

Number	Date	OriginTime	Lat ,N	Long ,W	Depth, km	Magnitude, m_N
13	1998/04/18	$16^h:22^m:52^s$	45.559°	74.997°	21.5	4.1

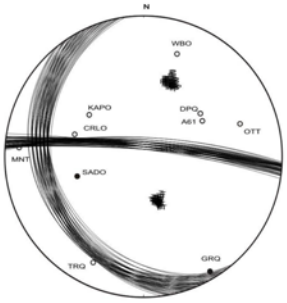

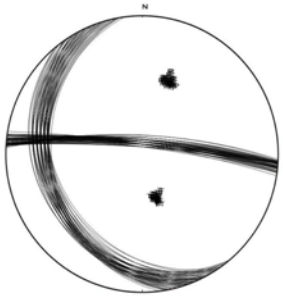

Average solution1

Dip(1)	Strike(1)	Rake(1)
80.39	275.22	73.77
± 5	± 3	± 6

Dip(2)	Strike(2)	Rake(2)
18.8	155.39	148.8
± 6	± 15	±15

10 Polarities, 0 allowed errors
50/224 acceptable solutions
Quality:A

Trend(P)	Plunge(P)	Tren(T)	Plunge(T)	Tren(B)	Plunge(B)
19.0	33.5	166.5	52.0	278.0	16.0
±7.0	± 4.0	±8.0	± 5.0	± 3.0	±5.0

Bent et al., 2003

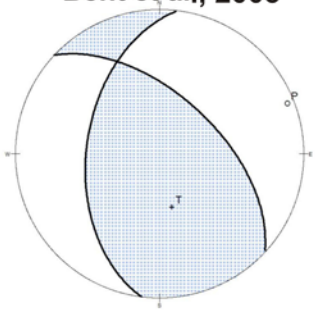

Lon	Lat
-74.96	45.58

Dip(1)	Strike(1)	Rake(1)
313.0	57.0	53.0

Dip(2)	Strike(2)	Rake(2)
188.0	48.0	133.0

Number	Date	OriginTime	Lat ,N	Long ,W	Depth, km	Magnitude, m_N
14	1998/07/30	$08^h57^m22^s$	46.227°	74.690°	10	4.4

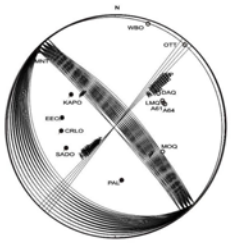

13 Polarities, 0 allowed errors
50/10414 acceptable solutions
Quality:C

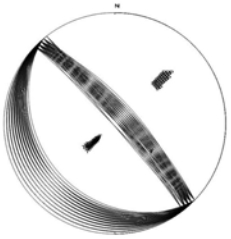

Average solution1

Dip(1)	Strike(1)	Rake(1)
34	174	90
± 2	± 6	± 0

Dip(2)	Strike(2)	Rake(2)
56	354	90
± 3	±10	± 0

Trend(P)	Plungr(P)	Trend(T)	Plunge(T)	Trend(B)	Plunge(B)
84	11	264	79	174	0
± 9	± 3	± 8	±3	± 9	±0

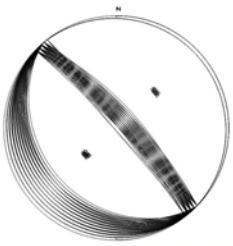

Average solution2

Dip(1)	Strike(1)	Rake(1)
10	114	90
± 2	± 4	± 0

Dip(2)	Strike(2)	Rake(2)
80	294	90
± 5	± 4	±0

Trend(P)	Plungr(P)	Trend(T)	Plunge(T)	Trend(B)	Plunge(B)
24	35	204	55	114	0
± 4	±5	±4	±5	±4	±0

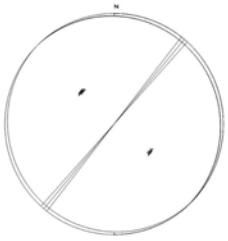

Average solution3

Dip(1)	Strike(1)	Rake(1)
90	222	90.43
± 0	± 2	± 0

Dip(2)	Strike(2)	Rake(2)
0	0	48
± 0	± 0	±2

Trend(P)	Plungr(P)	Trend(T)	Plunge(T)	Trend(B)	Plunge(B)
311.57	45.19	132.42	44.81	42	0.43
± 2	±0	±2	± 0	±2	±0

Bent et al., 2003

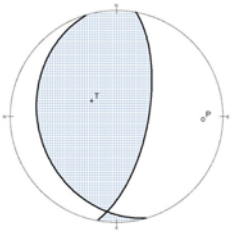

Lon	Lat
-74.80	46.19

Dip(1)	Strike(1)	Rake(1)
27.0	164.0	66.0

Dip(2)	Strike(2)	Rake(2)
78.0	15.0	107.0

Du et al., 2003

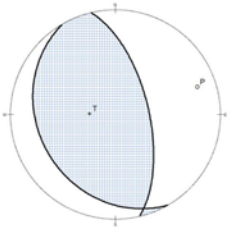

Lon	Lat	Depth
-74.72	46.17	12.0

Dip(1)	Strike(1)	Rake(1)
27.0	150.0	75.0

Dip(2)	Strike(2)	Rake(2)
64.0	347.0	98.0

Trend(P)	Plunge(P	Trend(T)	Plunge(T)
71.0	19.0	272.0	70.0

Number	Date	OriginTime	Lat ,N	Long ,W	Depth, km	Magnitude, m_N
15	1998/09/25	$19^h52^m55^s$	$41^\circ.34$	$80^\circ.143$	5	5.4

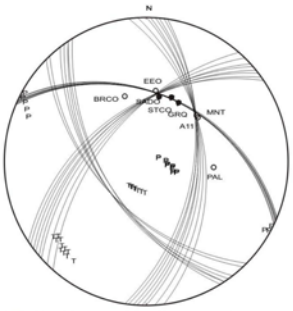

8 Polarities, 0 allowed errors
50/554 acceptable solutions
Quality:B

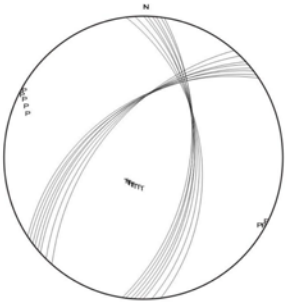

Average solution1

Dip(1)	Strike(1)	Rake(1)
46.49	356.42	52.81
± 1	± 3	± 1

Dip(2)	Strike(2)	Rake(2)
54.71	224.2	122.48
± 1	± 3	± 1

Trend(P)	Plunge(P	Trend(T)	Plunge(T)	Trend(B)	Plunge(B)
291.8	4.49	192.71	63.56	24	26
± 3	± 2	±6	± 0	± 2	± 0

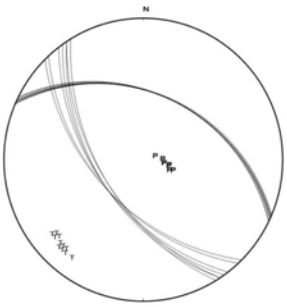

Average solution2

Dip(1)	Strike(1)	Rake(1)
39.58	305.1	-109.05
± 1	±11	± 7

Dip(2)	Strike(2)	Rake(2)
52.97	149.23	-74.9
± 1	± 5	±9

Trend(P)	Plunge(P	Trend(T)	Plunge(T)	Trend(B)	Plunge(B)
106.86	69.94	221.2	8.56	314	18
± 7	± 5	± 4	± 1	± 5	±9

Du et al., 2003

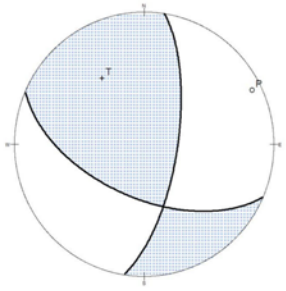

Lon	Lat	Depth
-80.39	41.50	2.0

Dip(1)	Strike(1)	Rake(1)
69.0	9.0	144.0

Dip(2)	Strike(2)	Rake(2)
57.0	114.0	25.0

Trend(P)	Plunge(P	Trend(T)	Plunge(T)
64.0	8)0	327.0	40.0

Number	Date	OriginTime	Lat ,N	Long ,W	Depth, km	Magnitude, m_N
16	1998/12/25	$13^h30^m26^S$	43.858°	77.820°		3.6

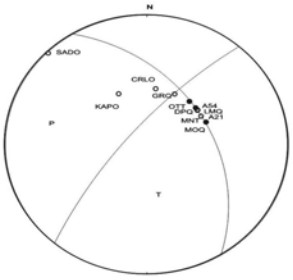

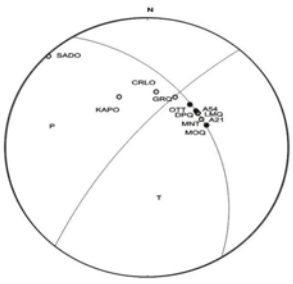

Average solution1

Dip(1)	Strike(1)	Rake(1)
42.23	328.59	23.64
± 0	± 0	± 0

Dip(2)	Strike(2)	Rake(2)
74.36	220.63	129.74
± 0	± 0	± 0

11 Polarities, 0 allowed errors
1 acceptable solutions
Quality:A

Trend(P)	Plungr(P)	Trend(T)	Plunge(T)	Trend(B)	Plunge(B)
281.98	19.45	170.86	45.58	28	38
± 0	± 0	±0	± 0	± 0	±0

Dineva et al., 2005

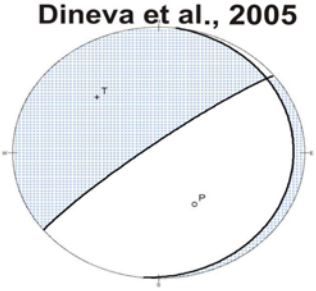

Lon	Lat	Depth
-77.9	43.8	13.0

Strike(1)	Dip(1)	Rake(1)
232.0	84.0	-84.0

Strike(2)	Dip(2)	Rake(2)
7.0	8.0	-135.0

Kim et al., 2006

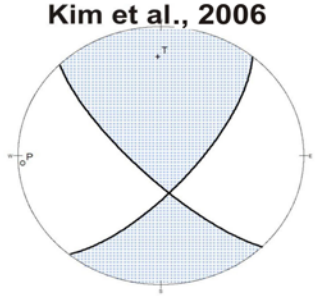

Lon	Lat	Depth
-77.9	43.8	2.0

Strike(1)	Dip(1)	Rake(1)
135.0	76.0	20.0

Strike(2)	Dip(2)	Rake(2)
40.0	70.0	165.0

Number	Date	OriginTime	Lat ,N	Long ,W	Depth, km	Magnitude, m_N
17	1999/06/18	$23^h19^m09^s$	$46^\circ.481$	$75^\circ.149$	27.5	3.5

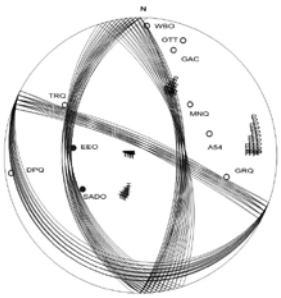

10 Polarities, 0 allowed errors
50/7730 acceptable solutions
Quality:B

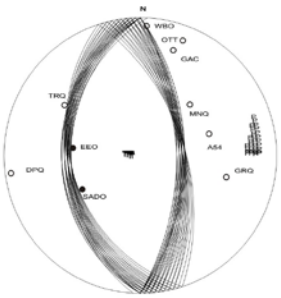

Average solution1

Dip(1)	Strike(1)	Rake(1)
34.0	178.0	90.0
±10.0	± 6.0	± 0.0

Dip(2)	Strike(2)	Rake(2)
56.0	358.0	90.0
± 6.0	±10.0	± 0.0

Trend(P)	Plungr(P)	Trend(T)	Plunge(T)	Trend(B)	Plunge(B)
88.0	11.0	268.0	79.0	178.0	0.0
±10.0	± 3.0	±10.0	± 3.0	±10.0	± 0.0

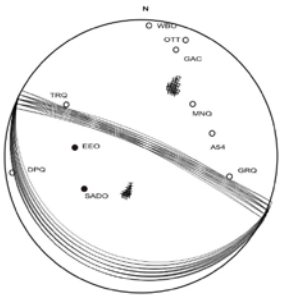

Average solution2

Dip(1)	Strike(1)	Rake(1)
10.0	114.0	90.0
± 4.0	± 4.0	± 0.0

Dip(2)	Strike(2)	Rake(2)
80.0	294.0	90.0
± 5.0	± 4.0	± 0.0

Trend(P)	Plungr(P)	Trend(T)	Plunge(T)	Trend(B)	Plunge(B)
24.0	35.0	204.0	55.0	114.0	0.0
± 4.0	± 5.0	± 4.0	± 5.0	± 4.0	± 0.0

Number	Date	OriginTime	Lat ,N	Long ,W	Depth, km	Magnitude, m_N
18	1999/11/26	$22^h33^m01^s$	43.664°	78.980°	9.9	3.7

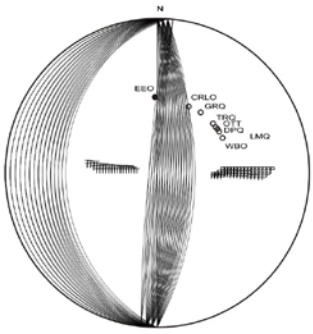

8 Polarities, 0 allowed errors
50/7833 acceptable solutions
Quality:A

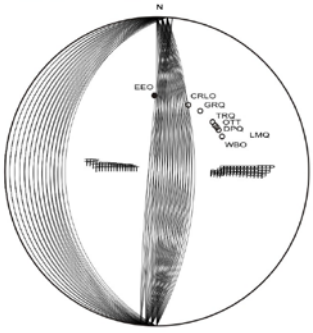

Average solution1

Dip(1)	Strike(1)	Rake(1)
72.0	2.0	90.0
±11.0	±2.0	±0.0

Dip(2)	Strike(2)	Rake(2)
18.0	182.0	90.0
±11.0	± 2.0	± 0.0

Trend(P)	Plungr(P)	Trend(T)	Plunge(T)	Trend(B)	Plunge(B)
92.0	27.0	272.0	63.0	2.0	0.0
±2.0	±11.0	±2.0	±11.0	± 2.0	± 0.0

Dineva et al., 2004

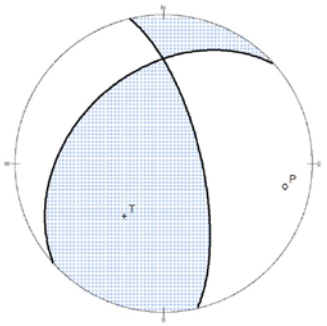

Lon	Lat	Depth
-78.97	43.70	9.2

Dip(1)	Strike(1)	Rake(1)
38.0	228.0	145.0

Dip(2)	Strike(2)	Rake(2)
69.0	347.0	58.0

Trend(P)	Plunge(P)	Trend(T)	Plunge(T)
101.0	18.0	218.0	54.0

Bent et al., 2003

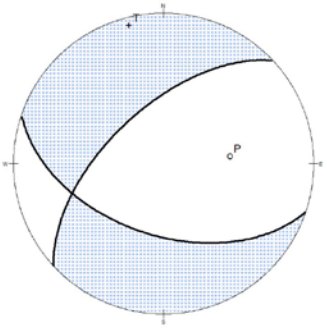

Lon	Lat	Depth
-78.99	43.71	18.0

Dip(1)	Strike(1)	Rake(1)
61.0	120.0	-28.0

Number	Date	OriginTime	Lat ,N	Long ,W	Depth, km	Magnitude, m_N
19	2000/01/01	$11^h22^m58^s$	46.870°	78.887°	14.6	5.2

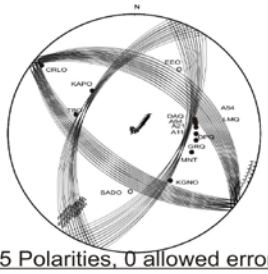

15 Polarities, 0 allowed errors
23173 acceptable solutions
Quality:B

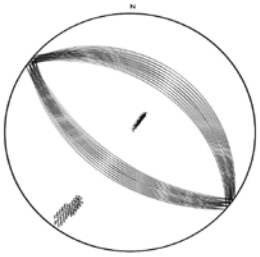

Average solution1

Dip(1)	Strike(1)	Rake(1)
56	126	90
± 9	± 3	±0

Dip(2)	Strike(2)	Rake(2)
34	306	90
± 9	± 3	±0

Trend(P)	Plungr(P)	Trend(T)	Plunge(T)	Trend(B)	Plunge(B)
216	11	36	79	126	0
± 3	± 9	± 3	± 9	± 3	±0

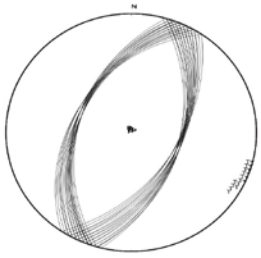

Average solution2

Dip(1)	Strike(1)	Rake(1)
42	204	-90
± 1	± 8	±1

Dip(2)	Strike(2)	Rake(2)
48	24	-90
± 1	±10	±1

Trend(P)	Plungr(P)	Trend(T)	Plunge(T)	Trend(B)	Plunge(B)
294	87	114	3	24	0
± 20	± 2	±9	±2	± 9	±1

Bent et al., 2003

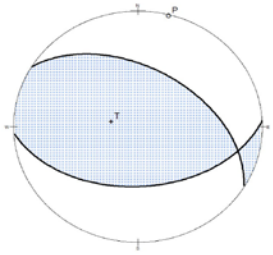

Lon	Lat
-78.42	46.82

Dip(1)	Strike(1)	Rake(1)
47.0	87.0	65.0

Dip(2)	Strike(2)	Rake(2)
49.0	302.0	11.0

Ma and adams., 2002

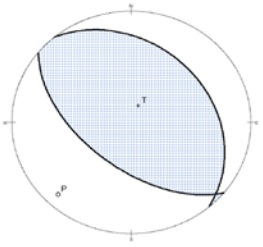

Lon	Lat	Depth
-78.93	46.84	13.0

Dip(1)	Strike(1)	Rake(1)
33.0	320.0	99.0

Dip(2)	Strike(2)	Rake(2)
57.0	130.0	84.0

Trend(P)	Plunge(P)	Trend(T)	Plunge(T)
224.0	12.0	21.0	77.0

Du et al., 2003

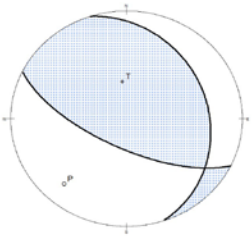

Lon	Lat	Depth
-78.90	46.87	10.0

Dip(1)	Strike(1)	Rake(1)
68.0	116.0	69.0

Number	Date	OriginTime	Lat ,N	Long ,W	Depth, km	Magnitude, m_N
20	2000/04/20	$08^h:46^m:55^s$	$43^\circ.927$	$74^\circ.264$	12.2	4

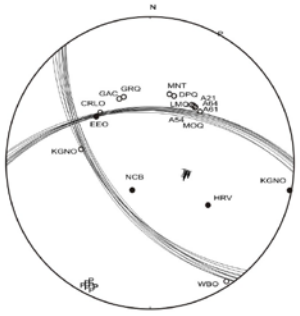

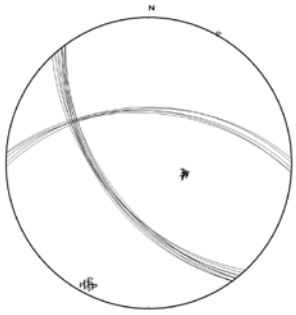

Average solution1

Dip(1)	Strike(1)	Rake(1)
48.99	270.46	51.53
± 1	± 3	±2

Dip(2)	Strike(2)	Rake(2)
53.79	140.91	125.58
± 3	± 3	±2

17 Polarities, 0 allowed errors
10 acceptable solutions
Quality:A

Trend(P)	Plungr(P)	Trend(T)	Plunge(T)	Trend(B)	Plunge(B)
206.6	2.7	111.6	61.8	298	28
± 2	± 2	±5	± 2	± 2	±2

Du et al., 2003

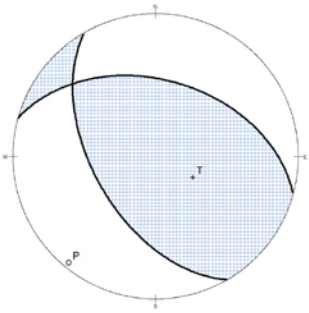

Lon	Lat	Depth
-74.25	43.95	8.0

Dip(1)	Strike(1)	Rake(1)
54.0	150.0	120.0

Dip(2)	Strike(2)	Rake(2)
46.0	286.0	55.0

Trend(P)	Plunge(P)	Trend(T)	Plunge(T)
219.0	5.0	119.0	66.0

Number	Date	OriginTime	Lat ,N	Long ,W	Depth, km	Magnitude, m_N
21	2000/08/06	$08^h:52^m:24^s$	$46^\circ.227$	$75^\circ.008$	25.1	4.2

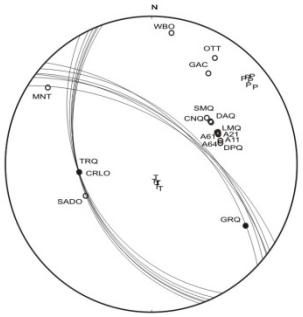

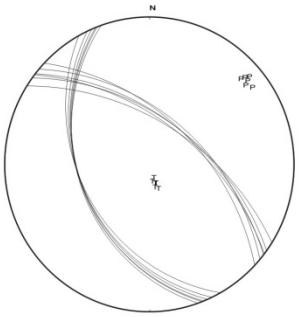

Average solution1

Dip(1)	Strike(1)	Rake(1)
55.23	308.03	72.87
± 2	± 5	±5

Dip(2)	Strike(2)	Rake(2)
38.28	156.42	112.99
± 1	± 5	±7

17 Polarities, 0 allowed errors
6 acceptable solutions
Quality:A

Trend(P)	Plungr(P)	Trend(T)	Plunge(T)	Trend(B)	Plunge(B)
50.2	8.7	171.2	73.4	318	14
± 3	± 2	±6	± 4	± 4	±4

Number	Date	OriginTime	Lat ,N	Long ,W	Depth, km	Magnitude, m_N
22	2000/10/06	$13^h:59^m:05^s$	$45^\circ.077$	$73^\circ.986$	20.1	3.8

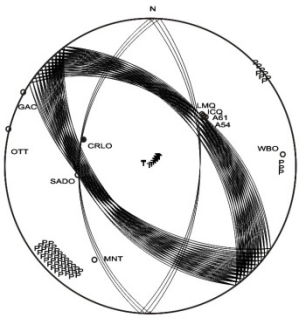

10 Polarities, 0 allowed errors
4586 acceptable solutions
Quality:B

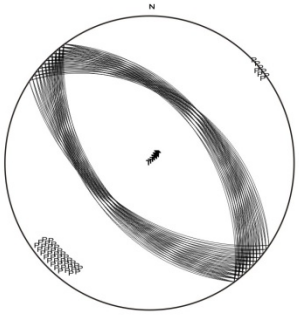

Average solution1

Dip(1)	Strike(1)	Rake(1)
50	134	90
± 3	±10	±0

Dip(2)	Strike(2)	Rake(2)
40	314	90
± 3	±10	±0

Trend(P)	Plungr(P)	Trend(T)	Plunge(T)	Trend(B)	Plunge(B)
224	5	44	85	134	0
±10	± 2	±10	± 3	±10	±0

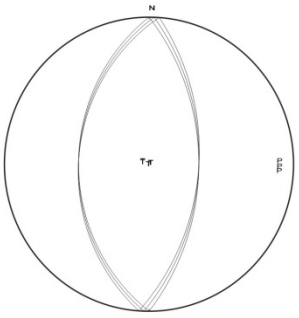

Average solution1

Dip(1)	Strike(1)	Rake(1)
52	2	90
± 0	± 2	±0

Dip(2)	Strike(2)	Rake(2)
38	182	90
± 0	± 2	±0

Trend(P)	Plungr(P)	Trend(T)	Plunge(T)	Trend(B)	Plunge(B)
92	7	272	83	2	0
± 2	± 0	±3	±0	± 2	±0

Number	Date	OriginTime	Lat ,N	Long ,W	Depth, km	Magnitude, m_N
23	2001/01/26	03^h:03^m:21^s	41°.912	80°.867	5	4.4

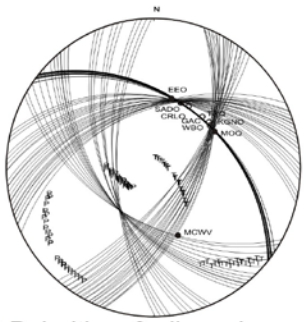

9 Polarities, 0 allowed errors
195 acceptable solutions
Quality:D

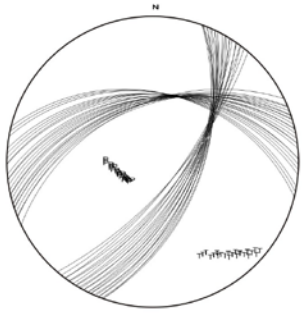

Average solution1

Dip(1)	Strike(1)	Rake(1)
42.95	258.84	-46.44
± 5	±20	±10

Dip(2)	Strike(2)	Rake(2)
60.41	26.43	-122.67
± 8	± 9	± 2

Trend(P)	Plungr(P)	Trend(T)	Plunge(T)	Trend(B)	Plunge(B)
246.49	60.08	139.21	9.7	44	28
±20	± 7	±12	± 7	± 6	± 4

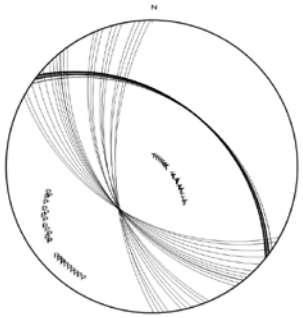

Average solution2

Dip(1)	Strike(1)	Rake(1)
40.13	308.8	67.95
± 0	± 2	± 20

Dip(2)	Strike(2)	Rake(2)
53.32	156.7	107.56
± 7	± 20	± 14

Trend(P)	Plungr(P)	Trend(T)	Plunge(T)	Trend(B)	Plunge(B)
234.3	6.79	119.09	74.38	326	14
± 20	± 8	±25	±12	±16	±15

Du et al., 2003

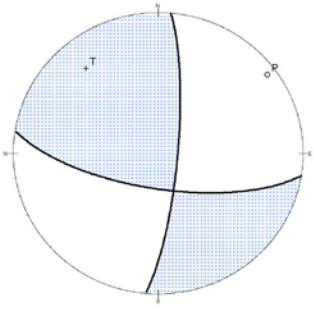

Lon	Lat	Depth
-80.83	41.99	2.0

Dip(1)	Strike(1)	Rake(1)
79.0	5.0	159.0

Dip(2)	Strike(2)	Rake(2)
69.0	99.0	12.0

Trend(P)	Plunge(P)	Trend(T)	Plunge(T)
53.0	7.0	320.0	23.0

Number	Date	OriginTime	Lat ,N	Long ,W	Depth, km	Magnitude, m_N
24	2001/03/19	$10^h40^m17^S$	$47^\circ.084$	$76^\circ.249$	20.5	3.9

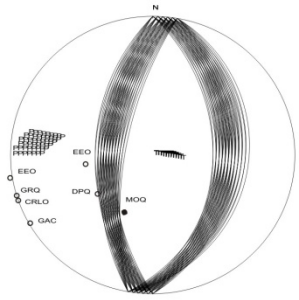

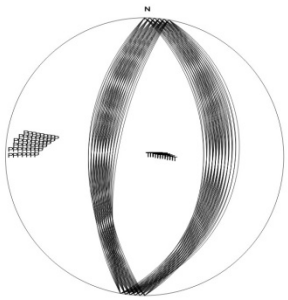

Average solution1

Dip(1)	Strike(1)	Rake(1)
34	4	90
± 10	± 3	± 0

Dip(2)	Strike(2)	Rake(2)
56	184	90
± 10	± 3	± 0

7 Polarities, 0 allowed errors
57422 acceptable solutions
Quality:B

Trend(P)	Plungr(P)	Trend(T)	Plunge(T)	Trend(B)	Plunge(B)
274	11	94	79	4	0
± 3	± 10	± 3	± 10	± 3	± 0

Number	Date	OriginTime	Lat ,N	Long ,W	Depth, km	Magnitude, m_N
25	2001/04/11	$21^h30^m50^S$	$47^\circ.107$	$76^\circ.103$	19.4	3.8

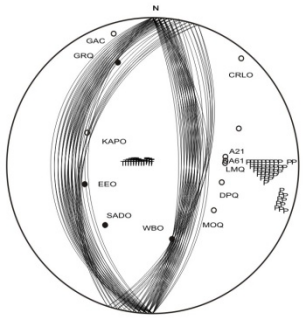

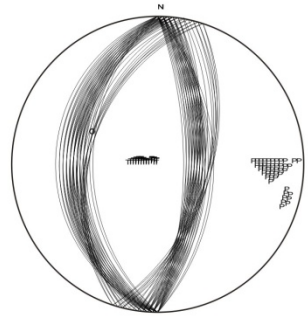

Average solution1

Dip(1)	Strike(1)	Rake(1)
58	8	90
± 10	± 15	± 0

Dip(2)	Strike(2)	Rake(2)
32	188	90
± 10	± 12	± 0

12 Polarities, 1 allowed errors
3597 acceptable solutions
Quality:B

Trend(P)	Plungr(P)	Trend(T)	Plunge(T)	Trend(B)	Plunge(B)
98	13	278	77	8	0
± 6	± 10	± 18	± 10	± 12	± 0

Number	Date	OriginTime	Lat ,N	Long ,W	Depth, km	Magnitude, m_N
26	2001/12/24	$04^h:58^m:22^s$	$46^\circ.905$	$76^\circ.488$	19.4	3.8

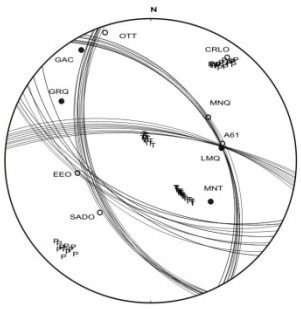

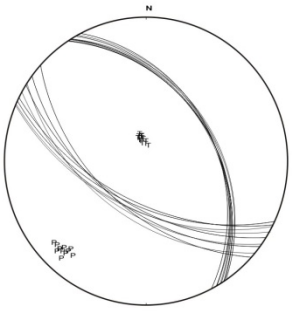

Average solution1

Dip(1)	Strike(1)	Rake(1)
64.91	278.99	54.19
± 11	± 11	± 7

Dip(2)	Strike(2)	Rake(2)
42.74	158.55	141.33
± 5	± 5	±17

10 Polarities, 0 allowed errors
31 acceptable solutions
Quality:B

Trend(P)	Plungr(P)	Trend(T)	Plunge(T)	Trend(B)	Plunge(B)
34	12.7	142.8	55	296	32
± 8	± 9	± 2	±10	±15	± 8

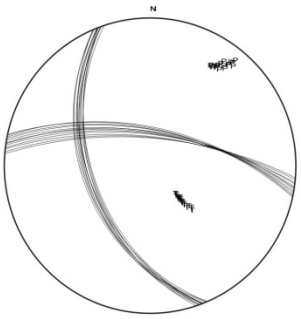

Average solution2

Dip(1)	Strike(1)	Rake(1)
55.23	122.03	72.87
± 2	± 8	± 6

Dip(2)	Strike(2)	Rake(2)
38.28	330.42	112.99
± 1	± 3	± 9

Trend(P)	Plungr(P)	Trend(T)	Plunge(T)	Trend(B)	Plunge(B)
224.2	8.7	345.2	73.4	132	14
± 5	± 1	±11	± 5	± 6	±5

Number	Date	OriginTime	Lat ,N	Long ,W	Depth, km	Magnitude, m_N
27	2002/02/11	$11^h:43^m:37^s$	$46^\circ.083$	$73^\circ.438$	15.9	3.8

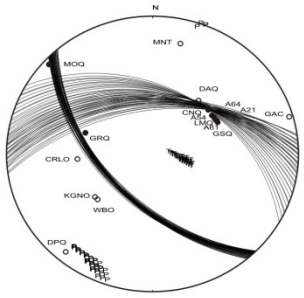

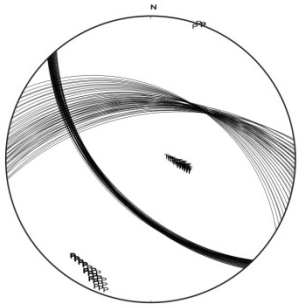

Average solution1

Dip(1)	Strike(1)	Rake(1)
46.45	273.41	58.88
± 7	±18	±14

Dip(2)	Strike(2)	Rake(2)
51.65	134.64	118.53
± 2	± 4	±10

16 Polarities, 0 allowed errors
206 acceptable solutions
Quality:B

Trend(P)	Plungr(P)	Trend(T)	Plunge(T)	Trend(B)	Plunge(B)
206.9	2.8	110	67.8	298	22
±10	± 3	±11	± 8	±10	±11

Number	Date	OriginTime	Lat ,N	Long ,W	Depth, km	Magnitude, m_N
28	2002/04/20	$10^h 50^m 47^s$	44.523°	73.728°	17.4	5.5

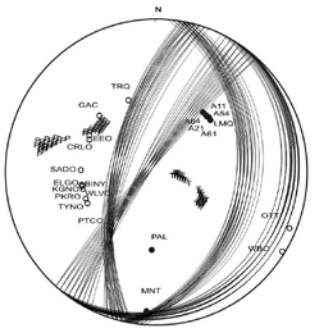

22 Polarities, 0 allowed errors
50/17032 acceptable solutions
Quality:B

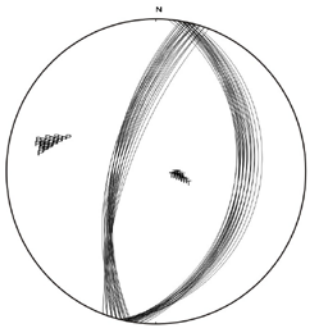

Average solution1

Dip(1)	Strike(1)	Rake(1)
28.07	10.24	85.75
± 7	± 5	± 3

Dip(2)	Strike(2)	Rake(2)
62.02	195.06	92.26
± 7	± 5	± 1

Trend(P)	Plungr(P)	Trend(T)	Plunge(T)	Trend(B)	Plunge(B)
283.39	16.99	110.51	72.89	14	2
± 6	± 5	±6	± 6	± 5	± 1

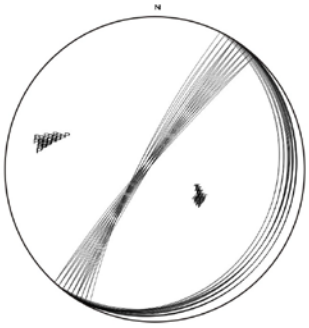

Average solution2

Dip(1)	Strike(1)	Rake(1)
6	36	90
± 1	± 8	± 0

Dip(2)	Strike(2)	Rake(2)
84	216	90
± 4	± 8	±0

Trend(P)	Plungr(P)	Trend(T)	Plunge(T)	Trend(B)	Plunge(B)
306	39	126	51	36	0
± 8	± 4	±8	±4	± 8	±0

Ma and Adams., 2002

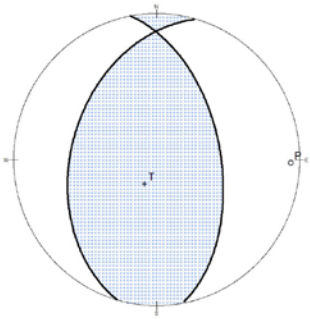

Lon	Lat	Depth
-73.7	44.5	10.0

Dip(1)	Strike(1)	Rake(1)
40.0	196.0	111.0

Dip(2)	Strike(2)	Rake(2)
53.0	349.0	73.0

Trend(P)	Plunge(P)	Trend(T)	Plunge(T)
91.0	7.0	207.0	75.0

Number	Date	OriginTime	Lat ,N	Long ,W	Depth, km	Magnitude, m_N
29	2002/04/20	$11^h 04^m 41^s$	44.483°	73.683°	7.9	4.1

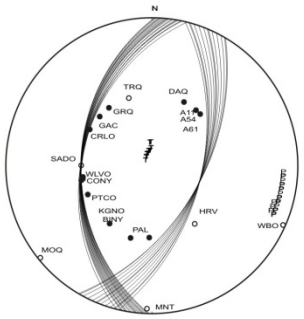

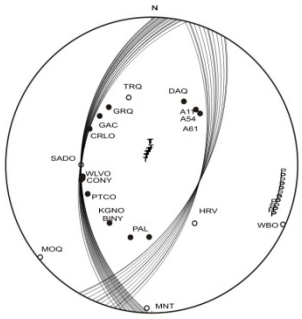

19 Polarities, 1 allowed errors
21 acceptable solutions
Quality:A

Average solution1

Dip(1)	Strike(1)	Rake(1)
38.4	188.4	80.3
± 1.0	±7.0	±10.0

Dip(2)	Strike(2)	Rake(2)
52.2	20.7	97.6
± 2.0	±13.0	± 7.0

Trend(P)	Plungr(P)	Trend(T)	Plunge(T)	Trend(B)	Plunge(B)
105.3	7.0	326.4	80.8	196.0	6.0
± 9.0	± 1.0	± 27.0	± 3.0	± 8.0	± 5.0

Number	Date	OriginTime	Lat ,N	Long ,W	Depth, km	Magnitude, m_N
30	2002/09/07	$21^h 27^m 45^s$	47.047°	76.237°	24.5	3.7

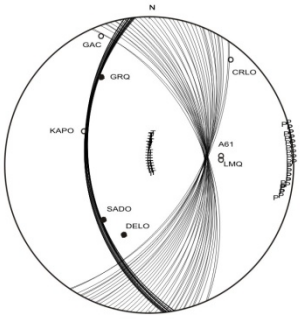

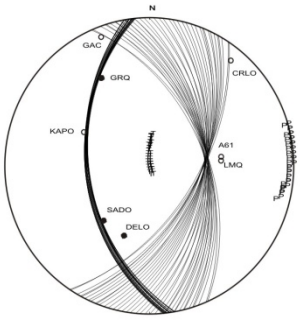

9 Polarities, 0 allowed errors
38 acceptable solutions
Quality:B

Average solution1

Dip(1)	Strike(1)	Rake(1)
42.96	173.08	75.24
± 3	± 5	±12

Dip(2)	Strike(2)	Rake(2)
48.78	12.89	103.35
± 5	±10	± 4

Trend(P)	Plungr(P)	Trend(T)	Plunge(T)	Trend(B)	Plunge(B)
93.48	2.95	347.21	79.56	184	10
± 6	± 3	±15	± 8	± 6	± 5

Number	Date	OriginTime	Lat ,N	Long ,W	Depth, km	Magnitude, m_N
31	2003/04/08	$15^h:06^m:15^s$	44.630°	74.362°	19	3.7

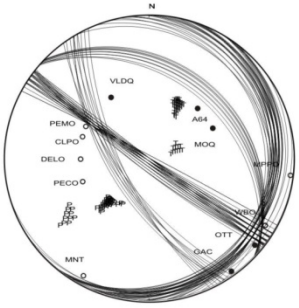

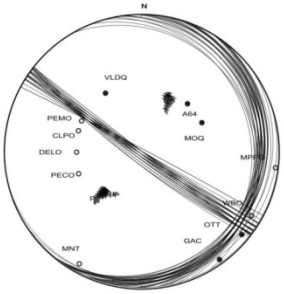

Average solution1

Dip(1)	Strike(1)	Rake(1)
86.04	127.44	81.98
± 5	± 3	± 3

Dip(2)	Strike(2)	Rake(2)
8.94	11.32	153.6
± 4	±25	±30

12 Polarities, 0 allowed errors
50/371 acceptable solutions
Quality:B

Trend(P)	Plungr(P)	Trend(T)	Plunge(T)	Trend(B)	Plunge(B)
224.9	40.52	28.9	48.36	128	8
± 7	± 5	± 6	± 5	±6	±3

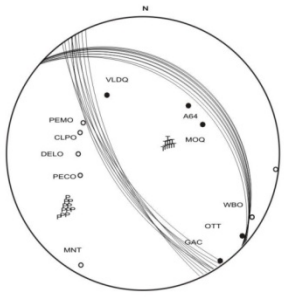

Average solution2

Dip(1)	Strike(1)	Rake(1)
26.64	311.9	76.52
± 4	± 1	±5

Dip(2)	Strike(2)	Rake(2)
64.15	146.92	96.67
± 5	±6	±2

Trend(P)	Plungr(P)	Trend(T)	Plunge(T)	Trend(B)	Plunge(B)
231.94	18.89	70.89	70.11	324	6
± 5	± 5	± 7	± 4	± 6	± 2

Number	Date	OriginTime	Lat ,N	Long ,W	Depth, km	Magnitude, m_N
32	2003/06/30	$19^h:21^m:16^s$	41.648°	81.150°	7	3.6

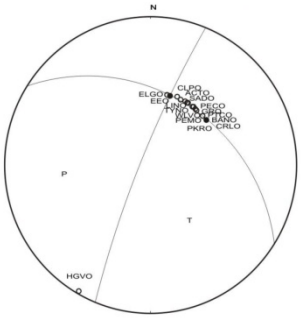

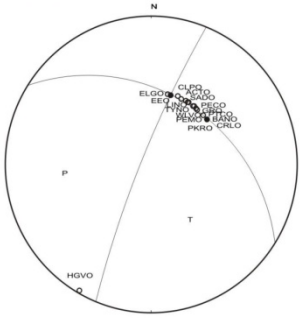

Average solution1

Dip(1)	Strike(1)	Rake(1)
39.1	302.0	12.5
± 0	± 0	± 0

Dip(2)	Strike(2)	Rake(2)
82.1	202.2	128.4
± 0	± 0	± 0

16 Polarities, 0 allowed errors
1 acceptable solutions
Quality:A

Trend(P)	Plungr(P)	Trend(T)	Plunge(T)	Trend(B)	Plunge(B)
262.7	26.9	147.3	40.2	16.0	38.0
± 0	± 0	±0	± 0	± 0	± 0

Number	Date	OriginTime	Lat ,N	Long ,W	Depth, km	Magnitude, m_N
33	2003/08/20	$01^h:58^m:18^s$	$46^\circ.012$	$74^\circ.951$	19	3.5

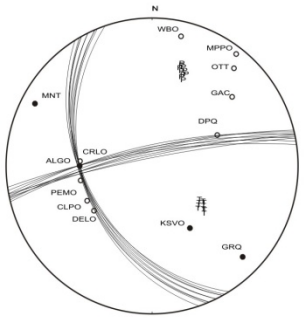

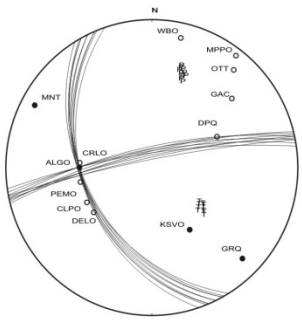

Average solution1

Dip(1)	Strike(1)	Rake(1)
34.6	301.8	57.0
± 3.0	±2.0	±2.0

Dip(2)	Strike(2)	Rake(2)
61.6	160.1	110.6
± 3.0	±3.0	±3.0

13 Polarities, 0 allowed errors
10 acceptable solutions
Quality:A

Trend(P)	Plungr(P)	Trend(T)	Plunge(T)	Trend(B)	Plunge(B)
235.3	14.2	109.0	66.7	330.0	18.0
±1.0	±3.0	±8.0	±1.0	±1.0	±2.0

Number	Date	OriginTime	Lat ,N	Long ,W	Depth, km	Magnitude, m_N
34	2003/10/20	$08^h:26^m:07^s$	$47^\circ.059$	$76^\circ.322$	21	4.5

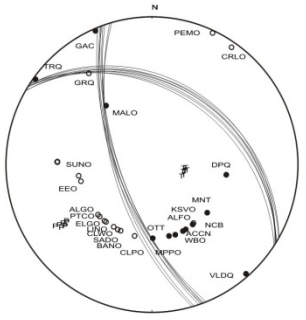

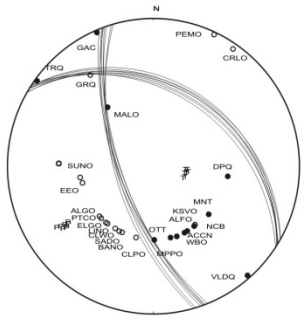

Average solution1

Dip(1)	Strike(1)	Rake(1)
34.6	301.8	57.0
± 3.0	±2.0	±2.0

Dip(2)	Strike(2)	Rake(2)
61.6	160.1	110.6
± 3.0	±3.0	±3.0

26 Polarities, 1 allowed errors
8 acceptable solutions
Quality:A

Trend(P)	Plungr(P)	Trend(T)	Plunge(T)	Trend(B)	Plunge(B)
235.3	14.2	109.0	66.7	330.0	18.0
± 1.0	± 3.0	± 8.0	±1.0	±1.0	±2.0

Number	Date	OriginTime	Lat ,N	Long ,W	Depth, km	Magnitude, m_N
35	2004/08/04	$23^h55^m26^s$	43.677°	78.241°	6.4	3.8

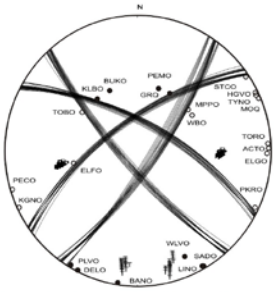

24 Polarities, 0 allowed errors
50/9279 acceptable solutions
Quality:B

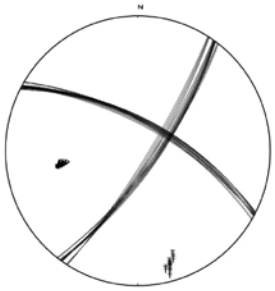

Average solution1

Dip(1)	Strike(1)	Rake(1)
65.51	298.09	-17.89
± 3	± 2	± 4

Dip(2)	Strike(2)	Rake(2)
73.76	35.71	-154.42
± 6	± 3	± 3

Trend(P)	Plungr(P)	Trend(T)	Plunge(T)	Trend(B)	Plunge(B)
258.65	29.39	165.56	5.47	66	60
± 2	± 3	±3	±6	±10	±2

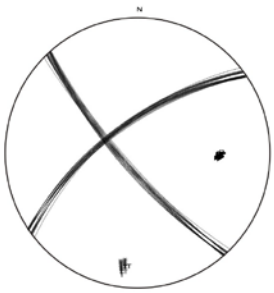

Average solution2

Dip(1)	Strike(1)	Rake(1)
77.27	137.15	-25.15
± 3	± 2	± 2

Dip(2)	Strike(2)	Rake(2)
65.51	233.06	-165.98
± 3	± 2	±3

Trend(P)	Plungr(P)	Trend(T)	Plunge(T)	Trend(B)	Plunge(B)
92.9	26.68	186.89	7.89	292	62
± 3	± 2	±2	±2	±7	±1

Kim et al., 2006

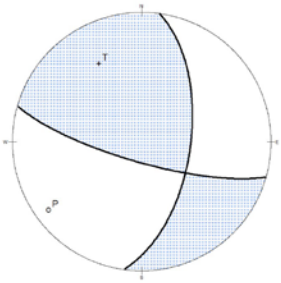

Lon	Lat	Depth
-78.2	43.7	4.0

Dip(1)	Strike(1)	Rake(1)
77.0	106.0	32.0

Dip(2)	Strike(2)	Rake(2)
59.0	8.0	165.0

Trend(P)	Plunge(P)	Trend(T)	Plunge(T)
234.0	12.0	331.0	31.0

Number	Date	OriginTime	Lat ,N	Long ,W	Depth, km	Magnitude, m_N
37	2005/05/25	$19^h22^m15^s$	$46^\circ.290$	$75^\circ.620$	23.8	3.7

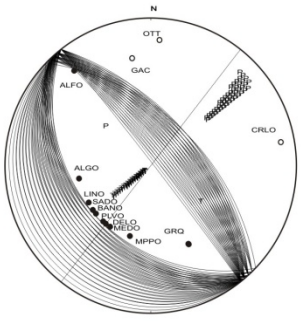

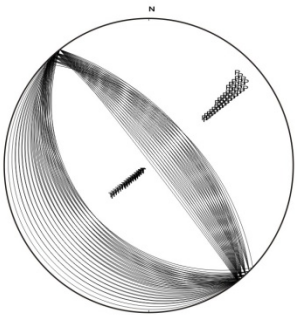

Average solution1

Dip(1)	Strike(1)	Rake(1)
24	138	90
± 15	± 3	± 0

Dip(2)	Strike(2)	Rake(2)
66	318	90
± 14	± 4	± 0

13 Polarities, 0 allowed errors
50/6918 acceptable solutions
Quality:B

Trend(P)	Plungr(P)	Trend(T)	Plunge(T)	Trend(B)	Plunge(B)
48	21	228	69	138	0
± 4	±18	±4	±12	± 4	±0

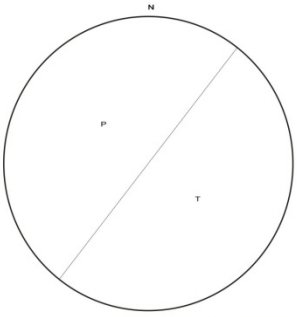

Average solution2

Dip(1)	Strike(1)	Rake(1)
0	0	52
± 0	± 0	± 0

Dip(2)	Strike(2)	Rake(2)
90	218	90.45
± 0	± 0	±0

Trend(P)	Plungr(P)	Trend(T)	Plunge(T)	Trend(B)	Plunge(B)
307.55	45.18	128.45	44.82	38	0.45
± 0	± 0	±0	±0	± 0	±0

Number	Date	OriginTime	Lat ,N	Long ,W	Depth, km	Magnitude, m_N
38	2005/07/04	$11^h47^m13^s$	$46^\circ.264$	$76^\circ.912$	16.7	3.6

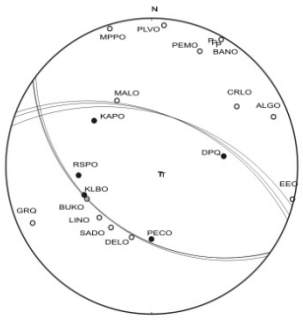

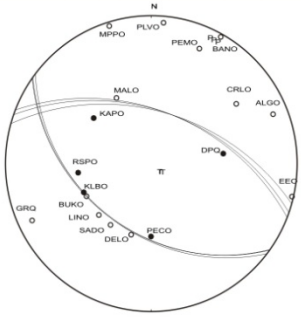

Average solution1

Dip(1)	Strike(1)	Rake(1)
50.5	289.3	79.6
± 0.0	±3.0	±1.0

Dip(2)	Strike(2)	Rake(2)
40.7	125.4	102.3
± 1.0	±1.0	±2.0

18 Polarities, 0 allowed errors
3 acceptable solutions
Quality:A

Trend(P)	Plungr(P)	Trend(T)	Plunge(T)	Trend(B)	Plunge(B)
26.7	5.0	148.1	80.6	296.0	8.0
±1.0	±0.0	±4.0	±1.0	±2.0	±1.0

Number	Date	OriginTime	Lat ,N	Long ,W	Depth, km	Magnitude, m_N
39	2005/07/23	$00^h:08^m:17^S$	$47^\circ.037$	$75^\circ.799$	19.5	3.5

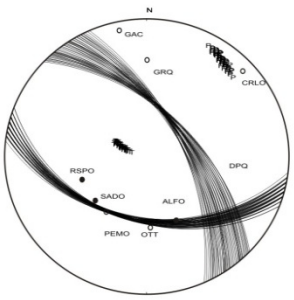

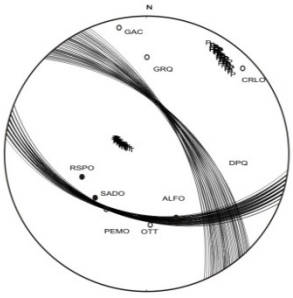

Average solution1

Dip(1)	Strike(1)	Rake(1)
40.52	102.79	58.23
± 2	± 7	±10

Dip(2)	Strike(2)	Rake(2)
56.47	321.95	114.22
± 4	±10	± 8

9 Polarities, 0 allowed errors
329 acceptable solutions
Quality:A

Trend(P)	Plungr(P)	Trend(T)	Plunge(T)	Trend(B)	Plunge(B)
34.9	8.45	283.15	68.14	128	20
±10	± 2	±10	± 7	±10	± 7

Number	Date	OriginTime	Lat ,N	Long ,W	Depth, km	Magnitude, m_N
40	2005/09/06	$14^h:10^m:52^S$	$46^\circ.282$	$75^\circ.287$	23.1	3.5

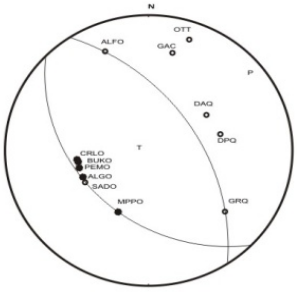

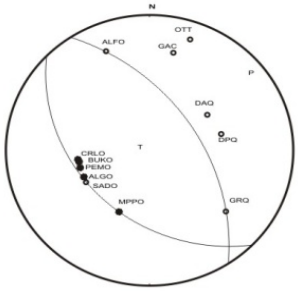

Average solution1

Dip(1)	Strike(1)	Rake(1)
38.4	134.4	80.3
± 0	± 0	± 0

Dip(2)	Strike(2)	Rake(2)
52.2	326.7	97.6
± 0	± 0	± 0

11 Polarities, 0 allowed errors
1 acceptable solutions
Quality:A

Trend(P)	Plungr(P)	Trend(T)	Plunge(T)	Trend(B)	Plunge(B)
52.0	7.0	272.4	80.8	142.0	6.0
± 0	± 0	±0	± 0	± 0	± 0

Number	Date	OriginTime	Lat ,N	Long ,W	Depth, km	Magnitude, m_N
41	2005/10/20	$21^h16^m29^s$	44.671°	80.470°	16.4	4.3

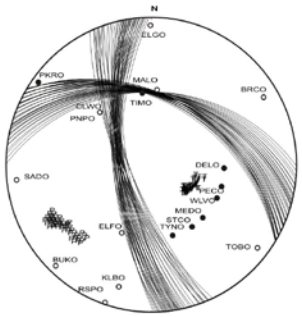

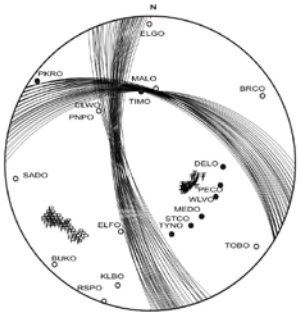

19 Polarities, 1 allowed errors
50/80 acceptable solutions
Quality:A

Average solution1

Dip(1)	Strike(1)	Rake(1)
40.1	290.8	39.1
±3.0	±16.0	±9.0

Dip(2)	Strike(2)	Rake(2)
66.0	168.9	123.2
± 6.0	±12.0	±2.0

Trend(P)	Plungr(P)	Trend(T)	Plunge(T)	Trend(B)	Plunge(B)
235.3	14.7	122.6	56.0	334.0	30.0
±11.0	±5.0	±16.0	±5.0	±10.0	±3.0

Dineva et al., 2007

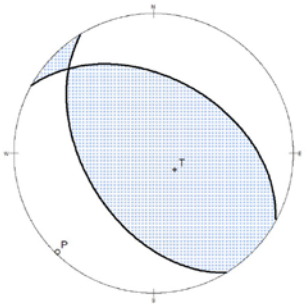

Lon	Lat	Depth
-80.5	44.7	12.0

Dip(1)	Strike(1)	Rake(1)
45.0	299.0	68.0

Dip(2)	Strike(2)	Rake(2)
49.0	149.0	110.0

Trend(P)	Plunge(P)	Trend(T)	Plunge(T)
242.0	2.0	127.0	75.0

Number	Date	OriginTime	Lat ,N	Long ,W	Depth, km	Magnitude, m_N
42	2006/01/09	$15^h35^m40^s$	45.031°	73.897°	15	4.2

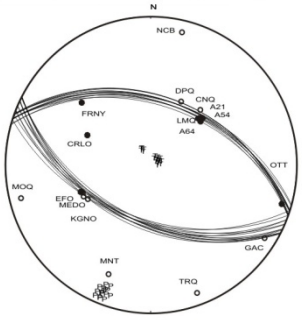

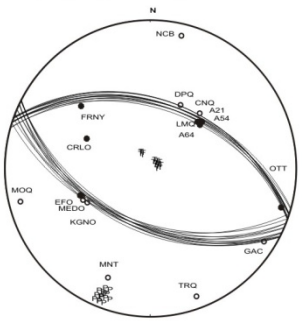

17 Polarities, 0 allowed errors
20 acceptable solutions
Quality:A

Average solution1

Dip(1)	Strike(1)	Rake(1)
40.0	289.6	86.9
± 0.0	± 0.0	±3.0

Dip(2)	Strike(2)	Rake(2)
50.0	113.7	92.6
± 0.0	± 3.0	±2.0

Trend(P)	Plungr(P)	Trend(T)	Plunge(T)	Trend(B)	Plunge(B)
201.8	5.0	43.8	84.6	292.0	2.0
±2.0	± 0.0	±10.0	±1.0	±1.0	±2.0

Number	Date	OriginTime	Lat ,N	Long ,W	Depth, km	Magnitude, m_N
43	2006/02/25	$01^h:39^m:22^s$	45.664°	75.246°	18.7	4.5

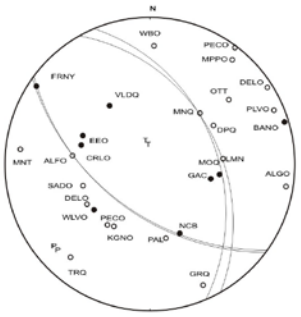

28 Polarities, 2 allowed errors
2 acceptable solutions
Quality:A

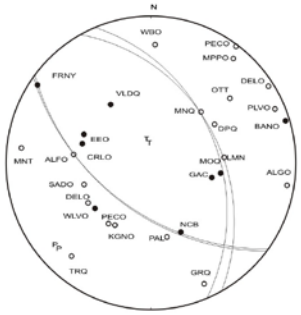

Average solution1

Dip(1)	Strike(1)	Rake(1)
53.7	125.8	70.0
± 1.0	± 0.0	± 0.0

Dip(2)	Strike(2)	Rake(2)
40.8	337.4	115.0
± 0.0	± 0.0	± 0.0

Trend(P)	Plungr(P)	Trend(T)	Plunge(T)	Trend(B)	Plunge(B)
230.0	6.8	342.0	72.5	138.0	16.0
±2.0	± 0.0	± 3.0	±4.0	±2.0	±4.0

Ma and Eaton., 2007

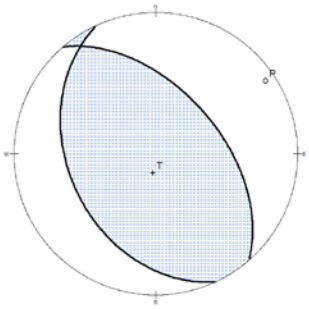

Lon	Lat	Depth
-75.2	45.7	19.0

Dip(1)	Strike(1)	Rake(1)
53.0	319.0	80.0

Dip(2)	Strike(2)	Rake(2)
38.0	155.0	103.0

Trend(P)	Plunge(P)	Trend(T)	Plunge(T)
56.0	8.0	188.0	80.0

Number	Date	OriginTime	Lat ,N	Long ,W	Depth, km	Magnitude, m_N
44	2006/06/20	$20^h:11^m:19^s$	41.799°	81.202°	9.1	3.7

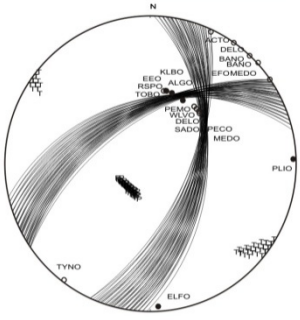

20 Polarities, 2 allowed errors
50/430 acceptable solutions
Quality:A

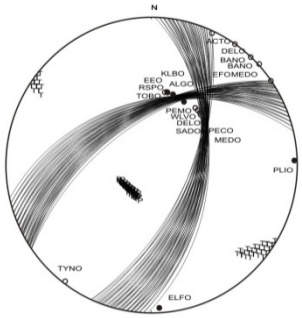

Average solution1

Dip(1)	Strike(1)	Rake(1)
49.0	243.5	-51.5
± 6.0	±10.0	± 5.0

Dip(2)	Strike(2)	Rake(2)
53.8	13.1	-125.6
± 7.0	±12.0	± 6.0

Trend(P)	Plungr(P)	Trend(T)	Plunge(T)	Trend(B)	Plunge(B)
222.4	62.0	127.4	2.6	36.0	28.0
± 20.0	±2.0	±7.0	± 5.0	± 5.0	± 2.0

Number	Date	OriginTime	Lat ,N	Long ,W	Depth, km	Magnitude, m_N
45	2007/03/12	$23^h 18^m 18^s$	$41^\circ.377$	$81^\circ.394$	7	3.7

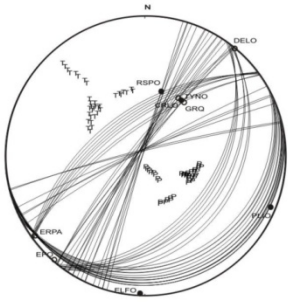

8 Polarities, 0 allowed errors
50/15929 acceptable solutions
Quality:C

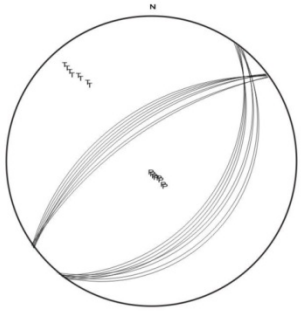

Average solution1

Dip(1)	Strike(1)	Rake(1)
56.38	233.36	-80.38
± 8	± 5	± 1

Dip(2)	Strike(2)	Rake(2)
34.82	36.34	-104.11
± 8	± 1	± 1

Trend(P)	Plungr(P)	Trend(T)	Plunge(T)	Trend(B)	Plunge(B)
173.6	76.43	316.45	10.89	48	8
±14	± 6	±1	±8	± 2	±1

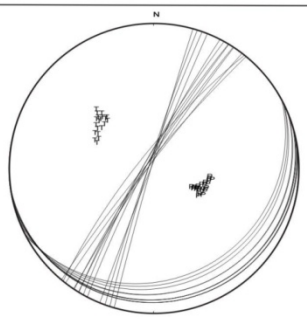

Average solution2

Dip(1)	Strike(1)	Rake(1)
8.48	74.84	-44.84
± 5	±16	± 20

Dip(2)	Strike(2)	Rake(2)
84.03	209.37	-96.03
± 6	± 10	± 1

Trend(P)	Plungr(P)	Trend(T)	Plunge(T)	Trend(B)	Plunge(B)
112.64	50.61	304.84	38.75	210	6
± 12	± 7	±11	±6	±12	±1

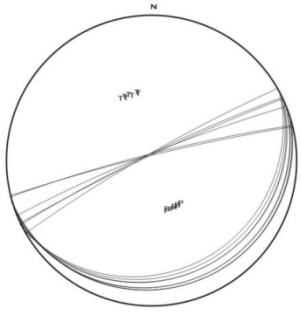

Average solution3

Dip(1)	Strike(1)	Rake(1)
4.47	81.41	-73.29
± 1	± 5	±5

Dip(2)	Strike(2)	Rake(2)
85.72	244.64	-91.29
± 1	±9	±1

Trend(P)	Plungr(P)	Trend(T)	Plunge(T)	Trend(B)	Plunge(B)
153.25	49.27	335.85	40.7	244.74	1.28
± 9	± 1	± 10	±1	± 10	±1

Number	Date	OriginTime	Lat ,N	Long ,W	Depth, km	Magnitude, m_N
46	2007/09/30	$17^h:35^m:35^s$	$46^\circ.924$	$76^\circ.510$	15.4	3.9

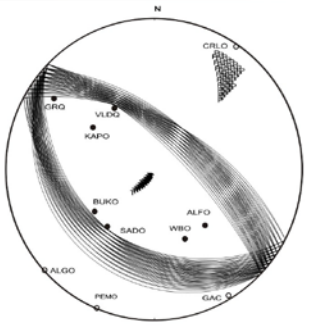

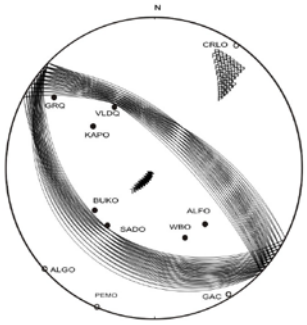

Average solution1

Dip(1)	Strike(1)	Rake(1)
30.0	126.0	90.0
± 8.0	±7.0	±0.0

Dip(2)	Strike(2)	Rake(2)
60.0	306.0	90.0
± 8.0	±8.0	±0.0

11 Polarities, 0 allowed errors
5o/2210 acceptable solutions
Quality:A

Trend(P)	Plungr(P)	Trend(T)	Plunge(T)	Trend(B)	Plunge(B)
36.0	15.0	216.0	75.0	126.0	0.0
±7.0	±9.0	± 8.0	±7.0	±8.0	± 0.0

Number	Date	OriginTime	Lat ,N	Long ,W	Depth, km	Magnitude, m_N
47	2007/10/01	$16^h:43^m:30^s$	$47^\circ.069$	$76^\circ.862$	19.8	4

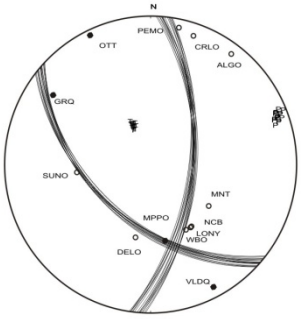

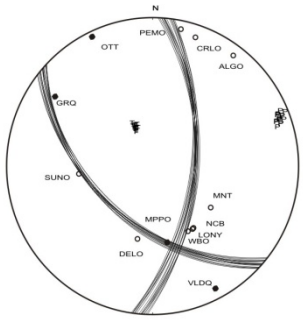

Average solution1

Dip(1)	Strike(1)	Rake(1)
47.0	131.4	46.8
± 1.0	±3.0	±5.0

Dip(2)	Strike(2)	Rake(2)
57.8	5.3	126.2
± 2.0	±3.0	±2.0

13 Polarities, 0 allowed errors
16 acceptable solutions
Quality:A

Trend(P)	Plungr(P)	Trend(T)	Plunge(T)	Trend(B)	Plunge(B)
70.5	6.0	330.2	59.3	164.0	30.0
± 3.0	± 3.0	± 3.0	± 4.0	± 4.0	± 3.0

Number	Date	OriginTime	Lat ,N	Long ,W	Depth, km	Magnitude, m_N
48	2007/12/23	$23^h48^m35^s$	$46.^\circ163$	$77.^\circ350$	25.9	3.6

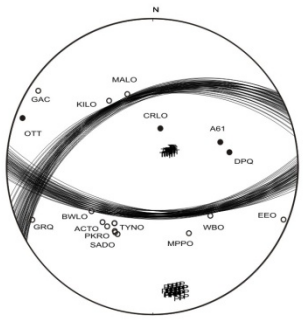

16 Polarities, 1 allowed errors
620 acceptable solutions
Quality:A

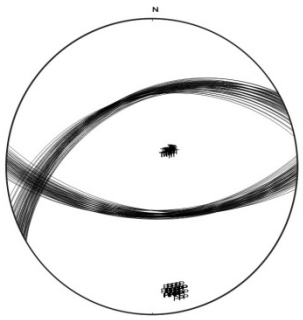

Average solution1

Dip(1)	Strike(1)	Rake(1)
37.7	248	70.1
± 3	± 9	± 9

Dip(2)	Strike(2)	Rake(2)
54.9	92.6	104.7
± 3	± 6	± 7

Trend(P)	Plungr(P)	Trend(T)	Plunge(T)	Trend(B)	Plunge(B)
172.1	8.8	46.7	75	264	12
± 6	± 3	±5	± 5	± 5	± 5

Number	Date	OriginTime	Lat ,N	Long ,W	Depth, km	Magnitude, m_N
49	2008/01/09	$01^h34^m47^s$	$41.^\circ758$	$81.^\circ395$	6	3.5

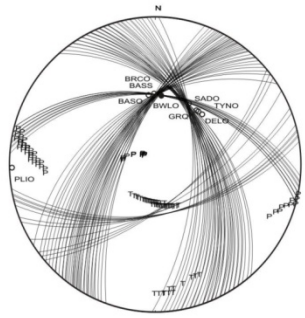

9 Polarities, 0 allowed errors
50/706 acceptable solutions
Quality:C

Average solution1

Dip(1)	Strike(1)	Rake(1)
48.07	335.85	44.57
± 10	±15	±10

Dip(2)	Strike(2)	Rake(2)
58.53	212.49	128.41
± 10	±15	± 5

Trend(P)	Plungr(P)	Trend(T)	Plunge(T)	Trend(B)	Plunge(B)
276.28	5.93	176.95	57.32	10	32
± 8	± 8	±18	±2	± 8	± 1

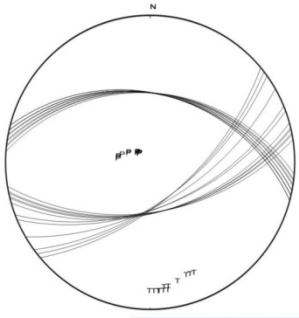

Average solution2

Dip(1)	Strike(1)	Rake(1)
39.58	280.9	-70.95
± 0	± 4	±13

Dip(2)	Strike(2)	Rake(2)
52.97	76.77	-105.1
± 5	±15	±8

Trend(P)	Plungr(P)	Trend(T)	Plunge(T)	Trend(B)	Plunge(B)
296.56	76.13	177.46	6.85	86	12
± 13	± 7	±5	±4	±13	±7

Number	Date	OriginTime	Lat ,N	Long ,W	Depth, km	Magnitude, m_N
50	2010/06/23	$17^h:41^m:42^s$	$45^\circ.882$	$75^\circ.495$	25.9	5.7

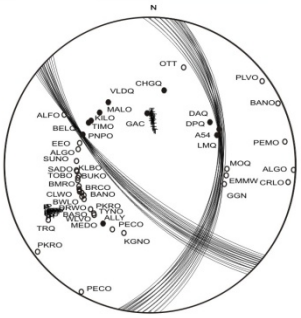

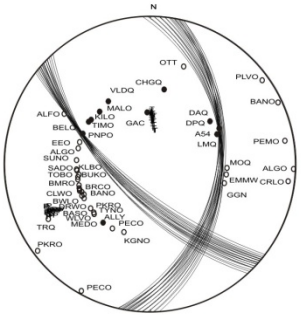

47 Polarities, 2 allowed errors
24 acceptable solutions
Quality:A

Average solution1

Dip(1)	Strike(1)	Rake(1)
65.5	132.0	58.9
± 4.0	± 5.0	± 6.0

Dip(2)	Strike(2)	Rake(2)
38.8	7.4	138.6
± 2.0	± 8.0	± 12.0

Trend(P)	Plungr(P)	Trend(T)	Plunge(T)	Trend(B)	Plunge(B)
244.2	15.0	359.1	57.6	146.0	28.0
± 3.0	± 3.0	± 4.0	± 7.0	± 5.0	± 6.0

Appendix D: Focal Mechanisms From Previous Studies Including the Canadian Stress Database.

Abbreviation for references:

CSDB = Canadian stress database (Adams, 1995)

GSC = Earthquakes Canada, GSC, *Earthquake Search (On-line Bulletin)*, http://seismo.nrcan.gc.ca/stnsdata/nedb/bull_e.php, Nat. Res. Can

SLU = Moment Tensor Solutions, Saint Louis Univ., Dep. Earth Atm. Sci.

http://www.eas.slu.edu/Earthquake_Center/MECH.NA/index.html.

PA = This study

Date: Date of the event:yyyymmdd.

Lon: Longitude of the event (°). Lat: Latitude of the event (°).

Depth: Focal depth of the event (km) M: Magnitude of the event

Strike(1), Dip(1) and Rake(1): strike, dip and rake of the plain(1)

Strike(2), Dip(2) and Rake(2): strike, dip and rake of the plain(2)

Pax: Trend of p axes Pp: Plunge of P axes

Tax: Trend of T axes Tp: Plung of T axes

Bax:trend of nodal plain Bp:plunge of nodal plain

Name: used name fro event for mapping the event.

Ref: Refrence

Date	Lon	Lat	Depth	M	Strike(1)	Dip(1)	Rake(1)	Strike(2)	Dip(2)	Rake(2)	Pax	Pp	Tax	Tp	Bax	Bp	Name	Ref
19351101	-79.1	46.8	10.0	6.1	130.0	45.0	80.0										T1	Bent(1996a)
19440925	-74.7	45.0	20.0	5.8	313.0	70.0	52.0										T2	Bent (1996b)
19660101	-78.2	42.8	2.0	4.1	13.0	71.0	159.0	110.0	70.0	20.0	62.0	1.0	331.0	28.0	154.0	62.0	T3	Herrmann (1979)
19670613	-78.2	42.9	3.0	4.4	-	-	-	-	-	-	74.0	11.0	336.0	53.0	172.0	36.0	C1	CSDB
19710508	-74.5	43.8	3.0	3.2	-	-	-	-	-	-	71.0	18.0	250.0	73.0	341.0	0.0	C2	CSDB
19721216	-75.2	45.8	18.0	3.9			-	-	-	-	155.0	10.0	260.0	75.0	65.0	20.0	C3	CSDB
19730615	-70.8	45.3	7.0	4.8mb	280.0	41.0		352.0	64.0		257.0	1.0	54.0	38.0			T4	Yang etall., 1981
19740607	-74.0	41.6	1.5	3.3			-			-	115.0	20.0	331.0	78.0	27.0	7.0	C4	CSDB
19740607	-74.0	41.6	1.5	3.3	280.0	59.0		120.0	32.0		295.0	23.0	151.0	75.0			T5	Yang etall., 1981
19750403	-74.2	45.7	5.0	3.1	-	-	-	-	-	-	268.0	3.0	10.0	35.0	169.0	50.0	C5	CSDB
19750607	-73.9	41.6	1.0	3.3Mb	-	-	-	-	-	-	50.0	15.0	230.0	74.0	140.0	0.0	C6	CSDB
19750609	-73.6	44.9	13.0	4.2Mb			-			-	73.0	8.0	255.0	84.0	163.0	0.0	C7	CSDB
19750712	-76.3	46.5	17.0	4.2Mb	-	-	-	-	-	-	206.0	25.0	26.0	65.0	296.0	0.0	C8	CSDB
19751102	-75.6	43.9	3.7	3.9mb	72.0	48.0		252.0	42.0		70.0	7.0	245.0	85.0	340.0	0.0	T6	Yang etall., 1981
19760311	-71.2	41.6	0.0	3.5mb	139.0	33.0		282.0	50.0		301.0	90.0	191.0	70.0			T7	Yang etall., 1981
19760413	-74.1	40.8	2.5	3mb	25.0	62.0		280.0	8.0		80.0	32.0	313.0	45.0			T8	Yang etall., 1981
19760713	-74.1	45.2	9.0	3.1			-			-	60.0	11.0	163.0	48.0	319.0	40.0	C9	CSDB
19770714	-74.4	46.0	18.0	3.4	-	-	-	-	-	-	250.0	30.0	115.0	50.0	0.0	20.0	C11	CSDB
19770928	-73.9	44.4	3.0	3.1	32.0	0.0		304.0	50.0		244.0	36.0	0.0	34.0			T9	Yang etall., 1981
19780218	-74.1	46.3	7.0	4.1mb	233.0	42.0		69.0	49.0		69.0	4.0	232.0	86.0			T10	Yang etall., 1981
19780730	-74.4	45.7	18.0	3.6	119.0	52.0	27.0	12.0	69.0	139.0	69.0	11.0	329.0	43.0	-	-	T11	Wahlstrom 1987
19780730	-74.4	45.6	<5	3.8mb	200.0	52.0		42.0	35.0		215.0	8.0	89.0	78.0			T12	Yang etall., 1981
19800606	-75.1	43.6	2.0	3.5	-	-	-	-	-	-	77.0	11.0	235.0	80.0	345.0	4.0	C12	CSDB
19810219	-74.9	46.0	18.0	3.3	-	-	-	-	-	-	1.0	25.0	100.0	25.0	233.0	55.0	C13	CSDB
19810704	-74.6	45.1	13.0	3.7	118.0	62.0	49.0	-	-	-	236.0	8.0	337.0	54.0	140.0	35.0	C14	CSDB
19810705	-74.6	45.2	13.0	3.4	252.0	36.0	14.0	-	-	-	213.0	28.0	94.0	42.0	324.0	35.0	C15	CSDB

19810707	-74.6	45.1	13.0	1.9	304.0	36.0	54.0										T13	Wahlstrom 1987
19810918	-75.0	46.1	0.0	3.5	308.0	80.0	-80.0	-	-	-	47.0	34.0	206.0	54.0	310.0	16.0	C16	CSDB
19810920	-74.4	45.8	18.0	2.8	69.0	40.0	82.0										T14	Wahlstrom 1987
19811021	-72.6	41.1	5.0	3.4	-	-	-	-	-	-	316.0	14.0	193.0	65.0	50.0	20.0	C17	CSDB
19820119	-71.6	43.5	8.0	4.2	200.0	35.0	120.0										T15	Nguyen&Herrmann (1992)
19820806	-75.5	45.9	19.0	3.7	271.0	65.0	4.0	-	-	-	228.0	14.0	132.0	20.0	349.0	65.0	C18	CSDB
19821031	-74.5	45.5	12.0	2.5	103.0	80.0	28.0										T16	Wahlstrom 1987
19821124	-73.4	45.4	18.0	2.9	203.0	75.0	27.0										T17	Wahlstrom 1987
19830913	-74.0	41.3	9.7	3.0	-	-	-	-	-	-	42.0	20.0	187.0	64.0	324.0	10.0	C19	CSDB
19831007	-74.3	43.9	7.5	5.1	-	-	-	-	-	-	112.0	0.0	210.0	90.0	22.0	0.0	C20	CSDB
19831007	-74.3	44.0	8.0	5.1Mb	-	-	-	-	-	-	267.0	22.0	108.0	66.0	0.0	7.0	C21	CSDB
19831011	-75.8	45.2	12.0	4.2	-	-	-	-	-	-	154.0	30.0	352.0	59.0	249.0	6.0	C22	CSDB
19831011	-75.8	45.2	12.0	4.1	224.0	22.0	63.0	-	-	-	155.0	25.0	0.0	63.0	250.0	10.0	C23	CSDB
19831012	-74.3	44.0	7.7	3.1	-	-	-	-	-	-	32.0	17.0	169.0	68.0	297.0	14.0	C24	CSDB
19831013	-75.8	45.2	12.0	1.2	52.0	77.0	59.0										T18	Wahlstrom 1987
19831016	-75.1	45.6	12.0	3.1	-	-	-	-	-	-	147.0	10.0	295.0	70.0	57.0	10.0	C25	CSDB
19831101	-73.9	45.7	18.0	3.4	104.0	61.0	78.0	-	-	-	203.0	15.0	347.0	72.0	110.0	10.0	C26	CSDB
19831210	-74.8	45.7	11.0	2.8	33.0	42.0	67.0										T19	Wahlstrom 1987
19831221	-74.0	45.2	10.0	3.0	-	-	-	-	-	-	97.0	25.0	345.0	40.0	207.0	35.0	C27	CSDB
19840117	-75.1	45.6	19.0	3.0	87.0	51.0	-8.0	-	-	-	52.0	32.0	308.0	22.0	190.0	50.0	C28	CSDB
19840628	-75.8	46.3	12.0	3.1	37.1	87.9	-39.4	305.3	50.6	-177.2	164.2	25.0	268.0	28.4			T20	Mareschal etal.,1989
19840802	-73.3	44.5	11.5	3.2	112.8	71.2	41.0	218.5	51.0	155.0	68.8	41.8	169.7	12.2			T21	Mareschal etal.,1989
19840820	-73.5	45.0	18.0	3.1	-	-	-	-	-	-	350.0	25.0	200.0	55.0	86.0	20.0	C29	CSDB
19841126	-75.1	45.2	5.0	3.3	299.0	41.0	41.0	-	-	-	242.0	13.0	132.0	57.0	340.0	30.0	C30	CSDB
19850130	-75.2	45.8	16.0	2.6	296.0	70.0	79.0										T22	Wahlstrom 1987
19850516	-75.7	46.9	12.0	3.2	232.3	85.4	62.7	331.1	27.7	170.1	168.7	53.0	299.0	34.7			T23	Mareschal etal.,1989

19850824	-76.7	45.6	9.0	3.1	272.0	57.0	66.0	-	-	-	18.0	9.0	132.0	68.0	285.0	20.0	C31	CSDB
19860107	-77.3	45.8	13.0	3.4	147.0	26.1	29.3	263.7	77.6	113.1	147.0	51.9	12.2	28.9			T24	Mareschal etal.,1989
19860110	-77.3	45.8	14.0	3.4	-	-	-	-	-	-	272.0	17.0	167.0	40.0	20.0	45.0	C32	CSDB
19860131	-81.1	41.6	6.0	5.0	-	-	-	-	-	-	68.0	9.0	335.0	17.0	183.0	70.0	C33	CSDB
19860503	-78.6	46.4	12.0	3.0	170.7	63.5	10.8	265.6	80.3	153.0	131.2	25.7	35.6	11.4			T25	Mareschal etal.1989
19860530	-78.4	46.3	4.0	3.0	-	-	-	-	-	-	163.0	44.0	30.0	36.0	280.0	25.0	C34	CSDB
19860605	-75.1	46.4	13.0	3.2	118.0	62.0	11.0	-	-	-	73.0	12.0	337.0	27.0	185.0	60.0	C35	CSDB
19860618	-74.8	45.9	4.0	3.0	-	-	-	-	-	-	231.0	10.0	24.0	79.0	140.0	5.0	C36	CSDB
19860806	-75.2	46.4	16.0	3.5	-	-	-	-	-	-	30.0	0.0	120.0	65.0	300.0	25.0	C37	CSDB
19860813	-74.3	45.1	10.0	3.3	-	-	-	-	-	-	110.0	0.0	20.0	80.0	200.0	10.0	C38	CSDB
19870723	-79.5	43.5	10.0	3.4	-	-	-	-	-	-	214.0	57.0	1.0	29.0	100.0	15.0	C39	CSDB
19870817	-78.9	46.9	18.0	3.2	284.0	63.0	72.0										T26	Adams etal.,1988
19871023	-74.5	45.8	13.0	3.7	-	-	-	-	-	-	228.0	30.0	342.0	36.0	110.0	40.0	C40	CSDB
19871111	-75.3	45.8	17.0	3.5	-	-	-	-	-	-	82.0	10.0	215.0	76.0	350.0	10.0	C41	CSDB
19880310	-75.7	46.3	13.0	4.0	-	-	-	-	-	-	243.0	29.0	358.0	36.0	125.0	40.0	C42	CSDB
19880515	-75.6	45.2	18.0	3.3	-	-	-	-	-	-	210.0	0.0	120.0	81.0	300.0	9.0	C43	CSDB
19880809	-75.0	45.0	9.0	3.4	-	-	-	-	-	-	251.0	13.0	137.0	59.0	348.0	27.0	C44	CSDB
19891116	-76.6	46.6	18.0	4.0	-	-	-	-	-	-	226.0	14.0	342.0	61.0	130.0	25.0	C45	CSDB
19900303	-75.3	45.2	18.0	2.9	226.0	42.0	-50.0										G1	GSC
19900424	-72.6	45.9	18.0	2.8	66.0	72.0	64.0										G2	GSC
19901007	-75.2	46.3	18.0	3.9	27.0	55.0	84.0										G3	GSC
19901019	-75.6	46.5	12.0	4.5	158.0	45.0	121.0	298.0	52.0	62.0	47.0	4.0	146.0	68.0	-	-	T27	Lamontagne et al., 1994
19931116	-73.5	45.2	19.4	4.3	169.2	45.0	90.2	349.2	45.0	90.2	169.1	3.0	135.3	86.4	169.0	0.0	P1	PA
19931225	-75.5	46.5	19.2	4.1	136.0	40.0	90.0	316.0	50.0	90.0	46.0	5.0	226.0	85.0	136.0	0.0	P2	PA
19941002	-72.5	42.4	10.0	3.5	14.0	48.0	90.0	194.0	42.0	90.0	104.0	3.0	284.0	87.0	14.0	0.0	P3	PA
19950215	-75.1	45.9	18.3	3.5	124.8	60.6	64.5	348.9	38.2	127.3	232.9	12.0	349.7	64.6	138.0	22.0	P4	PA

19950603	-76.4	47.1	18.0	3.9	100.1	50.0	68.9	311.0	44.4	113.2	204.8	2.9	304.8	73.7	114.0	16.0	P5	PA
19950616	-71.9	44.3	6.0	3.7	95.0	50.0	40.0	337.0	61.0	132.0	38.0	6.0	300.0	53.0	-	-	T28	Du et al., 2003
19950912	-74.4	45.6	23.4	3.7	259.1	54.1	85.1	87.5	36.2	96.8	352.6	9.0	148.2	80.2	262.0	4.0	P6	PA
19951010	-78.8	46.4	30.0	3.5	133.8	44.9	75.8	333.5	46.8	103.8	53.8	1.0	318.3	80.0	144.0	10.0	P7	PA
19960314	-74.4	46.0	18.0	3.7	136.0	36.0	98.0	306.0	54.0	84.0	40.0	9.0	191.0	80.0	-	-	T29	Du et al., 2003
19960314	-74.5	46.2	30.0	4.4	96.2	69.0	59.8	334.5	36.2	142.6	208.2	18.5	327.3	55.5	108.0	28.0	P8	PA
19960821	-71.4	44.2	7.0	3.4	144.0	60.0	93.0	318.0	30.0	85.0	232.0	15.0	62.0	75.0	-	-	T30	Du et al., 2003
19970403	-72.3	46.0	17.0	3.6	78.4	8.9	-63.3	231.4	82.0	-94.0	136.7	52.8	325.0	36.9	232.0	4.0	P9	PA
19970524	-74.2	45.8	22.0	3.6	96.0	33.0	60.0	311.0	62.0	108.0	27.0	15.0	256.0	68.0	-	-	T31	Du et al., 2003
19970524	-74.2	45.9	22.2	4.2	116.5	36.2	83.2	304.9	54.1	94.9	31.4	9.0	235.8	80.2	122.0	4.0	P10	PA
19980225	-80.4	41.5	2.0	4.5	9.0	69.0	144.0	114.0	57.0	25.0	64.0	8.0	327.0	40.0	-	-	T32	Du et al., 2003
19980226	-76.4	46.1	15.2	3.7	308.8	42.4	52.9	174.5	57.5	118.8	244.3	8.2	136.7	64.5	338.0	24.0	P11	PA
19980418	-75.0	45.6	21.5	4.1	275.2	80.4	73.8	155.4	18.8	148.8	19.0	33.5	166.5	52.0	278.0	16.0	P12	PA
19980730	-74.7	46.2	10.0	4.4	174.0	34.0	90.0	354.0	56.0	90.0	84.0	11.0	264.0	79.0	174.0	0.0	P13	PA
19980925	-80.4	41.5	2.0	4.5	9.0	69.0	144.0	114.0	57.0	25.0	64.0	8.0	327.0	40.0	-	-	T33	Du et al., 2003
19980925	-80.1	41.6	5.0	5.4	356.4	46.5	52.8	224.2	54.7	122.5	291.8	4.5	192.7	63.6	24.0	26.0	P14	PA
19981225	-77.9	43.8	13.0	3.6	232.0	84.0	-84.0	7.0	8.0	-135.0	149.0	51.0	317.0	39.0	-	-	T34	Dineva et al., 2004
19981225	-77.9	43.8	2.0	3.6	135.0	76.0	20.0	40.0	70.0	165.0					-	-	T35	Kim et al., 2006
19981225	-77.8	43.9	15.0	3.6	328.6	42.2	23.6	220.6	74.4	129.7	282.0	19.5	170.9	45.6	28.0	38.0	P15	PA
19990618	-75.1	46.5	27.5	3.5	178.0	34.0	90.0	358.0	56.0	90.0	88.0	11.0	268.0	79.0	178.0	0.0	P16	PA
19991031	-74.3	45.8		4.2	95.0	68.0	44.0	355.0	47.0	165.0					-	-	T36	Bent et al., 2003
19991126	-79.0	43.7	9.2	3.8	228.0	38.0	145.0	347.0	69.0	58.0	101.0	18.0	218.0	54.0	-	-	T37	Dineva et al., 2005
20000101	-78.9	46.9	14.6	5.2	126.0	56.0	90.0	306.0	34.0	90.0	216.0	11.0	36.0	79.0	126.0	0.0	P17	PA
20000420	-74.3	43.9	12.2	4.0	270.5	49.0	51.5	140.9	53.8	125.6	206.6	2.7	111.6	61.8	298.0	28.0	P18	PA

20000524	-79.0	43.8	5.0	3.1	42.0	24.0	-54.0	183.0	71.0	-105.0					-	-	T38	Dineva et al., 2005
20000524	-79.1	43.8		3.1	16.0	25.0	52.0	237.0	71.0	106.0					-	-	T39	Bent et al., 2003
20001006	-74.0	45.1	20.1	3.8	134.0	50.0	90.0	314.0	40.0	90.0	224.0	5.0	44.0	85.0	134.0	0.0	P19	PA
20010126	-80.8	42.0	2.0	3.9	5.0	79.0	159.0	99.0	69.0	12.0	53.0	7.0	320.0	23.0	-	-	T40	Du et al., 2003
20010319	-76.2	47.1	20.5	3.9	4.0	34.0	90.0	184.0	56.0	90.0	274.0	11.0	94.0	79.0	4.0	0.0	P20	PA
20010411	-76.1	47.1	19.4	3.6	4.0	59.0	90.0	184.0	31.0	90.0	95.0	14.0	273.0	76.0	2.0	0.0	P21	PA
20011224	-76.5	46.9	19.4	3.8	279.0	64.9	54.2	158.6	42.7	141.3	34.0	12.7	142.8	55.0	296.0	32.0	P22	PA
20020211	-73.4	46.1	15.9	3.8	273.4	46.5	58.9	136.6	51.7	118.5	206.9	2.8	110.0	67.8	298.0	22.0	P23	PA
20020420	-73.7	44.5	10.0	5mw	196.0	40.0	111.0	349.0	53.0	73.0	91.0	7.0	207.0	75.0	-	-	T41	Ma and Adams (2002)
20020420	-73.7	44.5	7.3	4.1	188.4	38.4	80.3	20.7	52.2	97.6	105.3	7.0	326.4	80.8	196.0	6.0	P24	PA
20020420	-73.7	44.5	17.4	5.5	10.2	28.1	85.8	195.1	62.0	92.3	283.4	17.0	110.5	72.9	14.0	2.0	P25	PA
20020907	-76.2	47.0	24.5	3.7	173.1	43.0	75.2	12.9	48.8	103.4	93.5	3.0	347.2	79.6	184.0	10.0	P26	PA
20030408	-74.4	44.6	19.0	3.7	127.4	86.0	82.0	11.3	8.9	153.6	224.9	40.5	28.9	48.4	128.0	8.0	P27	PA
20030630	-81.2	41.6	7.0	3.6	302.0	39.1	12.5	202.2	82.1	128.4	262.7	26.9	147.3	40.2	16.0	38.0	P28	PA
20030820	-75.0	46.0	19.0	3.5	257.3	79.0	51.2	154.0	40.1	162.8	16.3	24.0	130.3	42.5	266.0	38.0	P29	PA
20031012	-76.3	47.1	21.0	4.5	301.8	34.6	57.0	160.1	61.6	110.6	235.3	14.2	109.0	66.7	330.0	18.0	P30	PA
20040804	-78.2	43.7	4.0	3.1	106.0	77.0	32.0	8.0	59.0	165.0	234.0	12.0	331.0	31.0	-	-	T42	Kim et al., (2006)
20040804	-78.3	43.7	3.0	3.2	125.0	65.0	35.0										S1	SLU
20040804	-78.2	43.7	6.4	3.8	298.09	65.51	-17.89	35.71	73.76	-154.42	258.65	29.39	165.56	5.47	66	60	P31	PA
20050303	-74.2	45.0	18.4	3.5	140.0	68.0	90.0	320.0	22.0	90.0	230.0	23.0	50.0	67.0	140.0	0.0	P32	PA
20050525	-75.6	46.3	23.8	3.7	138.0	24.0	90.0	318.0	66.0	90.0	48.0	21.0	228.0	69.0	138.0	0.0	P33	PA
20050704	-76.9	46.3	16.7	3.6	289.3	50.5	79.6	125.4	40.7	102.3	26.7	5.0	148.1	80.6	296.0	8.0	P34	PA
20050723	-75.8	47.0	19.5	3.5	102.8	40.5	58.2	322.0	56.5	114.2	34.9	8.5	283.2	68.1	128.0	20.0	P35	PA
20050906	-75.3	46.3	23.1	3.5	134.4	38.4	80.3	326.7	52.2	97.6	52.0	7.0	272.4	80.8	142.0	6.0	P36	PA
20051020	-80.5	44.7	16.4	4.3	290.8	40.1	39.1	168.9	66.0	123.2	235.3	14.7	122.6	56.0	334.0	30.0	P37	PA
20060109	-73.9	45.0	15.0	4.2	289.6	40.0	86.9	113.7	50.0	92.6	201.8	5.0	43.8	84.6	292.0	2.0	P38	PA

20060225	-75.2	45.7	18.7	4.5	125.8	53.7	70.0	337.4	40.8	115.0	230.0	6.8	342.0	72.5	138.0	16.0	P39	PA
20060620	-81.2	41.8	9.1	3.7	243.5	49.0	-51.5	13.1	53.8	-125.6	222.4	62.0	127.4	2.6	36.0	28.0	P40	PA
20070312	-81.4	41.4	7.0	3.7	233.4	56.4	-80.4	36.3	34.8	-104.1	173.6	76.4	316.5	10.9	48.0	8.0	P41	PA
20070930	-76.5	46.9	15.4	3.9	126.0	30.0	90.0	306.0	60.0	90.0	36.0	15.0	216.0	75.0	126.0	0.0	P42	PA
20071001	-76.9	47.1	19.8	4.0	131.4	47.0	46.8	5.3	57.8	126.2	70.5	6.0	330.2	59.3	164.0	30.0	P43	PA
20071223	-77.4	46.2	25.9	3.6	248.0	37.7	70.1	92.6	54.9	104.7	172.1	8.8	46.7	75.0	264.0	12.0	P44	PA
20080109	-81.4	41.8	6.0	3.5	335.9	48.1	44.6	212.5	58.5	128.4	276.3	5.9	177.0	57.3	10.0	32.0	P45	PA
20100623	-75.5	45.9	25.9	5.7	132.0	65.5	58.9	7.4	38.8	138.6	244.2	15.0	359.1	57.6	146.0	28.0	P46	PA

Appendix E: Errors of Hypocentre and Focal Mechanism Estimations

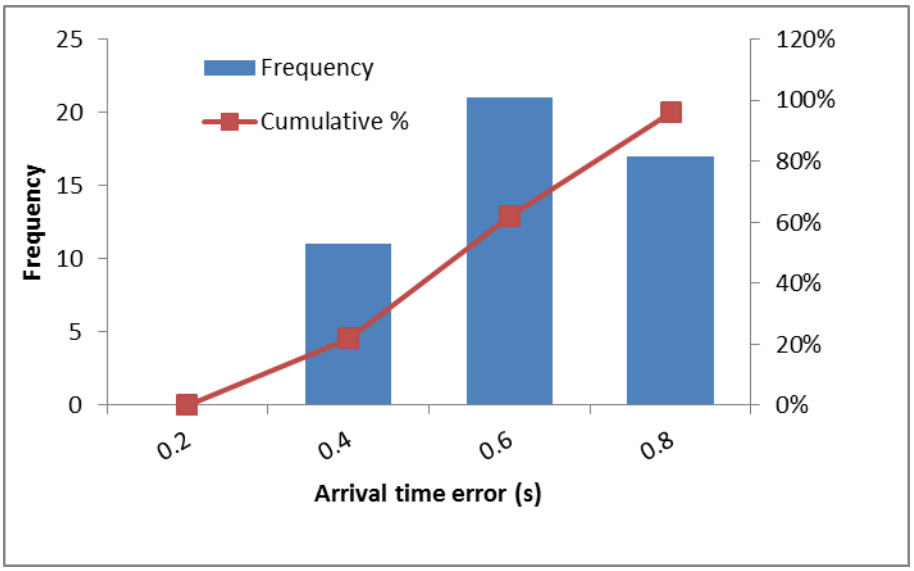

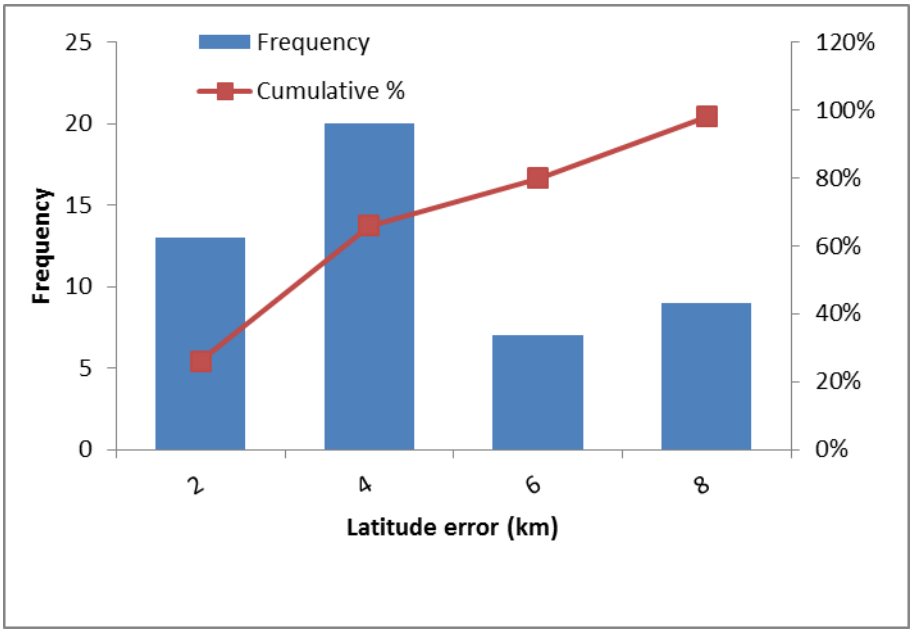

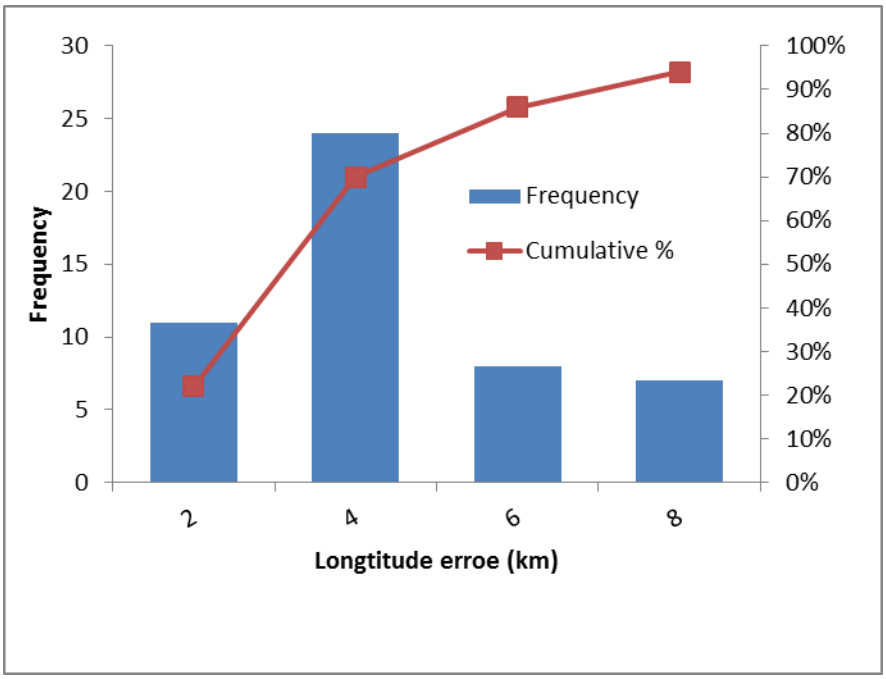
30
25
20
15
10
5
0
Frequency
100%
90%
80%
70%
60%
50%
40%
30%
20%
10%
0%
Frequency
Cumulative %
2
4
6
8
Longtitude erroe (km)

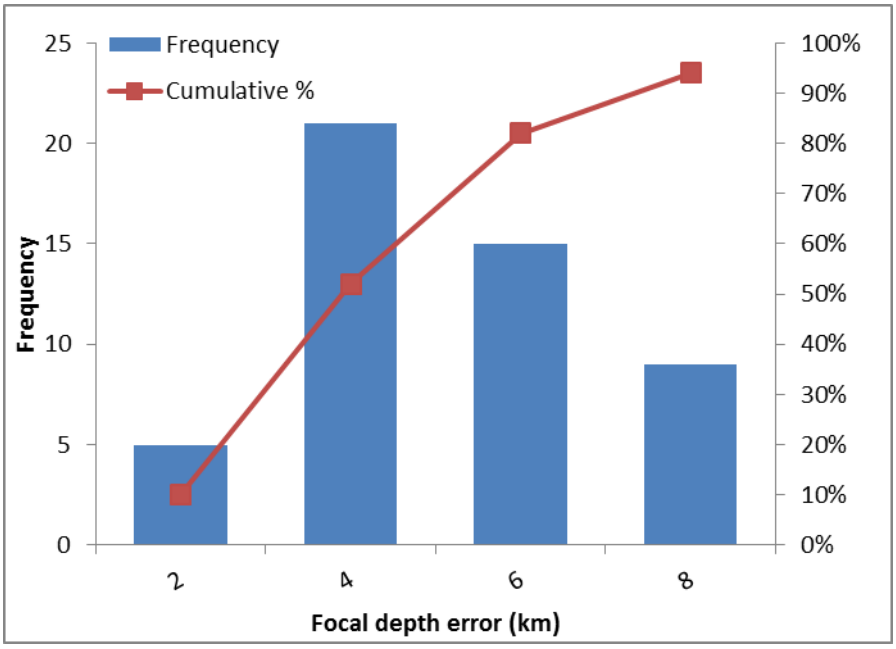
25
20
15
10
5
0
Frequency
Frequency
Cumulative %
100%
90%
80%
70%
60%
50%
40%
30%
20%
10%
0%
2
4
6
8
Focal depth error (km)

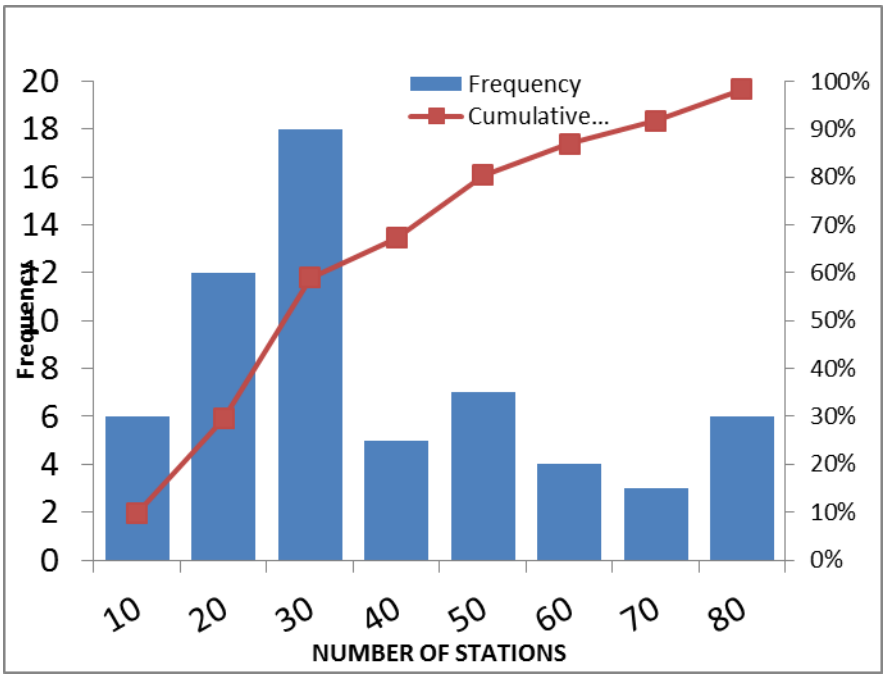
Frequency
Cumulative...
Frequency
NUMBER OF STATIONS
0
2
4
6
8
10
12
14
16
18
20
0%
10%
20%
30%
40%
50%
60%
70%
80%
90%
100%
10
20
30
40
50
60
70
80

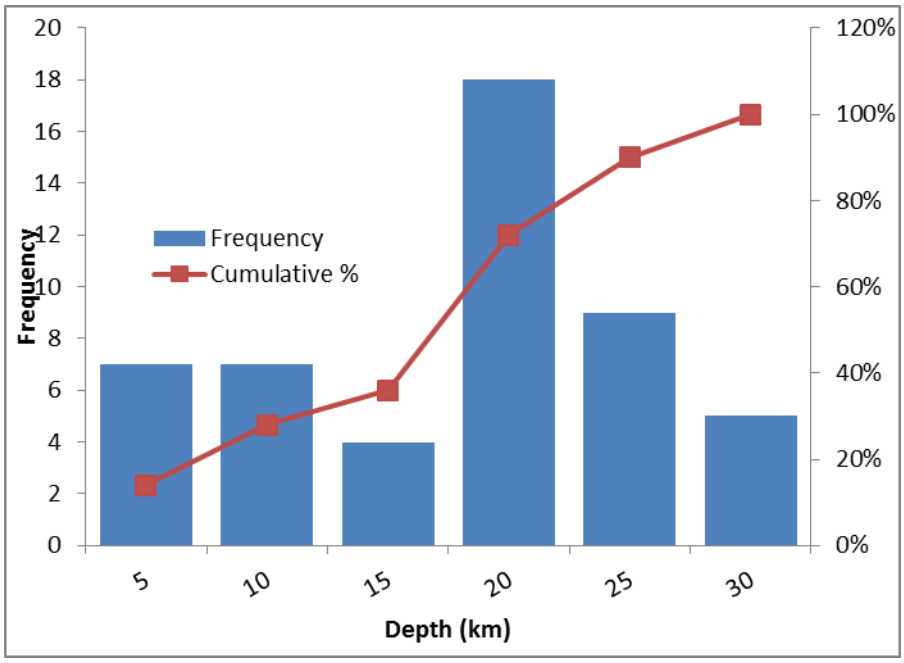
Frequency
Cumulative %
Frequency
Depth (km)
0
2
4
6
8
10
12
14
16
18
20
0%
20%
40%
60%
80%
100%
120%
5
10
15
20
25
30

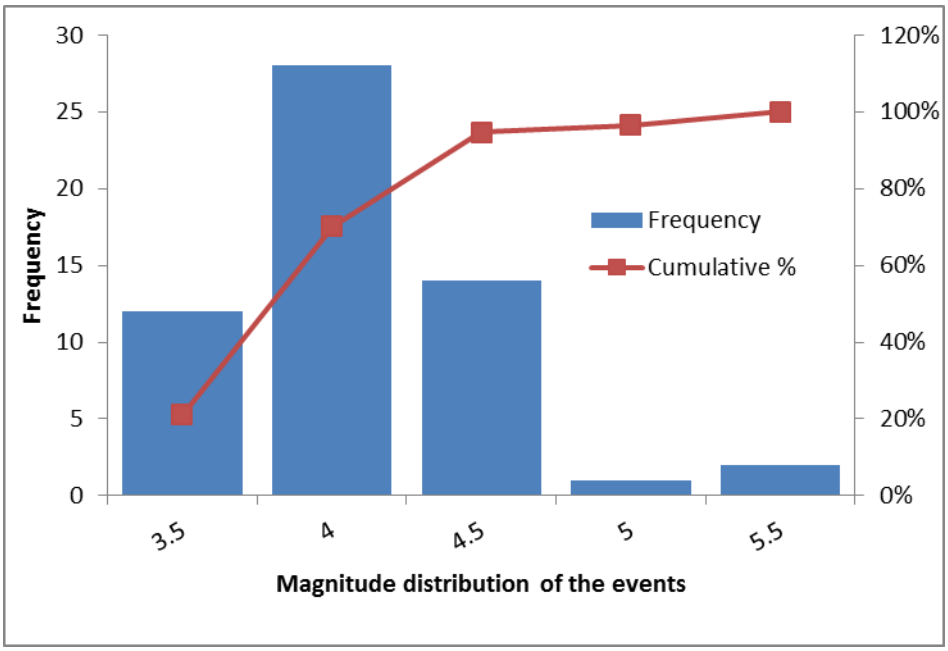
30
25
20
15
10
5
0
120%
100%
80%
60%
40%
20%
0%
Frequency
Frequency
Cumulative %
3.5
4
4.5
5
5.5
Magnitude distribution of the events

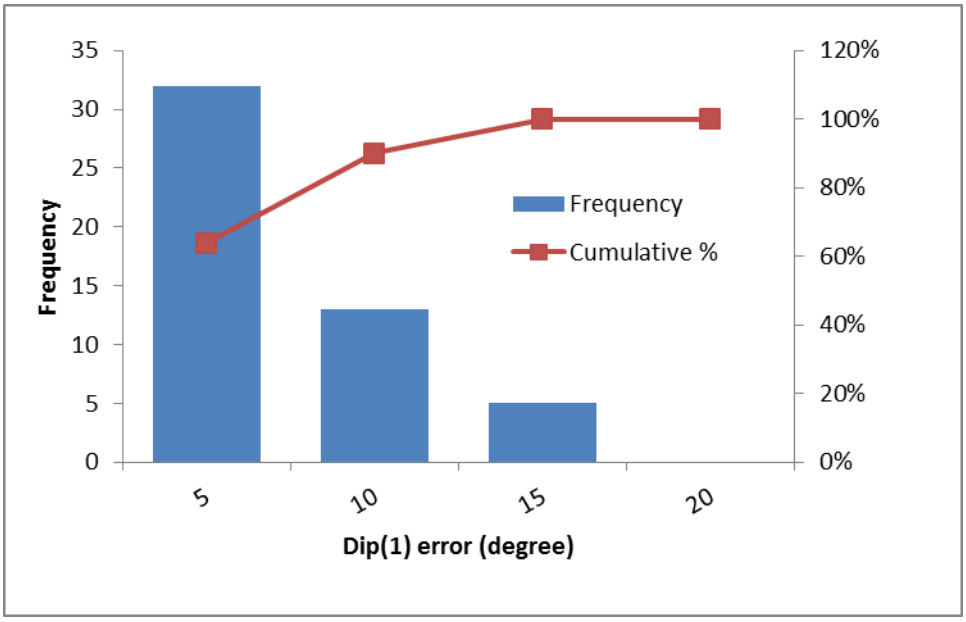
35
30
25
20
15
10
5
0
120%
100%
80%
60%
40%
20%
0%
Frequency
Frequency
Cumulative %
5
10
15
20
Dip(1) error (degree)

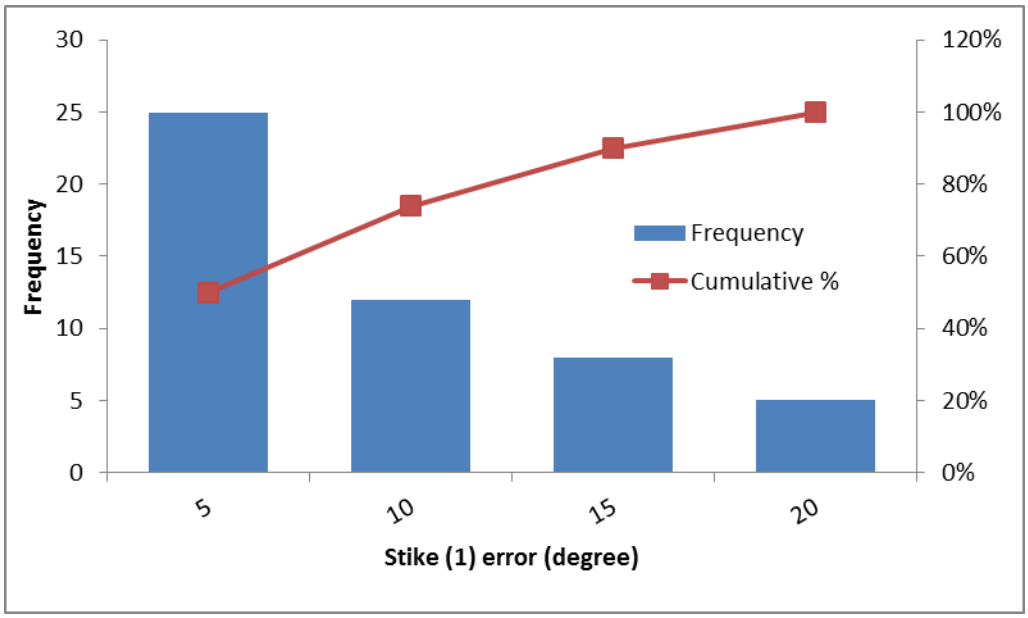
30
25
20
15
10
5
0
120%
100%
80%
60%
40%
20%
0%
Frequency
Frequency
Cumulative %
5
10
15
20
Stike (1) error (degree)

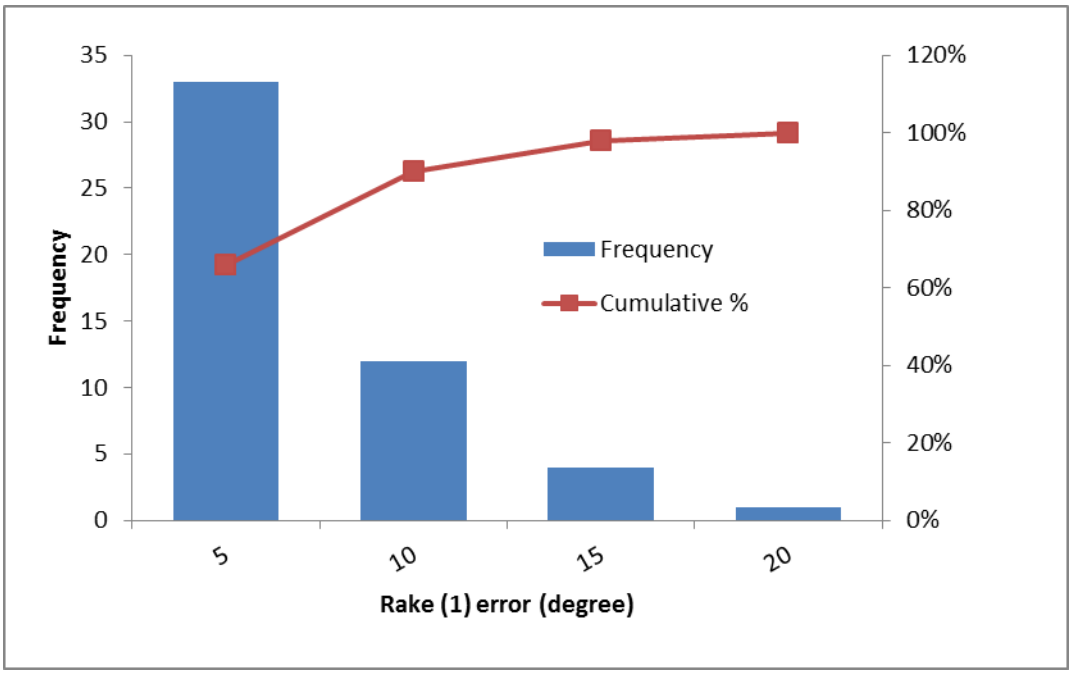
35
30
25
20
15
10
5
0
120%
100%
80%
60%
40%
20%
0%
Frequency
Frequency
Cumulative %
5
10
15
20
Rake (1) error (degree)

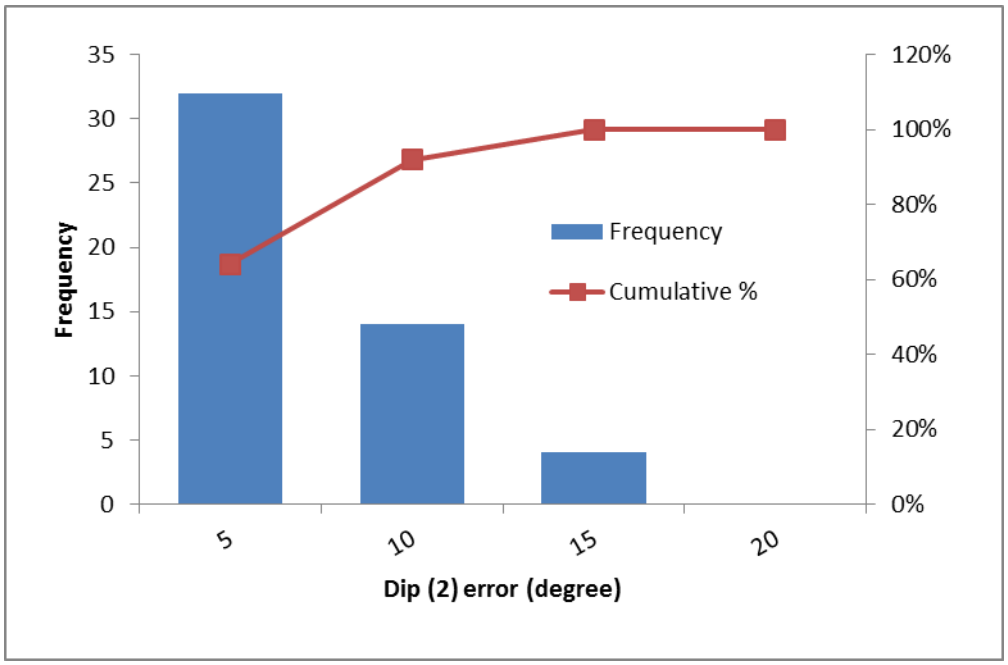
35
30
25
20
15
10
5
0
Frequency
120%
100%
80%
60%
40%
20%
0%
Frequency
Cumulative %
5
10
15
20
Dip (2) error (degree)

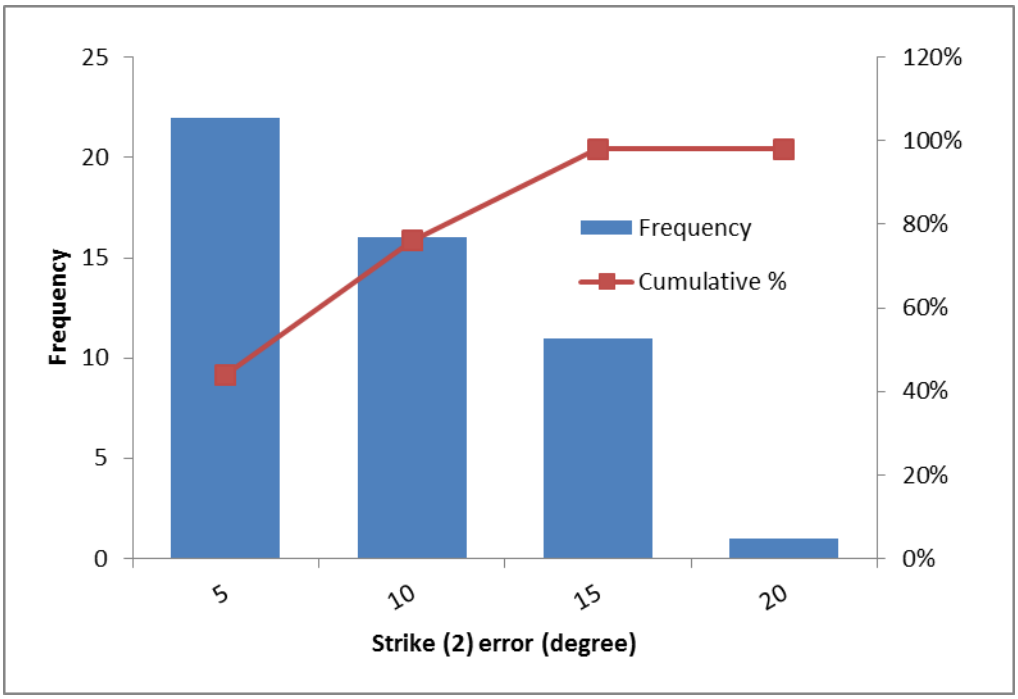
25
20
15
10
5
0
Frequency
120%
100%
80%
60%
40%
20%
0%
Frequency
Cumulative %
5
10
15
20
Strike (2) error (degree)

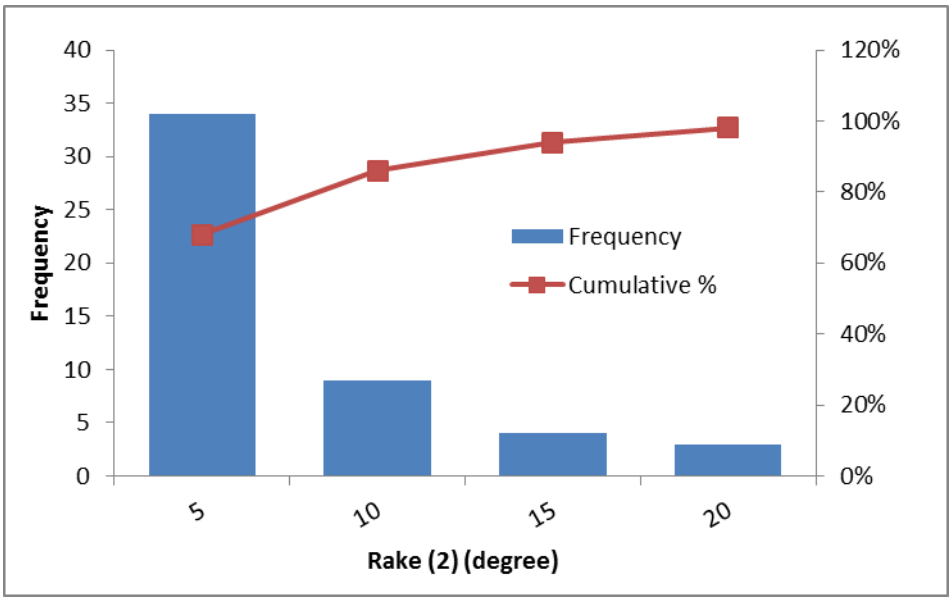
40
35
30
25
20
15
10
5
0
Frequency
120%
100%
80%
60%
40%
20%
0%
Frequency
Cumulative %
5
10
15
20
Rake (2) (degree)

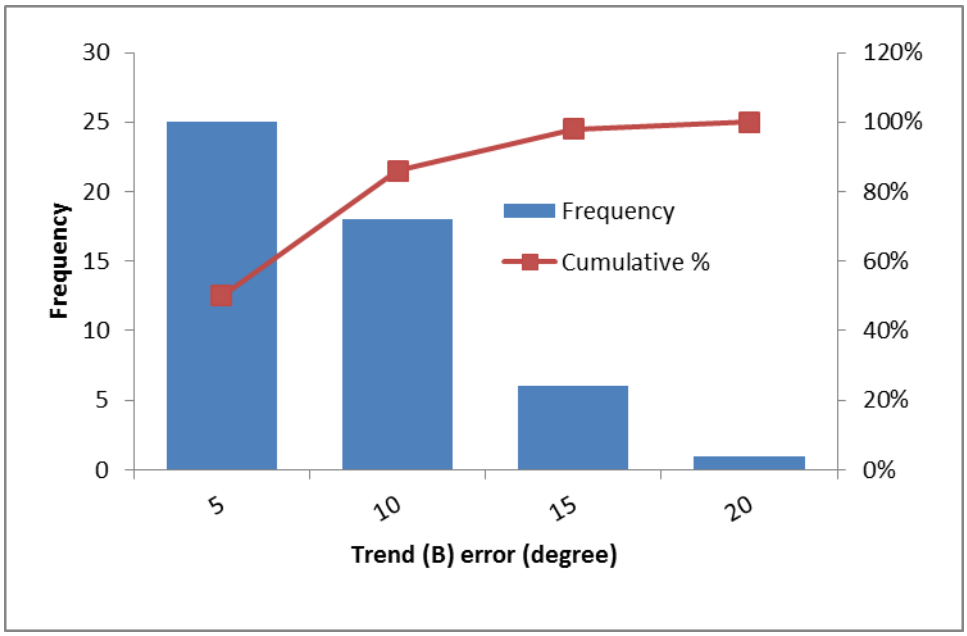
30
25
20
15
10
5
0
Frequency
120%
100%
80%
60%
40%
20%
0%
Frequency
Cumulative %
5
10
15
20
Trend (B) error (degree)

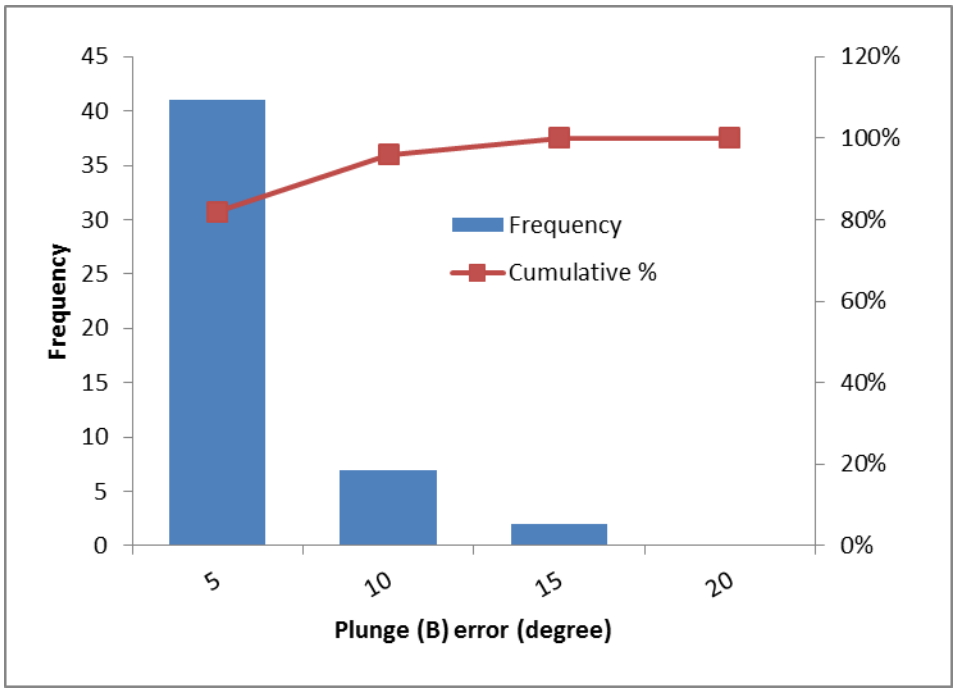
45
40
35
30
25
20
15
10
5
0
Frequency
120%
100%
80%
60%
40%
20%
0%
Frequency
Cumulative %
5
10
15
20
Plunge (B) error (degree)

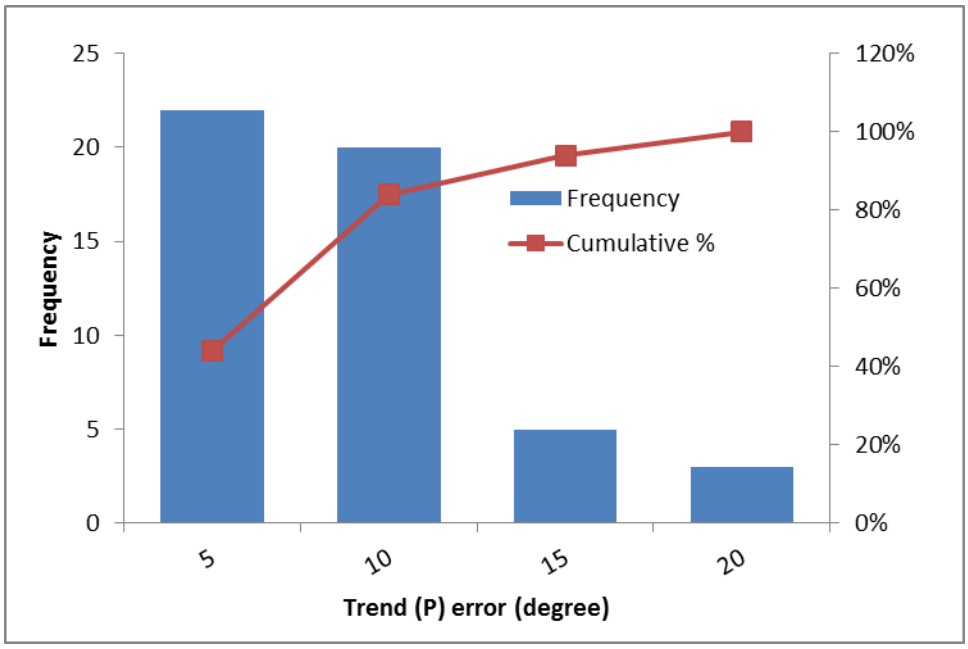
25
20
15
10
5
0
Frequency
120%
100%
80%
60%
40%
20%
0%
Frequency
Cumulative %
5
10
15
20
Trend (P) error (degree)

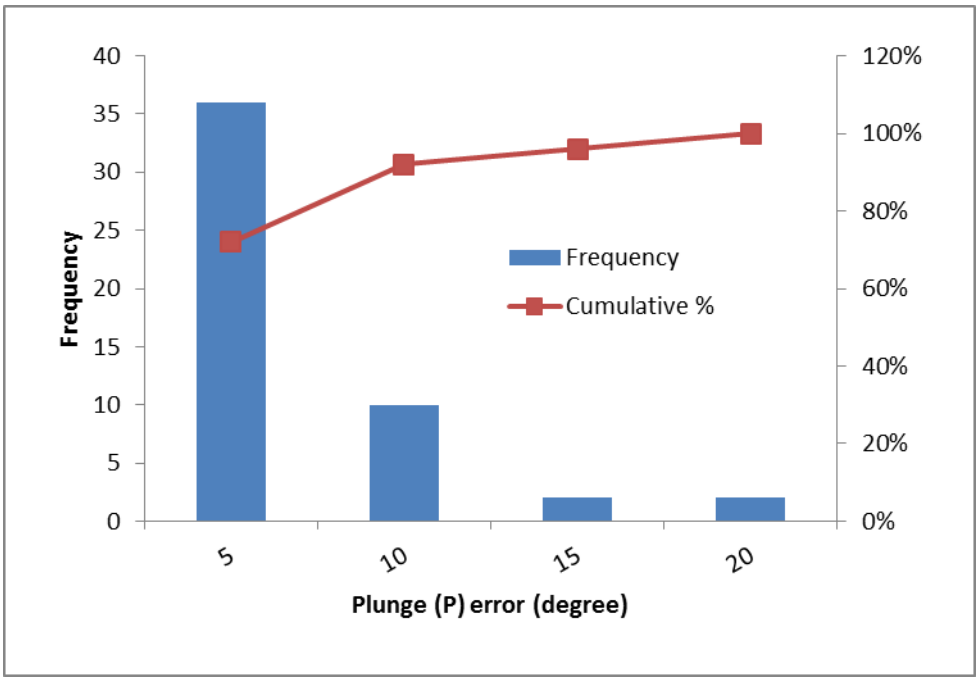
40
35
30
25
20
15
10
5
0
Frequency
120%
100%
80%
60%
40%
20%
0%
Frequency
Cumulative %
5
10
15
20
Plunge (P) error (degree)

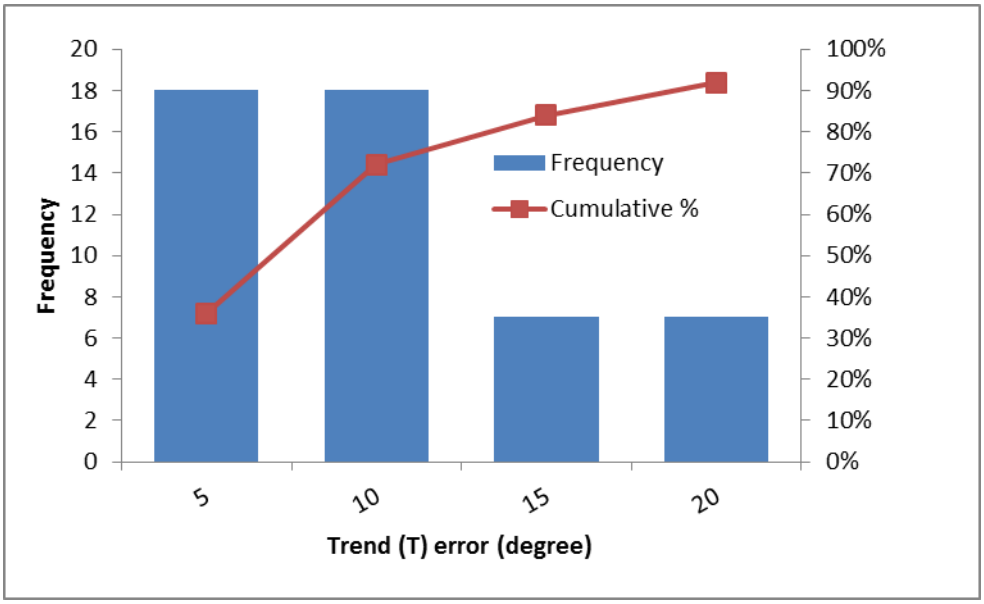
20
18
16
14
12
10
8
6
4
2
0
Frequency
100%
90%
80%
70%
60%
50%
40%
30%
20%
10%
0%
Frequency
Cumulative %
5
10
15
20
Trend (T) error (degree)

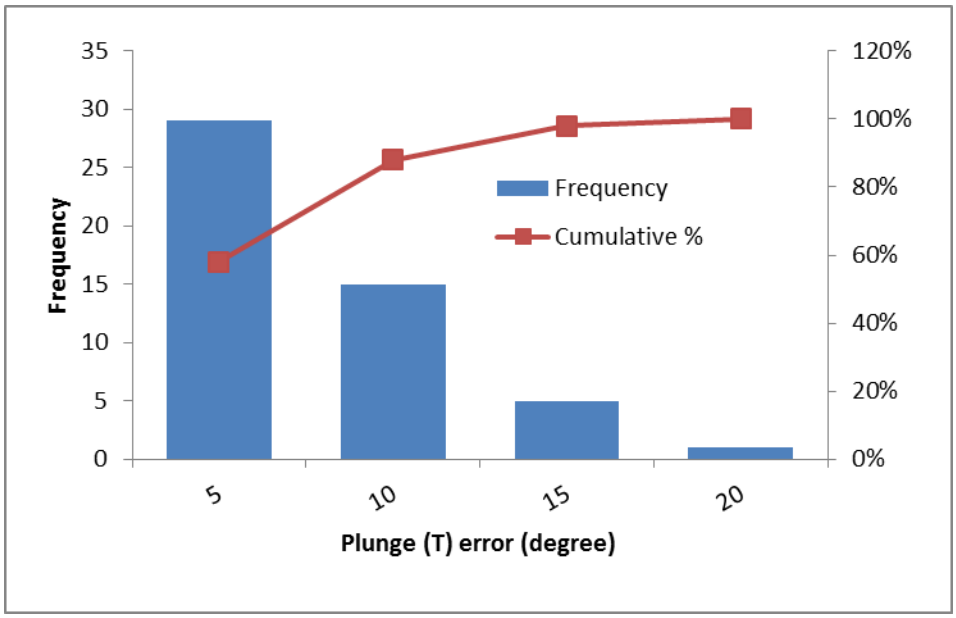
35
30
25
20
15
10
5
0
Frequency
120%
100%
80%
60%
40%
20%
0%
Frequency
Cumulative %
5
10
15
20
Plunge (T) error (degree)

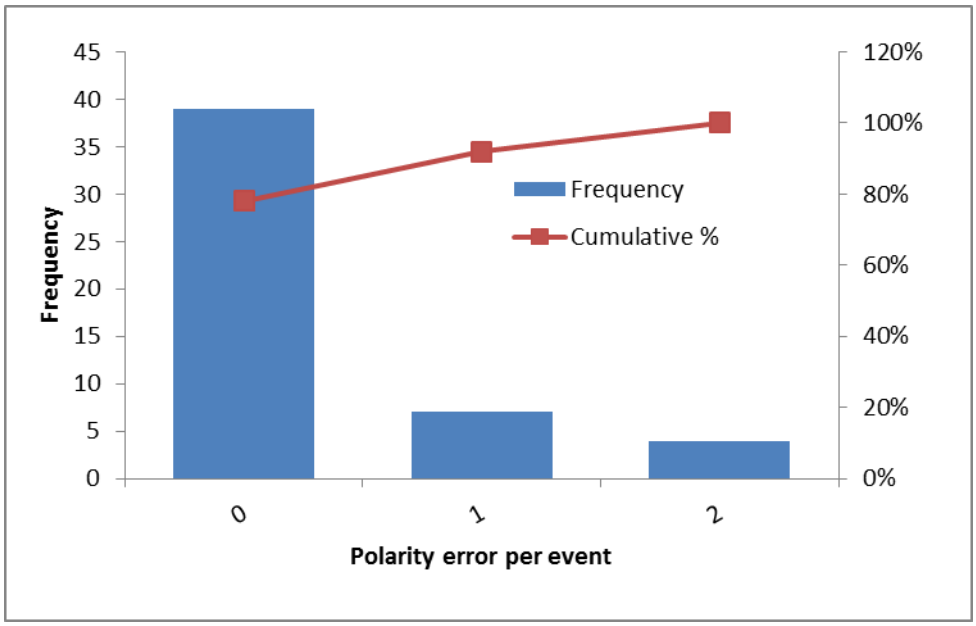
45
40
35
30
25
20
15
10
5
0
Frequency
120%
100%
80%
60%
40%
20%
0%
Frequency
Cumulative %
0
1
2
Polarity error per event

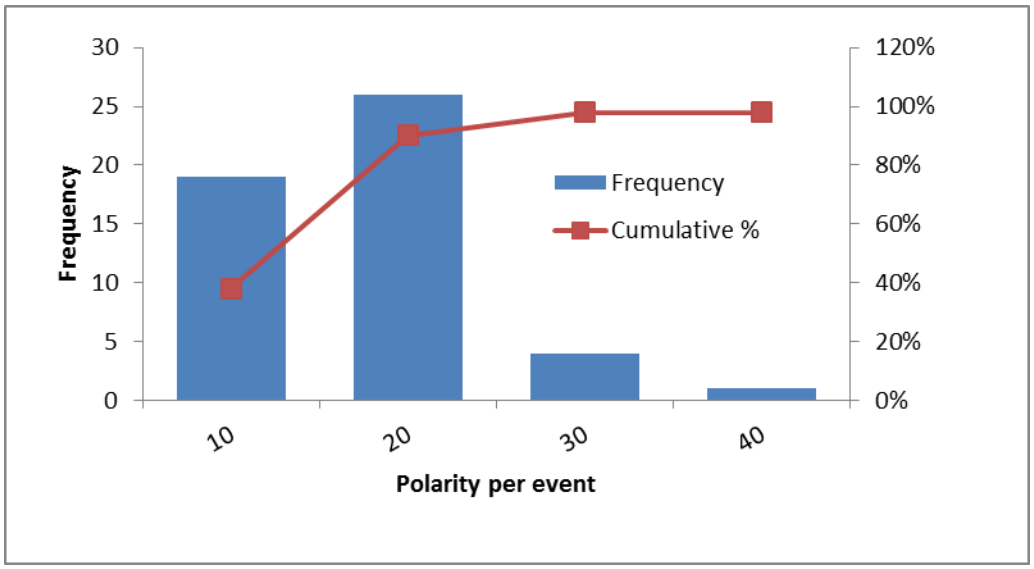
30
25
20
15
10
5
0
Frequency
120%
100%
80%
60%
40%
20%
0%
Frequency
Cumulative %
10
20
30
40
Polarity per event

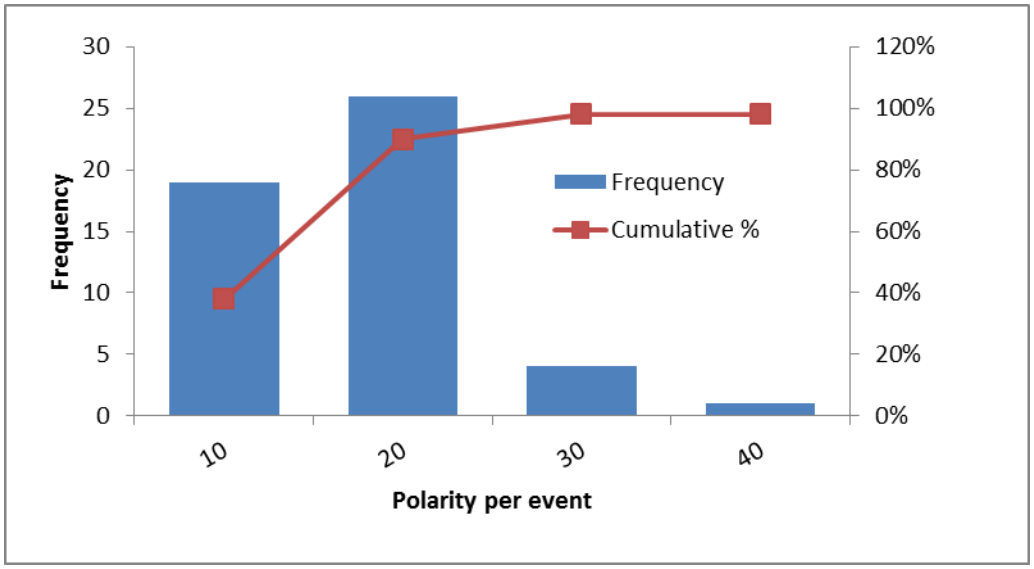
30
25
20
15
10
5
0
Frequency
120%
100%
80%
60%
40%
20%
0%
Frequency
Cumulative %
10
20
30
40
Polarity per event